Phase Noise in Coherent Optical Communications

by

MURAT AZIZOĞLU

B.S. Middle East Technical University
(1985)
M.S. Ohio State University
(1987)

Submitted in Partial Fulfillment
of the Requirements for the
Degree of

Doctor of Philosophy
in Electrical Engineering and Computer Science

at the

Massachusetts Institute of Technology
September 1991

Signature of Author _____

Department of Electrical Engineering and Computer Science
August 1, 1991

Certified by _____

Pierre A. Humblet
Thesis Supervisor

Accepted by _____

Campbell L. Searle
Chairman, Departmental Committee on Graduate Students

Phase Noise in Coherent Optical Communications

by

Murat Azizoğlu

Submitted to the
Department of Electrical Engineering and Computer Science
on August 1, 1991 in partial fulfillment of the requirements
for the Degree of Doctor of Philosophy

Abstract

Phase noise is an important factor in the design, analysis and performance of the future optical communication networks. We analyze the performance limitations imposed by phase noise on optical communications, for both transmitter–receiver pairs and networks. We consider various modulation schemes, in particular amplitude, frequency and phase modulation. For each modulation scheme, a number of reception strategies at intermediate-frequency (IF) are analyzed, and their error performances are compared. Optimum receiver structures are also obtained and seen to be very complex.

We also consider a class of communication strategies in which a reference signal is transmitted to alleviate the effects of phase noise. We show that systems in which power is equally divided between information-carrying and reference signals are limited to the performance of conventional single-carrier systems with orthogonal modulation. On the other hand, optimal allocation of power between the information and reference signals results in significant performance improvement. This is due to the fact that the reference signal occupies a smaller bandwidth, and hence it can be tightly filtered at the receiver.

We then take a signal space approach to detecting phase noisy sinusoidals in additive white Gaussian noise. By obtaining the Karhunen-Loeve expansion of the signal with phase noise, we demonstrate that the number of relevant signal directions increases from a few to infinity with the introduction of phase noise. Consequently the complexity of optimum detection with phase noise is very high.

Lastly, we consider the effect of phase noise in Frequency Division Multiple Access networks. We show that phase noise induced spectral broadening decreases the efficiency in which the available frequency band can be allocated to users in such a network. We specify this degradation for both single detector and balanced detector reception strategies.

Thesis Supervisor: Pierre A. Humblet

Title: Professor of Electrical Engineering, Department of Electrical Engineering and Computer Science

Acknowledgments

It is an impossible task to express my gratitude to all the people that made this thesis a reality. Nonetheless, I must try.

I am grateful to my advisor Pierre A. Humblet for everything. Throughout the years, he has thought me how to think, how to suspect, and how to work. Whatever is good in this thesis is due to his high standards, and his contagious energy and enthusiasm. I feel very fortunate to have the opportunity to benefit from his insight and wisdom.

Professors Robert G. Gallager and Robert S. Kennedy, my thesis readers, have helped improve this work by valuable feedback and suggestions.

Laboratory for Information and Decision Systems (LIDS) is an ideal environment to do research. The motivating and friendly atmosphere is due to everybody, faculty, staff and students, who is in LIDS. I would like to thank them all for making this a pleasant and valuable experience. I can only mention a few people who are especially important to me. John S. Young and I have spent countless hours discussing small problems (our research) and large problems (the world). I know I have a very close friend and colleague in John. Manos Varvarigos has been an equally important friend: we have shared many pleasant times, discussing politics, playing bridge, etc. Emre Telatar has been a constant source of help and friendship. Other friends at LIDS whom I should thank include Walid Hamdy, George Stamoulis, Muriel Medard, Peter Li, Phil Lin, David Tse and Ying Li. Professors Sanjoy Mitter and Dimitri Bertsekas have always provided valuable advise and friendly insight.

As I always do, I have postponed the most difficult part till it is no longer possible. I don't know how to thank my family. Whatever I accomplish in life is due to my mother, who so selflessly has put her own life on indefinite hold just to see her children happy and successful. My brother and sister will be more happy for me than I can ever be for anyone including myself.

This Ph.D. adventure has placed most demands on my dear wife Jaleh. She has had to tolerate the unbearable heaviness of being of a tense researcher while trying to do her own Ph.D. and more recently raising our little baby daughter. There is absolutely no way that I know of to thank her enough.

Finally, the most painful part is to acknowledge the driving force of my life. My beloved father, Dr. Yusuf Azizoğlu, had left this world 21 years ago, before I ever started going to school. Yet, he has always been with me. I used to see him in the classroom in the primary school when my classmates would go out in the breaks. I no longer see him. I wish he could be here today at the end of my schooling. He would have been happy to see me educated. But then, who knows that he does not? This thesis is dedicated to his memory, and to the Kurdish people he so dearly loved.

I acknowledge the financial support provided for my graduate work by NSF under grant NSF/8802991-NCR and by DARPA under grant F19628-90-C-0002.

Contents

List of Figures

Chapter 1

Introduction

Coherent optical communication technology offers great promise in realizing high data rate, long-distance communication networks. The advance of low loss single mode optical fibers with bandwidth in the order of 10 THz (10^{13} Hz) and compact and economical semiconductor lasers has made it possible to communicate at data rates that are orders of magnitude larger than that of electronic systems. This possibility has motivated a large amount of research in the emerging field of fiber-optic communications. In the twenty years that followed the introduction of the laser and the silica fiber, several research directions have achieved ground breaking progress. These research efforts may be broadly categorized into three groups. The first one is the development of devices to be employed in a communication system, such as semiconductor lasers, optical filters and amplifiers, glass fibers, photodetectors, etc. The second major research concentration is in the design and analysis of communication systems. Finally, there have been experimental efforts to demonstrate the feasibility and to improve the performance of these systems.

These three categories of research have had considerable interaction among, and influence on, each other. For example, the lack of spectral purity of the semiconductor lasers has led system researchers to design systems that will be robust against this nonideal effect, and experimental research has tested the designed systems. Similarly, the need for amplification of lightwaves for improving the system performance has motivated the device researchers to concentrate their efforts on optical amplifiers. The rapid progress of fiber-optic communications from a mere concept in early 1970s to practical systems in early 1990s owes much to this interaction.

The focus of this thesis falls in the second category above. This work will concentrate on an inherent nonideal phenomenon, phase noise in semiconductor lasers. We will investigate methods to remedy the effects of phase noise, and find the limitations that phase noise

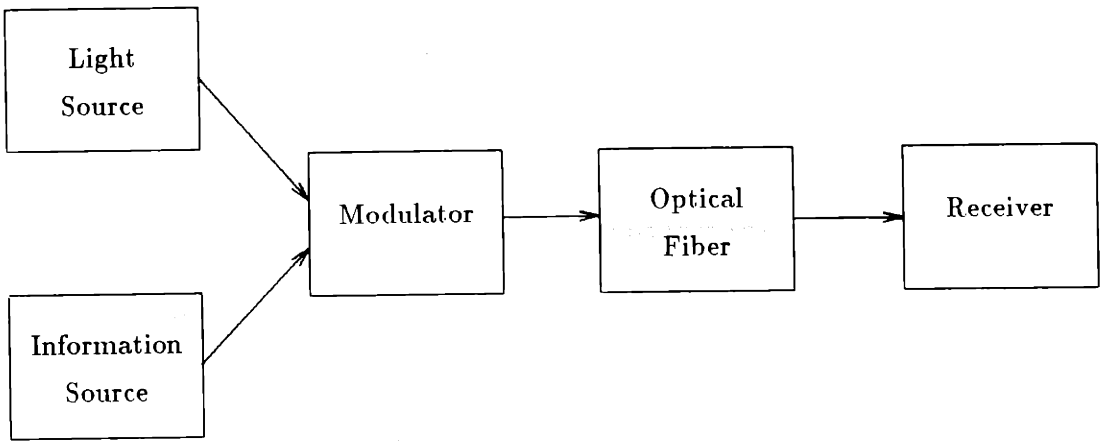

Figure 1-1: Basic block diagram of a fiber-optic communication system

imposes on communication systems.

This work is intended to be a comprehensive treatment of phase noise in coherent optical systems. A considerable amount of research has been performed on phase noise as the list of references would suggest. However, there does not exist a study of phase noise that treats the phase noise problem comprehensively, that investigates the different modulation formats with a consistent model and a uniform set of assumptions. The problem of optimum detection of phase noisy signals has not been adequately addressed. The network implications of phase noise has also received little attention. It is our goal to provide a study of this rather broad problem. In attempting to achieve this goal, we take the viewpoint of a communication theorist who tries to predict the performance of various communication schemes. Communication theory has addressed many problems which are similar in nature to the ones encountered in optical communications. Nonetheless, tools developed through many years in communication theory are not fully utilized by the optical communications community. This work is an attempt to narrow the existing gap in the specific problem of phase noise. It is hoped that the results we obtain will be helpful to both the optical communications community by providing theoretical performance limits that must be aimed in practice, and to the communication theory community by pointing out that many open problems remain in optical communication that can be attacked via communication-theoretic methods.

Before going into the details of the problems in the next chapters, we briefly describe the techniques used in optical communications below.

1.1 Fiber-optic Communication Systems

The basic features of a fiber-optic communication system are outlined in Figure 1-1. The light source in the figure is typically a laser or a light emitting diode (LED). The information source produces what we would like to send to the receiving end. While the information can be analog, e.g. voice, video, text, etc., or digital, e.g. data from a computer, the framework that we are interested in is that of digital communications. Therefore it is assumed that the information source produces digital, most often binary, data. If the underlying information is analog, it has been converted into digital form via sampling and quantization. The modulator is a means of impressing the digital data onto the lightwave output of the laser (or LED). It does not have to be a distinct device, and in fact it is possible to modulate the laser output directly by using the data in the driving circuitry of the laser.

After the digital information is impressed onto the optical field, the resulting lightwave is transmitted via the optical fiber which connects the source of the information to the desired destination. The receiver converts the received lightwave back to electrical data. The way the receiver operates depends on the modulation format, as well as optical detection strategy. In general, one of the two optical detection techniques is used: *direct detection* or *coherent detection*. In direct detection, the front end of the receiver is a photodetector which outputs an electrical signal proportional to the intensity of the received lightwave. In particular if the received optical field is

$$r_{opt}(t) = A(t)e^{j\alpha(t)}$$

then the average current output of the photodetector will be

$$i(t) = K|A(t)|^2$$

where K is a constant that will be elaborated on later. The current $i(t)$ will be processed electronically to recover the data. Note that the frequency and phase information of the lightwave is lost during the photodetection process. Therefore the information about the data must be embedded into the intensity of the transmitted lightwave. This is called *intensity modulation* (IM). The simplest and most commonly used form of IM is on-off-keying.

In coherent detection the incoming optical field is combined with a local oscillator field

before photodetection. If the incoming field is

$$r_{\text{in}}(t) = A(t)\exp(j(2\pi\nu_0 t + \theta(t)))$$

and the local oscillator field is

$$r_{\text{LO}}(t) = A_{LO}(t)\exp(j(2\pi\nu_1 t + \theta_{LO}(t)))$$

then the average output of the photodetector will be

$$\begin{aligned} i(t) = \quad & K \quad \left[|A(t)|^2 + |A_{LO}(t)|^2\right] + \\ & 2K \quad \text{Re}\left[A(t)A^*_{LO}(t)\exp(j(2\pi(\nu_0 - \nu_1)t + \theta(t) - \theta_{LO}(t)))\right] \end{aligned}$$

which has a baseband component as well as an intermediate frequency (IF) component at frequency $f_{IF} = \nu_0 - \nu_1$. The frequency and phase information is then preserved, up to a translation.

There are several characteristic differences between coherent detection and direct detection. Some important ones are the following:

1. Coherent detection allows electronic processing of the received signal at IF, while this is not possible at direct detection.

2. Frequency and phase modulation is possible with coherent detection, while intensity modulation is the only option with direct detection. (Frequency and phase modulation can be used with direct detection when measures are taken to convert the modulation to intensity modulation prior to photodetection. Some examples of this are wide-deviation frequency shift keying with optical filters at the receiver, and differential phase shift keying with optical delay and combining elements.)

3. Coherent detection results in better sensitivity (defined as the required signal power to achieve a given bit error rate) than direct detection. This is due to the effective amplification of the signal power by the mixing of the local oscillator signal. With the advance of optical amplifiers, direct detection systems will also improve in their sensitivity.

4. Since the optical spectrum can be shifted to different IF frequency values, frequency division multiplexing of different users can be more easily accomplished in coherent detection.

5. While direct detection is essentially a power measurement, which can be easily implemented using the current state-of-the-art, coherent detection is more involved, and thus requires certain practical obstacles to be overcome.

The last item above involves the matching of the polarization of the received and local fields among other coherence problems, and is the primary reason why almost all fiber-optic communication systems implemented to date employ direct detection. However, due to the advantages mentioned above, coherent detection has received much attention. Feasibility experiments are being performed in research laboratories worldwide. While a large number of technological problems have to be resolved before coherent systems can be regarded as a practical alternative, the progress in the field is certainly encouraging. It remains to be seen as to which of the two techniques will be widely used in the communication systems of the future. It will not be far-fetched to imagine the two to coexist, just as AM and FM do in today's radio systems.

1.2 Phase Noise

Phase noise is a phenomenon associated with spontaneous emissions that occur during the operation of a laser. The photon emission in a laser is primarily of two kinds. The first is stimulated emission in which an electron in a high energy level interacts with an incoming photon to release some of its energy and emit a photon. The result is an amplification of light. This is the intended mode of laser operation. (In fact, the name "laser" originates from Light Amplification via Stimulated Emission of Radiation). However, there are also spontaneous emissions in which an electron in a higher energy level emits a photon in a random fashion. The difference between the two types of emissions is that stimulated emission results in a light with the same frequency and phase as the incoming light while spontaneous emission results in a random phase. Each spontaneously emitted photon contributes a random incremental change in the overall phase of the laser output field. Thus the phase of the laser output executes a random walk from its nominal value. As the rate of the spontaneous emission events increases, the phase can be modeled as a Brownian motion process [1]. This randomness in the phase is commonly referred to as *phase noise*. While phase noise is common to all lasers, and more generally to most oscillators [2], it is especially strong in semiconductor lasers. It was observed in 1981 that the phase noise in semiconductor lasers is 30-50 times greater than the theoretical prediction of the time [3]. It was later shown in [1] that this is due to a change in the real refractive index of the

laser cavity which follows a spontaneous emission. This implies that the phase noise in a semiconductor laser will be stronger by a factor of $(1+\alpha^2)$ compared with a gas laser where $\alpha \simeq 4.6 - 6.2$.

The output field of a semiconductor laser can then be represented as

$$s(t) = A\cos(2\pi\nu_0 t + \theta(t) + \phi) \tag{1.1}$$

where $\theta(t)$ is the phase noise and ϕ is a constant phase. The phase noise $\theta(t)$ is satisfactorily modeled as a Brownian motion process which can be expressed as an integral of a white Gaussian frequency noise, that is

$$\theta(t) = 2\pi \int_0^t \mu(\tau)\, d\tau\ . \tag{1.2}$$

The strength of the phase noise will depend on the (two-sided) spectral height N_1 of the white Gaussian process $\mu(t)$. It can be easily seen that the phase process $\theta(t)$ is a zero-mean Gaussian process with variance

$$\mathrm{Var}\,[\theta(t)] = (2\pi)^2 N_1 t\ . \tag{1.3}$$

This equation reveals an important property of the phase noise: the phase noise statistically grows with time. As time progresses the phase noise becomes gradually more degrading. In fact since the density of $\theta(t)$ is determined by its variance, it is a simple matter to show that

$$\Pr\left[|\theta(t)| \geq \Delta\right] = 2Q\left(\frac{\Delta}{2\pi\sqrt{N_1 t}}\right)$$

where $Q(\cdot)$ is the complementary distribution function of a Gaussian random variable with zero-mean and unit variance. Thus we see that as $t \to \infty$, $\theta(t)$ gets large with probability 1. At the steady state, the modulo 2π equivalent of $\theta(t)$ becomes a uniform phase over $(-\pi, \pi]$.

We now investigate the spectral properties of the phase noisy laser output of Equation (1.1). Note that since $\theta(0) = 0$ by definition the constant phase ϕ corresponds to the initial phase. When ϕ is nonrandom, the process $s(t)$ is nonstationary. In order to be able to discuss the spectral distribution we need to make the process stationary without changing the power in its spectral components. The standard method to accomplish this is to introduce a randomness in the time origin, i.e. to make ϕ uniform over $(-\pi, \pi]$. (An uncertainty in the measurement of time origin will clearly not change the spectral characteristics of a

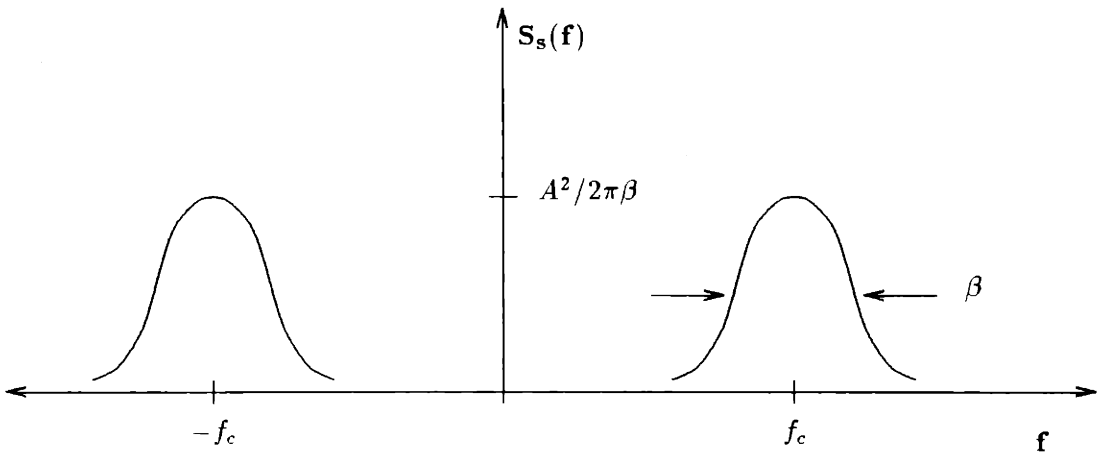

Figure 1-2: Power spectral density of a phase noisy sinusoid.

signal.) Then, the autocorrelation function of $s(t)$ is obtained as [4]

$$R_s(\tau) = \frac{A^2}{2}\cos(2\pi\nu_0\tau)\, e^{-2\pi^2 N_1|\tau|} \tag{1.4}$$

and the power spectral density is obtained via Fourier transform as

$$S_s(f) = \frac{A^2 N_1}{4}\left[\frac{1}{(f-\nu_0)^2 + (\pi N_1)^2} + \frac{1}{(f+\nu_0)^2 + (\pi N_1)^2}\right] . \tag{1.5}$$

The power spectral density is shown in Figure 1-2. This density is called *Lorentzian.* The 3-dB bandwidth of the signal is easily seen to be equal to $2\pi N_1$. (When there is no phase noise, the spectrum consists of two impulses as expected.) This bandwidth is commonly taken as a measure of the spectral broadening induced by phase noise. Thus the *linewidth* of a laser is defined as

$$\beta \triangleq 2\pi N_1 . \tag{1.6}$$

The linewidth has the advantage of being directly observable from the spectrum of the signal[1]. A typical semiconductor laser has a linewidth in the range 5-100 MHz. There are ongoing efforts to reduce the linewidth of semiconductor lasers. Since phase noise is a major impairment on fiber-optic communication systems, success in these efforts will improve the performance of such systems to a considerable extent. There have been reports of lasers

[1]This does not imply that observing the spectrum of a lightwave is an easy task in practice. Elaborate techniques, called self-homodyning, are used for this purpose[5].

with linewidth as low as 1 kHz in the literature [6], but such a low linewidth is accomplished at the expense of compactness and cost. It seems likely that practical lasers that will be used in future communications systems will have linewidths of at least 1 MHz [4, 7, 8]. Therefore it is essential that communication systems be designed taking phase noise into account, and that fundamental limitations due to phase noise be understood.

Phase noise has two important effects on optical networks. The first is *spectral broadening*, which causes every user in a Frequency Division Multiplexed (FDM) network to occupy a larger portion of the frequency band and consequently requires wider interchannel spacing. The result is an inefficient use of the available fiber bandwidth relative to ideal coherent detection. This is especially dominant at low data rates where channels occupy small bandwidth, and the overhead due to linewidth becomes a significant part of the bandwidth needed by an individual user. The second effect of phase noise is the incomplete knowledge and time-varying nature of the phase, which makes the correct retrieval of the transmitted data more difficult at the receiver. This causes a degradation of the bit error rate of the transmitter/receiver pairs.

A note on the phase noise model that will be used in this work is in order. While the Lorentzian spectrum matches the experimental observations quite well [9, 10], the Brownian motion model is still a simplified model. A more accurate description would incorporate a low frequency component of $1/f$ characteristics in the frequency noise spectrum in addition to the white noise that we assume. However, this low frequency component is significant only up to 1 MHz and is dominated by the white noise component beyond that range. It has been demonstrated that the low frequency components can be tracked and compensated [11]. Therefore the $1/f$ noise will be neglected in our model to avoid unnecessarily complicating the analyses that will be performed. Another idealization of the assumed model is that the relaxation oscillations that follow the spontaneous emissions are ignored. Strictly speaking, the variance of the phase noise process $\theta(t)$ contains not only the linear time component in Equation (1.2) but also a damped sinusoid of the form $e^{-at}\cos\omega t$ [12]. This effect is usually neglected in phase noise models since the rate of decay (more than 1 GHz) is typically much faster than the bit rate.

Since phase noise does not affect the amplitude directly, it may seem at first glance that amplitude (intensity) modulation systems will be immune to the adverse effects of phase noise. However there is another noise phenomena which has to be taken into consideration. This is the *shot noise* which is inherent to the photodetection process as we explain below.

1.3 Photodetection and Shot Noise

A photodetector is a power detector that produces an output current in response to the input optical field. There are various types of photodetectors, e.g. vacuum tubes, semiconductor photodiodes, avalanche photodiodes, all of which obey the same principle but differ in details. We concentrate on semiconductor (nonavalanche) photodiodes, because of their smaller size, lower cost and lower power supply requirements. Such a photodiode would ideally emit one electron per incoming photon. However in practical photodiodes the average number of emitted electrons per photon is η, where η is between 0 and 1 and it is called the quantum efficiency of the diode.

When the incoming lightwave has instantaneous power $P(t)$ and frequency ν_0, the electron emissions obey an inhomogeneous Poisson process with rate $\lambda(t) = \eta P(t)/h\nu_0$, where h is the Planck constant. Therefore the output current is a Poisson impulse train[2] given by

$$i(t) = q \sum_k \delta(t - \tau_k) \tag{1.7}$$

where $\{\tau_k\}$ are the arrival times of the Poisson process and q is the electron charge [13]. It is known that $i(t)$ has mean $q\eta P(t)/h\nu_0$ and covariance function $K_i(t,s) = q^2\lambda(t)\delta(t-s)$. Thus $i(t)$ can be written as a sum of a deterministic current and a zero mean noise process with this covariance function. When coherent detection with a large local oscillator power is used the noise process becomes Gaussian and white [4, 13]. The photodetection process may then be modeled as an addition of a white Gaussian noise to the instantaneous power of the sum of received field and local oscillator field.

There are two other noise processes that are associated with photodetection. They are dark current and thermal noise. As the name implies, dark current is due to random electron emissions in the absence of an optical input. These emissions also obey a Poisson law but with a fixed rate. Thermal noise is due to the electrical circuitry of the photodetector. Dark current and thermal noise powers are independent of the local oscillator power while shot noise power is proportional to this power. Therefore in the regime of large local oscillator power, dark current and thermal noise may be neglected. This is often called the shot-noise-limited (or quantum limited) regime. We will always assume that the receivers operate in this regime. An interesting property of the quantum limited regime is that the signal-to-

[2] Here we have assumed that the electron emissions are instantaneously observable at the current output, i.e. that the photodetector has infinite bandwidth. The conclusions in this section remain valid with a finite detector bandwidth with minor modifications.

noise ratio of the photodetector output is independent of the local oscillator power and is equal to the average number of received signal photons per unit time [4, 14]. This allows us to neglect the local oscillator and treat the problem as a standard additive white Gaussian noise problem that is so common to communication systems.

1.4 Phase Noisy Detection Problem

Having identified the relevant noise processes and the photodetection model, we can now formulate the problem of detecting information signals. The IF signal at the photodetector output is the sum of phase noisy modulated signal and shot noise. This signal can be written as

$$r(t) = s\left(t, \theta(t), \{a_n\}\right) + n(t) \tag{1.8}$$

where $n(t)$ is a white Gaussian noise with two sided spectral density $N_0/2$, $\{a_n\}$ is the sequence of information symbols, and $s(\cdot)$ is the modulated signal at IF frequency f_c which is the difference of the optical frequencies of the received and local oscillator signals:

$$s\left(t, \theta(t), \{a_n\}\right) = \mathrm{Re}\left[m\left(t, \{a_n\}\right) \exp\left(j\left(2\pi f_c t + \theta(t)\right)\right)\right] \tag{1.9}$$

and $m(\cdot)$ is the baseband modulation. For example, with binary on-off keying (OOK)

$$m\left(t, \{a_n\}\right) = \sum_n a_n p(t - nT) \quad a_n = 0, 1$$

with binary phase-shift keying (PSK)

$$m\left(t, \{a_n\}\right) = \sum_n (1 - 2a_n) p(t - nT) \quad a_n = 0, 1$$

and with binary frequency shift keying (FSK)

$$m\left(t, \{a_n\}\right) = \sum_n \left[a_n\, e^{-j2\pi f_d t} + (1 - a_n)\, e^{j2\pi f_d t}\right] p(t - nT) \quad a_n = 0, 1$$

where

$$p(t) = \begin{cases} 1 & \text{for } 0 < t < T \\ 0 & \text{otherwise} \end{cases}$$

and T is the bit duration.

The receiver is to obtain an estimate of the data sequence with the performance measure

being the probability of error defined as

$$P_e = \Pr(\hat{a}_n \neq a_n) .$$

We will look at different modulation formats and different receiver structures, and evaluate their error probability performances. We will mostly concentrate on binary modulation formats and in particular on FSK, differential PSK and OOK. These modulation formats are both analytically and practically simpler and well-understood. It seems unlikely, at least in the infancy stage of coherent optical communications, that more complicated modulation schemes will be implemented.

We will also look at different IF receiver structures, optimal receiver structures and more practical suboptimal receivers, for different modulation formats. The performance of any of these receivers will depend on two key parameters: the IF signal-to-noise ratio ξ, and the ratio of the combined linewidth of transmitter and local oscillator lasers to the bit rate, β/R, where $\beta = \beta_T + \beta_{LO}$. The latter quantity is proportional to the variance of phase wander within a bit period, since

$$\mathrm{Var}\,[\theta(t) - \theta(t-T)] = 2\pi\beta T \stackrel{\triangle}{=} \gamma .$$

We will refer to γ as the *phase noise strength.* For small γ the effect of phase noise during a bit interval is small and vice versa.

In the next three chapters we consider frequency, phase and amplitude modulation formats in detail. We obtain optimal detection strategies and suboptimal receivers derived form them. We also perform accurate analyses for the performance of these modulation formats.

A method to alleviate the effect of phase noise is to have the transmitter send two copies of the same carrier, one modulated and one unmodulated. The receiver can then use the unmodulated signal to obtain a phase reference for the modulated signal. We show that systems in which the available power is equally divided between the information signal and the reference signal are limited to the performance of conventional single carrier systems with orthogonal modulation. Optimal allocation of power between these signals as well as an optimal assignment of the filter bandwidths according to the signal-to-noise ratio and the phase noise strength result in significant performance improvement. This transmitted reference scheme shows promise as a practical alternative to the conventional single carrier systems. We will describe and analyze this scheme in Chapter 5.

The detection problem may be viewed as finding the projections of the received signal on relevant signal directions and processing these projections according to a certain decision rule. This signal space approach is particularly helpful in the problem of known signal in additive white Gaussian noise; the optimum matched-filter receiver can be obtained with relatively little effort with this approach [15]. This is due to the fact that white Gaussian noise has independent projections in orthogonal signal directions; all but finitely many signal detections become irrelevant to the detector. Similarly in the problem of detecting a sinusoidal signal with an unknown but constant phase, the well-known envelope detector can be easily obtained by recognizing that in-phase and quadrature sinusoids are the only relevant signal directions.

The same principle may be applied to the detection of the phase noisy sinusoid in additive white Gaussian noise. The signal directions may be obtained by employing the Karhunen-Loeve analysis. We pursue this approach in Chapter 6 and find the eigenfunctions. There we will find that introduction of phase noise increases the number of relevant signal directions from a few to infinity. This is an indicator of the difficulty of optimally detecting phase noisy signals.

1.5 Network Implications of Phase Noise

The advantage of fiber-optic communications is best utilized in a multi-user network environment where different communication sessions are taking place simultaneously. Bandwidth has traditionally been a scarce resource in networking. With the advance of optical networking, the available bandwidth increases by several orders of magnitude. Therefore, optical fibers promise a revolution in the high speed networks of the future. The design of optical networks involves a myriad of issues ranging from multiple access mechanisms to network topology to routing and flow control. It is beyond the scope of this thesis to address these issues. We will briefly consider the efficiency of bandwidth utilization for a particular multiaccess scheme in the presence of phase noise.

Apart from deteriorating the end to end error performance of a communication system, phase noise also affects channel allocation in a Frequency Division Multiplexed (FDM) optical network. This is due to spectral broadening as we have previously explained. Users must be allocated wider frequency bands due to spectral broadening. We will obtain the exact band occupancies of different modulation formats. We will also investigate the crosstalk in a multichannel environment that occurs due to photodetection. As a result we will obtain rules governing the channel allocation in a FDM network. We consider both receivers with

single photodetectors and receivers that use a pair of photodetectors in a balanced configuration [16, 17]. We observe that balanced receivers improve the efficiency of spectrum allocation considerably.

Chapter 2

Envelope Detection of Orthogonal Signals

In this chapter we consider the effect of phase noise on the error performance of communication systems. In the presence of phase noise, the incomplete knowledge and the time-varying nature of the phase makes the correct retrieval of the transmitted data bits more difficult for the receiver. This causes a degradation of the bit error rate of the point-to-point communication links. It is our goal to quantify this degradation for different modulation formats and receiver forms. This problem has received much attention in the recent years. Various performance analyses for different modulation formats and receiver structures exist in the literature [4, 8, 18, 19, 20, 21]. However, since researchers use different sets of assumptions and approximations in their work, it is difficult to reconcile their results and to agree on the quantitative effect of phase noise on coherent systems. The difficulty seems to arise from the fact that the Brownian motion model of the phase noise, which is well-tested and agreed upon, results in a random process that is both nonlinear and nonstationary. Thus, as one moves through different stages of a nontrivial receiver, the exact statistical characterization of the randomness due to phase noise becomes increasingly difficult. One needs to invoke a sequence of assumptions and approximations to overcome these difficulties. Naturally, the confidence that the real systems will operate within a reasonable margin of the predictions of the analyses depends on the number and the nature of these assumptions and approximations.

It is reasonable to expect that the modulation formats which suffer the least from phase noise will be those with asymmetric constellations in signal space, e.g. on-off-keying (OOK) and frequency-shift-keying (FSK). These two modulation formats were considered recently by Foschini and his colleagues in [8]. They formulated and treated the problem with a minimal number of approximations. Their work provides a rigorous framework upon which the researchers in the field may agree and improve. As a result, a considerable number

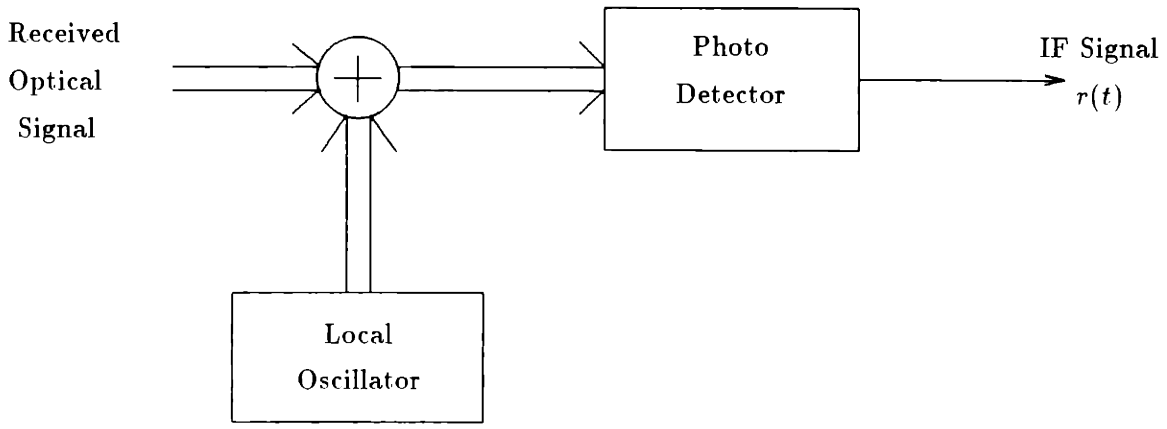

Figure 2-1: The optical heterodyne receiver.

of papers have resulted from their model in a relatively short time [21, 22, 18]. The work reported in this chapter also conforms to the receiver model of [8]. We consider orthogonal modulation formats here, e.g. FSK and orthogonal polarization modulation. We describe the receiver models and the problem in the next section. We obtain closed-form expressions for the probability of error conditional on the squared envelope of a normalized phase noisy signal, for different receiver forms. We provide an approximation that is close to the actual envelope and whose moments are readily available. We compute the probability density function of this approximate envelope from its moments using a method based on Legendre polynomials. We then use this density function to remove the conditioning on the error probability and, thus, to obtain the error performance of the systems under consideration. We also provide a lower bound to the error probability of the double-filter receiver which is very close to the actual error probability. Therefore this lower bound, which is very easy to compute, can be used to estimate the performance.

Finally, we extend the analysis to the case of N-ary FSK where we provide very tight upper and lower bounds to the bit error probability.

2.1 Problem Description

The received optical signal is first processed by an optical heterodyne receiver shown in Figure 2-1 for FSK signals. Polarization modulation would require a polarization beam splitter and a pair of photodetectors. Optical heterodyning transforms the signal from

optical frequency to intermediate frequency. The IF signal output $r(t)$ is to be further processed by the IF receiver. This IF processing is the main focus of this chapter.

The IF receiver structure that we consider in this chapter is shown in Figure 2-2 where the incoming signal is corrupted by phase noise and additive noise. The front end of this receiver is the standard quadrature receiver that performs envelope detection of FSK signals. The correlators and integrators perform a bandpass filtering to limit the noise power corrupting the signal. Since the integrators integrate their inputs over a duration T' the effective bandwidth of the filter is $1/T'$. For a uniformly distributed phase uncertainty which is constant over the bit duration the optimum value of T' is the bit duration T. However, when the signal is corrupted by phase noise, the spectrum of the signal is broadened. Therefore a wider filter bandwidth, equivalently smaller integration times, may be necessary. For analytical convenience, we only consider the case where the ratio T/T' is a positive integer M as in [8].

The outputs of the in-phase and quadrature branch integrators in Figure 2-2 are squared and then added to perform the envelope detection. The remaining processing depends on the value of M. For $M = 1$, the adder outputs are sampled at the end of the bit duration and the two values are compared to reach a decision about the transmitted data bit. We call the receiver with $M = 1$ a *single sample receiver* since only one sample is taken during a bit duration. For $M \geq 2$, the adder outputs are sampled every T' seconds resulting in M samples per bit. The way these samples are processed depends on the complexity that one desires. One simple strategy is to discard all but the last one of these samples and to use the last sample as in the single sample receiver. A more efficient way is to average these M samples and compare the two averages. This averaging is not the optimal processing of the samples. However, since it can be performed by a lowpass filter it is a practical reception strategy to implement.

We classify the reception strategies above into three categories. The first is the single sample receiver, the second one is the multisample receiver with single filtering and the third one is the multisample receiver with double filtering. These receiver structures were first suggested by Kazovsky et. al. in [23] for ASK multiport homodyne receivers [1]. In the framework of [23], the single sample receiver is the conventional matched-filter receiver, the single-filter receiver is the conventional receiver with a widened filter, and the double filter receiver is the wide-band filter-rectifier-narrowband filter (WIRNA) structure. It was

[1] A homodyne receiver uses the same frequency for the local oscillator as the received signal so that the photodetector output is at baseband.

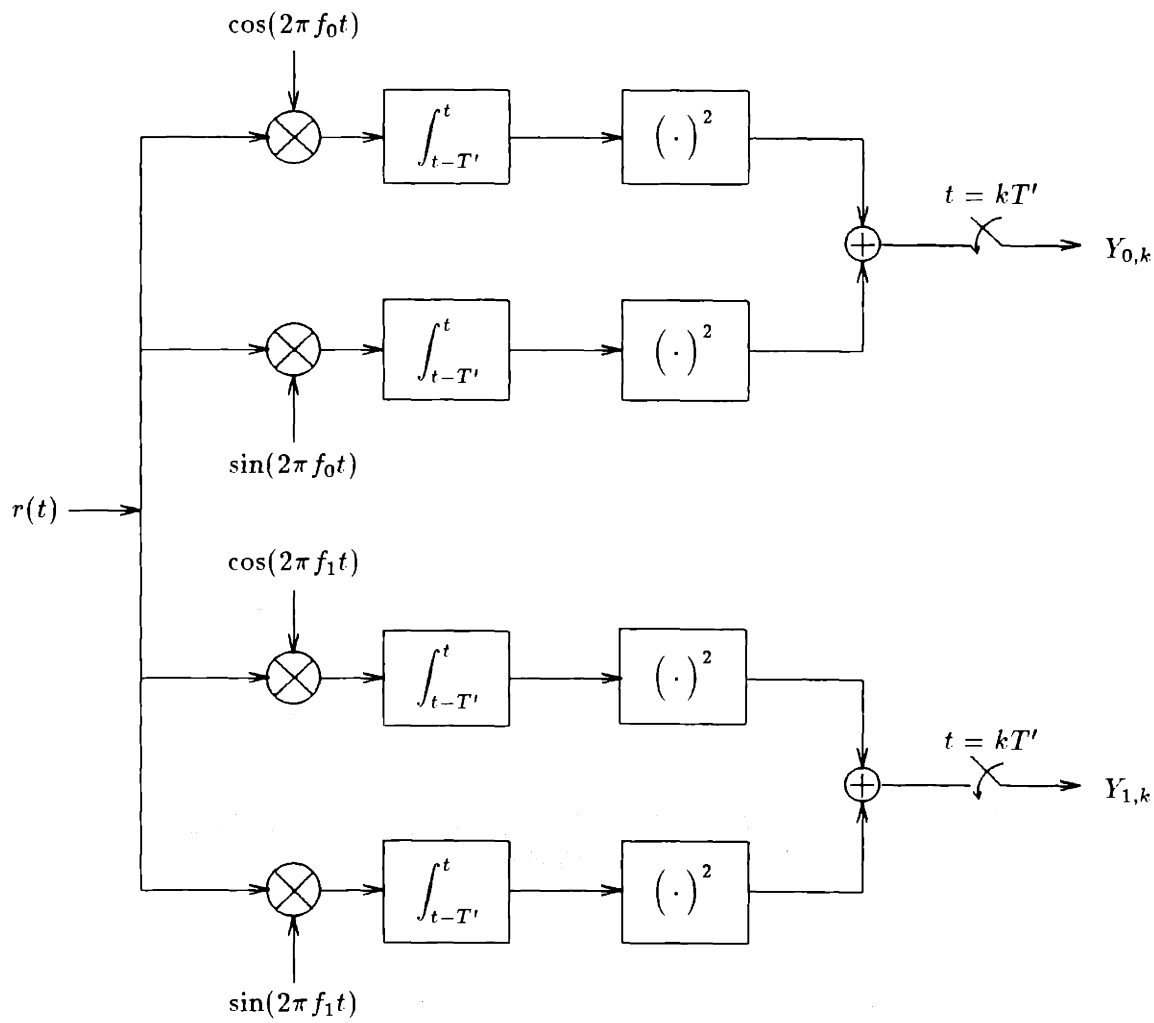
cos(2πf0t)
∫ t t−T'
(·)²
t = kT'
Y0,k
sin(2πf0t)
r(t)
cos(2πf1t)
∫ t t−T'
(·)²
t = kT'
Y1,k
sin(2πf1t)

a)

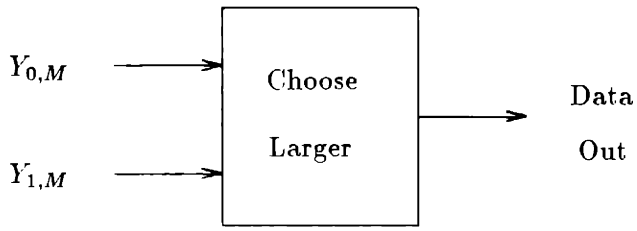

b)

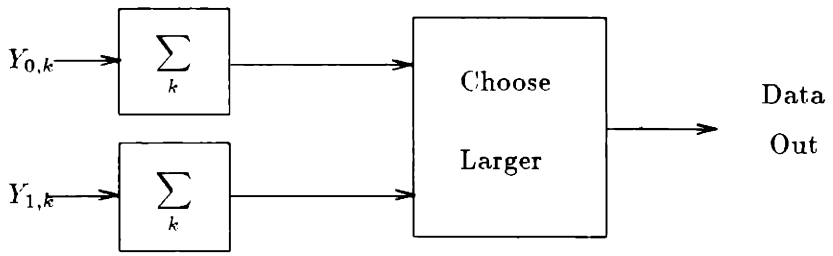

c)

Figure 2-2: The IF receiver, a) Front end, b) Sample processing for single sample and single filter receivers, c) Sample processing for double filter receiver.

also noticed in [23] that if the M samples of the double filter receiver are viewed as coming from M distinct channels (or from a fast frequency-hopped spread spectrum system), then the receiver is functionally equivalent to the noncoherent receiver for multichannel signaling treated in [24]. Some of our results, in particular the conditional error probability given by Equation (2.19), may be obtained by using the results of [24]. However, we will proceed independently in order to derive additional properties.

2.1.1 Single Sample Receiver

We first consider the single sample receiver. This receiver is the optimal receiver when the phase of the received signal has uniform distribution and is time-invariant. The error probability for this case has a simple closed-form ($1/2\ e^{-E_b/2N_0}$) [25]. We will see that a similar (but more complicated) result can be obtained in the phase noisy case.

We assume that the received IF signal is the FSK signal corrupted by additive noise and phase noise:

$$r(t) = A\cos(2\pi f_i t + \theta(t)) + n(t) \quad i = 0, 1 \tag{2.1}$$

where f_0 and f_1 are the frequencies for "0" and "1" respectively. The phase noise $\theta(t)$ is a Brownian motion process described by

$$\theta(t) = 2\pi \int_0^t \mu(\tau)\, d\tau \tag{2.2}$$

with $\mu(\tau)$ being a zero-mean white Gaussian process with two-sided spectral density $\beta/2\pi$. Then $\theta(t)$ is a zero-mean Gaussian process with zero-mean and variance $2\pi\beta t$; β is the combined linewidth of the source and local oscillator lasers. The additive noise $n(t)$ in (2.1) is a white Gaussian process with two-sided spectral density $N_0/2$. We assume that the difference between f_1 and f_0 is much larger than the filter bandwidth $1/T'$, so that when a "0" is transmitted, the integrator outputs of the lower branch integrators in Figure 2-2a contain no signal component, and vice versa. With this assumption, when a "0" is transmitted the sampler outputs at time $t = T$ can be written as

$$\begin{aligned} Y_0 &= \left| \frac{A}{2} \int_0^T e^{j\theta(t)}\, dt + n_{c0} + j n_{s0} \right|^2 \\ Y_1 &= |n_{c1} + j n_{s1}|^2 \end{aligned} \tag{2.3}$$

where n_{ci} and n_{si} are statistically independent and identically distributed (i.i.d.) Gaussian

random variables with zero-mean and variance $\sigma^2 = N_0T/4$. Due to symmetry, the error probability is given by

$$P_e = \Pr(Y_0 \leq Y_1) \ . \tag{2.4}$$

We will now condition the error probability on the amplitude of the phase noise integral in (2.3). We define

$$Y \triangleq \left| \frac{A}{2} \int_0^T e^{j\theta(t)}\, dt \right| \ . \tag{2.5}$$

Then the conditional density of Y_0 can be easily found as[2]

$$p(y_0|Y) = \frac{1}{2\sigma^2} e^{-(y_0+Y^2)/2\sigma^2} I_0\left(\frac{Y\sqrt{y_0}}{\sigma^2}\right) \tag{2.6}$$

while Y_1 has an exponential density given by

$$p(y_1) = \frac{1}{2\sigma^2} e^{-y_1/2\sigma^2} \ . \tag{2.7}$$

Therefore the conditional error probability comes as a result of the classical problem of incoherent detection of orthogonal signals as [25]

$$P_e(Y) = \frac{1}{2} e^{-Y^2/2\sigma^2} \ . \tag{2.8}$$

Let's now express Y in a different form. From (2.5), we have

$$Y = \frac{AT}{2} \left| \int_0^1 e^{j\theta(Tu)}\, du \right| \ .$$

Since $\theta(Tu)$ has variance $2\pi\beta Tu$, Y can be written in terms of standard Brownian motion $\psi(t)$ (i.e. that with variance t) as

$$Y = \frac{AT}{2} \left| \int_0^1 e^{j\sqrt{\gamma}\psi(t)}\, dt \right|$$

where $\gamma \triangleq 2\pi\beta T$. Now if we define the random variable $X(\gamma)$ as

$$X(\gamma) \triangleq \left| \int_0^1 e^{j\sqrt{\gamma}\psi(t)}\, dt \right|^2 \tag{2.9}$$

[2] For notational convenience we indirectly address the random variable that a density function refers to with its argument, i.e., $p(y)$ stands for $p_Y(y)$ in the more standard notation.

(2.8) can be written in terms of X as

$$P_e(X) = \frac{1}{2}e^{-\xi X(\gamma)/2} \tag{2.10}$$

where $\xi = A^2T/2N_0$ is the signal-to-noise ratio. Therefore P_e is given by

$$P_e = E_X\left[\frac{1}{2}e^{-\xi X(\gamma)/2}\right] . \tag{2.11}$$

In the case with no phase noise ($\gamma = 0$), this reduces to $1/2e^{-\xi/2}$ as it should.

An immediate implication of (2.11) is that there does not exist a bit-error-rate-floor, i.e. a nonzero error probability that exists even when ξ tends to ∞, for the single sample receiver, provided that the probability density function of $X(\gamma)$ does not contain a delta function at the origin [3].

To determine P_e from (2.11) we have to obtain either the probability density function or the moment generating function of X. Therefore the random variable X plays a key role in the performance analysis of the single sample receiver. In the next section, we will show that this is also true for the multisample receivers that we consider.

2.1.2 Multisample Receivers

In the previous section, we mentioned that the receiver may use a shorter integration time T' than the full bit duration T. The advantage of this scheme is that the phase is not allowed to wander too much so that the amount of collected signal energy may not drop below undesirable levels. Equivalently, the bandwidth of the IF filter is increased to pass more of the signal power. If only the last of the M samples, the one at $t = T$, is used, then the received signal is effectively processed only during the interval $(T - T', T)$, hence there is a drop in the received signal-to-noise ratio by a factor of $1/M$. However, since the phase is allowed to change in an interval of length T', the effective value of γ also drops by a factor of $1/M$. (This can be observed by repeating the calculations of the previous section when T is replaced by T'.) Therefore the probability of error for the multisample receiver with single filter is given by

$$P_e = E_X\left[\frac{1}{2}e^{-\xi X(\gamma/M)/2M}\right] . \tag{2.12}$$

[3] If one takes the finite frequency separation $f_1 - f_0$ into account, then there is an inherent error floor in FSK [14, 19]. This has been neglected in our model in (2.3).

An inspection of (2.12) shows that when the signal-to-noise ratio and/or the phase noise strength is small, the optimal value of M will be small. However, for large signal-to-noise ratios and large phase noise values, it may be worthwhile to sacrifice from the signal energy while alleviating the effect of phase noise.

The single-filter receiver uses only one of the M available samples. Thus the single-filter receiver is, in fact, a single sample receiver with widened front end filter bandwidth. The efficiency of this receiver would be improved if all the M samples were used in the decision process. A simple processing of these samples is averaging, which may be accomplished by low-pass-filtering the sum of the outputs of the square-law devices [8]. The result is the multisample double-filter receiver that we analyze below. Note that this receiver is not the (still unknown) receiver which minimizes the probability of error. It is closely related to the optimal receiver for the case where the phase noise process $\theta(t)$ is piecewise constant and takes M independent uniformly distributed values during a bit interval. In this case, the optimal receiver averages the square root of the samples when the signal-to-noise ratio is high.

In the case of a "0" being transmitted, the lowpass filter outputs will be

$$Y_0 = \sum_{k=1}^{M} |x(k) + n_{c0}(k) + jn_{s0}(k)|^2 \tag{2.13}$$

$$Y_1 = \sum_{k=1}^{M} |n_{c1}(k) + jn_{s1}(k)|^2 \tag{2.14}$$

where $x(k)$ is given by

$$x(k) = \frac{A}{2} \int_{(k-1)T'}^{kT'} e^{j\theta(t)}\, dt$$

and all the additive noise samples are i.i.d. zero-mean Gaussian with variance

$$\alpha^2 = N_0 T'/4 \,.$$

It can be seen that since $\theta(t)$ has independent increments, the variables $|x(k)|$ are statistically independent. Furthermore, since $\theta(t)$ has stationary increments, $|x(k)|$ will be identically distributed[4]. Then each of the terms in (2.13) and (2.14) obey the distributions in (2.6) and (2.7) respectively. (Y in (2.6) is replaced by $|x(k)|$.) In particular, since each term in

[4]This also implies that the envelopes preserve their statistical properties from one bit to another. So we can consider the first bit in the performance analysis without loss of generality.

(2.14) has i.i.d. exponential distribution, Y_1 has a Gamma distribution with parameters M and $1/2\alpha^2$. It is convenient to normalize Y_0 and Y_1 via

$$V_i = \frac{Y_i}{2\alpha^2} \quad i = 0, 1 .$$

Then V_1 has the density function

$$p(v_1) = \frac{v_1^{M-1}}{(M-1)!} e^{-v_1} \quad v_1 \geq 0 . \tag{2.15}$$

Due to symmetry, the probability of error is given by

$$P_e = \Pr(V_0 \leq V_1) .$$

Now using the density of V_1 and conditioning the error probability on V_0, we obtain

$$P_e = \int_0^\infty \sum_{k=0}^{M-1} \frac{v_0^k}{k!} e^{-v_0} p(v_0)\, dv_0 \tag{2.16}$$

where $p(v_0)$ is the density function of V_0. This density appears to be difficult to obtain in closed-form. Therefore, we will first condition (2.16) on the phase noisy envelopes. Given $\{x(k) : 1 \leq k \leq M\}$, V_0 is the sum of squares of $2M$ independent Gaussian random variables, the density of which is given by [25]

$$p(v_0|\{x(k)\}) = \left(\frac{v_0}{r}\right)^{(M-1)/2} e^{-(v_0+r)} I_{M-1}\left(\sqrt{4rv_0}\right) \quad v_0 \geq 0 \tag{2.17}$$

where $I_{M-1}(\cdot)$ is the modified Bessel function of order $M-1$ and r is defined as

$$r = \frac{1}{2\alpha^2} \sum_{k=1}^{M} |x(k)|^2 .$$

Note that the conditional density of V_0 depends on $\{x(k)\}$ only through the sum of their squared amplitudes. This enables us to proceed further and to express the error probability conditioned on r as

$$P_e(r) = \Pr(V_0 \leq V_1|r)$$

$$= \sum_{k=0}^{M-1} \frac{1}{k!} \int_0^\infty e^{-x} x^k \left(\frac{x}{r}\right)^{(M-1)/2} e^{-(x+r)} I_{M-1}\left(\sqrt{4rx}\right)\, dx\,. \qquad (2.18)$$

It is shown in Appendix 2.A that $P_e(r)$ can be expressed as

$$P_e(r) = \frac{e^{-r/2}}{2^M} \sum_{n=0}^{M-1} \frac{(r/2)^n}{n!} \sum_{k=n}^{M-1} \binom{k+M-1}{k-n} \frac{1}{2^k}\,. \qquad (2.19)$$

Now we relate r to the envelope of the standard Brownian motion using the techniques of the previous section. From the definition of r and $x(k)$ we have

$$\begin{aligned} r &= \frac{A^2}{8\alpha^2} \sum_{k=1}^{M} \left| \int_{(k-1)T/M}^{kT/M} e^{j\theta(t)} dt \right|^2 \\ &= \frac{A^2}{8\alpha^2} \left(\frac{T}{M}\right)^2 \sum_{k=1}^{M} \left| \int_{k-1}^{k} e^{j\sqrt{\gamma/M}\psi(t)} dt \right|^2 \end{aligned}$$

where $\psi(t)$ is the standard Brownian motion. Defining

$$X_k(\gamma) = \left| \int_{k-1}^{k} e^{j\sqrt{\gamma}\psi(t)} dt \right|^2$$

and using the definitions of the additive noise variance α^2 and the signal-to-noise ratio (SNR) ξ, we obtain

$$r = \xi \frac{1}{M} \sum_{k=1}^{M} X_k(\gamma/M)\,. \qquad (2.20)$$

Therefore r is the SNR weighted by the sample average of the M normalized phase noisy envelope squares, it can be viewed as a phase noisy signal-to-noise ratio. As $M \to \infty$, the sample average tends to the mean of X_k with probability 1, by the law of large numbers. Also, the mean of $X_k(\gamma/M)$ tends to 1 as $M \to \infty$. Therefore r tends to ξ, which is the maximum value it can assume since $X_k \leq 1$ by the Schwartz inequality.

The conditional error probability given by (2.19) is shown in Figure 2-3 as a function of r. As expected $P_e(r)$ decreases as r gets larger while M is fixed. However, for a fixed value of r, $P_e(r)$ increases with M. Thus, there is a tradeoff between the collected energy of the phase noisy signal and the additive noise energy corrupting the signal as M changes. There must exist an optimum value of M which balances the two conflicting noise effects. This behavior is also observed in [8].

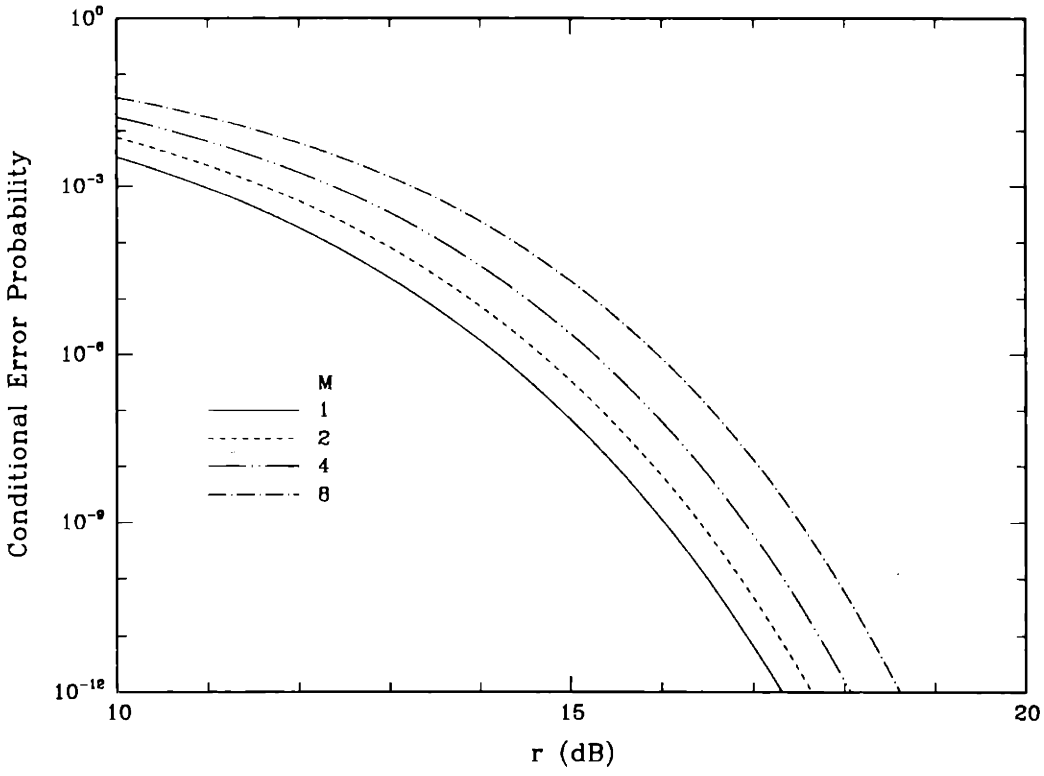

Figure 2-3: Error probability of the double-filter receiver conditioned on the phase-noisy signal to noise ratio.

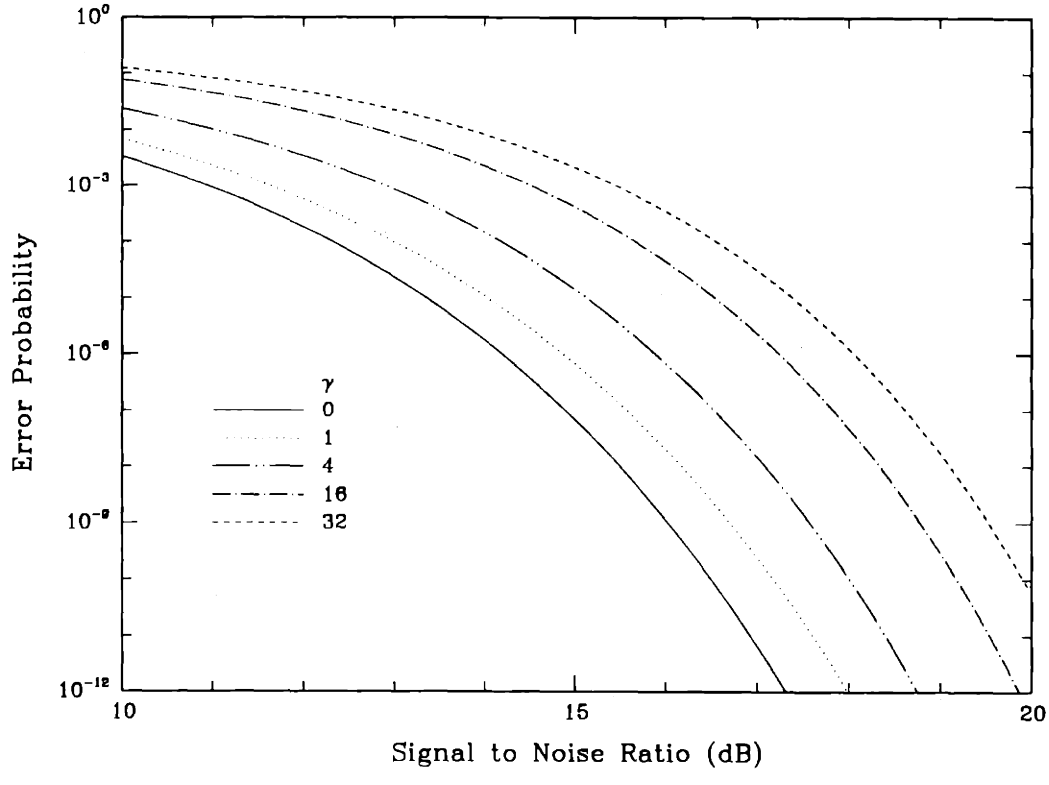

Figure 2-4: Lower bound on the error probability obtained by Jensen's inequality.

We can readily obtain a lower bound to the error probability without calculating the density of $X(\gamma)$. We show in Appendix 2.B that $P_e(r)$ as given by (2.19) is a convex $\cup$ function of r for any value of M. The unconditional error probability is the expected value of $P_e(r)$; thus replacing r by its mean results in a lower bound by Jensen's inequality [26]. Using (2.20), one has

$$P_e \geq P_e\left(E\left[X(\gamma/M)\right]\right) . \tag{2.21}$$

The expected value of $X(\gamma)$ will be found in the next section. Figure 2-4 shows the lower bound in (2.21) with the use of (2.34) of the next section. At each value of SNR ξ and the phase noise strength γ, the lower bound has been minimized with respect to M.

The overall error probability P_e is obtained from $P_e(r)$ by removing the conditioning over r. If $p_a(r)$ denotes the probability density function of r, then we have

$$P_e = \int P_e(r) p_a(r)\, dr . \tag{2.22}$$

Since r is a weighted average of i.i.d. random variables X_k as given by (2.20), the density of r is given in terms of the density of X_k by an M-fold convolution. Then, we see that the density of the phase noisy squared-envelope is again the only information we need to obtain the error probability. The convolutions must be performed anew for each M since the individual densities to be convolved correspond to the envelope with phase noise strength γ/M. Therefore the computation becomes very costly with many convolutions to be performed. We describe an alternative method which eliminates the need for convolutions. From (2.19), the error probability can be written as

$$P_e = E_r\left[\sum_{n=0}^{M-1} a_n \left(\frac{r}{2}\right)^n e^{-r/2}\right] \tag{2.23}$$

where the coefficients a_n are defined as

$$a_n = \frac{1}{2^M n!} \sum_{k=n}^{M-1} \binom{k+M-1}{k-n} \frac{1}{2^k} . \tag{2.24}$$

Using the sample average expression for r given in (2.20) one gets

$$P_e = \sum_{n=0}^{M-1} a_n \left(\frac{\xi}{2M}\right)^n E\left[\left(\sum_{k=1}^{M} X_k(\gamma/M)\right)^n \exp\left(-\frac{\xi}{2M}\sum_{k=1}^{M} X_k(\gamma/M)\right)\right] .$$

Finally expanding the expression above in a multinomial sum and using the independence of the X_k we obtain

$$P_e = \sum_{n=0}^{M-1} a_n \left(\frac{\xi}{2M}\right)^n \sum_{\substack{k_1,\ldots,k_M \\ k_1+\cdots+k_M=n}} \frac{n!}{k_1!\cdots k_M!} \prod_{i=1}^{M} \alpha(k_i) \tag{2.25}$$

where

$$\alpha(k) = E\left[X^k(\gamma/M)\exp\left(-\frac{\xi}{2M}X(\gamma/M)\right)\right] . \tag{2.26}$$

The need for convolutions is eliminated by this expansion. All that is necessary about the envelope is a set of tilted moments $\alpha(k)$. This reduces the computations considerably. Further computational savings can be obtained by observing that the inner summation in (2.25) contains many identical terms: any permutation of an M-tuple $(k_1, k_2, \ldots, k_M)$ results in the same term. Therefore the summation may be limited to ordered tuples with $k_1 \geq k_2 \geq \cdots \geq k_M$ with the introduction of a scaling factor that counts the number of permutations. This scaling factor depends on how distinct the entries of the tuple are. If all the entries in a tuple $\vec{k}$ are distinct, then $\vec{k}$ has $M!$ permutations. If an entry k_i is repeated $r(k_i)$ times in $\vec{k}$, then every distinct permutation has $r(k_i)!$ copies. Then, the scaling factor with ordered indices is

$$N(\vec{k}) = \frac{M!}{\prod_i r(k_i)!}$$

where the product is taken over i for which k_i are distinct.

2.2 An Approximation to the Phase Noisy Envelope

In the previous sections, we have seen that the squared-envelope of a phase noisy sinusoid plays a critical role in the performance analysis of the incoherent IF reception of heterodyne FSK system. This squared-envelope is the random variable X defined in (2.9) which we repeat here for convenience:

$$X = \left|\int_0^1 e^{j\sqrt{\gamma}\psi(t)}\,dt\right|^2 \tag{2.27}$$

where we have removed the explicit argument γ for notational simplicity. Due to its importance in the performance analysis, the determination of the probability density of X, or equivalently its moment generating function, has received considerable attention. Foschini and his coworkers provided the first comprehensive treatment of this problem in [8] and [27]. We summarize their approach below, since it is directly related to our subsequent analysis.

Foschini et. al. expand the complex exponential into its power series and retain the first order γ terms. The resulting approximation, X_L, is linear in γ and is given by

$$X_L = 1 - \gamma \left[\int_0^1 \psi^2 \, dt - \left(\int_0^1 \psi \, dt \right)^2 \right] . \tag{2.28}$$

(We use the subscript L to emphasize the linear nature of this approximation.) The linear approximation X_L is in fact a lower bound to the phase noisy envelope X. This can be seen easily by rewriting (2.27) as a double integral, using the fact that X is real, and finally using $\cos x \geq 1 - x^2/2$.

When $\psi(t)$ is expanded in Fourier cosine series on $(0,1)$ one obtains [27]

$$X_L = 1 - \gamma \mathbf{z}^T D \mathbf{z} \tag{2.29}$$

where $\mathbf{z}$ is an infinite dimensional vector of independent, identically distributed Gaussian random variables with zero-mean and unit variance, and D is an infinite dimensional diagonal matrix with $d_{ii} = 1/(i\pi)^2$. Thus, $\mathbf{z}^T D \mathbf{z}$ is a compact notation for $\sum_{i=1}^{\infty} z_i^2/(i\pi)^2$. The basis used in obtaining (2.29) is not arbitrary. In fact, the basis $\cos(\pi n x), x \in (0,1), n = 0, 1, \ldots$ is a remarkable one. It is not the solution to the Karhunen-Loeve equation for $\psi(t)$. However, one can expand the derivative of $\psi(t)$, which is white and Gaussian, in the sine basis and integrate to get a complete expansion in the cosine basis augmented by the constant function. Since this augmentation does not destroy orthogonality (cosine's integrate to zero), one can use Parseval's theorem to obtain (2.29). Humblet recently discovered that if a new random process is defined from $\psi(t)$ as $y(t) = \psi(t) - \int_0^1 \psi(\tau) \, d\tau$, this cosine basis is the solution to the Karhunen-Loeve equation for the new process [28, 29].

The moment generating function of X_L is then found as [27]

$$M_{X_L}(s) \triangleq E\left(e^{sX_L}\right) = e^s \prod_{k=1}^{\infty} \left(1 + \frac{2\gamma s}{k^2 \pi^2}\right)^{-1/2} = e^s \sqrt{\frac{\sqrt{2\gamma s}}{\sinh \sqrt{2\gamma s}}} \quad \mathrm{Re}(s) > -\frac{\pi^2}{2\gamma} \tag{2.30}$$

and is inverse Laplace-transformed to obtain the density function of X in semi-closed form.

Equation (2.30) can be used in conjunction with (2.11) to obtain the error probability for the single sample receiver with the linear approximation. The result is obtained as

$$P_e = \begin{cases} \frac{1}{2} e^{-\xi/2} \left(\sqrt{\xi\gamma} / \sin \sqrt{\xi\gamma} \right)^{1/2} & \xi\gamma < \pi^2 \\ \infty & \xi\gamma \geq \pi^2 \end{cases} \tag{2.31}$$

where the first case follows via $\sinh(jx) = j\sin(x)$, while the second case follows from the derivation of (2.30) in [27]. It is seen that this approximation fails to give sensible results at high SNR values. This is due to the fact that although X can take values only between 0 and 1, X_L can become negative. In fact, the density of X_L has a nonzero tail for negative arguments, which becomes increasingly dominant as γ increases. According to (2.31), this negative tail of the density function $p_{X_L}(x)$ decays exponentially, as $\exp(\pi^2 x/2\gamma)$ for $x < 0$, so that when $\xi > \pi^2/\gamma$ the integral of $e^{-\xi x/2}p_{X_L}(x)$ diverges. This problem is not observed in the numerical results of [8] due to the truncation of the negative tail of the probability density function. The linear approximation gives a loose upper bound to the error probability without the truncation, and it is not clear how tight the results become with the truncation.

We seek a better approximation to the random variable X by forcing the range of the approximate random variable, say $\bar{X}$, to match the range of X, namely $(0, 1)$. Therefore we require a good approximation to satisfy

1. $O \leq \bar{X}(\gamma) \leq 1$ for all $\gamma \geq 0$ and all Brownian sample paths $\psi(t)$,

2. $\bar{X}(\gamma)$ and $X(\gamma)$ match to the first order in γ for all $\psi(t)$.

The range constraint above suggests that $\bar{X}(\gamma)$ can be written as

$$\bar{X}(\gamma) = \exp\left[-G(\sqrt{\gamma}\psi)\right]$$

where G is a functional whose domain is the set of functions defined on $[0, 1]$ which vanish at 0, and whose range is $[0, \infty)$. We force G to satisfy

1. $G(f) \geq 0$ for all $f(t)$, with equality if and only if $f(t) \equiv 0$

2. $G(f) = G(-f)$ for all $f(t)$,

where the second property is due to the fact that the two sample paths $\psi(t)$ and $-\psi(t)$ result in the same value of $X(\gamma)$. For $X(\gamma)$ and $\bar{X}(\gamma)$ to be identical to the first order in γ, $X(0) = \bar{X}(0)$ and $\bar{X}'(0) = X'(0)$ must be satisfied. where 'prime' denotes the first derivative with respect to γ. We state one functional $G(f)$ that satisfies these requirements in the following lemma.

Lemma 2.1 *If* $G(f) = \int_0^1 f^2\,dt - \left(\int_0^1 f\,dt\right)^2$, *then* $X(\gamma)$ *and* $\bar{X}(\gamma)$ *are identical to the first order in* γ.

Proof. Since $X(0) = 1$, $G(0) = 0$ is needed for $X(0) = \bar{X}(0)$. On the other hand, it is straightforward, but somewhat lengthy, to show that

$$X'(0) = \left(\int_0^1 \psi \, dt\right)^2 - \int_0^1 \psi^2 \, dt \, .$$

For a G that satisfies $G(0) = 0$,

$$\bar{X}'(0) = -\frac{\partial G(\sqrt{\gamma}\psi)}{\partial \gamma}|_{\gamma=0} \, .$$

It is easily seen that the functional given in the statement of the lemma satisfies both of the requirements. □

Note that the functional of the Lemma 2.1 satisfies the positivity and evenness conditions as well. Therefore the random variable X_E defined as

$$X_E(\gamma) \stackrel{\triangle}{=} \exp(-\gamma \mathbf{z}^T D \mathbf{z}) \tag{2.32}$$

with $\mathbf{z}$ and D as defined previously, promises to be a good approximation to X. We use the subscript E to denote the exponential nature of this approximation.

To summarize, we have obtained an approximation that retains the desirable feature of that of Foschini et. al. while having the additional feature that it takes values that are in the same range as the original random variable. However, the exponential approximation does not provide a lower bound to the phase noisy envelope. Therefore our performance results will not be upper bounds to the exact performance.

A nice property of the random variable X_E is that its moments are easily obtained from (2.30) as

$$\begin{aligned} \mu(t) &\stackrel{\triangle}{=} E(X_E^t) \\ &= \sqrt{\frac{\sqrt{2\gamma t}}{\sinh(\sqrt{2\gamma t})}} \end{aligned} \tag{2.33}$$

for all real $t \geq -\pi^2/2\gamma$. For $t \leq -\pi^2/2\gamma$, the t'th moment of X_E is infinite.

An indication of how well the two approximations model X is the behavior of the first two moments as γ varies. The moments of X_E are already found in (2.33). We now evaluate the first two moments of X. Rewriting (2.27) as a double integral and taking the expectation

we obtain

$$E(X) = \int_0^1 \int_0^1 E\left\{\exp\left[j\sqrt{\gamma}\left(\psi(t) - \psi(s)\right)\right]\right\} dt\, ds\ .$$

Now we use the fact that $\sqrt{\gamma}\left(\psi(t) - \psi(s)\right)$ is Gaussian with zero-mean and variance $\gamma\,|t-s|$ and get

$$\begin{aligned} E(X) &= \int_0^1 \int_0^1 \exp\left(-\gamma\,|t-s|\,/2\right) dt\, ds \\ &= \frac{4}{\gamma}\left[1 - \frac{2}{\gamma}\left(1 - e^{-\gamma/2}\right)\right]\ . \end{aligned} \tag{2.34}$$

The calculation of $E\left(X^2\right)$ follows along the same lines: we first express X^2 as a four-fold integral, take the expectation and express the integrand as a Gaussian characteristic function while observing the dependencies of the random variables. We finally obtain

$$E\left(X^2\right) = \frac{16}{\gamma^2}\left[2 - \frac{15}{\gamma} + \frac{87}{2\gamma^2} - \left(\frac{20}{3\gamma} + \frac{392}{9\gamma^2}\right)e^{-\gamma/2} + \frac{1}{18\gamma^2}e^{-2\gamma}\right]\ . \tag{2.35}$$

The first two moments of X as given by Equations (2.34) and (2.35) are in agreement with previous calculations of the mean and the variance in [23] and [14].

Finally we calculate the first two moments of X_L (without truncation). The first moment is obtained as

$$\begin{aligned} E\left(X_L\right) &= 1 - \gamma E\left(\mathbf{z}^T D \mathbf{z}\right) \\ &= 1 - \gamma \sum_{n=1}^{\infty} \frac{1}{(n\pi)^2} \\ &= 1 - \frac{\gamma}{6} \end{aligned} \tag{2.36}$$

and the second moment is obtained as

$$\begin{aligned} E\left({X_L}^2\right) &= 1 - 2\gamma E\left(\mathbf{z}^T D \mathbf{z}\right) + \gamma^2 E\left((\mathbf{z}^T D \mathbf{z})^2\right) \\ &= 1 - 2\gamma \sum_{n=1}^{\infty} \frac{1}{(n\pi)^2} + \gamma^2 \sum_{n=1}^{\infty}\sum_{m=1}^{\infty} \frac{E(z_n^2\, z_m^2)}{(n\pi)^2 (m\pi)^2} \\ &= 1 - \frac{\gamma}{3} + \gamma^2 \sum_{n=1}^{\infty} \frac{3}{(n\pi)^4} + \gamma^2 \sum_{n\neq m}\sum_{m=1}^{\infty} \frac{1}{(n\pi)^2}\frac{1}{(m\pi)^2} \\ &= 1 - \frac{\gamma}{3} + \frac{\gamma^2}{20} \end{aligned} \tag{2.37}$$

where we have used $E(z_n^4) = 3$ and $\sum_{n=1}^{\infty} n^{-4} = \pi^4/90$ [30]. The first two moments of X, X_E and X_L as given by Equations (2.33)-(2.37) are shown in Figure 2-5 as functions of γ. It can be seen from the figure that the moments of X_L agree with those of the actual random variable X only for very small γ while the moments of X_E are very close to the actual moments for all γ. Therefore we expect the exponential approximation to be an accurate one.

2.3 Density of X_E

The moments of X_E as given by (2.33) provides complete information about its statistical behavior. In principle, one could compute the moment generating function of X_E from the moments $\{\mu(n)\}$ as

$$F(s) \triangleq E\left(e^{-sX_E}\right) = \sum_{n=0}^{\infty} \frac{(-s)^n}{n!}\mu(n)$$

and find the density function as the inverse-Laplace transform. However, since the series above is slowly converging, especially for large s, this is not a computationally attractive approach. Instead, we use an indirect approach which is based on orthogonal polynomials for finding the density. We first prove the following about the value of the density function at the origin.

Lemma 2.2 *Let $q(x)$ denote the probability density function of X_E. Then $q(0)$ has the following property:*

$$q(0) = \begin{cases} 0 & \text{if } \gamma < \pi^2/2 \\ \infty & \text{if } \gamma > \pi^2/2\,. \end{cases} \tag{2.38}$$

Proof. We prove the first part of the lemma by using Chernoff bound [31]. We have

$$q(0) = \lim_{\epsilon \to 0} \frac{1}{\epsilon} \Pr\left(0 \le X_E < \epsilon\right)\,.$$

From the definition of X_E the probability above is

$$Pr\left(0 \le X_E < \epsilon\right) = \Pr\left(\mathbf{z}^T D\mathbf{z} > -\frac{1}{\gamma}\ln\epsilon\right)\,.$$

We now bound the right hand side by using the Chernoff bound on $\mathbf{z}^T D\mathbf{z}$ via (2.33) to obtain

$$Pr\left(0 \le X_E < \epsilon\right) \le \epsilon^{s/\gamma}\left(\frac{\sqrt{2s}}{\sin(\sqrt{2s})}\right)^{1/2} \quad \text{for } 0 \le s \le \pi^2/2\,.$$

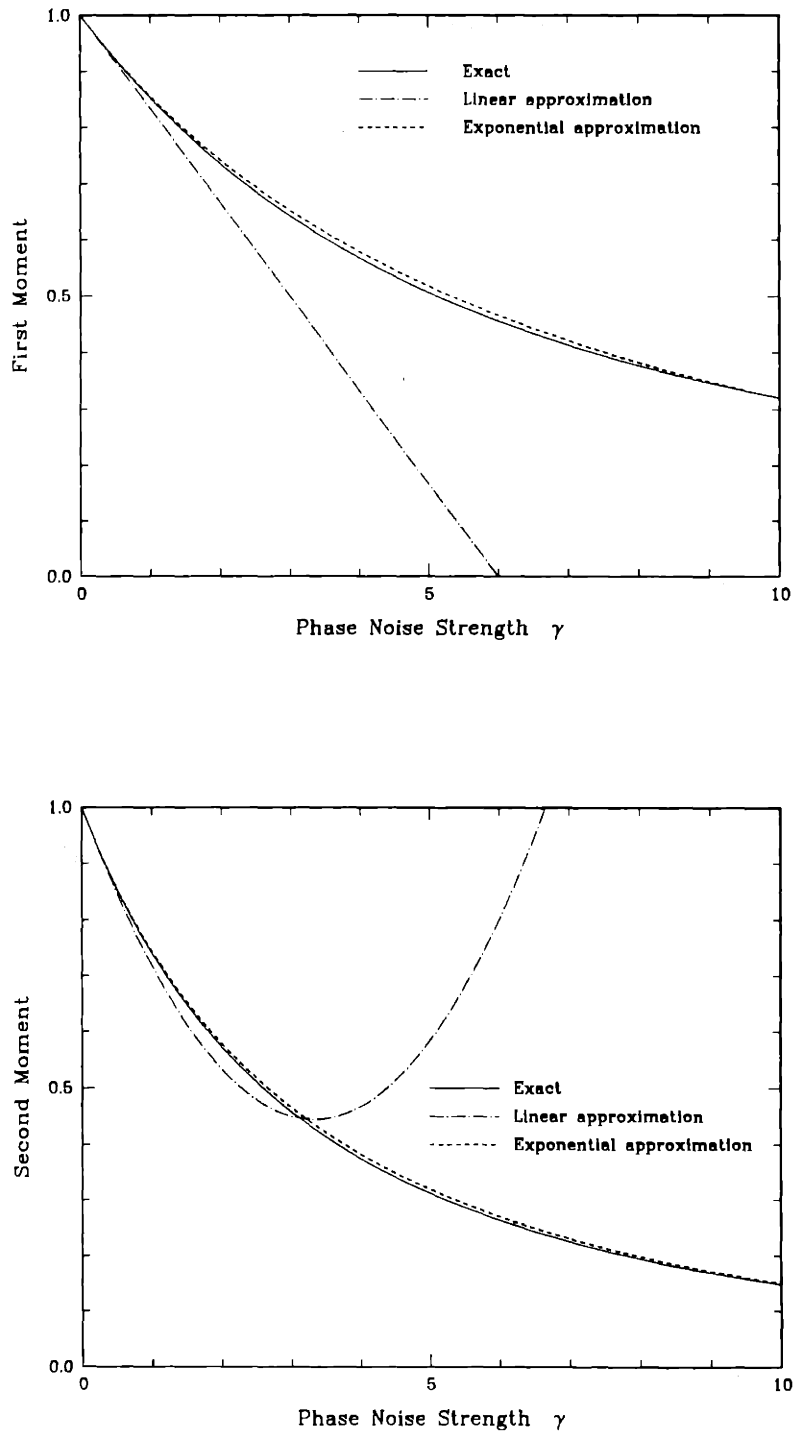

Figure 2-5: Comparison of means and second moments of the actual envelope and its linear and exponential approximations.

Dividing both sides by ϵ and taking the limit we obtain

$$q(0) \leq \lim_{\epsilon \to 0} \epsilon^{s/\gamma - 1} \left(\frac{\sqrt{2s}}{\sin(\sqrt{2s})} \right)^{1/2} \quad \text{for } 0 \leq s \leq \pi^2/2 \, .$$

The limit above is 0 if $s/\gamma > 1$, which is possible for some s in the allowed range if $\gamma < \pi^2/2$. Since $q(x) \geq 0$, $q(0) = 0$.

For the second part of the proof, we use the fact that each of the random variables in the series of $\mathbf{z}^T D \mathbf{z}$ are nonnegative to obtain the following lower bound.

$$Pr\,(0 \leq X_E < \epsilon) = \Pr\left(\mathbf{z}^T D \mathbf{z} > -\frac{1}{\gamma} \ln \epsilon \right) \geq \Pr\left(\frac{1}{\pi^2} z_1^2 > -\frac{1}{\gamma} \ln \epsilon \right) \, .$$

The rightmost probability is $2Q(\sqrt{-\pi^2 \ln \epsilon / \gamma})$ where $Q(x)$ is the complementary distribution function for the unit normal random variable. Proceeding as before we obtain

$$q(0) \geq \lim_{\epsilon \to 0} \frac{2}{\epsilon} Q\left(\sqrt{-\frac{\pi^2}{\gamma} \ln \epsilon} \right) \, .$$

Finally we use $Q(x) \sim \frac{1}{\sqrt{2\pi}x} e^{-x^2/2}$ as $x \to \infty$ [15] to obtain

$$q(0) \geq \sqrt{\frac{2\gamma}{\pi^3}} \lim_{\epsilon \to 0} \frac{\epsilon^{\pi^2/2\gamma - 1}}{\sqrt{-\ln \epsilon}} \, .$$

The limit above is infinite if $\gamma > \pi^2/2$, this completes the proof. □

The lemma above indicates that the density of X_E changes its form as γ exceeds a critical value, $\pi^2/2$. The left tail of the density, i.e. $q(x)$ for small x, strongly affects the probability of error, since P_e is the integral of the product of $q(x)$ (or convolution of $q(x)$ with itself) and some rapidly decaying function such as $e^{-\xi x/2}$. Therefore the behavior of $q(x)$ for $x \ll 1$ is of special interest for accurate calculation of error probability. The following lemma indicates that this behavior is polynomial.

Lemma 2.3 $q(x) = O\left(x^{\frac{\pi^2}{2\gamma} - 1} \right)$ *for* x *small, where* $f(x) = O\,(g(x))$ *is equivalent to* $\lim_{x \to 0} f(x)/g(x) = c$ *for a positive finite* c.

Proof. From (2.33) we have

$$\int_0^1 x^t q(x)\,dx = \begin{cases} (\sqrt{2\gamma t}/\sinh(\sqrt{2\gamma t}))^{1/2} & t > 0 \\ \left(\sqrt{2\gamma|t|}/\sin(\sqrt{2\gamma|t|})\right)^{1/2} & 0 > t > -\pi^2/2\gamma \\ \infty & t < -\pi^2/2\gamma\ . \end{cases}$$

Since $\int_0^\delta x^{-\beta}\,dx$ converges for $\beta < 1$ and diverges for $\beta \geq 1$ for any $\delta > 0$, we must have

$$x^{-\frac{\pi^2}{2\gamma}} q(x) = c(x)\frac{1}{x}$$

for some function $c(x)$ with finite and positive $c(0)$, where we have assumed that $q(x)$ is continuous at $x = 0$. Then the claim is proved. □

This lemma is in agreement with the previous lemma in predicting the value of $q(0)$. Moreover, it suggests that for accurate calculation of $q(x)$ for small x it is better to calculate the tilted density $q(x)/x^{\frac{\pi^2}{2\gamma}-1}$. Before we describe a method to perform this calculation, we exploit a useful property of $X_E(\gamma)$ that will enable us to compute the density function for a single value of γ, say $\gamma = 1$, and to obtain all other density functions from this computed one. From the definition of $X_E(\gamma)$ we have

$$X_E(\gamma)^{1/\gamma} = e^{-\mathbf{z}^T D \mathbf{z}}\ .$$

Then for any positive γ_1 and γ_2, the associated X_E's satisfy

$$X_E(\gamma_1)^{1/\gamma_1} = X_E(\gamma_2)^{1/\gamma_2}$$

which specifies a one-to-one mapping from $X_E(\gamma_1)$ to $X_E(\gamma_2)$ via

$$g(x) = x^{\gamma_2/\gamma_1}\ .$$

Then the densities of the two random variables are related via [32]

$$q_{\gamma_2}(x) = \frac{q_{\gamma_1}\left(g^{-1}(x)\right)}{|g'\left(g^{-1}(x)\right)|}$$

where we introduced a subscript to the density function to emphasize its dependence on γ. Upon manipulation, we obtain

$$q_{\gamma_2}(x) = \alpha x^{\alpha-1} q_{\gamma_1}(x^\alpha) \tag{2.39}$$

where $\alpha = \gamma_1/\gamma_2$.

The calculation of $q(x)$ for a given γ, as will be seen shortly, is a computationally intensive effort. Therefore the simple relation (2.39) introduces a big saving in the required numerical work.

The moments of a random variable are the projections of its density function on a sequence of polynomials. Therefore, the density can be reconstructed from these moments via a complete orthonormal polynomial basis. The even (or odd) indexed Legendre polynomials constitute such a basis on the interval $(0,1)$ [33]. Any piecewise continuous function $f(x)$ on $(0,1)$ that has left and right derivatives at every point in the interval can be expressed as

$$f(x) = \sum_{\substack{n=0 \\ n \text{ even}}}^{\infty} (2n+1) F_n P_n(x) \tag{2.40}$$

where $P_n(x)$ is the n'th Legendre polynomial and F_n is given by

$$F_n = \int_0^1 f(x) P_n(x)\, dx \,. \tag{2.41}$$

Specializing to the case of

$$f(x) = \frac{q(x)}{x^h}$$

where we have defined

$$h \triangleq \frac{\pi^2}{2\gamma} - 1$$

we obtain

$$F_n = E\left[X_E^{-h} P_n(X_E)\right] \,. \tag{2.42}$$

To obtain the coefficients F_n in terms of the moments, we first expand $P_n(x)$ in its Taylor series as [33]

$$P_n(x) = \sum_{\substack{k=0 \\ k \text{ even}}}^{n} a_{nk} x^k \tag{2.43}$$

where the coefficients a_{nk} are given by

$$a_{nk} = \frac{1}{2^n}(-1)^{(n-k)/2}\binom{n}{(n-k)/2}\binom{n+k}{k} . \tag{2.44}$$

Now we can compute the expectation in (2.42) in terms of the moments given by (2.33) as

$$F_n = \sum_{\substack{k=0 \\ k \text{ even}}}^{n} a_{nk}\mu(k-h) \tag{2.45}$$

and, consequently, the density function as

$$q(x) = x^h \sum_{\substack{n=0 \\ n \text{ even}}}^{\infty} (2n+1)P_n(x) \sum_{\substack{k=0 \\ k \text{ even}}}^{n} a_{nk}\mu(k-h) . \tag{2.46}$$

The convergence of the series in (2.46) is quite fast. Note that the moments always remain finite since $k - h > -\pi^2/2\gamma$ for all $k \geq 0$. It is also worth mentioning that although the formula above remains valid for any value of h, in particular for $h = 0$ which corresponds to the direct computation of $q(x)$ without tilting, the value that we use is the most appropriate one because it captures the polynomial behavior of $q(x)$ in the small x region.

The results of the computation is shown in Figure 2-6 for various γ values. As expected the density is more concentrated around unity for small γ. As γ increases, the density gets flat until $\gamma = \pi^2/2$, and becomes peaked at $x = 0$ thereafter. The density function is observed to have a sharp decay around its $x = 1$ tail. In Appendix 2.C, we show that the nature of this decay is exponential in $\gamma/(1-x)$, provided that $q(x)$ is bounded and non-oscillatory.

The density function of X_E can also be calculated with another method. The distribution function of the random variable $\mathbf{z}^T D\mathbf{z}$ is given in [8], from which the distribution function of X_E can be directly computed, the density function is then obtained by differentiation. It was observed that this method yields results which are in perfect agreement with Figure 2-6.

In the next section, we will use the density we have obtained to evaluate the performance of the receivers under consideration.

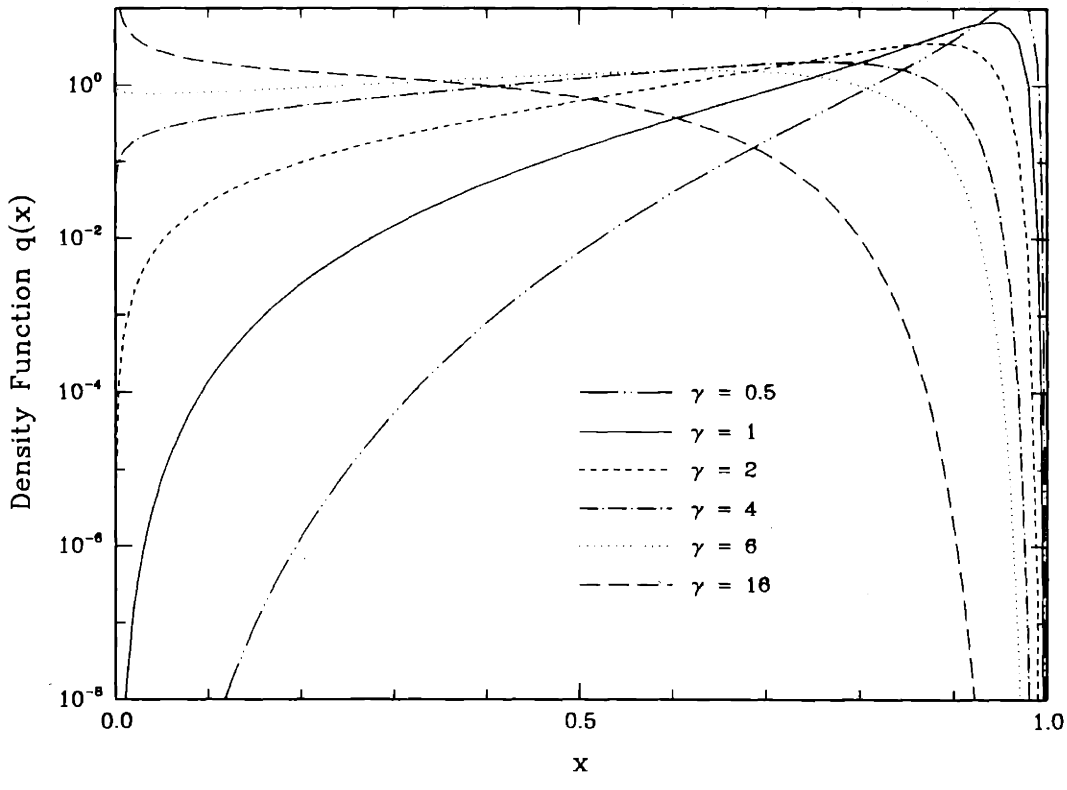

Figure 2-6: Probability density function $q(x)$ for various γ values.

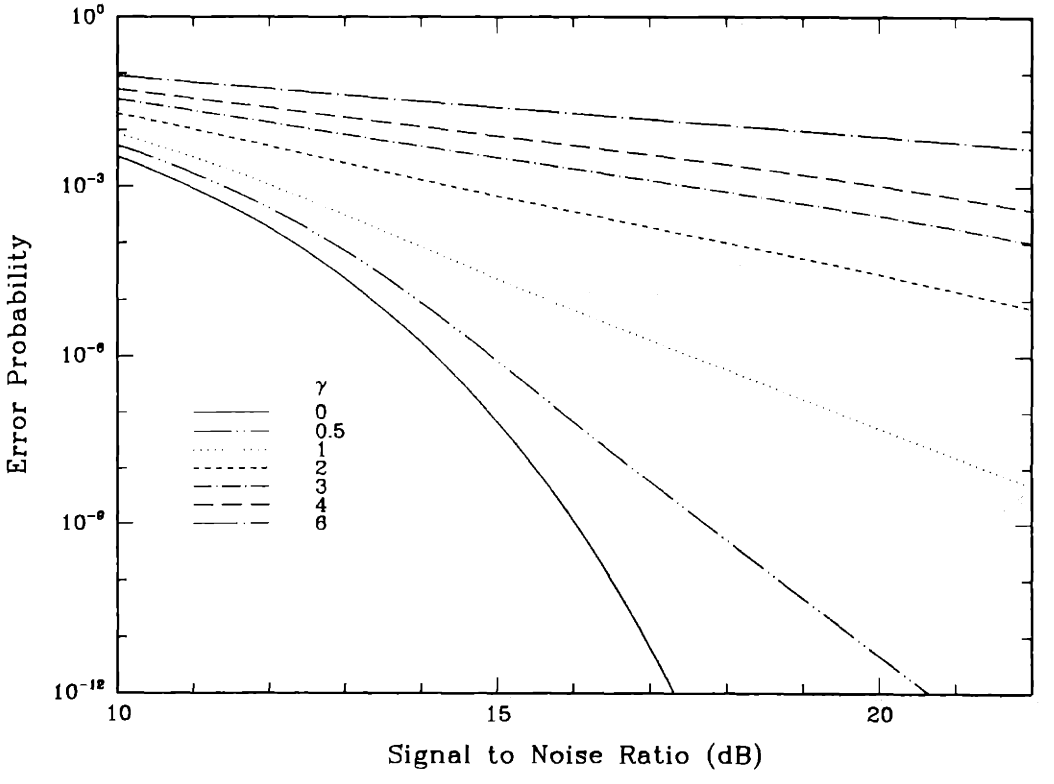

Figure 2-7: Error probability of single sample receiver as a function of signal to noise ratio.

2.4 Results and Discussion

The error probability for the single sample receiver is given by (2.11) as

$$P_e = \frac{1}{2}\int_0^1 e^{-\xi x/2} q_\gamma(x)\, dx\ .$$

We have computed the error probability using this integral. The result of this computation is shown in Figure 2-7. It is seen from this figure that the error probability is above 10^{-4} for $\gamma \geq 2$ and $\xi \leq 22$ dB. The single sample receiver cannot combat the phase noise effectively for large γ, and the bit error rate severely degrades with increasing phase noise strength.

The error probability calculation is more involved for the multisample receivers. For the

single-filter receiver, the error probability is given by (2.12) which can be written as

$$P_e = \frac{1}{2}\int_0^1 \exp(-\xi x/2M) q_{\gamma/M}(x)\, dx\ . \tag{2.47}$$

Using (2.39) with $\gamma_1 = \gamma$ and $\gamma_2 = \gamma/M$, we can rewrite (2.47) as

$$P_e = \frac{1}{2}\int_0^1 \exp(-\xi x/2M) M x^{M-1} q_{\gamma}(x^M)\, dx$$

which with the change of variable $y = x^M$ yields

$$P_e = \frac{1}{2}\int_0^1 \exp(-\xi y^{1/M}/2M) q_{\gamma}(y)\, dy\ . \tag{2.48}$$

We want to find the value of M that minimizes (2.48). Since no closed form for $q(\cdot)$ is available, this optimization involves evaluating this equation for $M = 1, 2, 3, \ldots$ until the optimum is reached[5]. Equation (2.48) has the desired form since the density function has the same parameter γ for all M.

The result of the computation of the bit error rate via (2.48) is shown in Figure 2-8. The plotted bit error rate values have been optimized over M. The optimal value of M increases with SNR and the phase noise strength. This is because as the SNR increases the receiver prefers to use a smaller portion of signal energy to reduce the effect of the phase noise with the same factor.

Finally we focus on the performance of the double filter multisampling receiver. In Section 2.1.2, we showed that the bit error rate for this receiver can be computed by first finding the M-fold convolution of the density function of $X(\gamma/M)$ and then removing the conditioning on r in Equation (2.19). However, the density function, $q_{\gamma/M}(x)$, changes with M, thus this method is computationally prohibitive. Therefore, we use the alternative approach which resulted in Equations (2.25) and (2.26). One can further reduce the complexity by expressing $\alpha(k)$ in terms of $q_\gamma(x)$ as follows:

$$\begin{aligned}\alpha(k) &= \int_0^1 x^k \exp(-\xi x/2M) q_{\gamma/M}(x)\, dx \\ &= \int_0^1 y^{k/M} \exp(-\xi y^{1/M}/2M) q_{\gamma}(y)\, dy\ .\end{aligned} \tag{2.49}$$

[5] In fact, we could search for optimal non-integer M for the single-filter receiver. This does not seem to be necessary since the observed transitions with integer values were smooth.

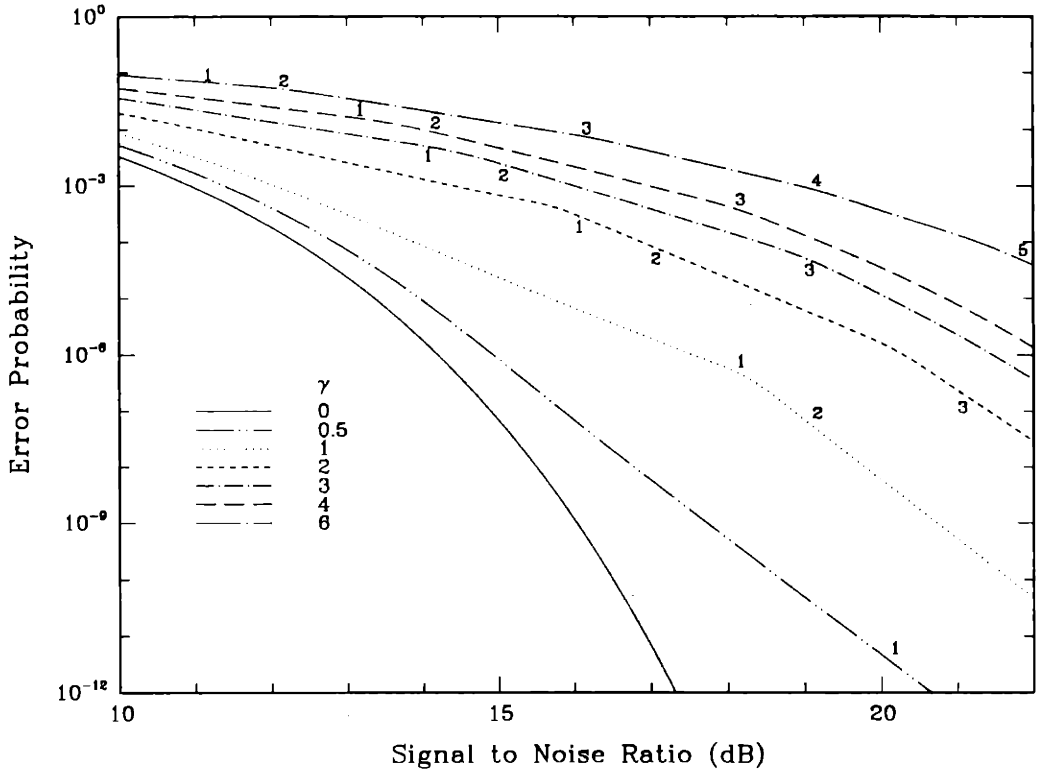

Figure 2-8: Error probability of multisample single-filter receiver as a function of signal to noise ratio. Optimal values of M are also shown.

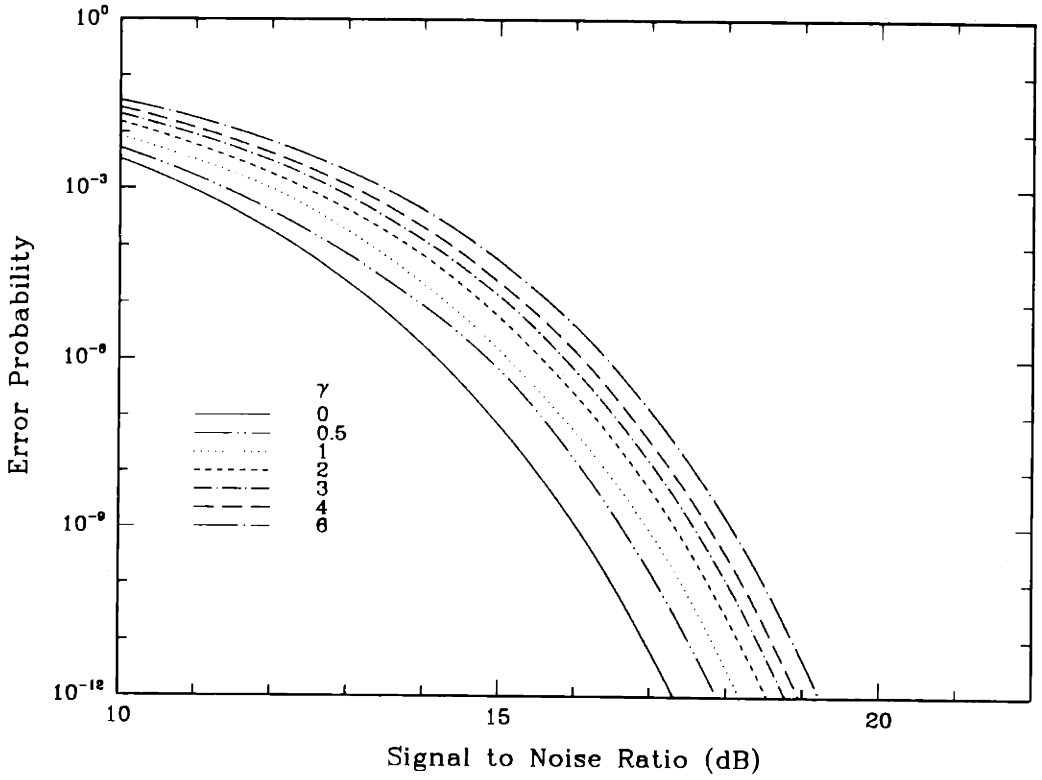

Figure 2-9: Error probability of multisample double-filter receiver as a function of signal to noise ratio.

where we have used the same transformation used in obtaining (2.48).

Equation (2.25) in conjunction with (2.49) provides a method for the error probability computation. In performing the numerical computation the symmetry between the terms in the inner summation was exploited as outlined in Section 2.1.2. The resulting computation is a very efficient one in comparison with the direct convolutions. The results are shown in Figure 2-9. The bit error rates are again optimized with respect to M as in the single filter case. A comparison of the performance curves for the single sample receiver and multisample receiver with and without double filtering reveals that the increased receiver complexity by oversampling the signal and additional lowpass filtering may improve the error performance to a significant extent when the signal-to-noise ratio is high and the phase noise is strong. This can be seen from Figure 2-10 which shows the performance of the three receivers for $\gamma = 1$ and $\gamma = 4$. For low SNR values (up to 12 dB for $\gamma = 1$ and 9 dB for $\gamma = 4$), the

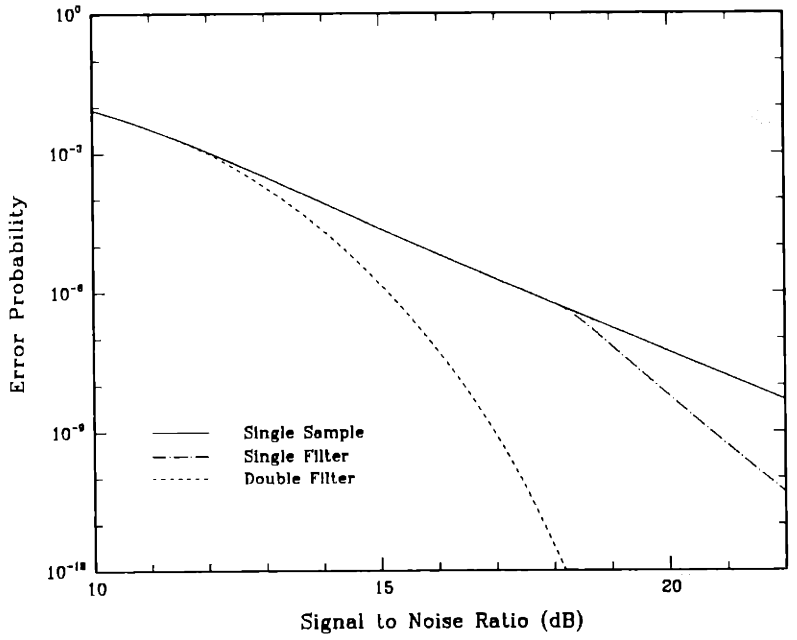

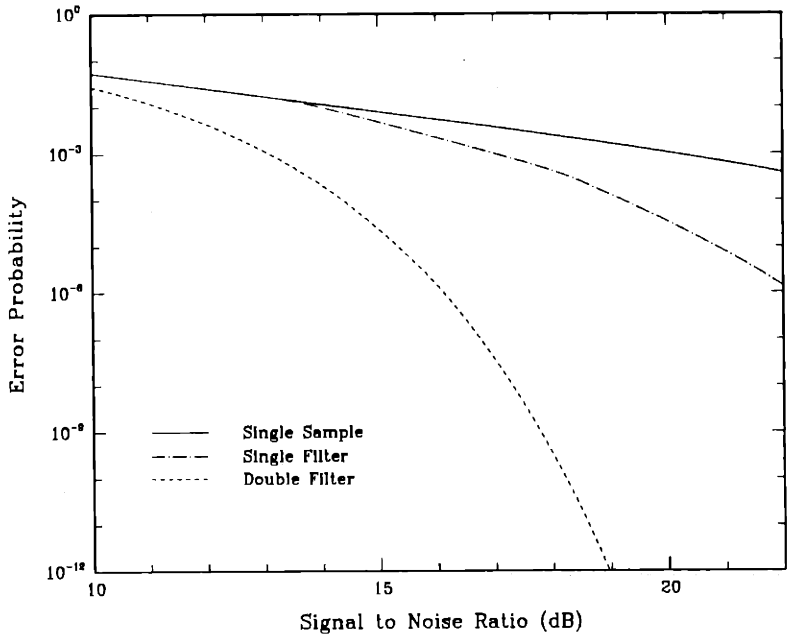

Figure 2-10: Comparison of bit error performances of the three receivers under consideration for $\gamma = 1$ and $\gamma = 4$.

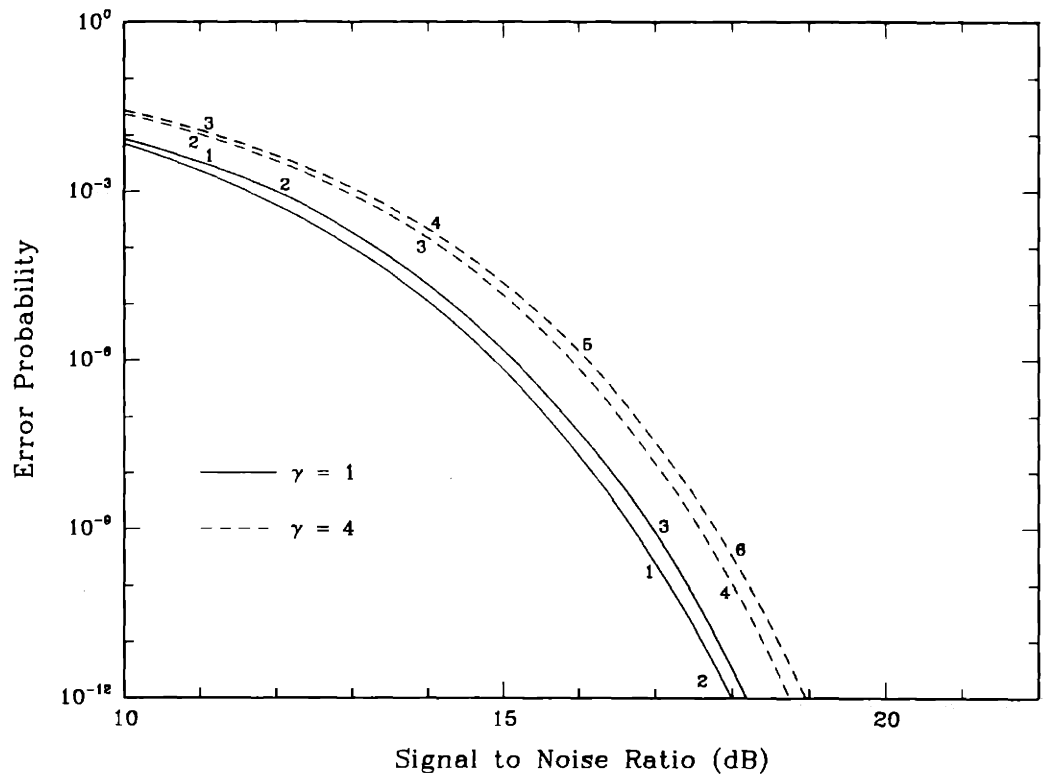

Figure 2-11: Error probability of multisample double-filter receiver together with its lower bound for $\gamma = 1$ and $\gamma = 4$. Optimal values of M are also shown.

best receiver is the simplest one, i.e. the optimal value for the multisampling receivers is $M = 1$. Only when the SNR is further increased, an increase in the receiver complexity is warranted. At a bit error rate of 10^{-9} with $\gamma = 1$, the double filter receiver has about 3.5 dB gain over multisample single-filter receiver and about 6 dB gain over the single sample receiver.

The error probability for the double filter receiver is very close to the lower bound obtained in Section 2.1.2, as illustrated by Figure 2-11 for $\gamma = 1$ and $\gamma = 4$. Therefore the simple lower bound expression

$$P_e \simeq P_e\left(\xi\frac{4M}{\gamma}\left[1-\frac{2M}{\gamma}(1-e^{-\gamma/2M})\right]\right) \tag{2.50}$$

in conjunction with (2.19) provides a simple and reliable approximation to the probability

of error. With the use of this closed-form result, the performance of a system with a given SNR and phase noise strength can be found by a straightforward optimization over M. It should be noted that the value of M that optimizes (2.50) is, in general, lower than the exact optimal value. This is due to the fact that the variation of r from its mean is neglected in the Jensen's bound that results in (2.50).

Since the phase noisy SNR r in (2.20) is the average of M i.i.d. random variables, a Gaussian approximation for large SNR and phase noise strength is also plausible. In fact, approximating the density of r with a Gaussian density on the interval $(0, \xi)$ yields an error probability which is very close to that shown in Figure 2-9. However, a closed-form result that is obtained by extending the range to the real line yields a poor estimate due to the large negative tail of $P_e(r)$.

The performance of the double-filter receiver as predicted by Figure 2-9 and approximated by Equation (2.50) is very close to that predicted by Foschini and his coworkers in [8]. This is because the truncated density tail of the linear approximation to the phase-noisy envelope is extremely low for a phase noise strength of γ/M, when M is around the optimal value. This is in contrast with the single-filter case where the agreement of our results with [8] is not as strong due to smaller values for the optimal value of M.

The signal-to-noise ratio needed to remain below a certain predetermined bit error rate increases with the introduction of phase noise. The amount of increase in the SNR is referred to as *phase noise penalty.* In Figure 2-12 the penalties for the three receivers are shown as a function of γ for a bit error rate of 10^{-9}. While the difference in the penalties for the single sample receiver and the multisample double-filter receiver is less than 1 dB for $\gamma \leq 0.5$, the latter receiver outperforms the former at higher phase noise strengths. This is in support of increased receiver complexity that is tailored towards combating the phase noise especially when $\gamma > 1$.

Advancing optical technology promises fiber-optic networks with data rates in excess of 100 Mbps per user and semiconductor lasers with linewidths of 5 MHz or less. With these parameters, the phase noise strength γ is in the range of 0.6 for which the penalty is about 1 dB with the double filter receiver and 2 dB with the single sample receiver. This means not only that the phase noise will not be a very significant impairment on the bit error rate, but also that simple IF receivers will be sufficient for most future applications.

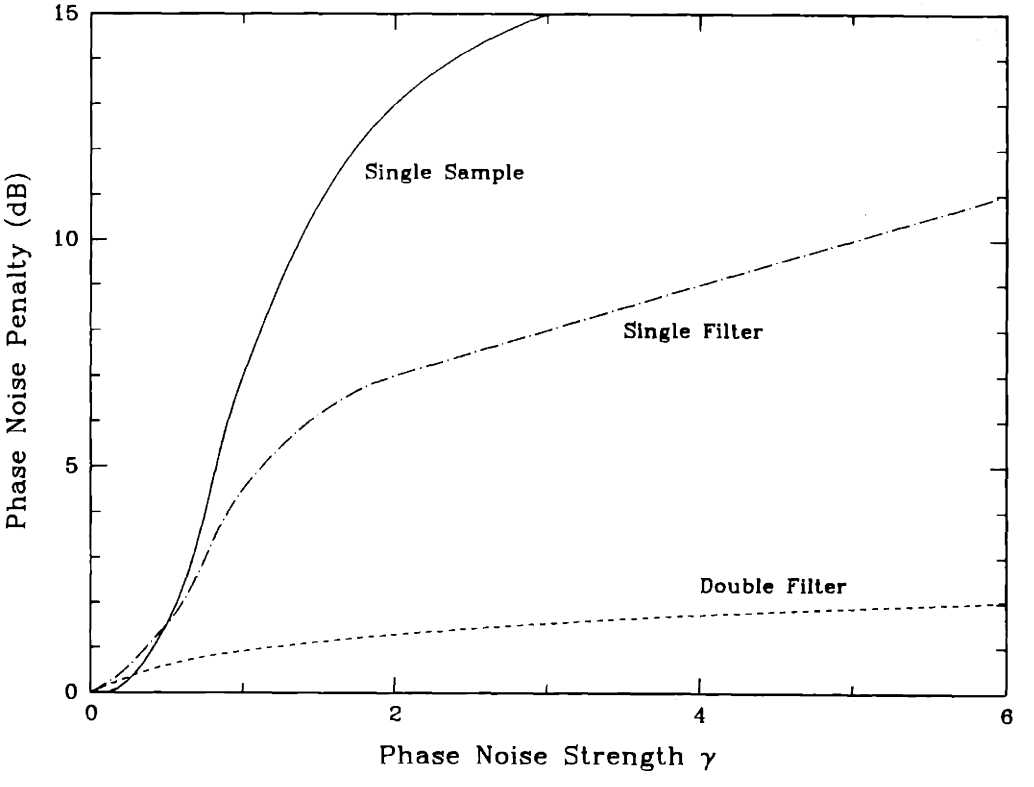

Figure 2-12: SNR penalty due to phase noise at a bit error rate of 10^{-9}.

2.5 Extension to N-FSK

The results of the previous sections about binary FSK can be extended to FSK with N hypotheses (N-FSK) without much difficulty. The receiver structure is the same as Figure 2-2 with the number of branches increased from 2 to N. We present an analysis to the performance of N-FSK below. It must be emphasized that we hold the transmission rate of data bits and the energy per data bit constant while making comparisons among different N-ary FSK schemes, as in [34].

Let the possible hypotheses be $0, 1, \ldots, N-1$. Let the normalized filter outputs be V_i, $i = 0, 1, \ldots, N-1$, and assume a "0" is transmitted. Then V_i will be independent random variables with the density functions found in Section 2.1 as

$$p(v_0|r) = \left(\frac{v_0}{r}\right)^{(M-1)/2} e^{-(v_0+r)} I_{M-1}\left(\sqrt{4rv_0}\right) \quad v_0 \geq 0 \tag{2.51}$$

$$p(v_i) = \frac{v_i^{M-1}}{(M-1)!} e^{-v_i} \quad v_i \geq 0 \quad i = 1, 2, \ldots, N-1\,. \tag{2.52}$$

Let $P_N(r)$ denote the probability of a symbol error conditioned on the phase-noisy SNR r. Since a symbol error will occur when any of the V_i for $i \neq 0$ is greater than V_0, we have

$$\begin{aligned} P_N(r) &= 1 - \Pr\left(V_0 \geq \max\{V_1, \ldots, V_{N-1}\}|r\right) \\ &= 1 - \int \left[\Pr(V_1 \leq v_0)\right]^{N-1} p(v_0|r)\, dv_0 \end{aligned}$$

where we have used the fact that V_i for $i \geq 1$ are i.i.d. conditioned on r. Then with the use of (2.52), we obtain

$$P_N(r) = 1 - \int \left[1 - \sum_{k=0}^{M-1} \frac{v_0^k}{k!} e^{-v_0}\right]^{N-1} p(v_0|r)\, dv_0$$

which does not seem to be easily brought to a closed-form similar to (2.19). Instead of computing $P_N(r)$ numerically we will find upper and lower bounds in closed-form. We first use $1 - (1-y)^{N-1} \leq (N-1)y$ for $0 \leq y \leq 1$, to obtain

$$P_N(r) \leq (N-1) \int \sum_{k=0}^{M-1} \frac{v_0^k}{k!} e^{-v_0} p(v_0|r)\, dv_0 = (N-1) P_2(r) \tag{2.53}$$

where $P_2(r)$ is the conditional error probability for binary FSK given by (2.19). The upper

bound in (2.53) is exactly the union bound. To obtain a lower bound to $P_N(r)$ we use

$$1-(1-y)^{N-1} \geq (N-1)y - \binom{N-1}{2} y^2$$

and we get

$$P_N(r) \geq (N-1)P_2(r) - \binom{N-1}{2} g_M(r)$$

where the function $g_M(r)$ is defined as

$$g_M(r) = \int \left(\sum_{k=0}^{M-1} \frac{v_0^k}{k!} e^{-v_0} \right)^2 p(v_0|r)\, dv_0 \,.$$

To obtain $g_M(r)$ in closed-form we first use

$$\begin{aligned} \left(\sum_{k=0}^{M-1} \frac{v_0^k}{k!} e^{-v_0} \right)^2 &= e^{-2v_0} \sum_{n=0}^{M-1} \sum_{m=0}^{M-1} \frac{v_0^{n+m}}{n!m!} \\ &= e^{-2v_0} \sum_{l=0}^{2(M-1)} \left[\frac{1}{l!} \sum_{k=0}^{\min(l,M-1)} \binom{l}{k} \right] v_0^l \end{aligned}$$

and we get

$$g_M(r) = \int e^{-2v_0} \sum_{l=0}^{2(M-1)} \frac{1}{l!} \beta_l v_0^l p(v_0|r)\, dv_0 \tag{2.54}$$

where we have defined

$$\beta_l \stackrel{\Delta}{=} \sum_{k=0}^{\min(l,M-1)} \binom{l}{k} . \tag{2.55}$$

We proceed exactly as in Appendix 2.A to evaluate the integral in (2.54) to obtain the result as

$$g_M(r) = \frac{e^{-2r/3}}{3^M} \sum_{n=0}^{2(M-1)} \frac{(r/3)^n}{n!} \sum_{l=n}^{2(M-1)} \binom{l+M-1}{l-n} \frac{\beta_l}{3^l} \tag{2.56}$$

which is quite similar to (2.19).

We finally have the bounds to the conditional error probability as

$$(N-1)P_2(r) - \binom{N-1}{2} g_M(r) \leq P_N(r) \leq (N-1)P_2(r) \tag{2.57}$$

in conjunction with Equations (2.19) and (2.56). Note that the two bounds are equal for $N = 2$. The bounds are tight for small N and large r. For $N \leq 16$ and $r \geq 14$ dB, the two bounds are within an order of magnitude for any M.

The symbol error probability P_N is obtained as the expected value of $P_N(r)$ optimized over M, i.e.

$$P_N = \min_M E_r \left[P_N(r) \right] .$$

Since only bounds to $P_N(r)$ are available in closed-form, we will perform the optimization for the upper bound and use the optimal value of M, say M^*, in the lower bound. The result is

$$(N-1)P_2 - \binom{N-1}{2} E_r \left[g_{M^*}(r) \right] \leq P_N \leq (N-1)P_2 \tag{2.58}$$

where P_2 is the binary FSK error probability found in the previous section. The bit error probability P_b is related to the symbol error probability as [25]

$$P_b = \frac{N/2}{N-1} P_N$$

which results in

$$\frac{N}{2} P_2 - \frac{N(N-2)}{4} E_r \left[g_{M^*}(r) \right] \leq P_b \leq \frac{N}{2} P_2 . \tag{2.59}$$

The upper bound to the actual bit error rate reveals that for N-FSK at a bit SNR value of ξ and a phase noise of γ is at most $N/2$ times the bit error rate of binary FSK at an SNR of $\xi \log_2 N$ and a phase noise strength of $\gamma \log_2 N$. The expectation in the lower bound can be computed without any convolutions, using the same method described in the previous section. Figure 2-13 shows the upper and lower bounds to P_b for $N = 4, 8, 16$ as well as the binary bit error rate for $\gamma = 1$. It is seen that the bounds are very close, and that the bit error rate improves with increasing N. At a bit error rate of 10^{-9} the improvement over binary FSK is 2.5 dB with $N = 4$, 4 dB with $N = 8$, and 4.8 dB with $N = 16$. Since the cost of the receiver and the bandwidth occupation are proportional to N, 4-FSK may be a desirable alternative to binary FSK for this value of phase-noise strength.

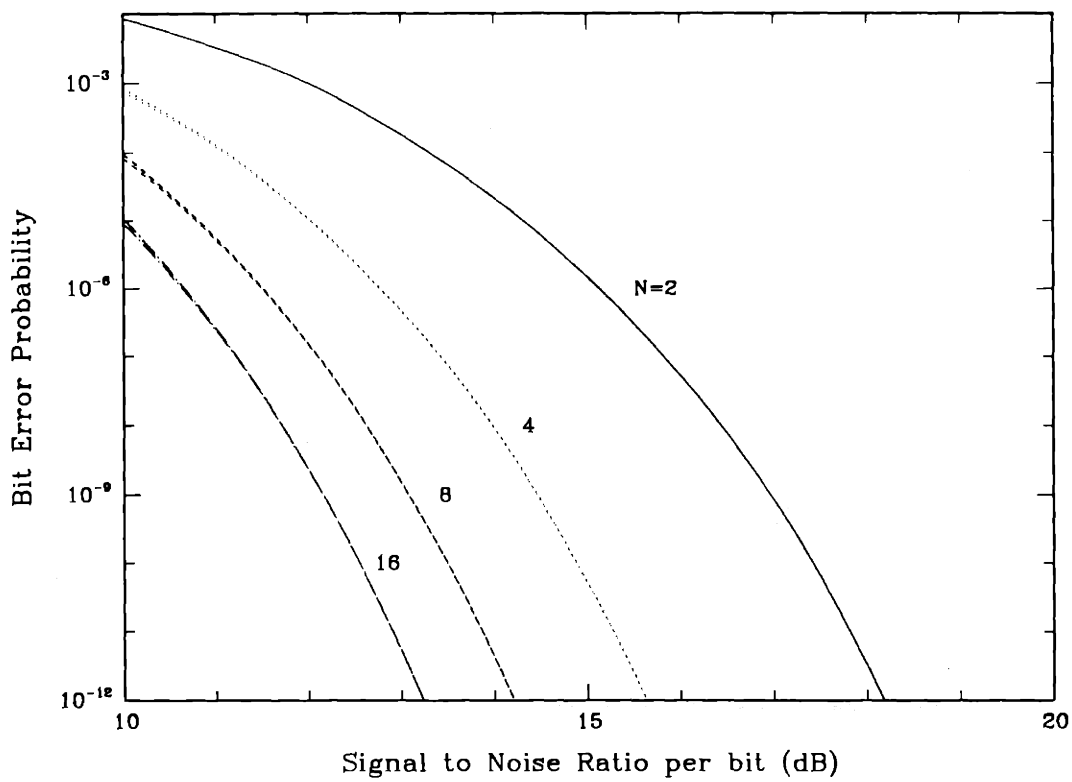

Figure 2-13: Upper and lower bounds to the bit error probability for N-FSK with $\gamma = 1$ and $N = 2, 4, 8, 16$.

Appendix

2.A Derivation of Conditional Error Probability for Double–Filter Receiver

In this appendix, we derive (2.19) which gives the error probability of the multisample double-filter receiver condition on phase-noisy signal-to-noise ratio r.

From (2.18) we have

$$P_e(r) = \sum_{k=0}^{M-1} E\left[\frac{V_0^k}{k!}e^{-V_0} \mid r\right] \tag{2.60}$$

where the expectation is taken with respect to the conditional probability density function given by (2.17). This can be performed by directly evaluating the density integral. It is simpler, however, to use a transform domain technique. The moment generating function of V_0 is given as [25]

$$\mu_M(s,r) \triangleq E\left(e^{-sV_0} \mid r\right) = \frac{1}{(1+s)^M}\exp\left(-\frac{sr}{1+s}\right) . \tag{2.61}$$

From (2.60) and (2.61) we have

$$P_e(r) = \sum_{k=0}^{M-1}\frac{(-1)^k}{k!}\left[\frac{\partial^k}{\partial s^k}\mu_M(s,r)\right]_{s=1} . \tag{2.62}$$

To simplify the notation in the following discussion, we introduce the following definition:

$$\mu_M^{(k)} \triangleq \frac{\partial^k}{\partial s^k}\mu_M(s,r)\mid_{s=1} .$$

The following lemma provides the intermediate result that will be used to obtain $P_e(r)$.

Lemma 2.4 *The derivatives $\mu_M^{(k)}$ are given by*

$$\mu_M^{(k)} = \frac{(-1)^k k!}{2^{M+k}}e^{-r/2}\sum_{i=0}^{k}\binom{M+k-1}{M+i-1}\frac{(r/2)^i}{i!} \tag{2.63}$$

for $k = 0, 1, \ldots, M-1$.

Proof. We will use induction on k. For $k = 0$, the claim is easily seen to be true with the

use of (2.61). Next we observe that

$$\frac{\partial}{\partial s}\mu_M(s,r) = -M\mu_{M+1}(s,r) - r\mu_{M+2}(s,r)$$

which implies

$$\mu_M^{(k+1)} = -M\mu_{M+1}^{(k)} - r\mu_{M+2}^{(k)} .$$

We now assume that the claim is true for k. Then by the last identity, we obtain

$$\mu_M^{(k+1)} = \frac{(-1)^{k+1}k!}{2^{M+k+1}}e^{-r/2}\sum_{i=0}^{k}\left[M\binom{M+k}{M+i} + \frac{r}{2}\binom{M+k+1}{M+i+1}\right]\frac{(r/2)^i}{i!}$$

We now split the series above into two, change the index in the second series, and obtain

$$\mu_M^{(k+1)} = \frac{(-1)^{k+1}k!}{2^{M+k+1}}e^{-r/2}\left[\sum_{i=0}^{k}M\binom{M+k}{M+i}\frac{(r/2)^i}{i!} + \sum_{i=1}^{k+1}i\binom{M+k+1}{M+i}\frac{(r/2)^i}{i!}\right]$$

We now isolate the $i = 0$ term in the first summation and $i = k+1$ term in the second summation, combine the remaining terms, and perform some straightforward manipulations to obtain

$$\mu_M^{(k+1)} = \frac{(-1)^{k+1}(k+1)!}{2^{M+k+1}}e^{-r/2}\sum_{i=0}^{k+1}\binom{M+k}{M+i-1}\frac{(r/2)^i}{i!}$$

as claimed. This concludes the proof. □

The lemma in conjunction with (2.62) results in

$$P_e(r) = \frac{e^{-r/2}}{2^M}\sum_{k=0}^{M-1}\frac{1}{2^k}\sum_{i=0}^{k}\binom{M+k-1}{M+i-1}\frac{(r/2)^i}{i!}$$

which upon interchange of summations yields

$$P_e(r) = \frac{e^{-r/2}}{2^M}\sum_{n=0}^{M-1}\frac{(r/2)^n}{n!}\sum_{k=n}^{M-1}\binom{M+k-1}{k-n}\frac{1}{2^k}$$

which is the equation given in (2.19).

2.B Convexity of Conditional Error Probability

In this appendix we prove that the error probability conditioned on phase-noisy SNR, $P_e(r)$, is a convex function of r [6]. From (2.19), we have

$$P_e(r) = \frac{e^{-r/2}}{2^M} \sum_{n=0}^{M-1} \frac{c_n(M-1)}{n!} \left(\frac{r}{2}\right)^n \tag{2.64}$$

where

$$c_n(M-1) = \sum_{k=n}^{M-1} \binom{k+M-1}{k-n} \frac{1}{2^k} . \tag{2.65}$$

Since the convexity of a function is not affected by multiplication by a positive constant and a scaling of its argument, it suffices to show the convexity of the function

$$h(r) = e^{-r} t(r)$$

where $t(r)$ is the polynomial of degree $M-1$ with coefficients $c_n(M-1)/n!$. The second derivative of $h(r)$ is

$$h''(r) = e^{-r} \left[t(r) - 2t'(r) + t''(r)\right]$$

where "prime"s denote derivatives. Thus, $P_e(r)$ is convex if and only if the polynomial

$$p(r) = t(r) - 2t'(r) + t''(r) \tag{2.66}$$

of degree $M-1$ is nonnegative for all $r \geq 0$. The latter will be satisfied if all the derivatives of $p(r)$ at $r = 0$ are nonnegative, by Taylor's theorem. The n'th derivative of $p(r)$ at $r = 0$ is given as

$$\begin{aligned} p^{(n)}(0) &= t^{(n)}(0) - 2t^{(n+1)}(0) + t^{(n+2)}(0) \\ &= c_n(M-1) - 2c_{n+1}(M-1) + c_{n+2}(M-1) \end{aligned}$$

Let $N = M-1$ and $d_n(N) = c_n(N) - c_{n+1}(N)$ for $n = 0, 1, \ldots, N$. Then we have

$$p^{(n)}(0) = d_n(N) - d_{n+1}(N) . \tag{2.67}$$

[6] For a shorter proof of this convexity result see the appendix of [35]. This version of the proof is given here because it uses interesting combinatorial identities.

Thus, we need to show that the coefficients $d_n(N)$ are nonincreasing in n for every N. To do this, we need an intermediate result given in the following lemma.

Lemma 2.5 *The binomial coefficients satisfy*

$$\sum_{k=0}^{j} 2^k \binom{J-k}{j-k} = \sum_{k=0}^{j} \binom{J+1}{k} \tag{2.68}$$

for $J = 0, 1, 2, \ldots$ *and* $j = 0, 1, \ldots, J$.

Proof. We will use induction on J. For $J = 0$, the claim is obviously true. For $J = 1$, the claim is easily verified for both $j = 0$ and $j = 1$. Now let's assume that the claim is true for J and for all $j \leq J$. We will show that this implies that the claim is also true for $J + 1$ and for all $j \leq J + 1$. Let $a_j(J)$ denote the left hand side of (2.68). For $0 \leq j \leq J$, we have

$$\begin{aligned}
a_{j+1}(J+1) &= \sum_{k=1}^{j+1} 2^k \binom{J+1-k}{j+1-k} + \binom{J+1}{j+1} \\
&= 2a_j(J) + \binom{J+1}{j+1} \\
&= 2\sum_{k=0}^{j} \binom{J+1}{k} + \binom{J+1}{j+1} \\
&= \binom{J+1}{0} + \sum_{k=0}^{j} \left[\binom{J+1}{k} + \binom{J+1}{k+1} \right] \\
&= \sum_{k=0}^{j+1} \binom{J+2}{k}
\end{aligned}$$

which is the desired result. (The second equality above follows by a change in the index of summation, the third one follows by induction hypothesis, the fourth one is a simple rearrangement of terms and the last one follows by the well-known property of the Pascal triangle.) Finally $a_0(J+1) = 1$ trivially satisfies (2.68). Thus the claim is true for all $j \leq J + 1$. This completes the proof by induction. □

A corollary to Lemma B.1 provides a closed-form to $d_n(N)$.

Corollary 2.1 *The difference coefficients* $d_n(N)$ *satisfy*

$$d_n(N) = \frac{1}{2^N} \binom{2N+1}{N-n} \quad n = 0, 1, \ldots, N. \tag{2.69}$$

Proof. From (2.65) we have

$$\begin{aligned} 2^N c_n(N) &= \sum_{k=n}^{N} 2^{N-k} \binom{k+N}{k-n} \\ &= \sum_{l=0}^{N-n} 2^l \binom{2N-l}{N-n-l} \end{aligned}$$

where we have used a change of index $l = N - k$. Now we use Lemma B.1 with $J = 2N$ and $j = N - n$ to get

$$c_n(N) = \frac{1}{2^N} \sum_{k=0}^{N-n} \binom{2N+1}{k}$$

which results in

$$\begin{aligned} d_n(N) &= c_n(N) - c_{n+1}(N) \\ &= \frac{1}{2^N} \binom{2N+1}{N-n} \end{aligned}$$

as claimed. □

As a result of this corollary, we see that for a fixed N, $d_n(N)$ are decreasing with n for $0 \leq n \leq N$. This means that the polynomial $p(r)$ is nonnegative for $r \geq 0$, and consequently that the conditional error probability $P_e(r)$ is convex for any M, as explained before.

An implication of the convexity of $P_e(r)$ is that the conditional error probability can not be improved by time-sharing between two phase-noisy SNRs r_1 and r_2, since $P_e(\lambda r_1 + (1-\lambda) r_2) \leq \lambda P_e(r_1) + (1-\lambda) P_e(r_2)$ for all $0 \leq \lambda \leq 1$.

2.C Tail Behavior of $q(x)$

In this appendix we concentrate on the decay properties of the density function $q(x)$ around its $x = 1$ tail. We prove that this decay is exponential as described in the following property.

Property 2.1 *The density function $q(x)$ has an exponential decay around $x = 1$, characterized as*

$$\lim_{x \to 1^-} (1-x) \ln q(x) = -\gamma/8 \,. \tag{2.70}$$

To prove this property we need two lemmas. We first define a transformation which is closely related to Mellin transform [36].

Definition: The *moment transform* of a function $f(x)$ defined on $(0,1)$ is given by

$$F(t) = \int_0^1 x^t f(x)\, dx \tag{2.71}$$

where $t \geq 0$.

It can be observed that for any bounded, continuous function the moment transform exists, and that it vanishes as $t \to \infty$. The behavior of a function in its $x = 1$ tail is related to the asymptotic behavior of its moment transform. The following lemma formalizes this notion.

Lemma 2.6 *Let f and g be two bounded, non-oscillatory functions on $(0,1)$ whose moment transforms satisfy $F(t) \leq G(t)$ for all $t \geq t_0$. Then there exists $\epsilon > 0$ such that $f(x) \leq g(x)$ for all $x > 1 - \epsilon$.*

Proof. Let $h = g - f$. h is bounded with moment transform $H = G - F$. Since h is non-oscillatory, there is a neighborhood of 1 in which h does not change sign, say $(1-\delta, 1)$ for some $\delta > 0$. Let

$$\begin{aligned} A &= \max\{|h(x)| : x \in (0,1)\} \\ B &= \int_{1-\delta}^1 h(x)\, dx\ . \end{aligned}$$

Suppose $h(x) \leq 0$ on $(1-\delta, 1)$. Then the following inequalities hold,

$$\begin{aligned} \int_0^{1-\delta} x^t h(x)\, dx &\leq \int_0^{1-\delta} x^t |h(x)|\, dx \leq A\frac{(1-\delta)^{t+1}}{t+1} \\ \int_{1-\delta}^1 x^t h(x)\, dx &\leq (1-\delta)^t B\ , \end{aligned}$$

which implies

$$H(t) \leq (1-\delta)^t \left[\frac{A(1-\delta)}{t+1} + B\right]\ . \tag{2.72}$$

However, since $A > 0$ and $B < 0$, t can be made large enough to make the right hand side of (2.72) negative. This is a contradiction, since $H(t) \geq 0$ for all $t \geq t_0$. The proof is complete with the choice of an ϵ with $0 < \epsilon < \delta$. □

The following lemma establishes a relation between the moment transform of a function and the Laplace transform of its $x = 1$ tail.

Lemma 2.7 *Let f be a bounded function on $(0,1)$ and let f_ϵ be defined as*

$$f_\epsilon(x) = \begin{cases} f(1-x) & 0 \le x < \epsilon \\ 0 & otherwise \end{cases}$$

for $0 < \epsilon < 1$. If $Q_\epsilon(t)$ is the Laplace transform of $f_\epsilon(x)$ and $F(t)$ is the moment transform of $f(x)$, then $Q_\epsilon(t) \simeq F(t)$ for large t and small ϵ.

Proof. $Q_\epsilon(t)$ is defined as

$$Q_\epsilon(t) = \int_0^\epsilon f(1-x)e^{-tx}\,dx\ .$$

With small ϵ we use $e^{-tx} \simeq (1-x)^t$ for $0 < x < \epsilon$, to obtain

$$Q_\epsilon(t) \simeq \int_0^\epsilon f(1-x)(1-x)^t\,dx = \int_{1-\epsilon}^1 f(x)x^t\,dx\ .$$

Since x^t becomes smaller in the interval $(0, 1-\epsilon)$ with increasing t, the rightmost integral will be arbitrarily close to $F(t)$ for large t. Therefore, the quantity $|Q_\epsilon(t) - F(t)|$ can be made arbitrarily close to 0 for sufficiently small ϵ and large t. □

With these two lemmas at hand we now proceed with the proof of the property stated at the beginning of this appendix.

Proof. Lemma C.2 states that the tail of the density function $q(x)$ around $x = 1$ can be found as the inverse Laplace transform of its moment transform for large arguments. The moment transform, $\mu(t)$, of $q(x)$ is given by (2.33) and can be written as

$$\mu(t) = \left(\frac{2\sqrt{2\gamma t}}{1 - e^{-\sqrt{2\gamma t}}}\right)^{1/2} e^{-\sqrt{2\gamma t}/2}\ .$$

For large t, the first factor is bounded between 1 and $\sqrt{t}$. Thus, for large t we have

$$e^{-\sqrt{2\gamma t}/2} \le \mu(t) \le \sqrt{t}e^{-\sqrt{2\gamma t}/2}\ . \tag{2.73}$$

Then from the two lemmas we proved, the function $q(1-x)$ for small x will be bounded by the two functions whose Laplace transforms yield the bounds in (2.73). With the use of Formula 29.3.82 of [30] we obtain

$$\sqrt{\frac{\gamma}{8\pi y^3}}e^{-\gamma/8y} \le q(1-y) \le \sqrt{\frac{\gamma}{8\pi y^3}}\left(\frac{\gamma}{4y} - 1\right)e^{-\gamma/8y}$$

for small y, which upon substitution of x for $1-y$ becomes

$$\sqrt{\frac{\gamma}{8\pi(1-x)^3}}e^{-\gamma/8(1-x)} \leq q(x) \leq \sqrt{\frac{\gamma}{8\pi(1-x)^3}}\left(\frac{\gamma}{4(1-x)}-1\right)e^{-\gamma/8(1-x)} \tag{2.74}$$

for x close to 1. We observe that the dominant tail behavior of $q(x)$ is exponential in $(-\gamma/8(1-x))$. Equivalently, by taking logarithms of all sides in (2.74), we obtain

$$\lim_{x\to 1^-}(1-x)\ln q(x) = -\frac{\gamma}{8} \tag{2.75}$$

where we have used $\lim_{x\to 0} x\ln x = 0$. This completes the proof. □

Chapter 3

Detection of Phase Modulated Signals

In Chapter 2 we have analyzed the performance of FSK modulation in the presence of phase noise. We have seen that phase noise can introduce significant penalty to the energy required to achieve a certain error rate. It is well known that for Additive White Gaussian Noise (AWGN) channels Phase Shift Keying (PSK) provides the most energy efficient binary modulation [37], since the signal points are maximally distant (antipodal) from each other on the signal space. In particular, PSK is 3 dB better than FSK with orthogonal signals in terms of energy utilization. In fiber-optic communication systems, the peak power output of a semiconductor laser is usually limited to a few miliwatts. Therefore, efficient use of energy is of primary importance in these systems. Phase modulation systems are of interest for this reason. However, the additional problem of phase noise may make phase modulation difficult since both the information and the noise is on the phase. In this chapter we attempt to quantify the performance of phase modulation in the presence of phase noise.

3.1 Differential Encoding and Simple Receivers

Let's first consider PSK modulation with no phase tracking. That is, the receiver looks only at a particular bit interval to decide about the corresponding bit and does not use any information about the past observations of the incoming signal. The phase noise process has a variance that increases linearly with time. Therefore in the steady state, the noise becomes a much stronger component of the total phase than the signal component, which is either 0 or π independent of the signal power. Thus, the probability of error would deteriorate with time, reaching a steady-state value of $1/2$.

From the foregoing discussion, it is clear that the phase of the received signal should be tracked so that the uncertainty in the phase is not allowed to reach undesired levels.

This means that the receiver should have memory and should use the past observations to decide about the present. This can be accomplished with decision-directed phase-locked-loops [4], for example. Another alternative is to have a differential reception strategy in which the receiver subtracts the phase of the previous bit interval from that of the current bit interval in the decision process. This would, ideally, yield the difference between the current information phase and the previous one. The danger is that of error propagation, since an error in the decision will cause all the following decisions to be erroneous, until phase noise causes another error to correct the situation. This can be modeled as a Markov chain with two states, a "good" state and a "bad" state, with a small transition probability between them. Since all the decisions in the "bad" state are in error, the steady-state error probability is again $1/2$.

The problem of error propagation can be easily eliminated by conveying the information not in the actual value of the phase but in its change from the previous value. This is *Differential Phase Shift Keying* (DPSK), which incorporates history in the modulation. The signal component of the received IF waveform is

$$s(t) = A\cos(2\pi f_c t + \theta(t) + b_n\pi) \quad (n-1)T < t < nT \tag{3.1}$$

where f_c is the IF carrier frequency, b_n is the n'th differentially encoded bit (0 or 1), and $\theta(t)$ and T are the phase noise and the bit duration as before. The energy per bit is, then, $E_b = A^2T/2$. The n'th information bit a_n is given as

$$a_n = b_n \oplus b_{n+1} ,$$

where $\oplus$ denotes exclusive-OR operation.

We neglect the additive noise $n(t)$ that corrupts the signal for the moment and we first consider a naive reception strategy. The receiver observes the phase of the signal at time t, subtracts from it the phase at time $t-T$, and averages the phase difference over a bit duration. We call this *phase averaging*. The average phase difference is

$$\overline{\Delta\phi} \stackrel{o}{=} \frac{1}{T}\int_{(n-1)T}^{nT} [\theta(t) - \theta(t-T)]\,dt + a_n\pi \tag{3.2}$$

where by the sign $\stackrel{o}{=}$ we mean modulo 2π equivalence. The first term in the right hand side of (3.2) is a Gaussian random variable with zero mean. Its variance, α, can be found as

follows. The random process $\Delta\theta(t) \stackrel{\triangle}{=} \theta(t) - \theta(t-T)$ can be written as

$$\Delta\theta(t) = 2\pi \int_{t-T}^{t} \mu(\tau) d\tau$$

where $\mu(\tau)$ is a white Gaussian process with spectral density $\beta/2\pi$ as before. Then the autocorrelation function of $\Delta\theta(t)$ can be written as

$$R(t,s) \stackrel{\triangle}{=} E[\Delta\theta(t)\Delta\theta(s)] = (2\pi)^2 \int_{t-T}^{t} \int_{s-T}^{s} \frac{\beta}{2\pi} \delta(u-v) du dv$$

which after some manipulations yields

$$R(t,s) = \begin{cases} 2\pi\beta\,(T - |t-s|) & |t-s| < T \\ 0 & \text{otherwise.} \end{cases} \tag{3.3}$$

Then we obtain

$$\begin{aligned} \alpha &= \frac{1}{T^2} \int_{(n-1)T}^{nT} \int_{(n-1)T}^{nT} R(t,s)\; dtds \\ &= \frac{4\pi}{3}\beta T = \frac{2}{3}\gamma \end{aligned} \tag{3.4}$$

with the use of $\gamma = 2\pi\beta T$.

A by-product of the calculation above is the observation that the differential phase noise process $\Delta\theta(t)$ is stationary while the original phase noise process $\theta(t)$ is nonstationary. This is the reason why differential PSK works better against phase noise than PSK.

The decision variable $\overline{\Delta\phi}$ is the modulo 2π equivalent of a Gaussian random variable, which has a mean of 0 or π and a variance of α. Therefore, for equally likely data bits 0 and 1, the optimal processing of $\overline{\Delta\phi}$ is the test

$$\left|\overline{\Delta\phi}\right| \underset{0}{\overset{1}{\gtrless}} \frac{\pi}{2} \tag{3.5}$$

where $\overline{\Delta\phi}$ is assumed to lie in $(-\pi, \pi]$.

We will frequently confront random variables that are derived from a Gaussian random variable (Grv) by the modulo 2π operation. For convenience, we will use the following definition.

Definition : A circularly Gaussian random variable (cGrv) y is defined from a Grv x as $y \stackrel{o}{=} x$, and $y \in (-\pi, \pi]$. If x is $N(a,b)$, we say that y is $CN(a,b)$.

With this definition, $\overline{\Delta\phi}$ is $CN(a_n\pi, \alpha)$. The probability of error for the phase averaging receiver is

$$P_e = \Pr\left(|CN(0,\alpha)| > \frac{\pi}{2}\right) \tag{3.6}$$

which can be computed as the area under the Gaussian density $N(0,\alpha)$ between the abscissa $x = 2k\pi + \frac{\pi}{2}$ and $x = 2k\pi + \frac{3\pi}{2}$ for $k = \ldots, -1, 0, 1, \ldots$. Therefore, we have

$$P_e = 2\sum_{k=0}^{\infty}(-1)^k Q\left((k\pi + \pi/2)/\sqrt{\alpha}\right) \tag{3.7}$$

where $Q(x)$ is the complementary distribution function of $N(0,1)$. Since the series in (3.7) has absolutely decreasing terms, it can be bounded as

$$P_e \leq 2Q\left(\frac{\pi}{2\sqrt{\alpha}}\right) \leq e^{-\pi^2/8\alpha}\ . \tag{3.8}$$

The upper bound in (3.8) will be tight for small α since $Q(x)$ is an exponentially decreasing function. However, we would like to compute P_e in a better precision than the bound. The following proposition gives us the desired form.

Proposition 3.1 *For a random variable y which is $CN(0,a)$ the following holds*

$$\Pr\left(|y| < \frac{\pi}{2}\right) = \frac{1}{2} + \frac{2}{\pi}\sum_{n=0}^{\infty}\frac{(-1)^n}{2n+1}e^{-a(2n+1)^2/2}\ . \tag{3.9}$$

Proof. Consider the periodic function $f(\theta)$ with period 2π one period of which is defined as

$$f(\theta) = \begin{cases} 1 & -\pi/2 < \theta < \pi/2 \\ 0 & \pi/2 < |\theta| < \pi\ . \end{cases}$$

This function has the Fourier series

$$f(\theta) = \frac{1}{2} + \frac{2}{\pi}\sum_{n=0}^{\infty}\frac{(-1)^n}{2n+1}\cos\left((2n+1)\theta\right)\ .$$

The probability that we are interested in can be written as

$$\Pr\left(|y| < \frac{\pi}{2}\right) = \int_{-\infty}^{\infty} f(\theta)N_\theta(0,a)d\theta$$

where $N_\theta(0,a)$ is the Gaussian density function with mean 0, variance a and argument θ.

Equivalently,

$$\Pr\left(|y| < \frac{\pi}{2}\right) = \frac{1}{2} + \frac{2}{\pi}\sum_{n=0}^{\infty}\frac{(-1)^n}{2n+1}E\left[\cos\left((2n+1)\theta\right) \ : \ N(0,a)\right]$$

where $E[g \ : \ p]$ denotes the expected value of the function g of a random variable with the distribution p. From the characteristic function of a Grv, we obtain

$$\Pr\left(|y| < \frac{\pi}{2}\right) = \frac{1}{2} + \frac{2}{\pi}\sum_{n=0}^{\infty}\frac{(-1)^n}{2n+1}e^{-a(2n+1)^2/2}$$

which is the desired result. □

With this result, and with the use of (3.6) and (3.4) we have

$$P_e = \frac{2}{\pi}\sum_{n=0}^{\infty}\frac{(-1)^n}{2n+1}\left(1 - e^{-\gamma(2n+1)^2/3}\right) \tag{3.10}$$

which has two advantages over (3.7). First, it involves standard exponential functions instead of Q functions; second and more importantly, it has better convergence properties due to the extra factor $1/(2n+1)$.

The performance of the phase averaging in the absence of additive noise is shown in Figure 3-1. Note that the error probability is very high for all but very small γ. For an error probability of 10^{-9} γ must be less than 0.1. This is an indication that DPSK is more vulnerable to phase noise than FSK. The receiver which performs phase averaging cannot do better in the presence of additive noise; therefore it is said to have an *error floor* predicted by the figure.

If we continue to neglect the presence of additive noise, we can do better than phase averaging. In particular, instead of smoothing out the change of phase by averaging over time, the receiver could look only at the bit transition times, the time instants at which the information component of the phase could possibly exhibit a discrete jump. Since the Brownian motion sample paths are continuous with probability 1, the phase noise component cannot have jumps. Thus, one could perform the detection with zero error probability, in the absence of additive noise, by just checking the continuity of the phase at the bit transition times. The problem with this strategy is that a receiver that can detect instantaneous phase changes must have infinite bandwidth, hence it is totally vulnerable to additive white noise.

From the foregoing discussion, we can expect that the optimal reception strategy will

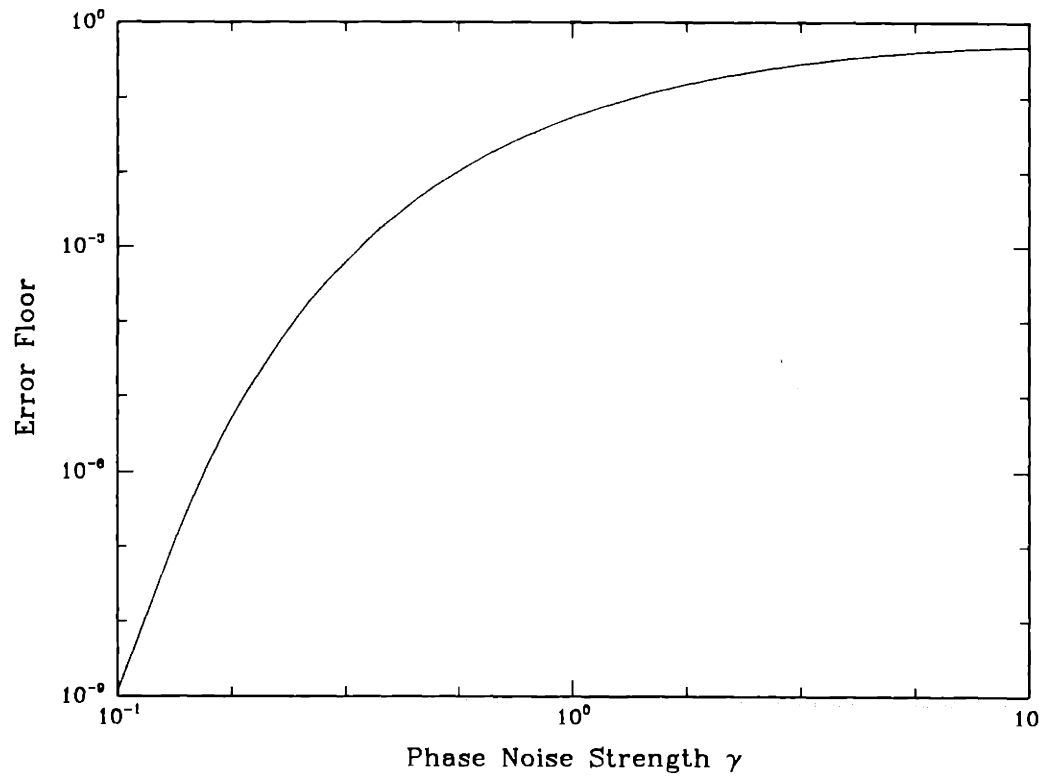

Figure 3-1: Error performance of phase averaging in the absence of additive noise.

depend on the relative strengths of the additive noise and the phase noise. The additive noise favors averaging, or equivalently lowpass filtering, operations for its effects to be smoothed, while the phase noise favors instantaneous decisions for its continuity to be exploited. Clearly, the optimum strategy will be a tradeoff between the two extremes. This was observed in a similar context in Chapter 2 for the noncoherent detection of FSK, where the optimum number of samples per bit M was determined via a tradeoff between the two noise phenomena; the phase noise favored large M (large bandwidth), while the additive noise favored small M (small bandwidth).

In the rest of this chapter, we will obtain the optimal receiver for DPSK. Our goal is not to obtain a practical receiver to implement, since the optimal receiver is likely to be a complex receiver due to the complexity of the problem. Rather, the goal is to have a conceptual understanding of the optimal receiver and its performance. The optimal receiver may also suggest simpler suboptimal receiver structures which are superior to the ones implemented in practice.

3.2 Optimal Receiver Formulation

The signal received by the IF receiver that follows the heterodyne detection is given as

$$r(t) = s(t) + n(t) \tag{3.11}$$

where s(t) is the phase noisy signal given by (3.1) and $n(t)$ is a white Gaussian process with spectral density $N_0/2$. The receiver first translates the signal to baseband by decomposing it into in-phase and quadrature components. This is accomplished by the front-end receiver shown in Figure 3-2. The lowpass filters serve the purpose of blocking the $2f_c$ components of the mixer outputs as well as limiting the additive noise power. Note that the signal $s(t)$ is not strictly band-limited, due to both modulation and phase-noise induced spectral broadening. However, the signal bandwidth is on the order of $R + \beta$ where R is the data rate, and the signal will pass the filter unaltered (simply shifted in frequency) provided that the filter bandwidth W satisfies

$$R + \beta \ll W \ll 2f_c \,. \tag{3.12}$$

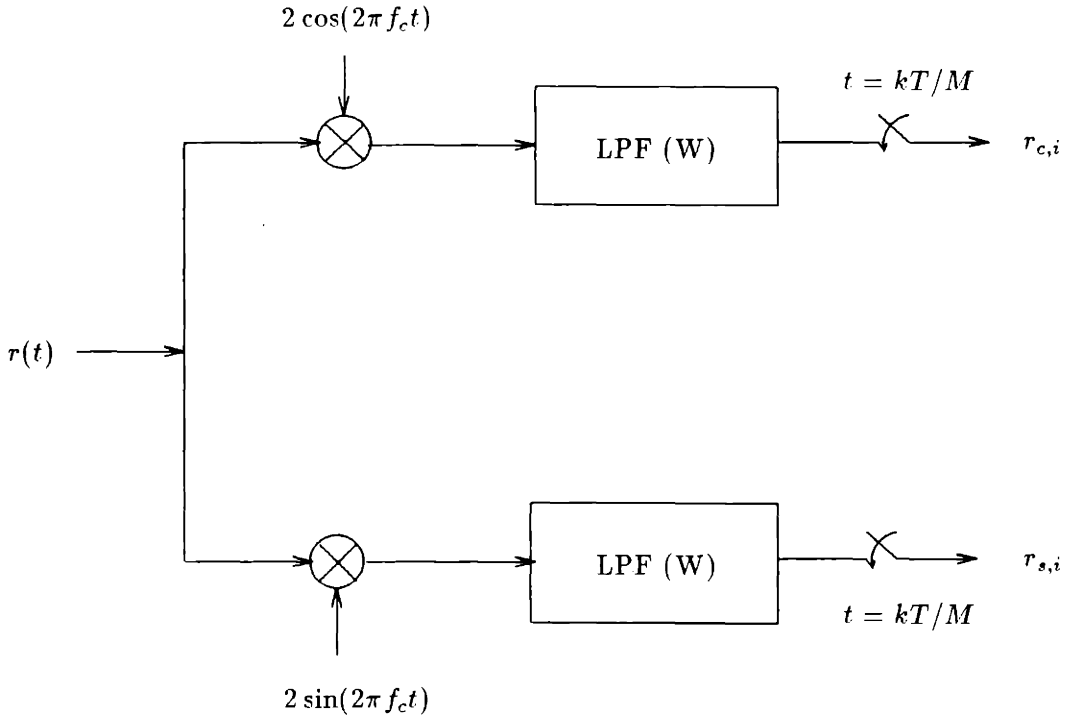

Figure 3-2: The front end of the optimal DPSK receiver. This converts the received signal into a set of vector samples, which will be further processed.

In that case, the filter outputs $r_c(t)$ and $r_s(t)$ are the real and imaginary components of the complex signal

$$x(t) = A \exp\left(j\left(\theta(t) + b_n\pi\right)\right) + n_b(t) \quad (n-1)T < t < nT \tag{3.13}$$

where

$$n_b(t) = 2\left(n(t)e^{-j2\pi f_c t}\right) * h(t)$$

and $h(t)$ is the impulse response of the filter. It can be easily shown that if the condition in (3.12) is satisfied, the real and imaginary parts of the bandlimited noise $n_b(t)$ are statistically independent. Thus, the filter outputs are two waveforms whose signal components are quadratures and whose noise components are statistically independent.

The next operation performed by the receiver is the sampling of the two waveforms with a sampling period of $T' = T/M$ for some integer M yet to be determined. The result is $2M$ samples per bit to be used by the rest of the receiver in the decision process.

One may, rightfully, question the compatibility of the front-end operations we have performed with optimal receiver structure. An optimal receiver can not have an arbitrary front end which processes the received signal. However, if the transformation from the received signal to the samples is reversible, then the optimal processing of the samples will result in the globally optimal receiver, since the sample processor can obtain the continuous signal back if necessary. The sampler must be sampling at a rate of at least the Nyquist rate so that the band-limited filter outputs can be recovered from the samples. This implies that the number of samples per bit must satisfy

$$M \geq 2WT\,. \tag{3.14}$$

We also require that the original signal be retrievable from the filter outputs. Since the white noise $n(t)$ has infinite spectral content it is not possible to retrieve $n(t)$ from its band-limited versions. However, the high-frequency component of the noise that is lost contains no information about the information bit and therefore is irrelevant. The real concern is whether the signal component $s(t)$ can be obtained from $r_c(t)$ and $r_s(t)$. It is easy to show that this can be done by another quadrature operation, that is

$$r_c(t)\cos 2\pi f_c t - r_s(t)\sin 2\pi f_c t = A\cos(2\pi f_c t + \theta(t) + b_n\pi) + n'(t)$$

where $n'(t)$ is a bandpass process which depends solely on $n(t)$. Hence, we have recovered

the relevant part of the original signal from the samples, which justifies that optimality has not been jeopardized by the front-end processing.

By going from the received signal to samples, we have converted the optimum detection problem from a continuous problem to a discrete problem, a problem in which the observation consists of $2M$ real numbers per bit duration. The bit decisions must be based on two consecutive bit intervals, so for the n'th data bit the observed samples are

$$\begin{aligned} c_i &\triangleq r_c\left((n-1)T + iT'\right) \\ s_i &\triangleq r_s\left((n-1)T + iT'\right) \quad i = 1, 2, \ldots, 2M \,. \end{aligned} \tag{3.15}$$

The explicit expression for c_i is

$$c_i = \begin{cases} A\cos(\theta_i + b_n\pi) + n_{c,i} & i = 1, \ldots, M \\ A\cos(\theta_i + b_{n+1}\pi) + n_{c,i} & i = M+1, \ldots, 2M \end{cases} \tag{3.16}$$

where θ_i and $n_{c,i}$ are the sampled values of $\theta(t)$ and $n_c(t)$ respectively, at time $t = (n-1)T + iT'$. The quadrature samples s_i are given by a very similar expression to (3.16) where cos is replaced by sin and $n_{c,i}$ is replaced by $n_{s,i}$.

For mathematical convenience, we would like to have the samples $n_{c,i}$ and $n_{s,i}$ to be statistically independent. Note that their cross independence is already true, since the processes $n_c(t)$ and $n_s(t)$ are independent. The condition for independence of $n_{c,i}$ and $n_{c.j}$ for $i \neq j$ (and similarly for the quadrature samples) is given in the following proposition.

Proposition 3.2 *Suppose the random process $a(t)$ is obtained from a Gaussian white noise process by ideal bandlimiting to W Hz. Then the samples $a(i\Delta)$ of $a(t)$ are statistically independent if $2W\Delta = 1$.*

Proof. Immediate with the observation that autocorrelation function of $a(t)$ is $R_a(\tau) = K\text{sinc}(2W\tau)$ for some constant K, where $\text{sinc}(x) = \sin(\pi x)/\pi x$. □

The proposition asserts that for the desired statistical independence the condition in (3.14) must be satisfied with equality, which results in sampling exactly at the Nyquist rate. In the following development we assume that this is the case.

If we regard c_i and s_i as the real and imaginary parts of a complex number $\mathbf{R}_i$, then we can use the useful geometric tool of phasor diagram, shown in Figure 3-3. In this phasor diagram, $\mathbf{R}_i$ is represented as a sum of three vectors. The first vector corresponds to the phase noisy sinusoid; it has a magnitude of A and a phase of $\theta_i + b_n\pi$. The other two vectors

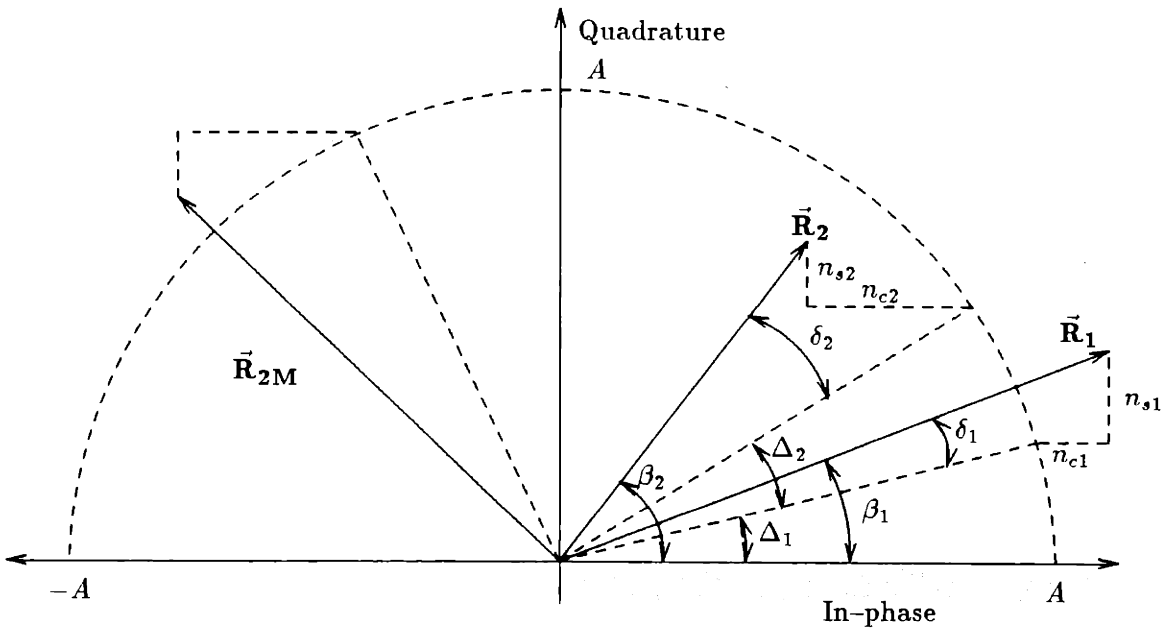

Figure 3-3: The phasor diagram of the sample vectors.

correspond to the additive noise components: a real vector $n_{c,i}$ and an imaginary vector $n_{s,i}$. In this diagram, the tip of $\mathbf{R}_i$ corresponds to the received signal at the sampling time; ideally it would be either the point $(A, 0)$ or the point $(-A, 0)$ depending on b_n. The phase noise rotates the vector from this ideal point and the additive noise perturbs the tip so that it is no longer on the sphere of radius A. The way in which the (unperturbed) tip rotates obeys a Markov process since the phase noise process has independent increments. In fact, the angle of rotation can be written as

$$\theta_i = \phi + \sum_{k=1}^{i} \Delta_k \quad 1 \leq i \leq M \tag{3.17}$$

where ϕ is the initial state of the phase ($\phi = \theta((n-1)T) + b_n\pi$) and Δ_k is the incremental phase noise accumulation between the $k-1$'st and k'th samples ($\Delta_k = \theta((n-1)T + kT') - \theta((n-1)T + (k-1)T')$). It is easily seen that $\{\Delta_k\}$ are independent, identically distributed zero-mean Grv's with variance

$$\alpha^2 \stackrel{\Delta}{=} \gamma/M\,. \tag{3.18}$$

For samples indexed $M+1 \leq i \leq 2M$, the phase change of $a_n\pi$ at $t = nT$ must also be

taken into account. This can be done by letting Δ_{M+1} have a mean of $a_n\pi$ instead of 0.

Then, the detection problem is to determine whether there is a deterministic phase shift between the M'th and $M+1$'st unperturbed vectors, using the observation vectors $\mathbf{R}_1, \ldots, \mathbf{R}_{2M}$. Intuitively, it may seem that only the vectors $\mathbf{R}_M$ amd $\mathbf{R}_{M+1}$ will be used in this decision. However, due to the perturbation by additive noise, the angles of the vectors $\mathbf{R}_i$, β_i is not a Markov process, although the unperturbed angle θ_i is. Therefore, all $2M$ vectors will be involved in the decision.

The common variance of the additive noise samples is found as

$$\sigma^2 = 2N_0W = \frac{N_0}{T}M \ . \tag{3.19}$$

While the phase noise increments $\{\Delta_k\}$ decrease in variance as M increases, the additive noise samples increase in variance linearly in M. This is because as M increases the lowpass filter has a wider passband, and thus passes a larger portion of the white noise spectrum, while the phase is sampled faster and thus the incremental phase changes decrease in their strength. An interesting relation between the two variances is that their product satisfies the relation

$$\alpha^2\sigma^2 = N_0\gamma/T = 2\pi\beta N_0 \tag{3.20}$$

which is independent not only of the number of samples M, but also of the bit rate $1/T$.

Let's now elaborate on the initial phase ϕ. Suppose we could get a good estimate on the state of the phase noise at time $t = (n-1)T$ using the observations of the previous bit interval. If the encoded bit b_n is correctly decided, then ϕ can be estimated within a small error. Then the coordinate frame of the phasor diagram can be rotated by this estimate $\hat{\phi}$ so that the observations lie in a coordinate frame with no initial phase. However if a detection error in deciding b_n is made, then the error in the estimate of ϕ will be in the neighborhood of π. Then a receiver which uses the absolute angles β_i in this coordinate frame, instead of the relative angles $\beta_i - \beta_{i-1}$ $(i \geq 2)$, may be in error for the next decision. This is the same phenomenon as the error propagation in nondifferential PSK, since the receiver is trying to detect b_n instead of $b_n \oplus b_{n+1}$.

To get rid of the problem above, we force our receiver to be *rotationally insensitive* in the sense that if the phasor diagram is rotated by a fixed amount the receiver's decision will not change. This can be accomplished in two ways. One is by letting $\phi = 0$ and having the receiver process only the relative angles $\beta_i - \beta_{i-1}$ for $i \geq 2$. This corresponds to differential phase processing with perfect phase tracking. An equivalent way results from

the observation that if β_1 was uniformly distributed over $(-\pi, \pi)$ the receiver would do the same processing, i.e. it would disregard β_1 and only use $\beta_i - \beta_1$. β_1 can be expressed as

$$\beta_1 = \phi + \Delta_1 + \delta_1$$

where the angle δ_1 that depends only on the additive noise on the first vector. Hence if ϕ is uniformly distributed over $(-\pi, \pi)$, the desired rotational insensitivity will be achieved. This corresponds to a receiver which makes no effort to track and compensate the state of the phase at bit transition times.

Now that we have completely specified the operating strategy of the receiver and the statistical distribution of the random variables involved in the phasor diagram, we can obtain the optimal decision rule. We first write the joint probability density function of the $2M$ vectors conditioned on ϕ, $\{\Delta_i\}$ and a_n in rectangular coordinates. This conditional density is a product of $4M$ Gaussian densities corresponding to additive noise samples. Then we convert this density to polar coordinates to obtain the joint conditional density of $\{(R_i, \beta_i)\}$, and remove the conditioning on $\{\Delta_i\}$ and on ϕ. Finally we form the Maximum Likelihood Test (MLT) using the densities for $a_n = 0$ and $a_n = 1$. We give only the result of this calculation here, the details may be found in Appendix 3.A. The resulting MLT is

$$L_0 \underset{1}{\overset{0}{\gtrless}} L_1 \tag{3.21}$$

where

$$L_0 = f(AR_1/\sigma^2, \ldots, AR_{2M}/\sigma^2, \quad \beta_2 - \beta_1 \quad , \ldots, \beta_M - \beta_1, \ldots, \beta_{2M} - \beta_1)$$

$$L_1 = f(AR_1/\sigma^2, \ldots, AR_{2M}/\sigma^2, \quad \beta_2 - \beta_1 \quad , \ldots, \beta_M - \beta_1, \tag{3.22}$$

$$\pi + \beta_{M+1} \quad -\beta_1, \ldots, \pi + \beta_{2M} - \beta_1) \tag{3.23}$$

The function $f(\cdot)$ in (3.22) is given by

$$f(x_1, \ldots, x_{2M}, \alpha_2, \ldots, \alpha_{2M}) = \sum_{k_2} \cdots \sum_{k_{2M}} I_{k_2 + \cdots + k_{2M}}(x_1) \left(\prod_{i=2}^{2M} I_{k_i}(x_i) \right) a(\vec{k}) \cos \left(\sum_{i=2}^{2M} k_i \alpha_i \right) \tag{3.24}$$

where

$$a(\vec{k}) = \exp \left[-\frac{\alpha^2}{2} \sum_{i=2}^{2M} \left(\sum_{l=i}^{2M} k_l \right)^2 \right] \tag{3.25}$$

and $I_k(\cdot)$ is the modified Bessel function of order k. The summations in (3.24) all run from $-\infty$ to ∞.

Because of the complexity of the function f, the optimal decision rule given by Equations (3.21)-(3.25), is not a practical rule to implement. More importantly, its performance cannot be evaluated to enable a comparison with other receiver structures. Therefore we consider special cases, where the decision rule reduces to simpler forms, in the following sections.

3.3 Optimal Receiver in Weak Additive Noise

The general formulation of the optimal receiver has resulted in a decision rule which is optimal for all signal and noise parameters. The complexity of this rule motivates us to investigate the special cases. One such case is that of weak additive noise. The variance of the additive noise samples satisfies $\sigma^2 = N_0 M/T$. When this variance is much less than the squared signal amplitude, i.e., $\sigma^2 \ll A^2$, we say that the additive noise is weak. The weak additive noise regime is, then, valid only for M values that are much less than the signal-to-noise ratio ξ. This may be the case in practice where ξ is, usually, larger than 10.

From the general decision rule of the previous section, with the use of $I_k(x) \simeq I_0(x)$ for large x, we can approximate the function f as

$$f(x_1, \ldots, x_{2M}, \alpha_2, \ldots, \alpha_{2M}) \simeq \left(\prod_{i=1}^{2M} I_0(x_i) \right) \sum_{k_2} \cdots \sum_{k_{2M}} a(\vec{k}) \cos \left(\sum_{i=2}^{2M} k_i \alpha_i \right) \tag{3.26}$$

for $x_i \gg 1$. The amplitude and phase dependence of this approximation are separated. Since L_0 and L_1 have the same amplitude arguments in f, the decision rule for the weak additive noise will only process the phases β_i. We now define the phase dependence of f as a new function g,

$$g(\alpha_2, \ldots, \alpha_{2M}) \triangleq \sum_{k_2} \cdots \sum_{k_{2M}} a(\vec{k}) \cos \left(\sum_{i=2}^{2M} k_i \alpha_i \right) \tag{3.27}$$

and show that this further simplifies as given in the following lemma.

Lemma 3.1 *The function $g(\cdot)$, defined in (3.27) satisfies*

$$g(\alpha_2, \ldots, \alpha_N) = \prod_{i=2}^{N} \left(2\pi \sum_n p(\alpha_i - \alpha_{i-1} + 2n\pi) \right) \tag{3.28}$$

where $\alpha_1 \equiv 0$ *and* $p(\cdot)$ *is the Gaussian density function* $N(0, \alpha^2)$.

The proof of this lemma is given in Appendix 3.B since it is not central to our discussion. With the use of the lemma and Equations (3.21) and (3.22) the optimal test becomes

$$\sum_n p(\beta_{M+1} - \beta_M + 2n\pi) \underset{1}{\overset{0}{\gtrless}} \sum_n p\left(\beta_{M+1} - \beta_M + (2n+1)\pi\right) \tag{3.29}$$

which reduces to

$$|\beta_{M+1} - \beta_M| \underset{0}{\overset{1}{\gtrless}} \frac{\pi}{2} \tag{3.30}$$

due to the symmetry of Gaussian density function. This is a test that simply looks at the angle between the vectors just before and just after the bit transition time, and checks whether this angle is closer to 0 or π. We will refer to this decision rule as *angle difference rule.*

We now analyze the performance of the angle difference rule in (3.30). Similar analyses can be found in [38, 39, 42]. The probability of error can be written as

$$P_e = \int_{|\beta_{M+1} - \beta_M| > \pi/2} p(\beta_M, \beta_{M+1}|0)\, d\beta_M\, d\beta_{M+1}\ . \tag{3.31}$$

Thus, we need the joint density of the angles β_M and β_{M+1} under the hypothesis $a_n = 0$. The x and y components of the ith sample under this hypothesis are

$$\begin{aligned} R_{i,x} &= A\cos(\sum_{j=1}^{i} \Delta_j + \phi + b_n\pi) + n_{c,i} \\ R_{i,y} &= A\sin(\sum_{j=1}^{i} \Delta_j + \phi + b_n\pi) + n_{s,i}\ . \end{aligned}$$

We are ultimately interested in the statistics of the difference $\beta_{M+1} - \beta_M$, thus we can manipulate the random variables that are common to both β_M and β_{M+1} without affecting that statistics. We have

$$\begin{aligned} \beta_M &= \theta_M + \delta_M \\ \beta_{M+1} &= \theta_M + \Delta_{M+1} + \delta_{M+1} \end{aligned}$$

where δ_i depends only on the additive noise on the ith sample. Therefore we can set $\theta_M = 0$

and let $\Delta_{M+1} = \Delta$. Then we have in Cartesian coordinates

$$\begin{aligned} p(R_{M,x}, R_{M,y}, R_{M+1,x}, R_{M+1,y}|\Delta) &= \frac{1}{(2\pi\sigma^2)^2} \exp\left[-\frac{1}{2\sigma^2}\left((R_{M,x} - A)^2 + R_{M,y}^2\right.\right. \\ &+ \left.\left.(R_{M+1,x} - A\cos\Delta)^2 + (R_{M+1,y} - A\sin\Delta)^2\right)\right] \end{aligned}$$

Now we make a transformation to polar coordinates and obtain

$$\begin{aligned} p(R_M, \beta_M, R_{M+1}, \beta_{M+1}|\Delta) &= \frac{R_M R_{M+1}}{(2\pi\sigma^2)^2} \exp(-(R_M^2 + R_{M+1}^2 + 2A^2)/2\sigma^2) \\ &\exp\left[\frac{A}{\sigma^2}(R_M \cos\beta_M + R_{M+1}\cos(\beta_{M+1} - \Delta))\right] \end{aligned}$$

Finally we remove the conditioning on Δ by first using the Bessel series:

$$\exp(z\cos u) = \sum_{k=-\infty}^{\infty} I_k(z)\cos(ku)$$

and then use the characteristic function of a Grv to obtain

$$\begin{aligned} p(R_M, \beta_M, R_{M+1}, \beta_{M+1}) &= \exp\left(-(R_M^2 + R_{M+1}^2 + 2A^2 - 2AR_M\cos\beta_M)/2\sigma^2\right) \\ &\cdot \frac{R_M R_{M+1}}{(2\pi\sigma^2)^2} \sum_{k=-\infty}^{\infty} I_k(AR_{M+1}/\sigma^2) e^{-k^2\alpha^2/2}\cos(k\beta_{M+1}) \end{aligned}$$

Since we only need the distribution of the angles we now integrate out the amplitudes:

$$p(\beta_M, \beta_{M+1}) = \frac{e^{-A^2/\sigma^2}}{(2\pi)^2} \sum_k \sum_l A_k A_l e^{-k^2\alpha^2/2}\cos(k\beta_{M+1})\cos(l\beta_M) \tag{3.32}$$

where we have defined the coefficients A_k as

$$\begin{aligned} A_k &\triangleq \frac{1}{\sigma^2}\int_0^\infty R e^{-R^2/2\sigma^2} I_k\left(\frac{AR}{\sigma^2}\right)\, dR \\ &= \int_0^\infty e^{-u} I_k\left(\sqrt{\frac{2A^2u}{\sigma^2}}\right)\, du \end{aligned} \tag{3.33}$$

Having obtained the density function for the angles, we can obtain the probability of error

from (3.31). We have

$$P_e = \frac{e^{-A^2/\sigma^2}}{(2\pi)^2} \sum_k \sum_l A_k A_l e^{-k^2\alpha^2/2} C_{kl}$$

where we have defined C_{kl} as

$$C_{kl} \triangleq \int_{|\beta_{M+1}-\beta_M|>\pi/2} \cos(k\beta_{M+1}) \cos(l\beta_M)\, d\beta_M\, d\beta_{M+1} .$$

It is easily found that

$$C_{kl} = \begin{cases} 2\pi^2 & \text{if } k = l = 0, \\ -(-1)^n 2\pi/(2n+1) & \text{if } |k| = |l| = 2n+1, \\ 0 & \text{otherwise.} \end{cases}$$

This results in

$$P_e = \frac{1}{2} e^{-A^2/\sigma^2} A_0^2 - \frac{2}{\pi} e^{-A^2/\sigma^2} \sum_{n=0}^{\infty} \frac{(-1)^n}{2n+1} A_{2n+1}^2 e^{-(2n+1)^2\alpha^2/2} .$$

From Equation (24.94) of [40] and (6.614.1) of [41] one gets

$$\begin{aligned} A_0 &= e^{A^2/2\sigma^2} \\ A_{2n+1} &= \sqrt{\frac{A^2\pi}{8\sigma^2}} e^{A^2/4\sigma^2} \left[I_n\left(\frac{A^2}{4\sigma^2}\right) + I_{n+1}\left(\frac{A^2}{4\sigma^2}\right) \right] \end{aligned}$$

which results in

$$P_e = \frac{1}{2} - \frac{\xi}{2M} e^{-\xi/M} \sum_{n=0}^{\infty} \frac{(-1)^n}{2n+1} \left[I_n\left(\frac{\xi}{2M}\right) + I_{n+1}\left(\frac{\xi}{2M}\right) \right]^2 e^{-(2n+1)^2\gamma/2M} \qquad (3.34)$$

which is the final result.

Equation (3.34) is obtained in [42] (with $M = 1$) for the performance of the "delay and correlate" receiver in which the receiver correlates the received signal with the signal corresponding to the previous bit interval and checks the sign of the result. This is equivalent to our model with $M = 1$: the receiver effectively samples once a bit and takes the inner product of the sampled vectors. For a general M, the receiver delays the signal by T/M and takes the inner product of the current and delayed samples.

The performance of the angle difference rule is shown in Figure 3-4. The bit error rates shown are optimized with respect to M. It is seen that angle difference receiver is

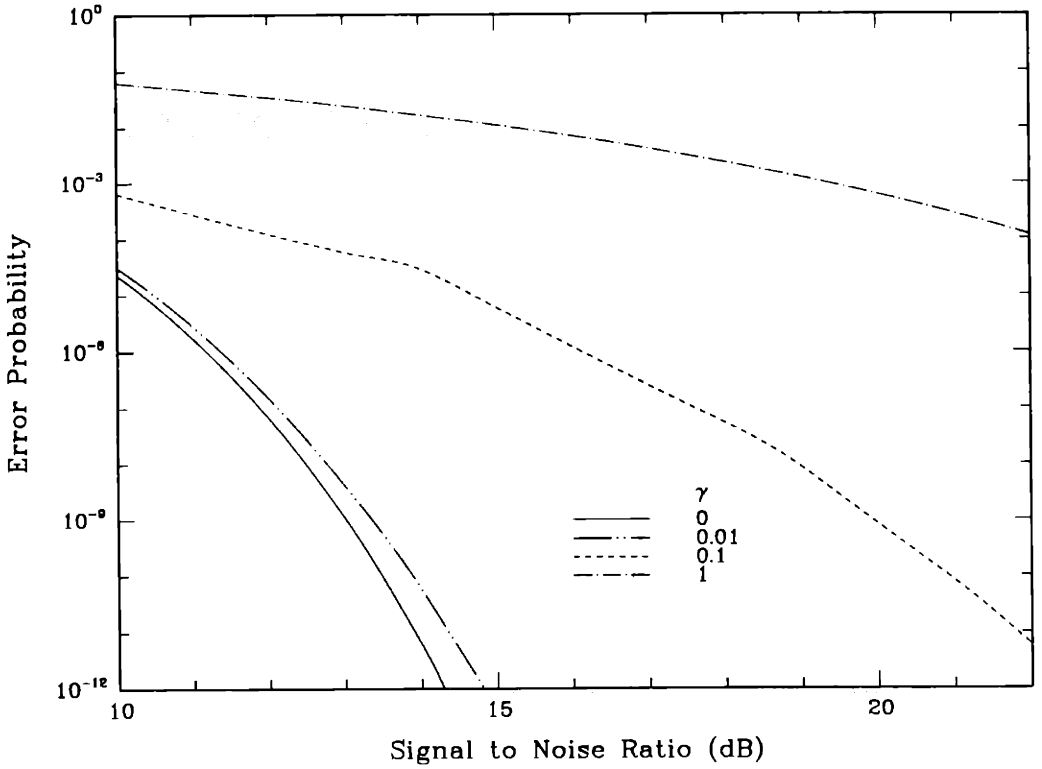

Figure 3-4: Error performance of angle difference rule.

very sensitive to phase noise. For $\gamma > 0.01$, there is a rapid deterioration in the system performance. In the case with no phase noise, $\gamma = 0$, the optimal value of M is always 1. As γ increases the optimal value also increases. However, the effect of phase noise cannot be compensated by looking at a smaller time interval; the increasing additive noise power dominates and the performance deteriorates dramatically.

It may be of interest to consider the asymptotic performance of this receiver for very high SNR values. Using the property

$$\lim_{x\to\infty} I_0(x)e^{-x}\sqrt{2\pi x} = 1$$

one obtains from (3.34) that as $\xi \to \infty$,

$$P_e = \frac{1}{2} - \frac{2}{\pi}\sum_{n=0}^{\infty}\frac{(-1)^n}{2n+1}e^{-\gamma(2n+1)^2/2M}$$

which is similar to the expression we obtained for the phase averaging in the absence of additive noise. For $M = 1$, the error floor is the same as that of phase averaging except an increase in γ by a factor of 1.5. This is due to the fact that there is no averaging, or post-filtering, in this receiver. Recalling the high floor of the phase averaging receiver we conclude that the standard delay and correlate receiver, i. e. the angle difference rule with M set at 1, has very poor phase noise tolerance. However the angle difference rule optimizes over M. In the absence of additive noise, the optimal value of M is infinite, the receiver just detects the polarity change (or lack of it) at the bit transition times and achieves zero error probability as

$$P_e(M \to \infty) = \frac{1}{2} - \frac{2}{\pi}\sum_{n=0}^{\infty}\frac{(-1)^n}{2n+1} = 0\,.$$

This tells us that if the receiver bandwidth is optimized with respect to the noise parameters, there will not exist a bit error rate floor. Thus, the error floor is not inherent to the phase modulation but to the receiver structure. However with nonzero noise levels the performance of this DPSK receiver is rather poor in comparison with FSK receivers we have previously considered.

There are two reasons for the poor sensitivity to phase noise. One is inherent in the DPSK modulation. The information is conveyed in the phase which is directly corrupted by the phase noise. Therefore one should not expect the tolerance of a DPSK receiver to phase noise to match that of a FSK or OOK receiver. The second reason is that the angle difference receiver was designed under the premise that the additive noise is weak. The

resulting decision rule used only one of the M available samples, thus reducing the effective SNR by a factor of M. In this sense, this receiver is similar to the single-filter receiver for the envelope detection of FSK. Both of these receivers operate with the principle that a reduction of SNR may be worthwhile if the phase noise strength is reduced by the same factor. The improvement introduced by both receivers is marginal. In the next section we will design receivers that use all the available samples as in the double-filter FSK receiver.

3.4 Optimal Receiver in Weak Phase Noise

In this section, we investigate the optimal receiver structure when the phase noise is weak. This case is realistic, since the variance of the incremental phase noise is γ/M, which is small for small γ and/or large M. First we concentrate on the case with no phase noise. The optimal decision rule with $\gamma = 0$ is, from (3.21)-(3.25),

$$L_0 \underset{0}{\overset{1}{\gtrless}} L_1 \tag{3.35}$$

$$\begin{aligned} L_0 &= \sum_{k_1+\cdots+k_{2M}=0} \cos\Big(\sum_{i=1}^{2M} k_i\beta_i\Big) \prod_{i=1}^{2M} I_{k_i}(AR_i/\sigma^2) \\ L_1 &= \sum_{k_1+\cdots+k_{2M}=0} \cos\Big(\sum_{i=1}^{M} k_i\beta_i + k_{i+M}(\beta_{i+M}-\pi)\Big) \prod_{i=1}^{2M} I_{k_i}(AR_i/\sigma^2)\ . \end{aligned}$$

While this decision rule still looks formidable, the following lemma simplifies it significantly:

Lemma 3.2 *L_0 given in (3.35) can be written as*

$$L_0 = I_0(\sqrt{E_0})$$

where

$$E_0 = \frac{A^2}{\sigma^4} \sum_{i,j=1}^{M} R_i R_j \cos(\beta_i - \beta_j)\ .$$

Proof. We first use

$$I_n(x) = \int_{-\pi}^{\pi} e^{x\cos u} \cos nu\ du$$

with $n = k_2 + \cdots + k_M$, to rewrite L_0 as

$$L_0 = \sum_{k_2 \cdots k_{2M}} \cos(\sum_{i=2}^{2M} k_i(\beta_i - \beta_1)) \left(\prod_{i=2}^{2M} I_{k_i}(b_i) \right) \frac{1}{2\pi} \int_{-\pi}^{\pi} e^{b_1 \cos u} \cos((k_2 + \cdots + k_{2M})u) \, du$$

where we have defined $b_i = AR_i/\sigma^2$. We now interchange the sum and the integral, expand the product of two cosines, and observe the symmetry with respect to u to obtain

$$L_0 = \frac{1}{2\pi} \int_{-\pi}^{\pi} e^{b_1 \cos u} \sum_{k_2 \cdots k_{2M}} I_{k_2}(b_2) \cdots I_{k_{2M}}(b_{2M}) \cos(\sum_{i=2}^{2M} k_i(\beta_i - \beta_1 + u)) \, du$$

Next we note that the inner summation can be simplified as

$$\begin{aligned} \sum_{k_2 \cdots k_{2M}} I_{k_2}(b_2) \cdots I_{k_{2M}}(b_{2M}) \cos(\sum_{i=2}^{2M} k_i x_i) &= \prod_{i=2}^{2M} \sum_{k_i} I_{k_i}(b_i) \cos(k_i x_i) \\ &= \prod_{i=2}^{2M} \exp(b_i \cos x_i) \\ &= \exp\left(\sum_{i=2}^{2M} b_i \cos x_i \right) \end{aligned}$$

where we have used

$$\sum_{k=-\infty}^{\infty} I_k(x) \sin ky = 0$$

and

$$\sum_{k=-\infty}^{\infty} I_k(x) \cos ky = \exp(x \cos y) \, .$$

Now we have

$$L_0 = \frac{1}{2\pi} \int_{-\pi}^{\pi} \exp\left[\sum_{i=2}^{2M} b_i \cos(\beta_i - \beta_1 + u) \right] \, du \tag{3.36}$$

We now let $\alpha_i = \beta_i - \beta_1$ and manipulate the exponent above as follows

$$\begin{aligned} \sum_{i=2}^{2M} b_i \cos(\alpha_i + u) &= \cos u \sum_{i=2}^{2M} b_i \cos \alpha_i - \sin u \sum_{i=2}^{2M} b_i \sin \alpha_i \\ &= \left[\left(\sum_{i=2}^{2M} b_i \cos \alpha_i \right)^2 + \left(\sum_{i=2}^{2M} b_i \sin \alpha_i \right)^2 \right]^{1/2} cos(u - v) \end{aligned} \tag{3.37}$$

where v is an angle which is independent of u. Letting

$$E_0 = \left(\sum_{i=2}^{2M} b_i \cos\alpha_i\right)^2 + \left(\sum_{i=2}^{2M} b_i \sin\alpha_i\right)^2$$

and inserting (3.37) into (3.36) we get

$$L_0 = I_0(\sqrt{E_0}) \,.$$

We finally bring E_0 to the form stated in the lemma.

$$\begin{aligned} E_0 &= \sum_{i,j=1}^{2M} b_i b_j \cos\alpha_i \cos\alpha_j + b_i b_j \sin\alpha_i \sin\alpha_j \\ &= \sum_{i,j=1}^{2M} b_i b_j \cos(\alpha_i - \alpha_j) \end{aligned}$$

which concludes the proof since $\alpha_i - \alpha_j = \beta_i - \beta_j$. □

Since $I_0(x)$ is an increasing function, the lemma simplifies the decision rule to

$$E_0 \underset{1}{\overset{0}{\gtrless}} E_1$$

where E_1 is appropriately defined with the π phase shifts for the second half of the angles. It can be easily seen that in terms of the samples one has

$$E_1 = \frac{A^2}{\sigma^4}\left[\sum_{i,j=1}^{M} + \sum_{i,j=M+1}^{2M} - 2\sum_{i=1}^{M}\sum_{j=M+1}^{2M}\right] R_i R_j \cos(\beta_i - \beta_j) \,.$$

Thus the test finally simplifies to

$$\sum_{i=1}^{M}\sum_{j=M+1}^{2M} R_i R_j \cos(\beta_i - \beta_j) \underset{1}{\overset{0}{\gtrless}} 0 \,. \tag{3.38}$$

An alternate way to state the same decision rule is the following:

$$\left(\frac{1}{M}\sum_{i=1}^{M} \mathbf{R_i}\right) \cdot \left(\frac{1}{M}\sum_{j=M+1}^{2M} \mathbf{R_j}\right) \underset{1}{\overset{0}{\gtrless}} 0 \,. \tag{3.39}$$

The receiver finds the average of the sample vectors corresponding to the current and previous bit intervals, and compares their inner product to zero. This is similar to the angle difference rule except that the average vectors are used instead of the Mth and $M+1$st vectors.

We will now provide a crude performance analysis for the receiver given by (3.39). Let's first find the conditional error probability when the phase noise angles θ_i are known. In this case, the in-phase and quadrature components of the averaged sample vectors are independent Gaussian random variables with known means and identical variance σ^2/M. If these components are viewed as the real and imaginary components of a complex variable, then the inner product reduces to the real part of the product of two Gaussian complex random variables. We define A_1, A_2, ϕ_1 and ϕ_2 as follows:

$$\begin{aligned} A_1 e^{j\phi_1} &= \frac{A}{M}\sum_{i=1}^{M} e^{j\theta_i} \\ A_2 e^{j\phi_2} &= \frac{A}{M}\sum_{i=M+1}^{2M} e^{j\theta_i} . \end{aligned} \tag{3.40}$$

Thus, A_1 and ϕ_1 are the amplitude and the phase of the phase-noisy signal vector for the first bit duration, respectively. Similarly, A_2 and ϕ_2 are the corresponding entities for the second bit duration. With these definitions the conditional error probability can be expressed as

$$P_e(A_1,\phi_1,A_2,\phi_2) = \Pr\left(\mathrm{Re}\left[(A_1e^{j\phi_1}+n_1)(A_2e^{j\phi_2}+n_2^*)\right] < 0 | A_1,\phi_1,A_2,\phi_2\right)$$

where n_1 and n_2 are i.i.d. complex Grv's with zero mean and component variance σ^2/M, they correspond to the additive noise averages. The probability above is a standard one in communication theory, it can be obtained as a special case of a more general probability treated in Appendix 4 of [25] as

$$P_e(A_1,\phi_1,A_2,\phi_2) = Q(a,b) - \frac{1}{2}I_0(ab)\exp(-(a^2+b^2)/2) \tag{3.41}$$

where a and b are given by

$$a = \left[\frac{M}{4\sigma^2}\left(A_1^2+A_2^2-2A_1A_2\cos(\phi_1-\phi_2)\right)\right]^{1/2}$$

$$b = \left[\frac{M}{4\sigma^2}\left(A_1^2 + A_2^2 + 2A_1A_2\cos(\phi_1 - \phi_2)\right)\right]^{1/2}$$

and $Q(\cdot,\cdot)$ is the Marcum's Q function defined as

$$Q(a,b) \triangleq \int_b^\infty e^{-(a^2+x^2)/2} I_0(ax)x\,dx\ .$$

Note that for given phase noisy signal vectors the conditional performance of the system is independent of M since σ^2/M is a constant. The phase noise has two negative effects on the performance. First, it causes $\phi_1 - \phi_2$ to be nonzero, and secondly it causes A_1 and A_2 to be less than the original amplitude A. The amplitude effect is of the same nature as the effect of phase noise on FSK, which is small when γ is small and SNR is large. The important deterioration in DPSK stems from the effect of phase noise on $\phi_1 - \phi_2$. Therefore, we will neglect the amplitude degradation and concentrate on the phase degradation. That is, we shall assume that $A_1 = A_2 = A$. Furthermore, for small γ, one can expand the complex exponential in (3.40) to the first order, and obtain

$$A_1 e^{j\phi_1} = A\left[1 + j\frac{1}{M}\sum_{k=1}^{M}\theta_k\right]$$

and the extension to the second set of samples is obvious. We see that the amplitude degradation is of second order in phase noise, while the phase deterioration is of first order. We also see that the phase of the average signal vector can be approximated by the average of the individual signal phases. This approximation results in

$$\phi_2 - \phi_1 \simeq \frac{1}{M}\sum_{k=1}^{M}(\theta_{k+M} - \theta_k) \tag{3.42}$$

which is similar to phase averaging. It can be shown that the variance of the phase difference with this approximation is

$$\begin{aligned}\mathrm{Var}(\phi_2 - \phi_1) &= \left[M^2 + 2\sum_{i=1}^{M-1} i^2\right]\frac{\alpha^2}{M^2} \\ &= \frac{\gamma}{3}\left(2 + \frac{1}{M^2}\right)\end{aligned}$$

which decreases with M. Therefore the optimum value of M is ∞. In this case we have

$$\phi_2 - \phi_1 = \frac{1}{T}\int_0^T [\theta(t) - \theta(t-T)]\ dt\ . \tag{3.43}$$

We have designed a receiver whose sensitivity to additive noise does not depend on M. Thus for efficient phase noise tracking we find that M should tend to ∞. The resulting receiver effectively performs phase averaging in the presence of additive noise. Another observation is that the improvement by optimization over M is not very large, since increasing M from 1 to ∞ reduces the phase noise variance only from γ to $2\gamma/3$.

The conditional error probability was found in (3.41). With the approximation $A_1 = A_2 = A$, the parameters a and b become

$$\begin{aligned} a &= \sqrt{2\xi \sin^2(\phi_2 - \phi_1)} \\ b &= \sqrt{2\xi \cos^2(\phi_2 - \phi_1)}\ . \end{aligned}$$

Assuming that the SNR is high and using the equations (A.20) and (A.21) of [43] Appendix A, one obtains

$$P_e(a,b) \simeq Q(b-a) \simeq \frac{1}{2}\exp(-(b-a)^2/2)\ . \tag{3.44}$$

The unconditional error probability can be obtained by taking the expectation of the conditional error probability over the Gaussian random variable $\Delta\phi = \phi_2 - \phi_1$ resulting in

$$P_e \simeq \frac{1}{2}\epsilon^{-\xi} E\left[\exp(\xi|\sin\Delta\phi|)\right]\ . \tag{3.45}$$

This error probability can be computed numerically, the result is shown in Figure 3-5. It is seen that this receiver is also vulnerable to phase noise. The error probability increases dramatically as the phase noise strength gets beyond 0.1. This is due to two reasons. One is that the receiver was designed to operate in the weak phase noise regime. The other and perhaps more important reason is again the inherent intolerance of phase modulation formats to phase noise.

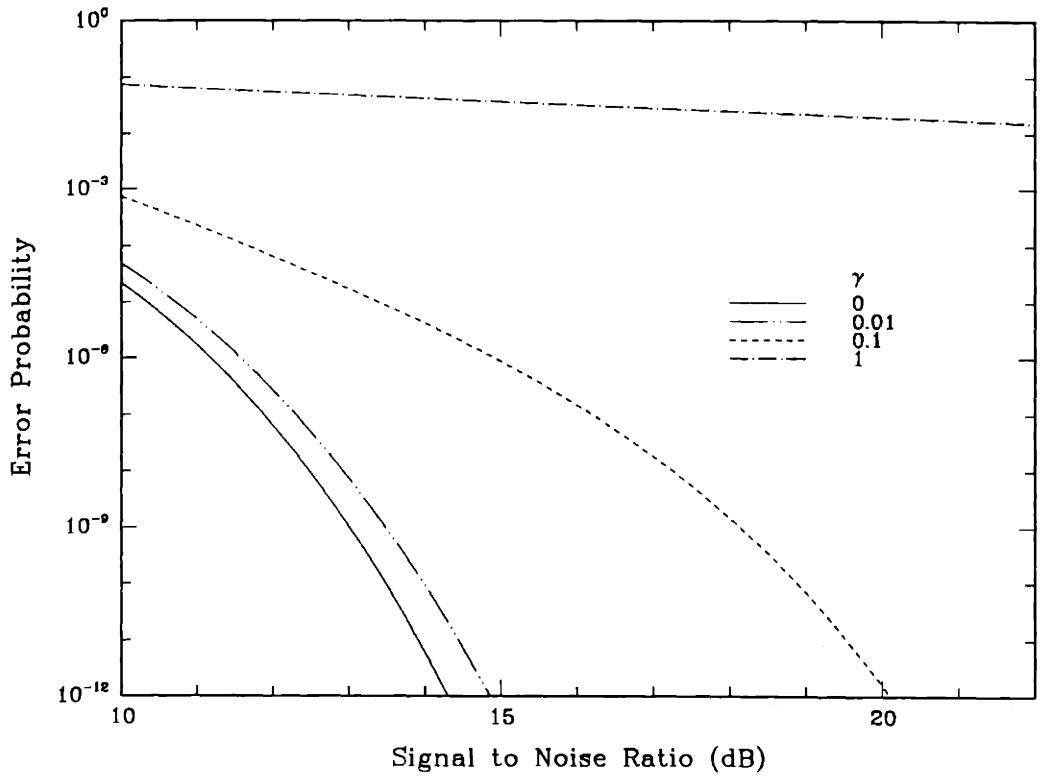

Figure 3-5: Error performance of inner product decision rule.

Appendix

3.A Derivation of the Maximum Likelihood Decision Rule

In this appendix, we derive the general Maximum Likelihood decision rule for DPSK to obtain Equations 3.21-3.25. Let c_i and s_i denote the x and y components of the observed vector $\mathbf{R}_i$. Then the joint conditional probability density function of the $2M$ vectors in rectangular coordinates can be written as

$$\begin{aligned} p_{0r}(\theta) &\triangleq p(\mathbf{R}_1, \ldots, \mathbf{R}_{2M} \mid \{\theta_i\}, a_n = 0) \\ &= \prod_{i=1}^{2M} (2\pi\sigma^2)^{-1} \exp\left[-\left((c_i - A\cos\theta_i)^2 + (s_i - A\sin\theta_i)^2\right)/2\sigma^2\right] \\ &= (2\pi\sigma^2)^{-2M} \exp\left(-\frac{1}{2\sigma^2}\sum_{i=1}^{2M}(c_i - A\cos\theta_i)^2 + (s_i - A\sin\theta_i)^2\right) . \end{aligned}$$

Now we will express this density in polar coordinates. This involves the substitution $c_i = R_i\cos\beta_i$, $s_i = R_i\sin\beta_i$ as well as the introduction of the Jacobian factor $\prod R_i$. Then we get

$$p_{0p}(\theta) = \left(\frac{e^{-A^2/2\sigma^2}}{2\pi\sigma^2}\right)^{2M} \left(\prod_{i=1}^{2M} R_i e^{-R_i^2/2\sigma^2}\right) \exp\left(\frac{A}{\sigma^2}\sum_{i=1}^{2M} R_i\cos(\beta_i - \theta_i)\right) . \tag{3.46}$$

Now we want to remove the conditioning on $\{\theta_i\}$. Note that the dependence of the conditional density on phase noise is only through the last exponential term. First let's recall from Equation 3.17 that $\theta_i = \theta_{i-1} + \Delta_i$, where Δ_i are i.i.d. normal with zero mean and variance α^2. Since Δ_{2M} enters only θ_{2M}, it is convenient to start the unconditioning with index $2M$ and proceed recursively. We obtain

$$\begin{aligned} E_{2M} &\triangleq E_{\Delta_{2M}} \exp\left(\frac{AR_{2M}}{\sigma^2}\cos(\beta_{2M} - \theta_{2M})\right) \\ &= \sum_{k_{2M}=-\infty}^{\infty} I_{k_{2M}}\left(\frac{AR_{2M}}{\sigma^2}\right)\cos(k_{2M}(\beta_{2M} - \theta_{2M-1}))e^{-k_{2M}^2\alpha^2/2} \end{aligned}$$

where we have first used the Bessel series [41, 40]

$$\exp(z\cos t) = \sum_{k=-\infty}^{\infty} I_k(z)\cos kt$$

and then used $E\cos k\Delta = e^{-k^2\alpha^2/2}$, $E\sin k\Delta = 0$ for $\Delta = N(0,\alpha^2)$. For removing the conditioning on Δ_{2M-1} we need to consider both the indices $2M-1$ and $2M$ in the exponential of (3.46). We now have

$$\begin{aligned} E_{2M-1} &\triangleq E_{\Delta_{2M-1},\Delta_{2M}} \exp\left(\frac{AR_{2M-1}}{\sigma^2}\cos(\beta_{2M-1}-\theta_{2M-1}) + \frac{AR_{2M}}{\sigma^2}\cos(\beta_{2M}-\theta_{2M})\right) \\ &= \sum_{k_{2M-1}}\sum_{k_{2M}} I_{k_{2M-1}}\left(\frac{AR_{2M-1}}{\sigma^2}\right) I_{k_{2M}}\left(\frac{AR_{2M}}{\sigma^2}\right) e^{-k_{2M}^2\alpha^2/2} \\ &\quad \cdot\ E_{\Delta_{2M-1}}\cos(k_{2M-1}(\beta_{2M-1}-\theta_{2M-2}-\Delta_{2M-1}))\cos(k_{2M}(\beta_{2M}-\theta_{2M-2}-\Delta_{2M-1}))\,. \end{aligned}$$

The latter expectation can be found as follows.

$$E_\Delta\ \cos(k(x-\Delta))\cos(l(y-\Delta)) = \frac{1}{2}e^{-(k+l)^2\alpha^2/2}\cos(kx+ly) + \frac{1}{2}e^{-(k-l)^2\alpha^2/2}\cos(kx-ly)$$

Since $I_k(x) = I_{-k}(x)$, the two terms above will have the same effect on the result, and we have

$$\begin{aligned} E_{2M-1} &= \sum_{k_{2M-1}}\sum_{k_{2M}} I_{k_{2M-1}}\left(\frac{AR_{2M-1}}{\sigma^2}\right) I_{k_{2M}}\left(\frac{AR_{2M}}{\sigma^2}\right) e^{-(k_{2M}^2+(k_{2M-1}+k_{2M})^2)\alpha^2/2} \\ &\quad \cdot\ \cos(k_{2M-1}(\beta_{2M-1}-\theta_{2M-2}) + k_{2M}(\beta_{2M}-\theta_{2M-2}))\,. \end{aligned}$$

By now, the recursive pattern has become clear. Removing the conditioning on each Δ_i introduces a new Bessel series with an additional exponential term. Thus after the expectation on Δ_1 is removed we have

$$\begin{aligned} E_1 &\triangleq E_{\Delta_1,\ldots,\Delta_{2M}} \exp\left(\frac{A}{\sigma^2}\sum_{i=1}^{2M} R_i\cos(\beta_i-\theta_i)\right) \\ &= \sum_{k_1}\cdots\sum_{k_{2M}}\left(\prod_{i=1}^{2M} I_{k_i}\left(\frac{AR_i}{\sigma^2}\right)\right) b(\vec{k})\cos\sum_{i=1}^{2M} k_i(\beta_i-\phi) \end{aligned}$$

where $b(\vec{k})$ is the collection of exponential terms given as

$$\begin{aligned} b(\vec{k}) &= \exp\left[-\frac{\alpha^2}{2}\left(k_{2M}^2 + (k_{2M}+k_{2M-1})^2 + \cdots + (k_{2M}+\cdots+k_1)^2\right)\right] \\ &= \exp\left[-\frac{\alpha^2}{2}\sum_{i=1}^{2M}\left(\sum_{l=i}^{2M} k_l\right)^2\right]\,. \end{aligned}$$

Finally we need to remove the conditioning on the initial phase ϕ. Since ϕ is uniformly distributed on $(-\pi, \pi)$, we have

$$E_\phi \cos(x - k\phi) = \begin{cases} \cos x & k = 0 \\ 0 & k \neq 0. \end{cases}$$

Thus only the terms with $k_1 + \cdots + k_{2M} = 0$ will not vanish in E_1. This results in a reduction of number of summations by one. We choose to eliminate the summation over k_1. Then

$$\begin{aligned} E_0 &\triangleq E_\phi E_1 \\ &= \sum_{k_2} \cdots \sum_{k_{2M}} I_{k_2+\cdots+k_{2M}} \left(\frac{AR_i}{\sigma^2}\right) \left(\prod_{i=2}^{2M} I_{k_i}\left(\frac{AR_i}{\sigma^2}\right)\right) a(\vec{k}) \cos \sum_{i=2}^{2M} k_i(\beta_i - \beta_1) \end{aligned}$$

where we have used $I_{-k}(x) = I_k(x)$ again, and we have slightly modified $b(\vec{k})$ to get $a(\vec{k})$ as given by (3.25). E_0 can be written in terms of the function $f(\cdot)$ defined in (3.24) as

$$E_0 = f\left(\frac{AR_1}{\sigma^2}, \ldots, \frac{AR_{2M}}{\sigma^2}, \beta_2 - \beta_1, \ldots, \beta_{2M} - \beta_1\right) \triangleq L_0 \, .$$

The unconditional density under $a_n = 0$ is now given by

$$p_0 = \left(\frac{e^{-A^2/2\sigma^2}}{2\pi\sigma^2}\right)^{2M} \left(\prod_{i=1}^{2M} R_i e^{-R_i^2/2\sigma^2}\right) L_0 \, . \tag{3.47}$$

The amplitudes $\{R_i\}$ are seen to be statistically independent while the phases are correlated through the function f. The density under $a_n = 1$ may be obtained from p_0 by the substitution $\beta_i \leftarrow \beta_i + \pi$ for $i = M+1, \ldots, 2M$. Thus

$$p_1 = \left(\frac{e^{-A^2/2\sigma^2}}{2\pi\sigma^2}\right)^{2M} \left(\prod_{i=1}^{2M} R_i e^{-R_i^2/2\sigma^2}\right) L_1 \tag{3.48}$$

where

$$L_1 \triangleq f\left(\frac{AR_1}{\sigma^2}, \ldots, \frac{AR_{2M}}{\sigma^2}, \beta_2 - \beta_1, \ldots, \beta_M - \beta_1, \pi + \beta_{M+1} - \beta_1, \ldots, \pi + \beta_{2M} - \beta_1\right) \, .$$

Therefore the Maximum Likelihood decision rule is obtained from (3.47) and (3.48) as

$$L_0 \underset{1}{\overset{0}{\gtrless}} L_1$$

as claimed in Equation 3.21.

3.B Proof of Lemma 3.1

In this appendix we will prove Lemma 3.1 which states that the function given by Equation (3.27) as

$$g(\alpha_2, \ldots, \alpha_N) = \sum_{k_2} \cdots \sum_{k_N} a(\vec{k}) \cos\left(\sum_{i=2}^{N} k_i \alpha_i\right)$$

where

$$a(\vec{k}) = \exp\left[-\frac{\alpha^2}{2} \sum_{i=2}^{N} \left(\sum_{l=i}^{N} k_l\right)^2\right]$$

satisfies

$$g(\alpha_2, \ldots, \alpha_N) = \prod_{i=2}^{N} \left(2\pi \sum_{n} p(\alpha_i - \alpha_{i-1} + 2n\pi)\right)$$

with

$$p(x) = \frac{1}{\sqrt{2\pi\alpha^2}} e^{-x^2/2\alpha^2}$$

and $\alpha_1 \equiv 0$.

To prove this result, we first rewrite $a(\vec{k})$ as

$$\begin{aligned} a(\vec{k}) &= \prod_{i=2}^{N} \exp\left[-\frac{\alpha^2}{2}\left(\sum_{l=i}^{N} k_l\right)^2\right] \\ &= \prod_{i=2}^{N} E_{\Delta_i}\left[\exp\left(-j\Delta_i \sum_{l=i}^{N} k_l\right)\right] \\ &= E_{\{\Delta\}} \exp\left[-j \sum_{i=2}^{N} \Delta_i \left(\sum_{l=i}^{N} k_l\right)\right] \end{aligned}$$

through the use of characteristic function of the Gaussian random variable Δ_i. Thus the

function $g(\cdot)$ can be written as

$$\begin{aligned} g(\alpha_2,\ldots,\alpha_N) &= \mathrm{Re}\, E \sum_{k_2}\cdots\sum_{k_N} \exp\left[j\sum_{i=2}^{N}\left(k_i\alpha_i - \Delta_i\sum_{l=i}^{N}k_l\right)\right] \\ &= \mathrm{Re}\, E \sum_{k_2}\exp\left[jk_2(\alpha_2-\Delta_2)\right]\sum_{k_3}\exp\left[jk_3(\alpha_3-(\Delta_2+\Delta_3))\right] \\ &\cdots \sum_{k_N}\exp\left[jk_N(\alpha_N-(\Delta_2+\cdots\Delta_N))\right] . \end{aligned}$$

Now we use the property

$$\sum_k e^{jkx} = 2\pi\sum_k \delta(x+2\pi k)$$

to obtain

$$\begin{aligned} g(\alpha_2,\ldots,\alpha_N) &= (2\pi)^{N-1}\mathrm{Re}\, E \sum_{k_2}\delta(\alpha_2-\Delta_2+2\pi k_2)\sum_{k_3}\delta(\alpha_3-(\Delta_2+\Delta_3)+2\pi k_3) \\ &\cdots \sum_{k_N}\delta(\alpha_N-(\Delta_2+\cdots+\Delta_N)+2\pi k_N) . \end{aligned}$$

Let E_i be the expectation above after the conditioning on Δ_i is removed. Then

$$\begin{aligned} E_N = \sum_{k_2}\delta(\alpha_2-\Delta_2+2\pi k_2) \quad &\cdots \quad \sum_{k_{N-1}}\delta(\alpha_{N-1}-(\Delta_2+\cdots\Delta_{N-1})+2\pi k_{N-1}) \\ &\cdot \quad \sum_{k_N} p(\alpha_N-(\Delta_2+\cdots+\Delta_{N-1})+2\pi k_N) . \end{aligned}$$

Applying the sifting property of the impulse to the last two terms and then taking the expectation over Δ_{N-1} one obtains

$$\begin{aligned} E_{N-1} &= \sum_{k_2}\delta(\alpha_2-\Delta_2+2\pi k_2)\cdots\sum_{k_{N-2}}\delta(\alpha_{N-2}-(\Delta_2+\cdots\Delta_{N-2})+2\pi k_{N-2}) \\ &\cdot \sum_{k_{N-1}}\sum_{k_N} p(\alpha_{N-1}-(\Delta_2+\cdots+\Delta_{N-2})+2\pi k_{N-1})p(\alpha_N-\alpha_{N-1}+2\pi(k_N-k_{N-1})) . \end{aligned}$$

By the time we remove all the conditionings through the use of sifting property we will have

$$E_1 = \sum_{k_2}\sum_{k_3}\cdots\sum_{k_N} p(\alpha_2+2\pi k_2)p(\alpha_3-\alpha_2+2\pi(k_3-k_2))\cdots p(\alpha_N-\alpha_{N-1}+2\pi(k_N-k_{N-1})) .$$

Now we let $n_2 = k_2$, $n_3 = k_3 - k_2, \ldots, n_M = k_N - k_{N-1}$ to get

$$E_1 = \prod_{i=2}^{N} \sum_{n_i} p(\alpha_i - \alpha_{i-1} + 2\pi n_i) = \prod_{i=2}^{N} \sum_{n} p(\alpha_i - \alpha_{i-1} + 2\pi n)$$

with the convention $\alpha_1 \equiv 0$. Since $g = (2\pi)^{N-1} E_1$, we have just proved the result

$$g(\alpha_2, \ldots, \alpha_N) = \prod_{i=2}^{N} \left(2\pi \sum_{n} p(\alpha_i - \alpha_{i-1} + 2\pi n) \right) . \square$$

Chapter 4

Detection of Amplitude Modulated Signals

In the previous two chapters, we studied frequency and phase modulation in the presence of phase noise. In this chapter we will investigate the detection of amplitude modulated signals. Amplitude modulation is a promising signaling format in the presence of phase noise since the coupling between the phase and the amplitude is likely to be weaker than the phase/phase and the phase/frequency coupling that limited the performance of phase and frequency modulation respectively. We consider binary On-Off-Keying (OOK) where the transmitted signal is a phase noisy sinusoid for a data bit of "1", and no signal is transmitted for a data bit of "0". Thus the received IF signal is

$$r(t) = a_k A \cos(2\pi f_c t + \theta(t)) + n(t) \quad (k-1)T < t < kT \tag{4.1}$$

where $a_k = 0$ or 1 and the rest of the parameters are as defined previously.

We start by considering optimum detection of OOK signals. This leads naturally to the envelope detection where several of the results from Chapter 2 can be used. We show that, with envelope detection, OOK has a higher probability of error at a given *peak* signal-to-noise ratio than FSK. However the penalty imposed by phase noise is less for OOK. Thus amplitude modulation is seen to exhibit more robustness against phase noise than frequency and phase modulation.

4.1 Optimal Receiver Formulation

The formulation of the optimal reception of OOK signals has many features in common with that of DPSK signals. The front end of the receiver has the same quadrature-filter-sample structure that we considered for phase modulation. The only difference is that the sample

processor processes only M samples that belong to the current bit interval. The in-phase components of the samples are given by

$$c_i = a_n A \cos\theta_i + n_{c,i} \quad i = 1, \ldots, M \tag{4.2}$$

and for the quadrature components s_i, cos is replaced by sin and $n_{c,i}$ is replaced by $n_{s,i}$. The phase samples θ_i obey, as before, the relation

$$\theta_i = \phi + \sum_{k=1}^{i} \Delta_k \quad 1 \leq i \leq M \tag{4.3}$$

where ϕ is the initial phase and Δ_k are the phase noise increments which are i.i.d. $N(0, \alpha^2)$ with $\alpha^2 = \gamma/M$. The additive noise samples are i.i.d. $N(0, \sigma^2)$ with $\sigma^2 = N_0 M/T$.

The role of the initial phase ϕ in the amplitude modulated system is not as important as the phase modulated counterpart. We will consider two scenarios in the following discussion. First, we will assume that the initial phase is perfectly tracked, i.e, $\phi = 0$. Later, we will assume that no phase tracking is performed, and hence ϕ is uniformly distributed on $(-\pi, \pi]$. We will obtain the optimal decision rules for both of these cases and evaluate their performances.

4.1.1 Known Initial Phase

In the case where the initial phase is perfectly known, one can include this phase in the correlators and assume $\phi = 0$. The probability density functions corresponding to the samples under the two hypotheses can then be found. The density for $a_n = 0$ is particularly simple since there is no phase noisy signal in this case. The amplitudes are i.i.d. Rayleigh distributed and the phases are i.i.d. uniform, and the amplitudes and the phases are mutually independent. For $a_n = 1$, the density can be found in the same way as in the previous chapter, first by conditioning on the phase noise. The resulting likelihood ratio test is

$$L \underset{0}{\overset{1}{\gtrless}} e^{A^2 M/2\sigma^2} \tag{4.4}$$

where

$$L = \sum_{k_1} \cdots \sum_{k_M} \left(\prod_{i=1}^{M} I_{k_i}\left(\frac{AR_i}{\sigma^2}\right)\right) \exp\left[-\frac{\alpha^2}{2}\sum_{i=1}^{M}\left(\sum_{l=i}^{M} k_l\right)^2\right] \cos\left(\sum_{i=1}^{M} k_i \beta_i\right) .$$

The decision rule is again complicated. We will specialize to the case of weak phase noise which is usually the case of interest, especially for large M. We approximate the decision variable as a first order perturbation around $\alpha^2 = 0$ as

$$L(\alpha^2) \simeq L(0) + \alpha^2 L'(0) \tag{4.5}$$

where the derivative is with respect to α^2. After some algebra that we give in Appendix 4.A, the decision rule reduces to

$$\frac{1}{M}\sum_{i=1}^{M} R_i \cos\beta_i + \frac{\gamma TA}{2N_0}\frac{1}{M^3}\sum_{i,j=1}^{M} \min(i,j) R_i \sin\beta_i R_j \sin\beta_j - \frac{\gamma}{2}\frac{1}{M^2}\sum_{i=1}^{M} i R_i \cos\beta_i \underset{0}{\overset{1}{\gtrless}} \frac{A}{2} \tag{4.6}$$

The interesting observation here is that the first term in the decision variable corresponds to that with no phase noise, and the other two terms act as correction terms which vanish as γ tends to 0. The quadrature components are correlated in the second term in a way in which the newer samples carry more weight. The same is true for the weighted sum of in-phase components in the third term.

As $M \to \infty$, the decision rule becomes

$$\frac{1}{T}\int_0^T r_c(t)\,dt + \frac{\gamma TA}{2N_0}\frac{1}{T^3}\int_0^T\int_0^T \min(t,\tau) r_s(t) r_s(\tau)\,dt\,d\tau - \frac{\gamma}{2}\frac{1}{T^2}\int_0^T t r_c(t)\,dt \underset{0}{\overset{1}{\gtrless}} \frac{A}{2} \tag{4.7}$$

The performance analysis of this decision rule, even in the limit of large M, seems to be difficult. A suboptimal version of this receiver with only the first term in (4.6) or (4.7) may be possible to analyze. The first term may be written as

$$\frac{1}{M}\sum_{i=1}^{M} R_i \cos\beta_i = \frac{a_n A}{M}\sum_{i=1}^{M}\cos\theta_i + \frac{1}{M}\sum_{i=1}^{M} n_{c,i}\ . \tag{4.8}$$

The error probability with a "0" sent is independent of the phase noise, and is easily found as

$$P_e(0) = Q\left(\sqrt{\xi/2}\right) \tag{4.9}$$

with $\xi = A^2T/2N_0$. The error probability with a "1" sent must be first conditioned on the

phase noise process. This yields

$$P_e\left(1|\theta(t)\right) = Q\left(\sqrt{2\xi}\left(\frac{1}{M}\sum_{i=1}^{M}\cos\theta_i - \frac{1}{2}\right)\right) . \tag{4.10}$$

To obtain the unconditional error probability we need to remove the conditioning on $\theta(t)$. A reasonably tight approximation may be obtained by interchanging the expectation and the Q function, although this is not a lower bound as in the FSK case since the Q function is not convex for negative arguments. We then obtain

$$P_e(1) \simeq Q\left(\sqrt{2\xi}\left(\frac{e^{-\gamma/2M} - e^{-(M+1)\gamma/2M}}{M(1-e^{-\gamma/2M})} - \frac{1}{2}\right)\right) . \tag{4.11}$$

In the limit as $M \to \infty$ the error probability becomes

$$P_e \simeq \frac{1}{2}Q\left(\sqrt{\xi/2}\right) + \frac{1}{2}Q\left(\sqrt{2\xi}\left[\frac{2}{\gamma}(1-e^{-\gamma/2}) - \frac{1}{2}\right]\right) . \tag{4.12}$$

This error probability is shown in Figure 4-1. It is seen that OOK has a better tolerance to phase noise than DPSK.

4.1.2 Unknown Initial Phase

When the receiver does not attempt to estimate the phase in the decision process, the initial phase may be modeled as a random variable which is uniformly distributed over $(-\pi, \pi]$. In this section, we will find the optimum receiver under this condition and evaluate its performance.

The maximum likelihood decision rule may be obtained in a way similar to the DPSK case to be

$$L \underset{0}{\overset{1}{\gtrless}} e^{A^2M/2\sigma^2} \tag{4.13}$$

where the decision variable L is now given by

$$L = \sum_{k_2}\cdots\sum_{k_M} I_{k_2+\cdots k_M}(AR_1/\sigma^2)\left(\prod_{i=2}^{M} I_{k_i}(AR_i/\sigma^2)\right) \quad \exp\left[-\frac{\alpha^2}{2}\sum_{i=2}^{M}\left(\sum_{l=i}^{M}k_l\right)^2\right] \cdot \cos\left(\sum_{i=2}^{M}k_i(\beta_i-\beta_1)\right)$$

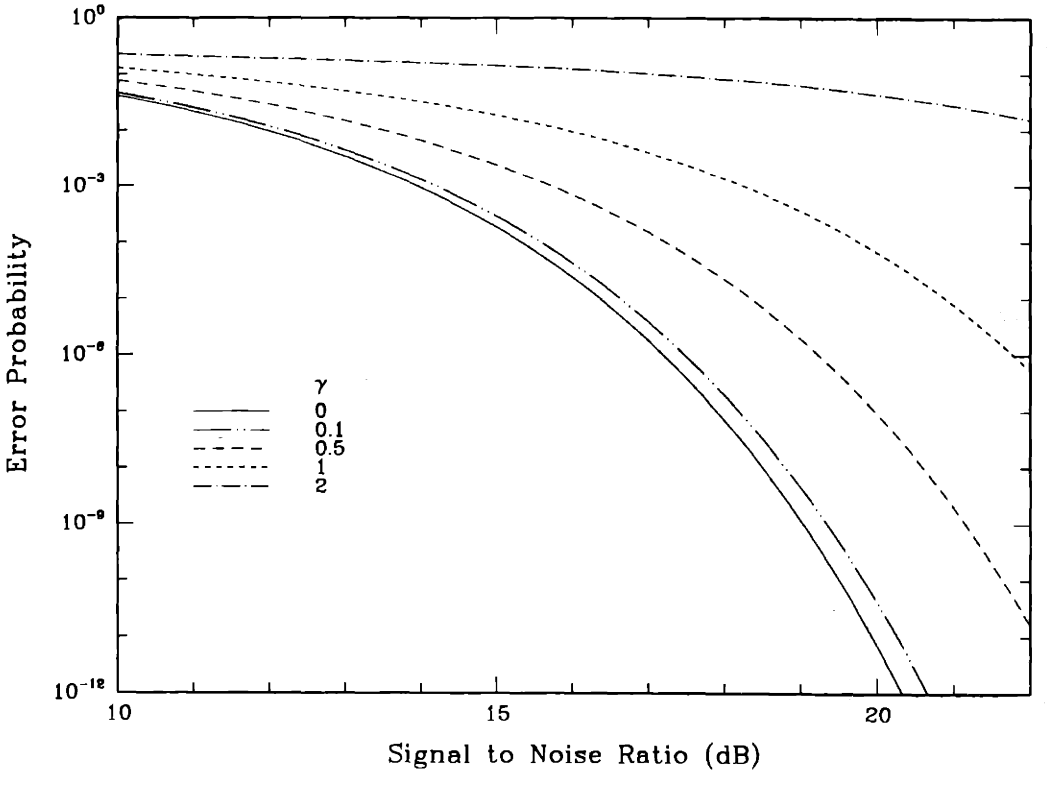

Figure 4-1: Error probability for the coherent OOK receiver.

which is again too complicated to implement or to analyze. Using the first order perturbation that we used for the case of known initial phase and applying techniques which are very similar to the ones in Appendix 4.A, we obtain the decision rule for the case of weak phase noise as

$$\frac{1}{M}\left|\vec{\mathbf{R}_1}+\cdots\vec{\mathbf{R}_M}\right|+\frac{\gamma}{2M^2}C\underset{0}{\overset{1}{\gtrless}}\frac{A}{2} \tag{4.14}$$

where C is given by

$$\begin{aligned} C = & \sum_{i,j=2}^{M} \min(i,j)\left(\frac{A}{\sigma^2 g^2}-\frac{1}{g^3}\right)\left[\sum_{m=1}^{M}\vec{\mathbf{R}_i}\otimes\vec{\mathbf{R}_m}\right]\left[\sum_{n=1}^{M}\vec{\mathbf{R}_j}\otimes\vec{\mathbf{R}_n}\right]-\frac{1}{g}\sum_{i=2}^{M} i\vec{\mathbf{R}_i}\cdot\vec{\mathbf{R}_1} \\ & - \frac{1}{2g}\sum_{i,j=2}^{M}|i-j|\vec{\mathbf{R}_i}\cdot\vec{\mathbf{R}_j} \end{aligned}$$

with

$$g=\left|\vec{\mathbf{R}_1}+\cdots\vec{\mathbf{R}_M}\right|$$

$$\vec{\mathbf{R}_i}\otimes\vec{\mathbf{R}_m}\triangleq R_i R_m\sin(\beta_i-\beta_m)\,.$$

We see that, once again, the decision variable is that of the optimal receiver perturbed by some complicated correction term. In the limit of large M, the decision rule becomes

$$\sqrt{\bar{c}^2+\bar{s}^2}+\gamma K\underset{0}{\overset{1}{\gtrless}}\frac{A}{2} \tag{4.15}$$

where

$$\begin{aligned} K = & \frac{1}{2}\left(\frac{AT}{N_0}-\frac{1}{\sqrt{\bar{c}^2+\bar{s}^2}}\right)\frac{1}{\bar{c}^2+\bar{s}^2}\frac{1}{T^3}\int_0^T\int_0^T \min(t,\tau)\left[\bar{c}r_s(t)-\bar{s}r_c(t)\right]\left[\bar{c}r_s(\tau)-\bar{s}r_c(\tau)\right]dt\,d\tau \\ & - \frac{1}{4}\frac{1}{\sqrt{\bar{c}^2+\bar{s}^2}}\frac{1}{T^3}\int_0^T\int_0^T |t-\tau|\left[r_c(t)r_c(\tau)+r_s(t)r_s(\tau)\right]\left[\bar{c}r_s(\tau)-\bar{s}r_c(\tau)\right]dt\,d\tau \end{aligned}$$

and

$$\begin{aligned} \bar{c} &= \frac{1}{T}\int_0^T r_c(t)\,dt \\ \bar{s} &= \frac{1}{T}\int_0^T r_s(t)\,dt\,. \end{aligned}$$

The first term in (4.15) corresponds to the standard envelope detector. The perturbation

term contains nonintuitive correlations between the in-phase and quadrature components that we will not elaborate on. Instead we will concentrate on the envelope detector structures in the remainder of this chapter.

4.2 Envelope Detection of OOK Signals

In this section, we will be consider the envelope detection of OOK modulated signals. We have seen in the previous section that for very small phase noise strength, the standard envelope detector is close to the optimal receiver in the absence of an initial phase estimate. The improvement obtained by modifying the envelope detector for FSK motivates us to explore the performance of a similar scheme for OOK. The IF receiver structure is shown in Figure 4-2. The receiver is similar to that of FSK, except that only one of the two branches of the FSK receiver is retained and the decision variable is compared to a threshold h. The front end consists of a quadrature demodulator, and a set of integrators of duration T'. The outputs of the integrators are squared and added, and then sampled.

We again consider three receiver forms. The first is a single sample receiver which samples once a bit, i. e. $T' = T$. This is the conventional envelope detector. The second receiver has $T' = T/M$ for some integer M, but still samples once at the end of the bit duration to obtain the decision variable Y. We call this a single filter receiver (with optimized bandwidth). The third receiver also has $T' = T/M$, but the decision variable is the sum of M samples, $Y = \sum_{k=1}^{M} Y_k$. This will be called a double filter receiver since the addition of M samples corresponds to a lowpass filtering operation. The value of M is to be determined for the latter two receivers to minimize the error probability.

Now we proceed to find the probability of error for these receiver structures. The method employed is similar to that of Chapter 2 in that we first condition the error probability on the phase noise process, then we remove this conditioning either by numerical integration or via analytical bounds.

We first consider the single sample receiver. The decision variable can be written as

$$Y = \left| \frac{A}{2} a_n \int_0^T e^{j\theta(t)}\, dt + n_c + j n_s \right|^2 \tag{4.16}$$

where n_c and n_s are independent identically distributed Gaussian random variables with zero mean and variance $\sigma^2 = N_0 T/4$. When $a_n = 0$, the decision variable has an exponential

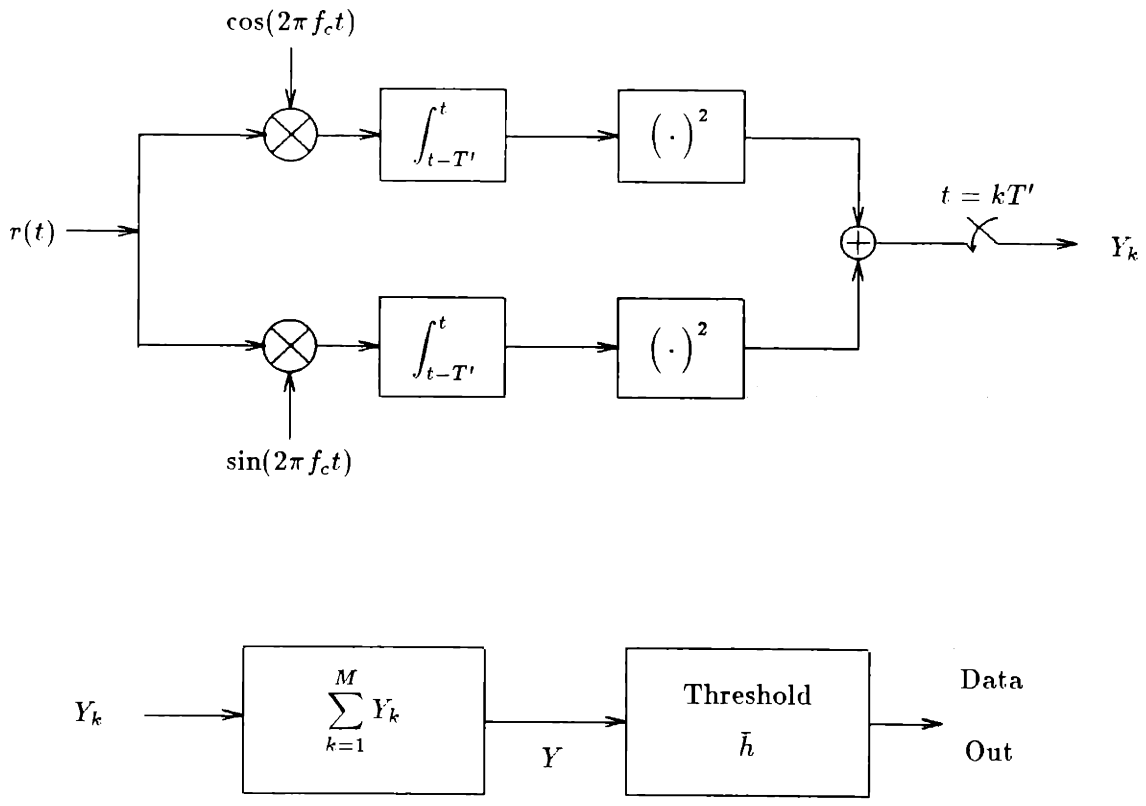

Figure 4-2: IF receiver for envelope detection of OOK signals. For single filter receiver the adder is absent, and $Y = Y_M$.

distribution given by

$$p(y) = \frac{1}{2\sigma^2} e^{-y/2\sigma^2} \quad y \geq 0 \, .$$

For $a_n = 1$, both additive noise and phase noise are present. We first condition the density on the phase noisy signal component

$$X' = \left| \frac{A}{2} \int_0^T e^{j\theta(t)} \, dt \right|^2$$

to obtain

$$p(y|X') = \frac{1}{2\sigma^2} e^{-(y+X')/2\sigma^2} I_0 \left(\frac{\sqrt{X'y}}{\sigma^2} \right)$$

which is a well known noncentral Chi-square distribution with two degrees of freedom.

Let $P_e(0)$ be the probability of error when $a_n = 0$, and let $P_e(1|X')$ be the conditional probability of error given $a_n = 1$ and X'. Then we have

$$\begin{aligned} P_e(0) &= \Pr[Y > h | a_n = 0] \\ &= \int_h^\infty \frac{1}{2\sigma^2} e^{-y/2\sigma^2} \, dy = e^{-h/2\sigma^2} \end{aligned}$$

and

$$\begin{aligned} P_e(1|X') &= \Pr[Y \leq h | a_n = 1, X'] \\ &= \int_0^h \frac{1}{2\sigma^2} e^{-(y+X')/2\sigma^2} I_0 \left(\frac{\sqrt{X'y}}{\sigma^2} \right) \, dy \\ &= 1 - Q\left(\sqrt{\frac{X'}{\sigma^2}}, \sqrt{\frac{h}{\sigma^2}} \right) \end{aligned}$$

where $Q(\cdot, \cdot)$ is the Marcum's Q function defined as

$$Q(a, b) \triangleq \int_b^\infty e^{-(a^2+x^2)/2} I_0(ax) x \, dx \, .$$

It is convenient to define a normalize threshold $\bar{h}$ as

$$\bar{h} = \frac{h}{2\sigma^2}$$

and to rewrite X' as follows

$$X' = \left| \frac{A}{2} \int_0^T e^{j\theta(t)}\, dt \right|^2 = \frac{A^2T^2}{4} \left| \int_0^1 e^{j\sqrt{\gamma}\psi(t)}\, dt \right|^2$$

where $\psi(t)$ is the standard Brownian motion and γ is the phase noise strength. Now with the previous definition of $X(\gamma)$ as

$$X(\gamma) = \left| \int_0^1 e^{j\sqrt{\gamma}\psi(t)}\, dt \right|^2$$

we have

$$\frac{X'}{2\sigma^2} = \xi X(\gamma)$$

where $\xi = A^2T/2N_0$ is the signal to noise ratio. Then the error probabilities become

$$\begin{aligned} P_e(0) &= e^{-\bar{h}} \\ P_e\left(1|X(\gamma)\right) &= 1 - Q\left(\sqrt{2\xi X(\gamma)}, \sqrt{2\bar{h}}\right) \end{aligned}$$

and the unconditional error probability is given by

$$P_e = \frac{1}{2}e^{-\bar{h}} + \frac{1}{2}\left[1 - E\left[Q\left(\sqrt{2\xi X(\gamma)}, \sqrt{2\bar{h}}\right)\right]\right] \tag{4.17}$$

which reduces to the well known OOK error probability for $\gamma = 0$.

The approximate probability density function, $q_\gamma(x)$, of $X(\gamma)$ was obtained in Chapter 2. Therefore the error probability in (4.17) can be evaluated numerically. The results are shown in Figure 4-3 for different γ values. The threshold $\bar{h}$ has been optimized at each point to minimize the error probability. It is seen that the performance of the single sample receiver deteriorates rapidly with the introduction of phase noise.

Next we consider the single filter receiver. The analysis for this case is very similar to that of the single sample receiver, since the decision variable consists of a single sample as well. The additive noise variances increase by a factor of M, while the effective phase noise strength decreases by the same factor. This is due to the reduction of the integration period by M. As a result, the error probability of the single filter receiver is given by

$$P_e = \frac{1}{2}e^{-\bar{h}} + \frac{1}{2}\left[1 - E\left[Q\left(\sqrt{2\xi X(\gamma/M)/M}, \sqrt{2\bar{h}}\right)\right]\right] \tag{4.18}$$

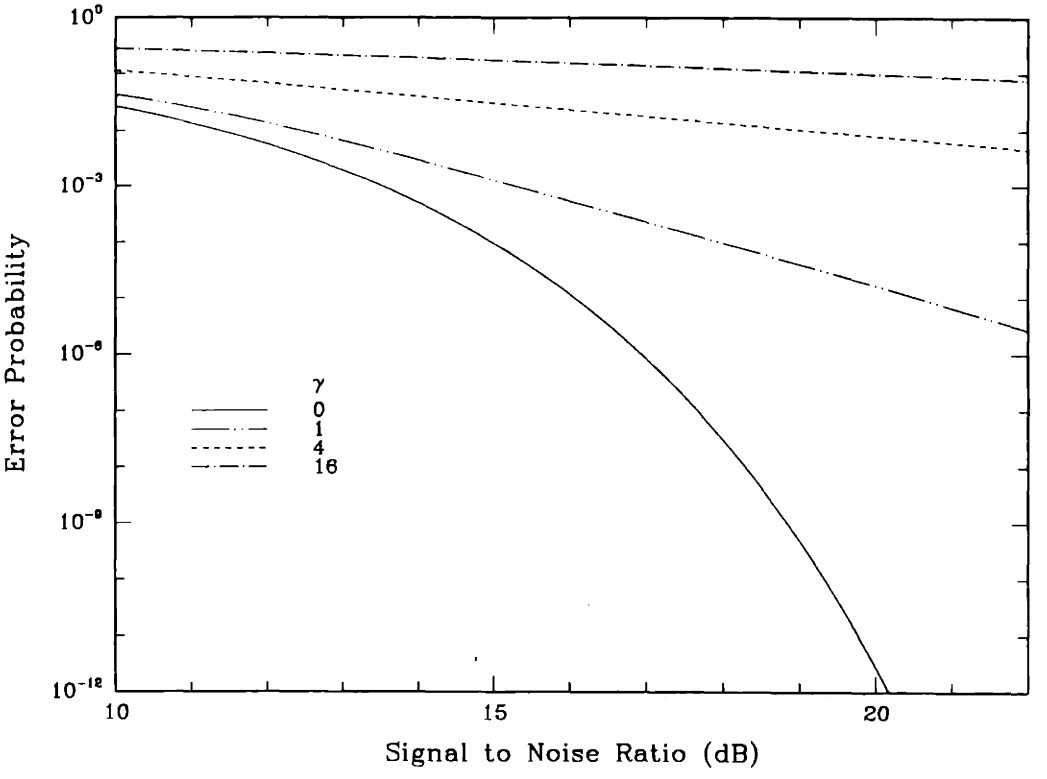

Figure 4-3: Error probability for the single sample receiver.

The value of M that minimizes P_e must be found as well as the normalized threshold $\bar{h}$. The former optimization poses a computational problem since the evaluation of the density function $q(x)$ for many values of γ/M is computationally prohibitive. However due to the exponential approximation for $X(\gamma)$ introduced in Chapter 2, this problem can be avoided as follows. We have

$$q_{\gamma/M}(x) = q_\gamma(x^M) M x^{M-1}$$

which results in

$$E\left[f\left(X(\gamma/M)\right)\right] = \int_0^1 f(x^{1/M}) q_\gamma(x)\, dx$$

for any function $f(\cdot)$ defined on $(0,1)$. Thus

$$P_e = \frac{1}{2} e^{-\bar{h}} + \frac{1}{2}\left[1 - \int_0^1 Q\left(\sqrt{2\xi x^{1/M}/M}, \sqrt{2\bar{h}}\right) q_\gamma(x)\, dx\right] \tag{4.19}$$

which requires only one density function, instead of possibly many. The resulting computation is very easy. Its results are shown in Figure 4-4. Again we see that the performance degradation due to phase noise is severe. The single filter receiver introduces an improvement over the single sample receiver at no additional hardware complexity. All that is needed is an estimate of the signal to noise ratio and the phase noise strength, and an a priori computation of the optimum bandwidth expansion factor M.

Finally we consider the performance of the double filter receiver. In this case, the decision variable is a sum of M statistically independent random variables, $\{Y_k\}$, under both hypotheses. The additive noise components are Gaussian with variance $\alpha^2 = N_0 T/4M$. It is convenient to normalize both the decision variable and the threshold as $V = Y/2\alpha^2$, $\bar{h} = h/2\alpha^2$. Then for $a_n = 0$, V is the sum of squares of $2M$ Gaussian random variables, thus it has a Gamma density given as

$$p(v) = \frac{v^{M-1}}{(M-1)!} e^{-v}\,.$$

Similar to our previous development, for $a_n = 1$, we first condition on the phase noise process, and obtain

$$p\left(v \mid \{\theta(t)\}\right) = \left(\frac{v}{r}\right)^{(M-1)/2} e^{-(v+r)} I_{M-1}(\sqrt{4rv})$$

where the dependence on the phase noise process is exhibited in the parameter r. This

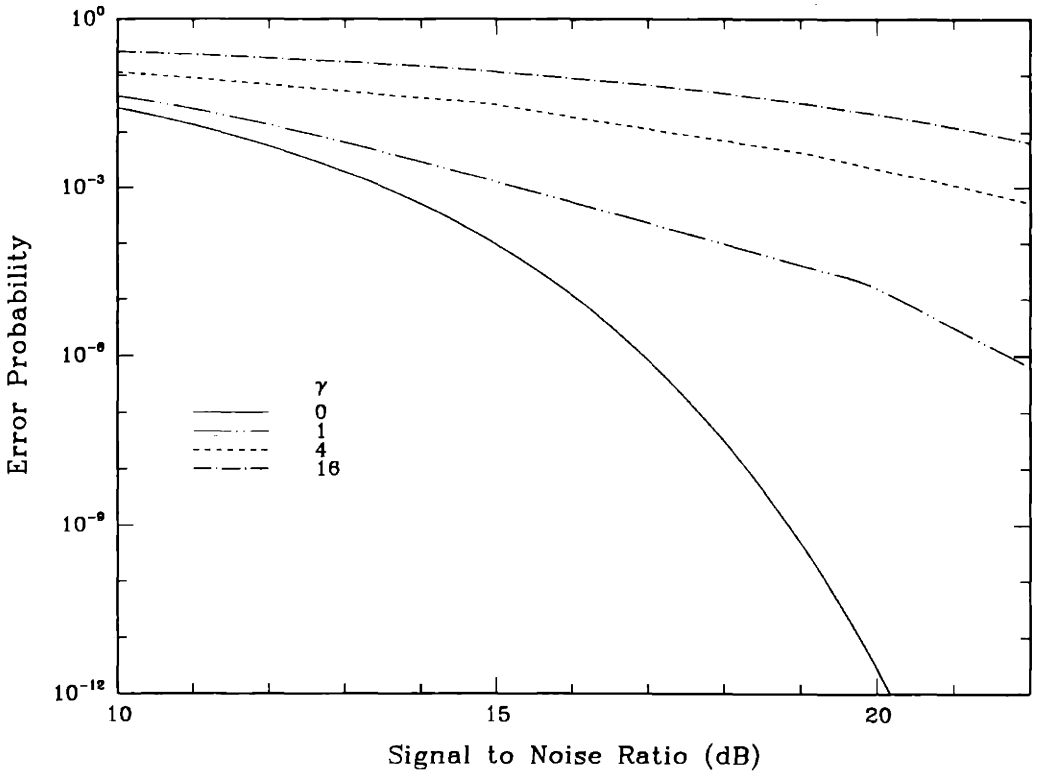

Figure 4-4: Error probability for the single filter receiver.

parameter is defined as

$$r = \frac{1}{2\alpha^2} \sum_{k=1}^{M} |x(k)|^2$$

where

$$x(k) = \frac{A}{2} \int_{(k-1)T/M}^{kT/M} e^{j\theta(t)}\, dt \quad k = 1, \ldots, M.$$

With a manipulation identical to the one employed for FSK, we obtain

$$r = \frac{\xi}{M} \sum_{k=1}^{M} X_k(\gamma/M) \tag{4.20}$$

where $X_k(\cdot)$ are independent observations of the random variable $X(\cdot)$. The parameter r is the phase noisy signal to noise ratio that we encountered before. It is always less than the actual SNR ξ, and approaches ξ with probability 1 as $M \to \infty$.

It is interesting to see that the dependence of error probability on phase noise is through a single random variable r. The error probability for $a_n = 0$ is easily seen to be

$$P_e(0) = \sum_{k=0}^{M-1} \frac{\bar{h}^k}{k!} e^{-\bar{h}}$$

while the error probability for $a_n = 1$ conditioned on r is obtained as

$$\begin{aligned} P_e(1|r) &= 1 - \int_{\bar{h}}^{\infty} \left(\frac{v}{r}\right)^{(M-1)/2} e^{-(v+r)} I_{M-1}(\sqrt{4rv})\, dr \\ &= 1 - Q_M(\sqrt{2r}, \sqrt{2\bar{h}}) \end{aligned}$$

where $Q_M(\cdot,\cdot)$ is the generalized Marcum's Q function [44] of order M defined as

$$Q_M(a,b) \triangleq \int_b^{\infty} \frac{x^M}{a^{M-1}} e^{-(x^2+a^2)/2} I_{M-1}(ax)\, dx$$

Note that there is no symmetry between $P_e(0)$ and $P_e(1)$ in OOK, unlike FSK. For a given r, $P_e(1|r)$ increases with M, as well as $P_e(0)$. On the other hand, for a given M, $P_e(1|r)$ decreases with r. However, r is a function of M as well, and it increases with probability 1 with M. Therefore there is a tradeoff in choosing M, between the additive and phase noise processes. The optimal values of M will be lower than those of FSK, since $P_e(0)$ is uniformly increasing in M.

The unconditional probability of error is given as

$$P_e = \frac{1}{2}\sum_{k=0}^{M-1}\frac{\bar{h}^k}{k!}e^{-\bar{h}} + \frac{1}{2}\left[1 - E\left[Q_M\left(\sqrt{2r}, \sqrt{2\bar{h}}\right)\right]\right] \tag{4.21}$$

which is to be optimized over M and $\bar{h}$. Since r is a sum of M independent identically distributed random variables, the expectation involves M-fold self-convolution of the density $q_{\gamma/M}(x)$. Thus we have, once again, the problem of many density computations as well as many convolutions. For the single filter receiver, this problem could be solved by a change of variable; for double filter FSK, the form of the conditional error probability allowed us eliminate the problem as well. However, this does not seem possible in this case, due to the fact that generalized Marcum's Q function does not have a compact explicit representation (for example, a finite series). Therefore, we will use three different techniques to obtain a reliable estimate of the error probability. First, we use Jensen's inequality to obtain a lower bound. We have found this inequality to provide a rather tight estimate of the error probability for FSK. Here we postulate that the quantity $P_e(1|r)$ is a convex $\cup$ function of r for a given threshold $\bar{h}$, so that an interchange of the expectation operator with the function Q_M will result in the following lower bound:

$$P_e \geq \frac{1}{2}\sum_{k=0}^{M-1}\frac{\bar{h}^k}{k!}e^{-\bar{h}} + \frac{1}{2}\left[1 - Q_M\left(\sqrt{2\xi\bar{X}(\gamma/M)}, \sqrt{2\bar{h}}\right)\right] \tag{4.22}$$

where $\bar{X}(\cdot)$ denotes the mean of $X(\cdot)$. From Chapter 2 we have

$$\bar{X}(\gamma) = \frac{4}{\gamma}\left[1 - \frac{2}{\gamma}(1 - e^{-\gamma/2})\right] . \tag{4.23}$$

Equation (4.22) in conjunction with (4.23) describe a lower bound that we will use in the following discussion. Note that the lower bound corresponds to an optimistic scenario where the random variable r does not deviate from its mean.

The second technique to be employed in estimating (4.21) is the Chernoff bound which states that

$$\Pr(V \leq \bar{h}) \leq e^{s\bar{h}}E(e^{-sV})$$

for all $s \geq 0$, which provides an upperbound to $P_e(1)$ in terms of the moment generating function of the decision variable under $a_n = 1$. This moment generating function will be

found in two stages. We first note that

$$V = \sum_{k=1}^{M} \left| \frac{x(k)}{\sqrt{2\alpha^2}} + \bar{n}_c(k) + j\bar{n}_s(k) \right|^2 \triangleq \sum_{k=1}^{M} V_k$$

where $x(k)$ are as previously defined, and $\bar{n}_c(k)$, $\bar{n}_s(k)$ are i.i.d. Gaussian with variance $1/2$. Therefore V_k are also independent with the conditional moment generating function [25]

$$E\left[e^{-sV_k} \mid x(k)\right] = \frac{1}{1+s} \exp\left(-\frac{s|x(k)|^2/2\alpha^2}{1+s}\right) .$$

Then the conditional moment generating function of V depends only on r, and is given by

$$E\left[e^{-sV} \mid r\right] = \frac{1}{(1+s)^M} \exp\left(-\frac{sr}{1+s}\right) .$$

Since r is a sum of M i.i.d. random variables, the conditioning on r is removed to yield

$$E\left[e^{-sV}\right] = \frac{1}{(1+s)^M} \left[E\left[\exp\left(-\frac{s\xi}{M(1+s)} X(\gamma/M)\right)\right]\right]^M$$

and finally the Chernoff bound is given by

$$P_e \leq \frac{1}{2} \sum_{k=0}^{M-1} \frac{\bar{h}^k}{k!} e^{-\bar{h}} + \frac{1}{2} \frac{1}{(1+s)^M} \left[\Phi_{\gamma/M}\left(\frac{s\xi}{M(1+s)}\right)\right]^M \tag{4.24}$$

where we denote the moment generating function of $X(\gamma)$ by $\Phi_\gamma(s) = E(e^{-sX(\gamma)})$. Lastly we relate $\Phi_{\gamma/M}(\cdot)$ to $q_\gamma(\cdot)$ as

$$\Phi_{\gamma/M}(s) = \int_0^1 \exp(-sx^{1/M}) q_\gamma(x)\, dx \tag{4.25}$$

which eliminates the need for computation of many density functions. An additional optimization needs to be performed over nonnegative s to obtain the tightest upper bound.

The Jensen bound and the Chernoff bound are shown in Figure 4-5 for various γ values. Note that the bounds are very close for all values of γ and ξ. Therefore, the computationally simpler lower bound may be used reliably.

A third approach in estimating the performance of the double filter receiver is Gaussian approximation. Since the normalized decision variable V is the sum of M independent identically distributed random variables under both hypotheses, it is tempting to use a

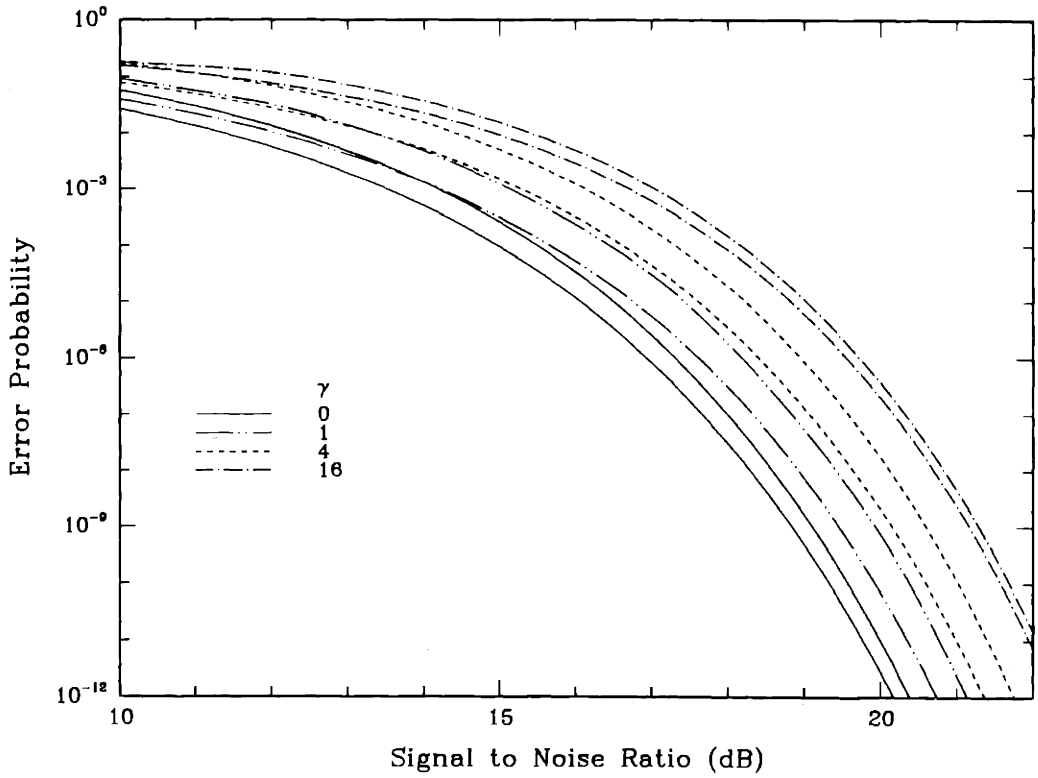

Figure 4-5: Comparison of Jensen and Chernoff bounds for the double filter receiver.

Gaussian approximation for V. For $a_n = 0$, both the mean and the variance of V are easily obtained to be M. For $a_n = 1$, the conditional mean of V is $M + r$, while its conditional variance is $M + 2r$. Therefore we have with the Gaussian approximation

$$\begin{aligned} P_e(0) &\simeq Q\left(\frac{\bar{h} - M}{\sqrt{M}}\right) \\ P_e(1|r) &\simeq Q\left(\frac{M + r - \bar{h}}{\sqrt{M + 2r}}\right) . \end{aligned}$$

Due to the difficulty of removing the conditioning exactly, we will further approximate $P_e(1)$ by

$$P_e(1) \simeq Q\left(\frac{M + E(r) - \bar{h}}{\sqrt{M + 2E(r)}}\right) .$$

Under these approximations the error probability becomes

$$P_e \simeq \frac{1}{2}Q\left(\frac{\bar{h} - M}{\sqrt{M}}\right) + \frac{1}{2}Q\left(\frac{M + \xi\bar{X}(\gamma/M) - \bar{h}}{\sqrt{M + 2\xi\bar{X}(\gamma/M)}}\right) \tag{4.26}$$

which is to be optimized over M and $\bar{h}$. This is the error probability of a system in which the decision variables are Gaussian with nonidentical variances. The optimal setting of the threshold is complicated. A conventional threshold setting is one that equalizes the two error probabilities. This results in an error probability of

$$P_e \simeq Q\left(\frac{\xi\bar{X}(\gamma/M)}{\sqrt{M} + \sqrt{M + 2\xi\bar{X}(\gamma/M)}}\right) \tag{4.27}$$

where the underlying threshold setting is

$$\bar{h}_G = M + \frac{\sqrt{M}\xi\bar{X}(\gamma/M)}{\sqrt{M} + \sqrt{M + 2\xi\bar{X}(\gamma/M)}} . \tag{4.28}$$

It is known that this nonoptimal threshold setting gives results that are very close to the optimal threshold setting for the Gaussian approximation [45]. The error probability predicted by the Gaussian approximation is compared with the previously obtained lower bound in Figure 4-6. For each γ value the Gaussian curve is the upper curve. It is seen that the two results are in good agreement uniformly over the set of γ and ξ values. Therefore we con-

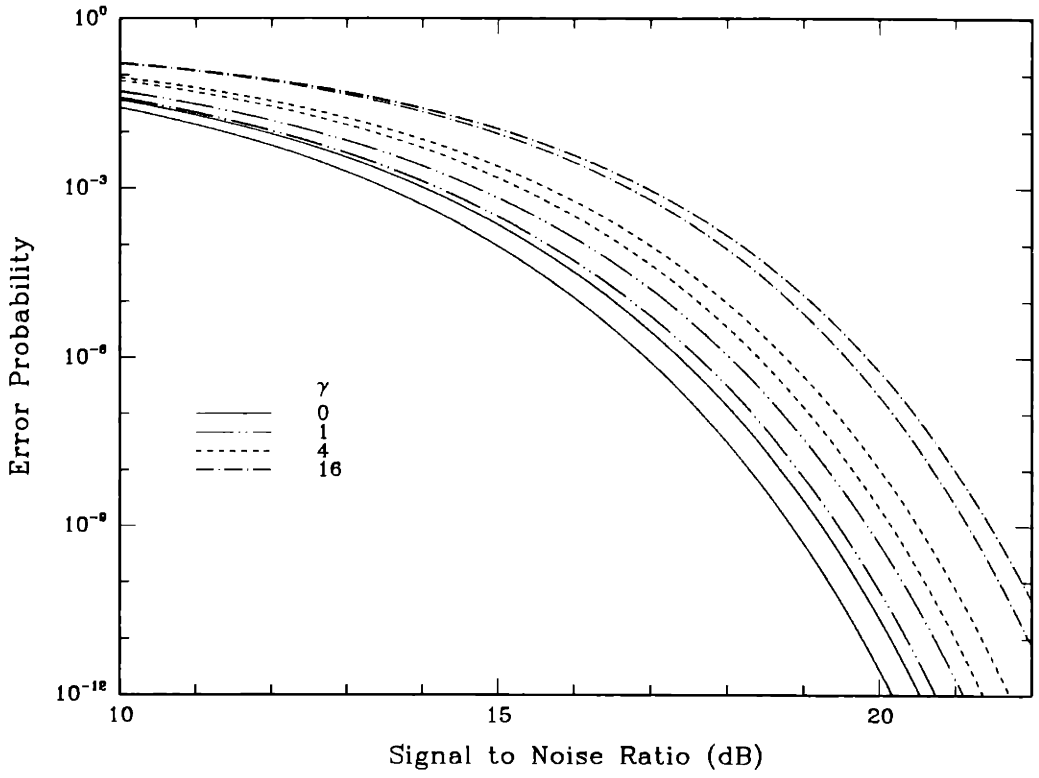

Figure 4-6: Comparison of Gaussian approximation and the lower bound for the double filter receiver.

clude that the lower bound given in Equation (4.22) satisfactorily predicts the performance of the double filter receiver.

The closeness of the error probability prediction of the Gaussian approximation to the exact performance was shown in [45] in the absence of phase noise. It was also noticed that the Gaussian threshold estimate is much lower than the actual optimal threshold. This is demonstrated in Figure 4-7. In the figure, the two error probabilities $P_e(0)$ and $P_e(1)$ are shown as functions of the normalized threshold for both the exact and the Gaussian results. It is seen that while the error probabilities at the respective optimal thresholds are very close, the optimal thresholds are very different. If the threshold is set according to the Gaussian approximation, the resulting performance would be far worse than what is predicted. This rather surprising result is true even when the value of M is large [45]. The presence of phase noise does not help correct this discrepancy as demonstrated in Figure 4-

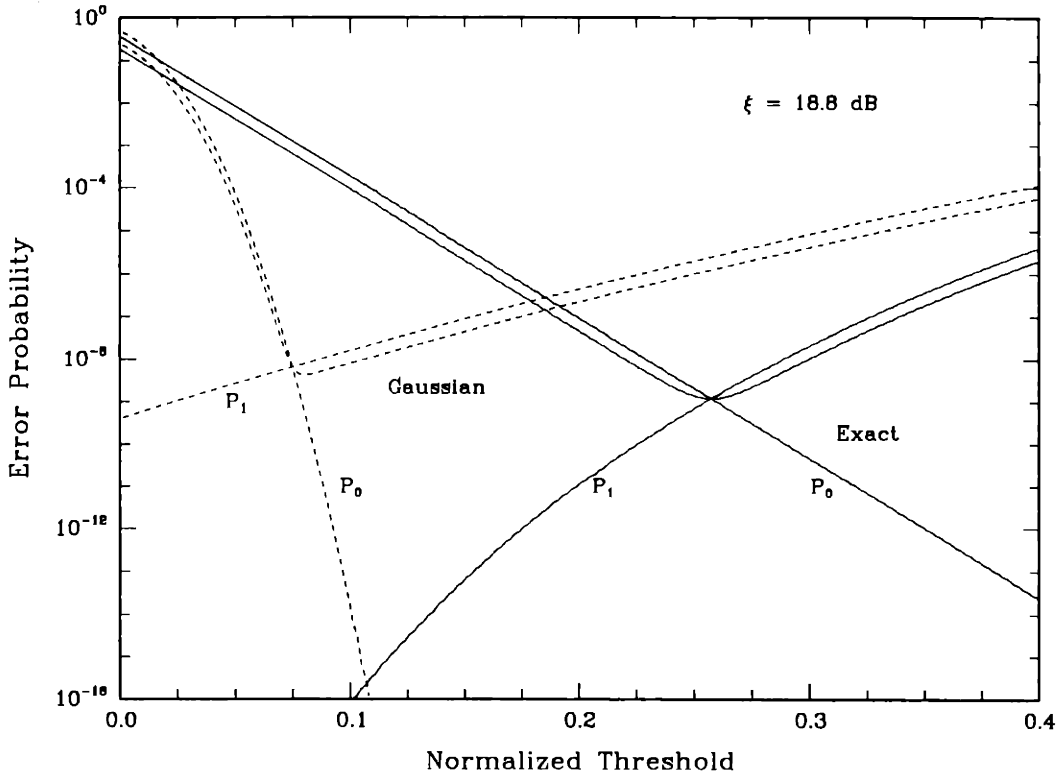

Figure 4-7: Error probabilities as functions of normalized threshold in the absence of phase noise.

8. Here we show the optimum threshold as a function of signal-to-noise ratio (SNR) for various values of γ. It is seen that the threshold predictions remain very different.

4.3 Comparison of OOK and FSK with Envelope Detection

A set of error probability curves of double filter envelope detection of OOK for a larger collection of γ values is given in Figure 4-9 for improved visual clarity. It is seen from the figure that at a bit error rate of 10^{-9}, the SNR penalty due to phase noise is 0.25 dB for $\gamma = 1$, 0.38 dB for $\gamma = 2$, 0.62 dB for $\gamma = 4$, 0.75 dB for $\gamma = 6$, and 1.13 dB for $\gamma = 16$. The robustness of OOK to phase noise surpasses that of FSK in terms of required excess signal energy to maintain a certain error probability level. This is seen clearly in Figure 4-10 which shows the penalty in SNR as a function of phase noise strength for both

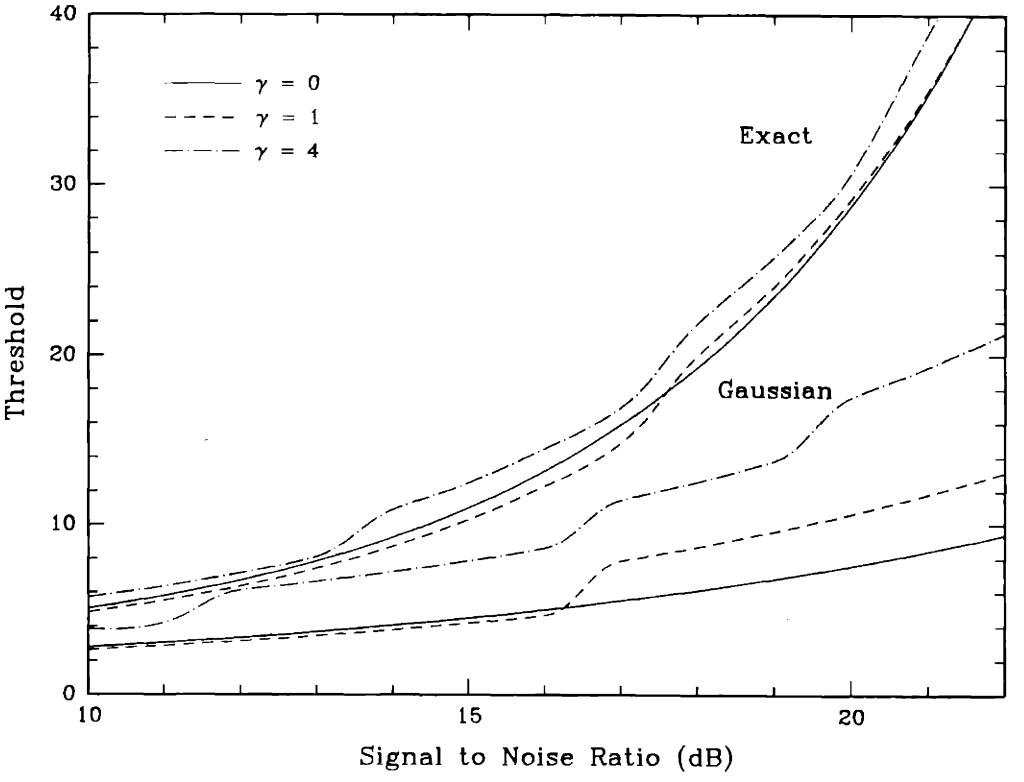

Figure 4-8: Optimal thresholds as functions of signal-to-noise ratio for various γ values.

OOK and FSK at an error probability of 10^{-9}. The improved robustness does not mean improved error performance, however. Since semiconductor lasers are limited in the peak power they can generate, as opposed to being average power limited, envelope detection of OOK will always have an inferior error probability with respect to envelope detection of orthogonal signals. This is demonstrated in Figure 4-11 for $\gamma = 0$ and $\gamma = 1$. The reason behind this conclusion can be seen as follows. In orthogonal signaling, envelope detection is performed for two frequencies, resulting in two decision variables. If one of the decision variables is neglected, and the other is compared to a fixed threshold for the decision, then the resulting performance will be identical to that of OOK. However, this clearly is a suboptimal processing of the available decision variables; symmetry dictates a comparison of the two decision variables for deciding on the most likely hypothesis. Nonetheless, OOK is still a modulation format of interest; the choice between OOK and FSK must be based on factors such as the amount of desired simplicity for the transmitters and the receivers, the achievability of orthogonality (i. e. wide frequency separation) in FSK, the severity of frequency dispersion during propagation along the fiber, etc.

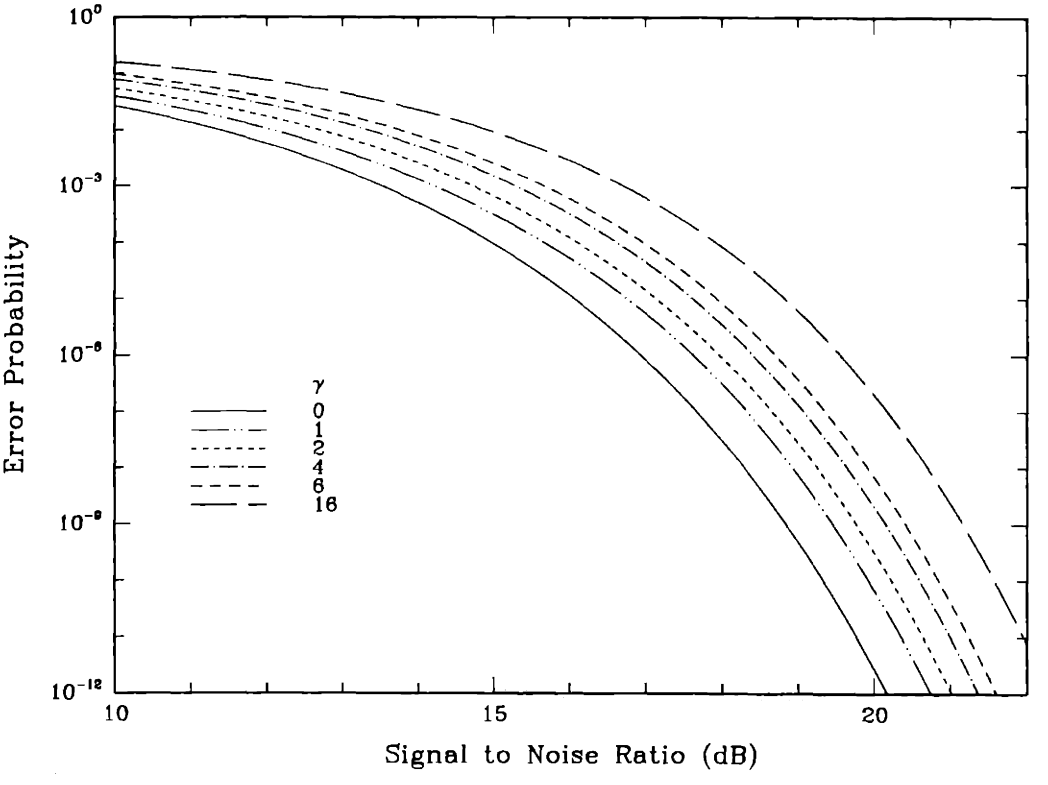

Figure 4-9: Estimated performance of the double filter receiver.

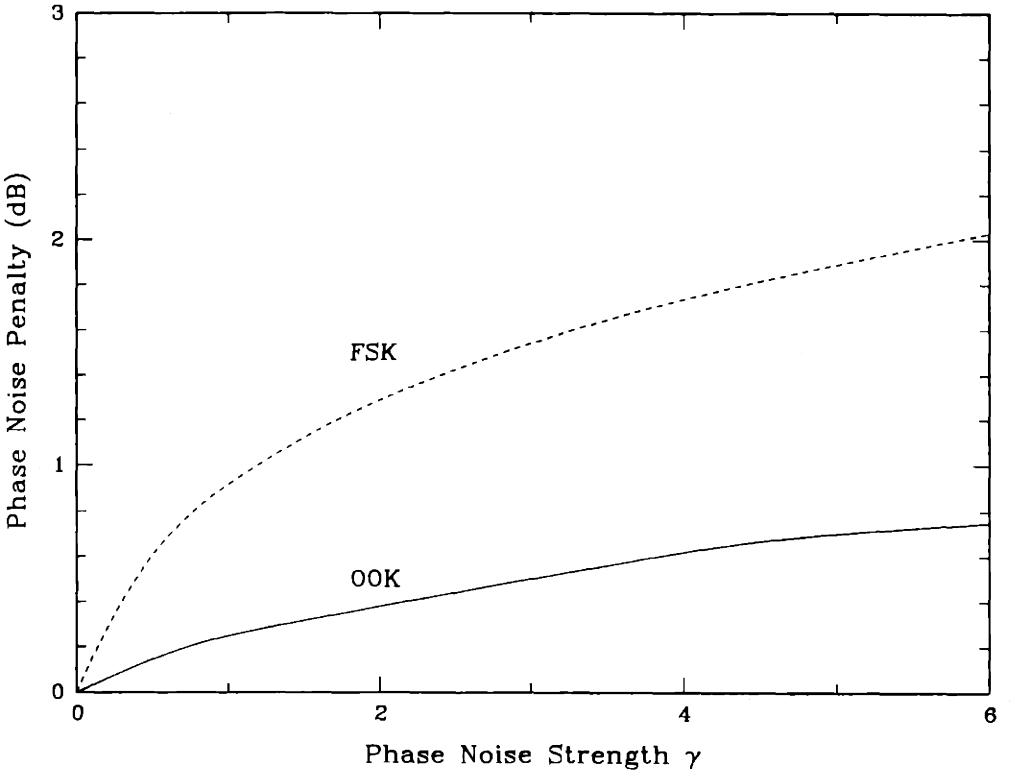

Figure 4-10: Comparison of SNR penalties for double-filter OOK and FSK due to phase noise.

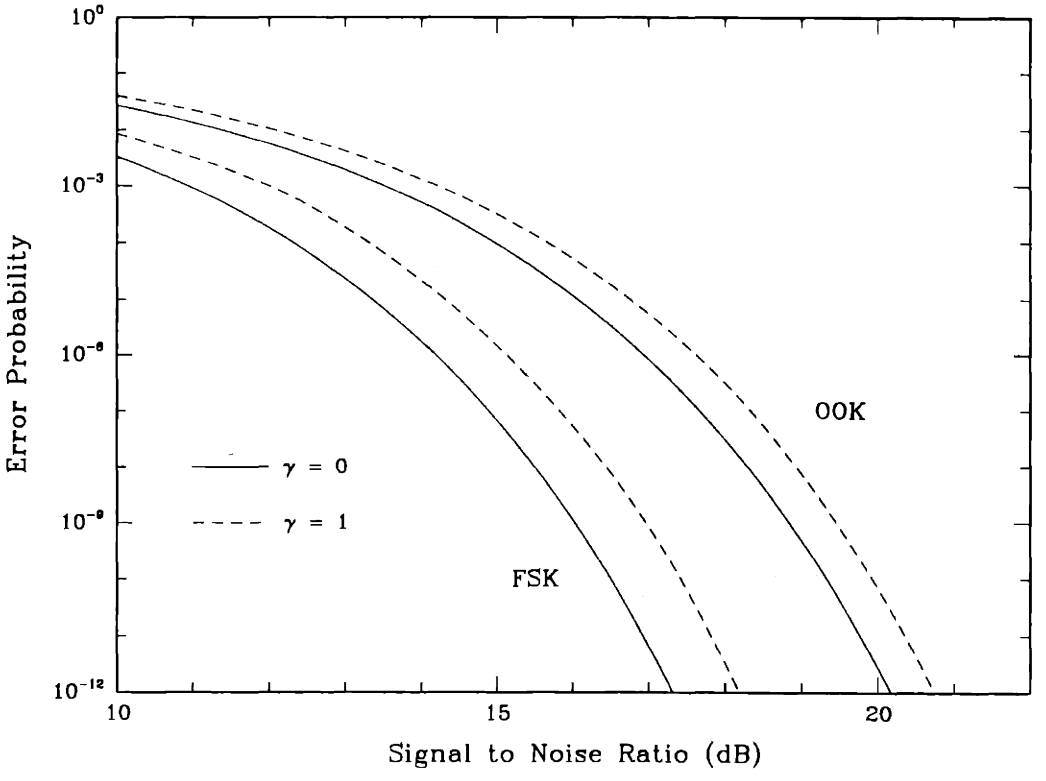

Figure 4-11: Comparison of error probabilities of double-filter OOK and FSK for $\gamma = 0$ and $\gamma = 1$.

Appendix

4.A Derivation of Equation (4.6)

In this appendix, we give the details in obtaining Equation (4.6). We start by writing the decision variable L in the decision rule of Equation (4.4) as

$$L(u) = \sum_{k_1} \cdots \sum_{k_M} \left(\prod_{i=1}^{M} I_{k_i} \left(\frac{AR_i}{\sigma^2} \right) \right) \exp \left[-\frac{u}{2} \sum_{i=1}^{M} \left(\sum_{l=i}^{M} k_l \right)^2 \right] \cos \left(\sum_{i=1}^{M} k_i \beta_i \right) \tag{4.29}$$

where $u = \alpha^2$. For small u, we can use the approximation

$$L(u) \simeq L(0) + uL'(0) .$$

First, we find $L(0)$. For $u = 0$ the exponential term in (4.29) vanishes. The cosine term can be written as a sum of 2^M terms: each term, apart from its sign, is a product of M sinusoidals which have arguments $k_i\beta_i$. All but one of these 2^M terms have at least one sine in the product. Since $\sin k_j\beta_j$ is an odd function of k_j, the sum $\sum_{k_j} I_{k_j}(AR_j/\sigma^2) \sin k_j\beta_j$ will vanish. Thus only the term with all cosine products contributes to $L(0)$ with the result

$$\begin{aligned} L(0) &= \prod_{i=1}^{M} \sum_{k_i} I_{k_i} \left(\frac{AR_i}{\sigma^2} \right) \cos k_i\beta_i \\ &= \prod_{i=1}^{M} \exp \left(\frac{AR_i}{\sigma^2} \cos k_i\beta_i \right) \\ &= \exp \left(\frac{A}{\sigma^2} \sum_{i=1}^{M} R_i \cos k_i\beta_i \right) . \end{aligned} \tag{4.30}$$

Note that (4.30) in conjunction with (4.4) gives the well known optimal receiver in the absence of phase noise.

Next, we find $L'(0)$. It is easily observed that

$$L'(0) = -\frac{1}{2} \sum_{k_1} \cdots \sum_{k_M} \left(\prod_{i=1}^{M} I_{k_i} \left(\frac{AR_i}{\sigma^2} \right) \right) \cos \left(\sum_{i=1}^{M} k_i \beta_i \right) g(\vec{k})$$

where we have defined $g(\vec{k})$ as

$$g(\vec{k}) = \sum_{i=1}^{M} \left(\sum_{l=i}^{M} k_l \right)^2 .$$

It can be easily shown (e. g. by induction or by a counting argument) that $g(\vec{k})$ can also be written as

$$g(\vec{k}) = \sum_{m,n=1}^{M} \min(m,n) k_m k_n$$

which results in

$$\begin{aligned} L'(0) &= -\frac{1}{2} \sum_{m,n=1}^{M} \min(m,n) \sum_{k_1} \cdots \sum_{k_M} k_m k_n \left(\prod_{i=1}^{M} I_{k_i} \left(\frac{AR_i}{\sigma^2} \right) \right) \cos \left(\sum_{i=1}^{M} k_i \beta_i \right) \\ &= \frac{1}{2} \sum_{m,n=1}^{M} \min(m,n) \frac{\partial^2}{\partial \beta_m \partial \beta_n} L(0) \end{aligned}$$

where we have used the fact

$$\frac{\partial^2}{\partial \beta_m \partial \beta_n} \cos \left(\sum_{i=1}^{M} k_i \beta_i \right) = -k_m k_n \cos \left(\sum_{i=1}^{M} k_i \beta_i \right)$$

as well as the definition of $L(0)$. Now using (4.30) one gets by differentiation

$$L'(0) = \frac{1}{2} \left(\sum_{m,n=1}^{M} \min(m,n) \frac{A^2 R_m R_n}{\sigma^4} \sin \beta_m \sin \beta_n - \sum_{m=1}^{M} m \frac{AR_m}{\sigma^2} \cos \beta_m \right) L(0)$$

so that

$$\begin{aligned} L(u) &\simeq L(0) \left[1 + \frac{u}{2} \left(\sum_{m,n=1}^{M} \min(m,n) \frac{A^2 R_m R_n}{\sigma^4} \sin \beta_m \sin \beta_n - \sum_{m=1}^{M} m \frac{AR_m}{\sigma^2} \cos \beta_m \right) \right] \\ &\simeq L(0) \exp \left[\frac{uA^2}{2\sigma^4} \sum_{m,n=1}^{M} \min(m,n) R_m \sin \beta_m R_n \sin \beta_n - \frac{uA}{2\sigma^2} \sum_{m=1}^{M} m R_m \cos \beta_m \right] \end{aligned}$$

where we also used $1 + x \simeq e^x$ for small x. Finally using Equations (4.4) and (4.30) in conjunction with the last equation, and substituting $u = \gamma/M$, $\sigma^2 = N_0 M/T$ one gets Equation (4.6).

Chapter 5

Transmitted Reference Systems

In the last three chapters we considered the performance of conventional modulation schemes in the presence of phase noise. In this chapter, we consider an alternative communication scheme which has been designed specifically for its robustness against phase noise. The approach we take is different from the previous chapters in the sense that we try to optimize the signaling mechanism as well as the receiver structure to achieve good performance.

The phase noise problem may be viewed as a lack of reference signal at the receiver which is identical to the transmitted signal except for modulation. Suppose we had a local oscillator which could produce a signal with the same phase noise as the received signal. Then the photodetector output would not be affected by phase noise at all; the identical phase processes would cancel out to yield a pure sinusoidal with embedded modulation. This simple observation suggests that systems designed to provide a reference to the receiver may help alleviate the performance degradation due to phase noise.

Let's first consider the transmission of the local oscillator signal directly from the transmitter in addition to the information carrying signal. A method in which this could be done is to use a beam splitter to separate the output of the transmitter laser into two branches, then to modulate one branch with data to generate the information signal and to use the other branch as the intended reference for the receiver. For conceptual simplicity let's suppose that two separate fibers can be used to transmit these two signals. If we further neglect the nonideal effects of propagation along the fiber on the signals, the receiver will be provided with an ideal reference signal in the sense mentioned above. The problem with this scheme is that this reference signal is not strong enough to be used as a local oscillator (LO) signal. The advantage of phase noise elimination will be overshadowed by the effects of thermal noise and dark current noise. The penalty of not operating in the shot noise limited regime is likely to be greater than the phase noise penalty which is at worst a few

dB's.

The idea of direct transmission of the LO signal may be feasible with the use of optical amplifiers. Optical amplifiers solve the power problem for the local signal, however they also introduce additive noise [45]. Therefore with the introduction of the amplifier both the information and reference signals contain noise in the optical domain. We will not consider this problem in this chapter, it remains to be seen whether this approach results in a performance improvement.

We consider a different scheme here. We do not attempt to provide a local oscillator signal to the receiver. The reference transmission will be used to help the receiver undo the adverse affects of phase noise *after the photodetection.* Before going into system details, let's first elaborate on how two signals can be transmitted simultaneously. The two-fiber channel in the example above is not practical. The fibers will inevitably have different dispersion characteristics so that the received signals will no longer have phase coherence. Therefore a common fiber must be used for both signals. Simultaneous transmission of two signals on a common channel requires that a certain orthogonality be provided so that the signals don't interfere with each other. This is essential for the receiver to be able to extract the two signals from their sum. Two main methods have been suggested to achieve this orthogonality [46, 47, 48]. The first employs two different optical carrier frequencies ν_1 and ν_2 for the information and the reference signals respectively. The two signals will occupy nonoverlapping frequency bands provided that the difference between ν_1 and ν_2 is much larger than the data rate and the linewidth. The receiver can separate the two signals by the use of coherent detection and appropriate IF filtering. Note that this is analogous to frequency division multiplexing in the multiuser context. A second method exploits two orthogonal polarizations. The transmitter laser produces a lightwave that contains both x and y polarization components. These two polarization components are separated by a polarization beam splitter, one of them is modulated with the data while the other one is used as the reference signal. The receiver can separate the two signals by using another polarization beam splitter.

In principle, both the frequency and polarization reference systems are the same when viewed at the IF domain. There are two copies of the phase noisy IF carrier, one modulated and the other unmodulated. These two copies can then be correlated to cancel the common phase noise term. Thus, at the first glance, perfect phase noise cancellation seems possible with this approach. However this is not true due to the additive noise introduced in the photodetection process as we will see in the next section.

5.1 Description of Transmitted Reference Systems

The transmitted reference systems considered here aim for the cancellation of phase noise by simultaneously sending a reference along with the information carrying signal. First we describe the reference transmission at a different frequency than the information signal. This method, which we call the *frequency reference*, was suggested independently by Chan et. al. in [46, 47] and Betti et. al. in [48]. In this method, the phase noisy output of the transmitter laser is split into two by a beam splitter. One of the two outputs is modulated via Phase Shift Keying (PSK) while the other one is shifted to another optical frequency, e.g. via an acousto-optic modulator. The two signals are combined by a coupler and transmitted along the fiber. The receiver adds a local oscillator field to the received optical field, and uses a photodetector to convert the received signal into IF domain. The resulting IF signal can be written as

$$r(t) = A_1 \cos(2\pi f_1 t + \theta(t) + \pi m(t)) + A_2 \cos(2\pi f_2 t + \theta(t)) + n(t) \tag{5.1}$$

where $\theta(t)$ is the combined phase noise of the transmitter and local oscillator lasers, $m(t)$ is the $0-1$ data waveform, $n(t)$ is a white Gaussian noise process which models the photodetector shot noise, and f_1, f_2 are the IF carrier frequencies for the information and reference signals respectively.

Assuming that f_1 and f_2 are sufficiently apart, the two signal components can be separated by two IF filters, to result in

$$\begin{aligned} r_1(t) &= A_1 \cos(2\pi f_1 t + \theta(t) + \pi m(t)) + n_1(t) \\ r_2(t) &= A_2 \cos(2\pi f_2 t + \theta(t)) + n_2(t) \end{aligned} \tag{5.2}$$

where $n_1(t)$ and $n_2(t)$ are independent white Gaussian noise processes with spectral height $N_0/2$.

Note that $r_1(t)$ and $r_2(t)$ in (5.2) have a common phase noise process. If we neglect the additive noise, the product $r_1(t)r_2(t)$ contains a term at frequency $f_2 - f_1$ which is free of phase noise, and a term at frequency $f_1 + f_2$ with doubled phase noise. Therefore in the absence of phase noise we could eliminate the phase noise entirely by filtering out the high frequency component, regardless of the strength of the original phase noise. While this observation is promising, it merely points out that there is no error floor in this transmitted reference scheme. An important question that needs to be answered is the robustness of

this phase noise cancellation to the additive noise. Filtering operations in the presence of phase noise must be analyzed with caution since the spectral broadening due to phase noise requires wider filters. Matched filters, which are optimal in the absence of phase noise, start deforming the desired signal with the introduction of phase noise. Wider filters introduce more additive noise at the output as well as more signal power. Therefore the tradeoff between the phase noise and additive noise must be accurately analyzed in the transmitted reference systems, as it is done for the conventional single carrier systems. The need for such an analysis was noted in [47, 48, 49].

A variety of polarization reference schemes also exist in the literature. The first one is the polarization PSK [50], which is equivalent to the frequency scheme in [47] except that the reference is at a polarization orthogonal to that of the PSK modulated signal instead of a different frequency. The implementation of this system is described in [51], and the principle of phase noise cancellation is demonstrated for extremely low linewidth (1 kHz) NdYAG lasers. The same scheme is also suggested in [47]. A scheme suggested in [48] incorporates hybrid frequency and polarization reference, in which the information and reference signals are transmitted in two orthogonal polarizations as well as two different frequencies. As a result this scheme is more robust against polarization crosstalk which may occur during propagation. Betti et. al. suggest two more polarization based reference transmission schemes in [48] which differ from [50] and [47] not in the signaling mechanism, but in the polarization compensation at the receiver.

An advantage of polarization reference schemes over frequency reference schemes is the ease of adjusting the power ratio of the two signals by controlling the angle of polarization of the transmitter laser. Frequency reference schemes can adjust the power ratio only via the coupling coefficient of the beam splitter. However this advantage may be balanced by polarization dispersion that accompanies propagation along the fiber. As a result of polarization dispersion the polarization vectors at the fiber output are not aligned with those at the input. Therefore the receiver must employ polarization diversity which results in a power penalty. The frequency reference schemes are prone to ferquency dispersion, but this seems to be of a lesser severity. The carrier wavelengths can be chosen near the zero-dispersion wavelength of the fiber (1300 nm), then a large separation in terms of IF frequency will correspond to a very small difference in the channel characteristics seen by the information and reference signals.

The concept of reference transmission is similar to DPSK where the carrier corresponding to the previous bit interval serves as a reference for the carrier of the current bit. Since phase noise is time-varying, the delay between the reference and the signal in DPSK is

detrimental as we have seen in Chapter 3. The transmitted reference schemes described here have the advantage of the signals being synchronous. In fact we will show in this chapter that through power and receiver optimization transmitted reference approaches the phase noise free performance of DPSK.

A common principle that connects all the transmitted reference schemes described above is that they all obey the key equation (5.2), neglecting the polarization crosstalk for the polarization based schemes. At the receiver two signals with the same phase noise is available. Various schemes differ in the values of A_1, A_2, f_1 and f_2, but the underlying structure is the same[1]. This enables us to provide a unified analysis of transmitted reference systems. We first outline the approaches to the analysis of these systems that exist in the literature to gain more insight to the problem.

5.2 Previous Performance Analyses

The need to analyze the performance of transmitted reference systems is first noted in [49], where it is correctly asserted that an accurate treatment of filtering operations and the additive noise/phase noise tradeoff is essential but difficult. The first attempt towards such an analysis may be found in [47, 53, 48]. It is first observed that two different frequencies are necessary only to enable the receiver extract $r_1(t)$ and $r_2(t)$ in (5.2) from the combined signal. Therefore once the two signals are separated, there is no need for distinct frequencies. The two signals can be brought to the same frequency, $f_c = (f_1 + f_2)/2$, by multiplying both with $\cos(\pi(f_2 - f_1)t)$. Therefore $f_1 = f_2 = f_c$ may be assumed without loss of generality. Two different IF receiver structures are considered. These are wideband single and double filter structures which we consider separately below.

5.2.1 Wideband Single Filter Receivers

Single filter receivers[2] with wide filter passbands are analyzed in both [47] and [48]. In such a system the information and reference signals are first filtered around the center frequency to limit the additive noise power, the bandpass filter outputs are mixed and sampled at the end of the bit period, the sampled value is compared to 0 to yield the decision. [47] assumes that the filters are identical; they have a bandwidth B that is large enough to pass

[1] A direct detection frequency reference scheme described in [52], where a pair of FSK tones is sent, does not fit into our formulation and will not be considered here.

[2] By a single filter structure we don't mean that there is a single filter in the receiver but a single filtering stage, i.e. that there is no post-mixing filter.

the signals *undistorted.* Then the standard results of [54] about the probability that the real part of the inner product of two complex Gaussian random variables is negative are invoked to obtain the error probability as

$$P_e = \frac{1}{2}\left[1 - Q(a,b) + Q(b,a)\right] \tag{5.3}$$

where a and b are given as

$$\begin{aligned} a &= \frac{1}{2\sqrt{N_0 B}}(A_1 + A_2) \\ b &= \frac{1}{2\sqrt{N_0 B}}|A_1 - A_2| \end{aligned}$$

and $Q(\cdot,\cdot)$ is the Marcum's Q function. The parameters a and b are the sum and difference of the means normalized by the standard deviations.

In the absence of phase noise, the filters are matched to the sinusoidals, so $B = 1/T$. Letting $\xi_i = A_i^2 T/2N_0$ for $i = 1, 2$, we get

$$\begin{aligned} a &= \frac{1}{\sqrt{2}}(\sqrt{\xi_1} + \sqrt{\xi_2}) \\ b &= \frac{1}{\sqrt{2}}\left|\sqrt{\xi_1} - \sqrt{\xi_2}\right| . \end{aligned}$$

For a fixed total transmitted energy, we have $\xi_1 + \xi_2 = \xi$ fixed, which is equivalent to $a^2 + b^2 = \xi$. Using the following property given in [15]

$$\begin{aligned} P_e &= \frac{1}{2}\left[1 - Q(a,b) + Q(b,a)\right] \\ &= \frac{1}{2}e^{-(a^2+b^2)/2}\left[I_0(ab) + 2\sum_{n=1}^{\infty}\left(\frac{b}{a}\right)^n I_n(ab)\right] \end{aligned}$$

we get

$$P_e \geq \frac{1}{2}e^{-\xi/2}I_0(ab) \geq \frac{1}{2}e^{-\xi/2} \tag{5.4}$$

with both of the inequalities satisfied with equality if and only if $b = 0$. Thus the power distribution which minimizes the error probability is given by $\xi_1 = \xi_2 = \xi/2$, i.e. the power must be equally divided between the reference and the information signals. The resulting error probability, $1/2e^{-\xi/2}$, is that of binary orthogonal signals. The reason for this can be

seen as follows. Let the filter outputs be $y_1(t)$ and $y_2(t)$. Since

$$y_1(t)y_2(t) = \frac{1}{4}\left[(y_1(t)+y_2(t))^2 - (y_1(t)-y_2(t))^2\right]$$

and since filtering is a linear operation, an equivalent receiver forms $r_1(t)+r_2(t)$ and $r_2(t)-r_1(t)$, and then performs standard envelope detection. On the other hand, with equal energy in $r_1(t)$ and $r_2(t)$, the sum and difference signals are orthogonal with independent noise components. Therefore the performance is the same as that of envelope detection of binary orthogonal signals. The resulting 3 dB degradation from DPSK even in the absence of phase noise is due to the selection of identical filters as we will show later.

In the presence of phase noise, the only change required to get the error probability is to increase BT from 1 to a value that is large enough to ensure that the phase noisy sinusoids pass the filters undistorted. Then ξ_1 and ξ_2 are now normalized by BT in the expressions for a and b. If we go through the power optimization, we see that the optimal power distribution is still such that $\xi_1 = \xi_2 = \xi/2$, and the error probability is given by

$$P_e = \frac{1}{2}e^{-\xi/2BT}\,. \tag{5.5}$$

Note that the effective signal-to-noise ratio (SNR) is reduced by a factor of BT which is large by assumption .

The same single filter receiver structure is also considered in [48] with the following fundamental observation. The reference signal is unmodulated and therefore occupies a smaller bandwidth than the information signal. Thus the reference signal $r_2(t)$ can be filtered with a filter of narrower passband reducing the additive noise power at the output. This can be viewed from the time domain as well. Since the bit duration has no relation to the reference signal, one can cross the bit boundaries to estimate the reference without any concern of intersymbol interference-like phenomena. This breaks the symmetry between the two signals, and allows an asymmetric power distribution. In fact, in the extreme case of no phase noise, the reference conveys no information, hence it should not be sent at all.

Let the filter bandwidths for the reference and information signals be W and B respectively. The processing of the filter outputs remains the same as before. Assuming that the signals pass the filters undistorted, the performance will still be given by (5.3) with the difference that the arguments are now given as

$$a = \frac{1}{2\sqrt{N_0}}\left(\frac{A_1}{\sqrt{B}} + \frac{A_2}{\sqrt{W}}\right)$$

$$b = \frac{1}{2\sqrt{N_0}} \left| \frac{A_1}{\sqrt{B}} - \frac{A_2}{\sqrt{W}} \right| . \tag{5.6}$$

It is difficult to find the optimal power distribution exactly. If it is assumed that the SNR is high in both channels to obtain the approximation

$$P_e \simeq Q(a - b)$$

where Q is the Gaussian error function, then the optimizing power ratio should maximize the minimum of ξ_1/W and ξ_2/B, subject to the constraint $\xi_1 + \xi_2 = \xi$. The solution is easily found as

$$\frac{\xi_1}{\xi} = \frac{B}{B+W} . \tag{5.7}$$

In the special case of identical filters this ratio becomes $1/2$ as expected. In the case with no phase noise, $W = 0$, we get the result that all the power should be sent at the information signal. With increasing linewidth more power is transferred to the reference, and in the large phase noise limit one gets the equal power distribution.

The resulting error probability when the power ratio is optimized is given in terms of the error function approximation in [48]. However, one can obtain a simpler result directly from (5.3) by observing that $b = 0$ at the optimal power ratio; then the error probability simplies to

$$P_e = \frac{1}{2} e^{-\xi/(B+W)T} . \tag{5.8}$$

A comparison of (5.8) with (5.5) shows that the power optimization has the potential of 3 dB improvement. The effective drop in the SNR with single filtering is a factor of T times the sum of the filter bandwidths. By making the reference filter narrower, one saves in the SNR. This is particularly important when the phase noise strength, $\gamma = 2\pi\beta T$, is small in which case $W/B \ll 1$. This is the reason why equal power distribution causes a 3 dB penalty in the limit of vanishing phase noise strength.

The analyses we have outlined here all assume that the phase noisy signals pass through the bandpass filters unaltered. Therefore the effect of phase noise on the performance is hidden in the bandwidths of the wideband filters. It is not clear how large B and W must be made as a function of phase noise strength for this assumption to be realistic. A heuristic relation first introduced in [4] and used by [47] and [48] takes

$$B = \frac{1}{T} + k\beta$$

$$W = k\beta \tag{5.9}$$

where β is the linewidth and k is a large constant. The motivation behind this is that the unmodulated phase noisy carrier has a 3 dB bandwidth of β, and the modulated phase-noise-free carrier has a bandwidth of the order of the bit rate. The predicted performance depends heavily on the assumed value for k. [47] uses filters with $BT = 7.1$ and lasers with $\beta T = 0.87$ resulting in $k \simeq 7$ in the experimental setup, while [48] uses $k = 8$ for its computations.

With the heuristic bandwidth setting of (5.9) the power distribution used in [48] is

$$\frac{\xi_1}{\xi} = \frac{1 + k\beta T}{1 + 2k\beta T} .$$

Note that, strictly speaking, this bandwidth setting is true only for large k, so the power distribution will be close to the even one for most phase noise strengths with this formalism. Figure 5-1 compares the performance predicted by Equation (5.8) and the performance prediction of the single filter receiver of Chapter 2 for a phase noise strength of $\beta T = 1$. It is seen that even without a power optimization, the filter optimization improves the performance considerably. This demonstrates that wideband filters are not required for good performance.

5.2.2 Wideband Double Filter Receivers

A double filter structure is also considered in [47]. The receiver now uses an integrator that integrates over the bit duration after the mixing. Assuming that the front end filters are identical with bandwidth B, and that the signals pass these filters undistorted, the mixer output will be

$$y_1(t)y_2(t) = \frac{1}{2}A_1A_2\cos(\pi m(t)) + \frac{1}{2}A_1A_2\cos(4\pi f_c t + 2\theta(t) + \pi m(t)) + n(t)$$

where $n(t)$ contains signal cross noise and noise cross noise terms. If B is much larger than the signal bandwidth, the signal cross noise terms can be taken to be Gaussian with flat spectral levels $A_i^2 N_0/4$ over $|f| < B$. The noise cross noise term will have a triangular spectrum over $|f| < B$ with peak $N_0^2 B$. This last term is neglected in [47] on the basis that the signal-to-noise ratio is large. However, the validity of this also depends on the phase noise strength: for large linewidths B must be made very large for the signal to remain undistorted, and the noise cross noise term may be important. We don't neglect this term

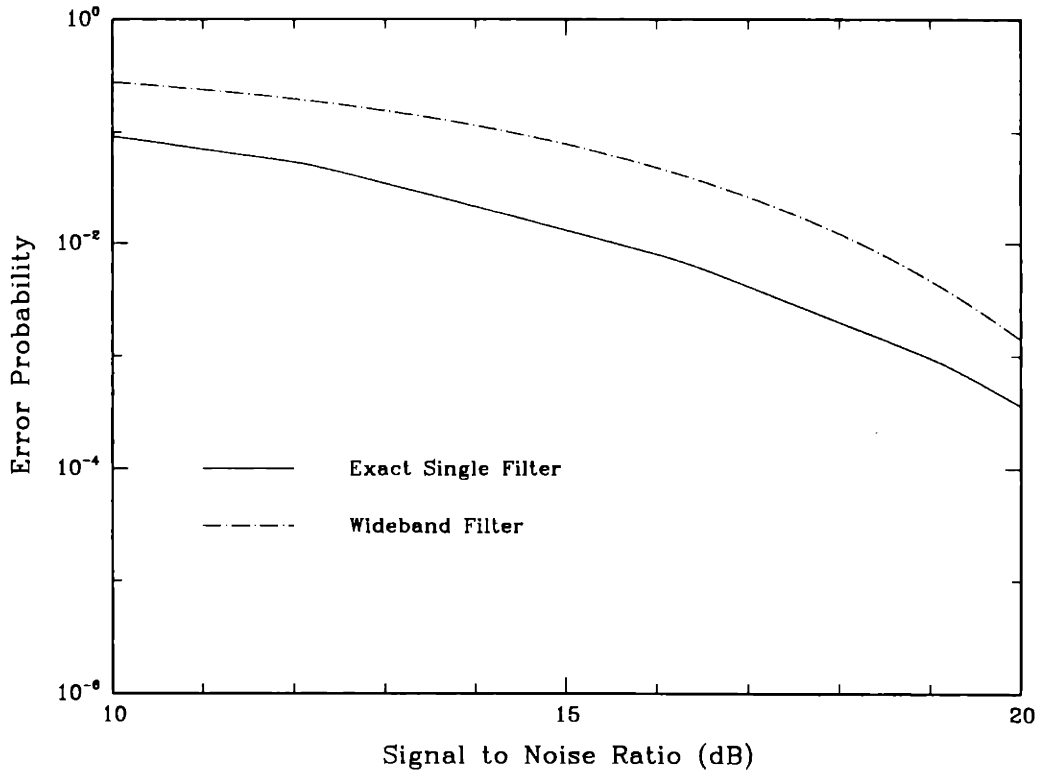

Figure 5-1: A comparison of the performance predictions for single-filter structures with $\beta T = 1$. The exact curve uses an even power distribution while the wideband filter curve has optimized power distribution via the heuristic bandwidth setting.

here, but we assume that it is Gaussian and that its spectrum may be replaced by a flat spectrum that results in the same power, i.e. with level $N_0^2 B/2$. After the integrator that integrates $y_1(t)y_2(t)$ over the bit duration, the resulting sample has an antipodal signal level corrupted by a Gaussian random variable. The error probability is easily found as

$$P_e = Q\left(\sqrt{\frac{2\xi_1\xi_2}{\xi + BT}}\right)$$

where $Q(\cdot)$ is the complementary error function. We see that the optimal power distribution still satisfies $\xi_1 = \xi_2 = \xi/2$ with the result

$$P_e = Q\left(\sqrt{\frac{\xi/2}{1 + BT/\xi}}\right) . \tag{5.10}$$

The error probability given by [47] does not have the second term in the denominator, and hence is valid only when $BT/\xi \ll 1$. Since the value of B that is needed to pass the signal undistorted may be very large this may not always hold. However when it does hold, (5.10) predicts a performance that is independent of the phase noise strength and is 3 dB worse than phase noise free FSK. That is, the double filter transmitted reference system with identical wideband filters has a uniform 3 dB phase noise penalty when the phase noise strength is not very large. However, we have seen that double filter FSK does not have this high of a penalty with the optimization of the filter bandwidth. This is shown in Figure 5-2 where the error probability of the receiver with wideband filter predicted by (5.10) is shown together with the error probability for the system with optimized filters from Chapter 2. It is seen that by performing the optimization of the filter bandwidth a better performance may be obtained although some signal power is sacrificed. The wideband filter assumption results in a weak phase noise dependence (with the correction), however the resulting performance is not good.

The existing analyses outlined here have two deficiencies. First, they don't adequately address the tradeoff between phase noise and additive noise by assuming wideband front end filters and, in the case of [47], identical filter bandwidths. The performance predictions do not reflect the true limits of the transmitted reference systems; the fact that wideband filters do not distort the signals is not critical for achieving good performance, furthermore heuristic bandwidth setting involves a free parameter whose setting arbitrarily determines the performance. This is best seen through the systems with even power allocation, these systems have the same performance as the corresponding (single or double filter) FSK

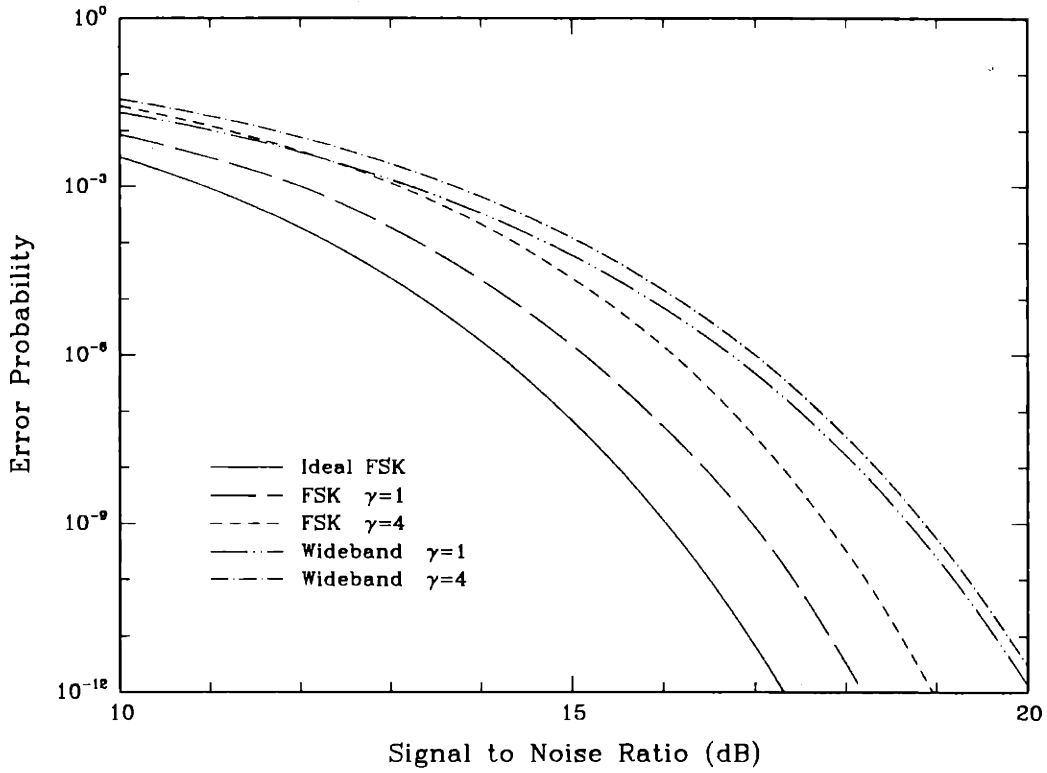

Figure 5-2: A comparison of the performance predictions for double-filter structures with $\gamma = 1$ and $\gamma = 4$, where both the wideband filter and the exact curves use an even power distribution.

system, while the outlined analysis predicts a phase noise independent, but poor, performance. The second deficiency is the lack of an analysis for the most promising transmitted reference system: the system with optimal power allocation between the information and reference signals and with a double filter receiver with optimal filter bandwidths. While [48] introduces the concept of adjusting the power distribution according to the strength of phase noise, it applies this concept only to single filter receivers with wideband filters. Consequently the resulting performance is not satisfactory, partly due to the inability of a single filter structure to combat phase noise effectively, and partly due to the wideband filter assumption which simplifies the analysis at the expense of degraded performance. In the rest of this chapter we will attempt to provide an analysis for the system without these deficiencies.

5.3 Transmitted Reference with Optimal Power Distribution and Optimal Receiver Bandwidths

In the previous section we have observed that allocating the available power optimally between the two transmitted signals, as well as optimally adjusting the filter bandwidths in a double filter receiver structure may achieve a superior performance for a transmitted reference system. We will now provide an analysis to quantify this observation and to obtain the settings of design parameters. We first restate the problem in order to make this section self-contained.

We assume that the receiver has the ability to extract the information and reference signals, and to bring them to a common frequency. Thus the inputs to the IF receiver are the two signals given as

$$\begin{aligned} r_1(t) &= A_1 \cos(2\pi f_1 t + \theta(t) + \pi d) + n_1(t) \\ r_2(t) &= A_2 \cos(2\pi f_2 t + \theta(t)) + n_2(t) \end{aligned} \tag{5.11}$$

where $d = 0, 1$ is the current data bit, $n_1(t)$, $n_2(t)$ are independent white Gaussian noise processes with spectral density $N_0/2$. These signals are first filtered by bandpass filters to limit the noise power. We model the bandpass filters as in-phase and quadrature demodulators followed by finite-time integrators. The integrators for the information signal $r_1(t)$ have a time duration of $T_1 = T/M$, while those for the reference signal $r_2(t)$ have their time duration K times longer, i.e. $T_2 = KT/M$. Thus, the information filter has a *bandwidth expansion factor* of M relative to a matched filter, while the reference filter has

a *bandwidth reduction factor* of K relative to the information filter, where $K, M \geq 1$ are to be found optimally. This reflects our previous observation that the reference signal can be more tightly filtered by virtue of being unmodulated. For analytical convenience we will assume that M and K are both integers.

We will consider two forms of timing alignment between the filter outputs. First we assume that both filters are causal: the integrator outputs at time t are the integrals of the inputs from time $t - T_i$ to t where $i = 1, 2$ for the information and reference filters respectively. We will also consider a centered filter structure in the Section 5.3.3 for potential performance improvement; the structure of this filter will be described in that section.

Let $x_I(t)$ and $x_Q(t)$ be the filter outputs of the in-phase and quadrature integrators of the information filter, and let $y_I(t)$ and $y_Q(t)$ be their reference filter counterparts. These real signals can be written compactly with the following complex notation:

$$\begin{aligned} x_I(t) + jx_Q(t) &= \pm\frac{A_1}{2}\int_{t-T_1}^{t} e^{j\theta(\tau)}\,d\tau + \int_{t-T_1}^{t} n_1(\tau)e^{j2\pi f_c\tau}\,d\tau \\ y_I(t) + jy_Q(t) &= \frac{A_2}{2}\int_{t-T_2}^{t} e^{j\theta(\tau)}\,d\tau + \int_{t-T_2}^{t} n_2(\tau)e^{j2\pi f_c\tau}\,d\tau \end{aligned}$$

where we have assumed that $f_cT_i \gg 1$ so that the double frequency components do not appear at the integrator output, the $\pm$ correspond to the data bit d being 0 or 1.

The remainder of the receiver structure is as follows. The in-phase and quadrature components are pairwise mixed and added resulting in the signal $x_I(t)y_I(t) + x_Q(t)y_Q(t)$. This signal is then processed via a lowpass filter which we model as a discrete-time adder after [8], as we did for the envelope detection of FSK and OOK signals in Chapters 2 and 4. Finally the lowpass filter output is sampled at the end of the bit duration and the sample is compared to 0 to yield the decision. The decision variable can be written as

$$Y = \sum_{k=1}^{M} Y_k$$

where

$$Y_k = x_I(kT_1)y_I(kT_1) + x_Q(kT_1)y_Q(kT_1)\,,$$

and the error probability is given by

$$P_e = \Pr(Y \leq 0 \mid d = 0)\,.$$

We will introduce some notation for a compact formulation in terms of matrices and vectors. First we define the conditional means given the phase noise process as

$$\begin{aligned} a_I(k) + ja_Q(k) &= \frac{A_1}{2}\int_{(k-1)T_1}^{kT_1} e^{j\theta(t)}\,dt \\ b_I(k) + jb_Q(k) &= \frac{A_2}{2}\int_{kT_1-T_2}^{kT_1} e^{j\theta(t)}\,dt \end{aligned}$$

and the independent discrete-time additive noise components as

$$\begin{aligned} w_I(k) + jw_Q(k) &= \int_{(k-1)T_1}^{kT_1} n_1(t)e^{j2\pi f_c t}\,dt \\ z_I(k) + jz_Q(k) &= \int_{(k-1)T_1}^{kT_1} n_2(t)e^{j2\pi f_c t}\,dt\,. \end{aligned}$$

These noise components are Gaussian random variables with zero mean and variance $\sigma^2 \triangleq N_0T_1/4$. The noise components on the reference signals (z_I and z_Q) are defined in this way because of the overlapping integration windows $(kT_1 - T_2, kT_1)$. With these definitions and with the use of $T_2 = KT_1$ we have

$$\begin{aligned} x_I(kT_1) &= a_I(k) + w_I(k) \\ y_I(kT_1) &= b_I(k) + \sum_{l=0}^{K-1} z_I(k-l) \quad k = 1,\ldots,M \end{aligned}$$

and same expressions for the quadrature components. We also define the M dimensional vectors $\vec{x}_I$, $\vec{x}_Q$, $\vec{y}_I$, $\vec{y}_Q$, $\vec{a}_I$, $\vec{a}_Q$, $\vec{b}_I$, $\vec{b}_Q$, $\vec{w}_I$ and $\vec{w}_Q$ in the generic form

$$\vec{\alpha}_\lambda = [\alpha_\lambda(1),\ldots,\alpha_\lambda(M)]^T$$

where $\alpha = x, y, a, b, w$ and $\lambda = I, Q$, and superscript T denotes transpose. ($\alpha_\lambda(k)$ must be understood as $\alpha_\lambda(kT_1)$ for $\alpha = x, y$.) The corresponding vectors for z's must be of larger dimension because of the longer span in the reference integrators. Thus we define the $(M + K - 1)$ dimensional vectors

$$\vec{z}_\lambda = [z_\lambda(-K+2), z_\lambda(-K+3),\ldots, z_\lambda(0),\ldots, z_\lambda(M)]^T$$

for $\lambda = I, Q$. Finally we define the $M \times (M + K - 1)$ matrix A as

$$A_{ij} = \begin{cases} 1 & \text{if } 0 \leq j - i \leq K - 1 \\ 0 & \text{otherwise,} \end{cases}$$

hence A is a Toeplitz matrix with K consecutive 1's in each row the first one being at the diagonal.

The decision variable Y can now be written in terms of the conditional mean vectors and additive noise vectors as

$$\begin{aligned} Y &= \vec{x}_I^T \vec{y}_I + \vec{x}_Q^T \vec{y}_Q \\ \vec{x}_\lambda &= \vec{a}_\lambda + \vec{w}_\lambda \\ \vec{y}_\lambda &= \vec{b}_\lambda + A\vec{z}_\lambda \end{aligned}$$

for $\lambda = I, Q$.

The approach that we took in the previous chapters for envelope detection of FSK and OOK with the same filter model was to obtain the exact error probability conditioned on phase noise, and then to remove the conditioning via an exponential approximation to the phase noisy envelope and/or via Jensen bound. Here, the conditional error probability is the probability that the inner product of two Gaussian vectors is negative. Finding this probability even in the case where there is no dependence between the elements of the Gaussian vectors is an involved task treated in Appendix 4B of [25]. However in this case the vectors $A\vec{z}_\lambda$ ($\lambda = I, Q$) have dependent entries unless $K = 1$. Even for the simple case of $M = 1$, where all the vectors (except z's) reduce to scalars, one gets a conditional error probability of the same form as (5.3) with parameters a and b containing two dependent phase noise variables. The complexity of conditional error probability even in this simple case motivates us to use Chernoff bounding techniques. We will later optimize the bound parameter to make the bound as tight as possible. The conditional Chernoff bound is

$$P_e\left(\theta(t)\right) \leq E\left(e^{-sY} \mid \theta(t)\right) \quad s \geq 0\,.$$

Since the in-phase and quadrature components are independent given the phase noise process, one can decouple Y as $Y = Y_I + Y_Q$ where $Y_I = \vec{x}_I^T \vec{y}_I$ and $Y_Q = \vec{x}_Q^T \vec{y}_Q$, obtain the moment generating function for Y_I and make proper substitutions for Y_Q. The following lemma gives the necessary result.

Lemma 5.1 *Let $\vec{x}$ and $\vec{y}$ be independent Gaussian vectors with means $\vec{a}$ and $\vec{b}$, and covari-*

ance matrices $\Lambda_x = \sigma^2 I$, $\Lambda_y = \sigma^2 B$ for some positive definite matrix B. Then the moment generating function of $\vec{x}^T\vec{y}$ is given by

$$E\left(\exp(-s\vec{x}^T\vec{y})\right) = |I - s^2\sigma^4 B|^{-1/2} \exp\left(-s\vec{a}^T\vec{b} + \frac{s^2\sigma^2}{2}\|\vec{b}\|^2 + \frac{1}{2}\vec{\alpha}^T\Lambda^{-1}\vec{\alpha}\right)$$

where $\vec{\alpha} = -s\vec{a} + s^2\sigma^2\vec{b}$ and $\Lambda = (B^{-1} - s^2\sigma^4 I)/\sigma^2$.

Proof. Since $\vec{x}$ has statistically independent elements, it is convenient to first condition the expectation on $\vec{y}$. Then it is easily observed from the moment generating function of Gaussian random variables that

$$E\left[\exp(-s\vec{x}^T\vec{y}) \mid \vec{y}\right] = \exp\left(-s\vec{a}^T\vec{y} + \frac{s^2\sigma^2}{2}\|\vec{y}\|^2\right) .$$

Then the desired expectation is given by

$$(2\pi\sigma^2)^{-M/2}|B|^{-1/2} \int \exp\left(-s\vec{a}^T\vec{y} + \frac{s^2\sigma^2}{2}\|\vec{y}\|^2 - \frac{1}{2\sigma^2}(\vec{y}-\vec{b})^T B^{-1}(\vec{y}-\vec{b})\right) d\vec{y}$$

which can be evaluated by completing the exponent to a quadratic to obtain the desired result. □

Using this lemma with $B = AA^T$ yields the Chernoff bound as

$$\begin{aligned} P_e\left(\theta(t)\right) \leq |I - s^2\sigma^4 AA^T|^{-1} \exp\Big[-s(\vec{a}_I^T\vec{b}_I + \vec{a}_Q^T\vec{b}_Q) \quad &+ \quad \frac{s^2\sigma^2}{2}(\|\vec{b}_I\|^2 + \|\vec{b}_Q\|^2) \\ &+ \quad \frac{1}{2}\vec{\alpha}_I^T\Lambda^{-1}\vec{\alpha}_I + \frac{1}{2}\vec{\alpha}_Q^T\Lambda^{-1}\vec{\alpha}_Q\Big] \end{aligned}$$

where

$$\begin{aligned} \alpha_\lambda &= -s\vec{a}_\lambda + s^2\sigma^2\vec{b}_\lambda \quad \lambda = I, Q \\ \Lambda &= \frac{1}{\sigma^2}\left[(AA^T)^{-1} - s^2\sigma^4 I\right] . \end{aligned}$$

The bound is finite for $s^2\sigma^4\lambda_{\max}(AA^T) < 1$, where $\lambda_{\max}(\cdot)$ denotes the maximum eigenvalue. Note that since A has full row rank AA^T is positive definite, hence the condition for finiteness also guarantees nonsingularity of Λ.

We now express the bound in terms of fundamental parameters and random variables.

Let's define two normalized phase noise integrals as

$$X_1(k) \triangleq \frac{1}{T_1}\int_{(k-1)T_1}^{kT_1} e^{j\theta(t)}\,dt \tag{5.12}$$

$$X_2(k) \triangleq \frac{1}{T_2}\int_{kT_1-T_2}^{kT_1} e^{j\theta(t)}\,dt = \frac{1}{K}\sum_{l=0}^{K-1} X_1(k-l) \tag{5.13}$$

where the second equality for $X_2(k)$ follows from $T_2 = KT_1$. Using the definitions of the conditional means, the first two terms in the exponent of the Chernoff bound can now be expressed as

$$-s(\vec{a}_I^T\vec{b}_I + \vec{a}_Q^T\vec{b}_Q) = -2s\sigma^2\sqrt{K\xi_1\xi_2}\mathrm{Re}\sum_{k=1}^{M} X_1(k)X_2^*(k) \tag{5.14}$$

$$\frac{s^2\sigma^2}{2}(\|\vec{b}_I\|^2 + \|\vec{b}_Q\|^2) = s^2\sigma^4 K\xi_2\sum_{k=1}^{M}|X_2(k)|^2 \tag{5.15}$$

where $\xi_i = A_i^2T_i/2N_0$ for $i = 1, 2$. We see that it is convenient to normalize the bound parameter as $u = s\sigma^2$. To get the third term of the bound exponent we use the definition of $\vec{\alpha}$'s and obtain after some manipulations

$$\frac{1}{2}\vec{\alpha}_I^T\Lambda^{-1}\vec{\alpha}_I + \frac{1}{2}\vec{\alpha}_Q^T\Lambda^{-1}\vec{\alpha}_Q = u^2\mathrm{Re}\sum_{i,j}^{M} \rho_{ij}\left[\xi_1 X_1(i)X_1^*(j) - 2u\sqrt{K\xi_1\xi_2}X_1(i)X_2^*(j) + u^2K\xi_2X_2(i)X_2^*(j)\right] \tag{5.16}$$

where ρ_{ij} is the (i,j)'th element of the matrix $(I - u^2AA^T)^{-1}AA^T$. When one invokes the natural vector notation for $X_i(k)$ $i = 1, 2$, and one combines the similar terms in (5.14)-(5.16) one obtains the conditional Chernoff bound as

$$P_e(\vec{X}_1, \vec{X}_2) \le |I - u^2AA^T|^{-1}\exp\left[-2u\sqrt{K\xi_1\xi_2}t_1 + u^2K\xi_2t_2 + u^2\xi_1t_3\right] \tag{5.17}$$

where

$$\begin{aligned} t_1 &= \mathrm{Re}\vec{X}_2^H(I - u^2AA^T)^{-1}\vec{X}_1 \\ t_2 &= \mathrm{Re}\vec{X}_2^H(I - u^2AA^T)^{-1}\vec{X}_2 \\ t_3 &= \mathrm{Re}\vec{X}_1^H(I - u^2AA^T)^{-1}AA^T\vec{X}_1 \end{aligned}$$

for $0 \leq u < u_{\max} = \lambda_{\max}^{-1/2}(AA^T)$ (superscript H denotes complex conjugate transpose). In obtaining (5.17) we have used the matrix identity $I + (I - B)^{-1}B = (I - B)^{-1}$ with $B = u^2 AA^T$.

Now we investigate some special cases of the Chernoff bound of (5.17) to gain more insight about it and to estimate its quality.

5.3.1 Special Cases for the Chernoff Bound

The formulation of the Chernoff bound can be applied to a variety of specific problems. Now we consider three of these problems.

1. Frequency Shift Keying: Setting $K = 1$ results in a bound for the conditional error probability of double filter FSK that we obtained exactly in Chapter 2. In this case $\vec{X}_1 = \vec{X}_2 = \vec{X}$, and we have

$$P_e(\vec{X}, K = 1) \leq (1 - u^2)^{-M} \exp\left[\frac{\|\vec{X}\|^2}{1 - u^2}\left(u^2(\xi_1 + \xi_2) - 2u\sqrt{\xi_1 \xi_2}\right)\right]$$

with $\xi_1 + \xi_2 = \xi/M$. One immediately sees that the optimal power distribution is even, a fact we have observed in the wideband filter analyses of Section 5.2. This distribution results in

$$P_e(\vec{X}, K = 1) \leq (1 - u^2)^{-M} \exp\left[-\frac{u}{1 + u}\frac{\xi}{M}\|\vec{X}\|^2\right] \quad 0 \leq u < 1 \,. \tag{5.18}$$

Note that $\|\vec{X}\|^2$ is now a sum of M independent identically distributed random variables, and $\xi\|\vec{X}\|^2/M$ is the phase noisy SNR r of Chapter 2. Thus in the notation of Chapter 2 we get

$$P_e(r) \leq (1 - u^2)^{-M} \exp\left(-\frac{ur}{1 + u}\right) \quad 0 \leq u < 1 \,.$$

If we further specialize to the case of no phase noise, we have $r = \xi$, and the optimal value of M becomes 1 as expected. Thus for phase noise free FSK we obtain the bound

$$P_e \leq \min_{0 \leq u < 1} (1 - u^2)^{-1} \exp\left(-\frac{u\xi}{1 + u}\right) \tag{5.19}$$

which gives the same exponential nature $e^{-\xi/2}$ as the true error probability as $u \to 1$. However since the coefficient also grows with u the bound is not arbitrarily tight as can be seen from Figure 5-3. Nonetheless it is still within 0.7 dB of the actual performance

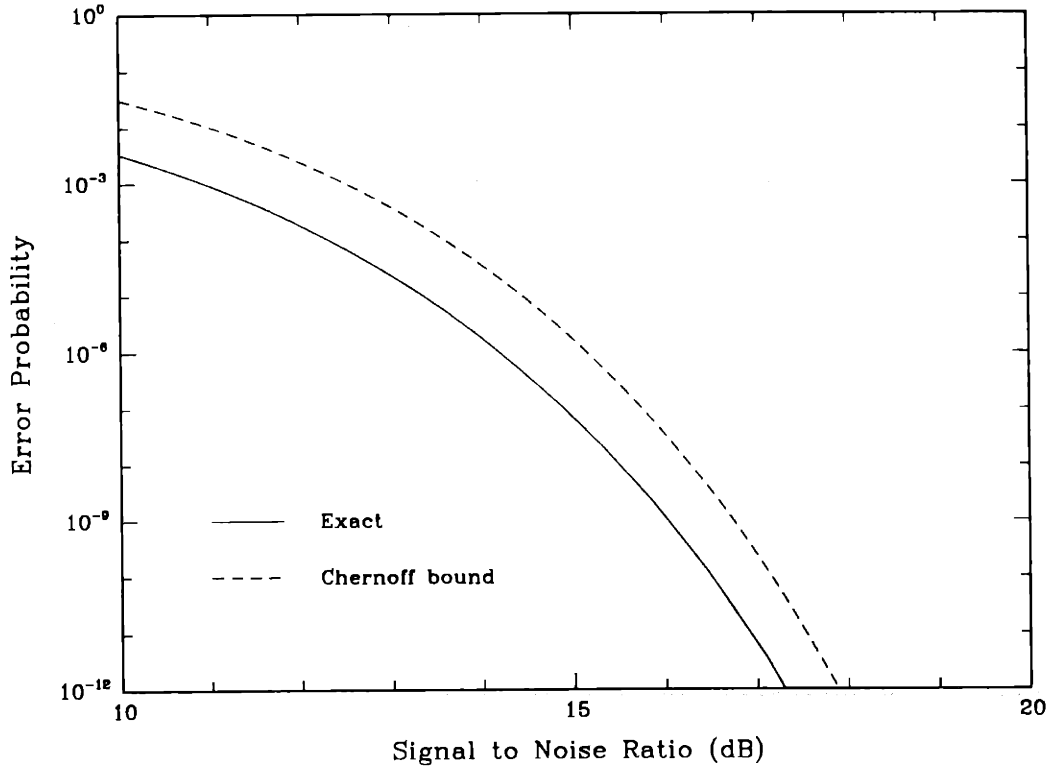

Figure 5-3: A comparison of the Chernoff bound with the actual performance for phase noise free FSK.

for low error probabilities. In fact, a parametric optimization of (5.19) for $\xi \gg 1$, $u \simeq 1$ yields the bound as $\xi e^{-\xi/2}/8$. (Here we first find the value of ξ for which u is optimal as $\xi = 2u(1+u)/(1-u)$, and we express the bound in terms of ξ when $u \simeq 1$.)

This example shows that Chernoff bound has the potential of retaining the essential features of the actual performance, e.g. the optimal power distribution, the filter bandwidth setting, and the rate of exponential decay of the error probability.

2. Single Filter Receiver: Another interesting special case of the obtained Chernoff bound is the single filter receiver in the absence of phase noise. In order to be able to treat the single filter case with an arbitrary integration time T_1, we set M to 1 in (5.17) but retain the M in $T_1 = T/M$. In this case we have $AA^T = K$, $\vec{X}_1 = \vec{X}_2 = 1$, and the

bound becomes,

$$P_e \leq (1 - Ku^2)^{-1} \exp\left[\frac{1}{1 - Ku^2}\left(Ku^2(\xi_1 + \xi_2) - 2u\sqrt{K\xi_1\xi_2}\right)\right] .$$

Letting $v = \sqrt{K}u$ and optimizing the numerator of the exponent over v one gets for the optimizing value

$$v^* = \frac{\sqrt{\xi_1\xi_2}}{\xi_1 + \xi_2} \leq \frac{1}{2}$$

with the resulting numerator being $-\xi_1\xi_2/(\xi_1 + \xi_2)$. We can bound the denominator and the coefficient using

$$\frac{3}{4} \leq 1 - (v^*)^2 \leq 1$$

so that the bound becomes

$$P_e \leq \frac{4}{3}\exp\left(-\frac{\xi_1\xi_2}{\xi_1 + \xi_2}\right)$$

which we want to minimize over ξ_1, ξ_2, K and M subject to the constraint

$$\xi_1 + \frac{\xi_2}{K} = \frac{\xi}{M} .$$

Clearly the function $\xi_1\xi_2/(\xi_1 + \xi_2)$ is less than both ξ_1 and ξ_2 with equality achieved when either one approaches ∞. Thus the optimal solution is obtained when $\xi_2 \to \infty$ and $K \to \infty$ such that $\xi_2/K \to 0$. In this case

$$P_e \leq \frac{4}{3}e^{-\xi}$$

which has the same exponential character as PSK. Note that since $\xi/K = A_2^2T/2N_0$ tends to 0, the optimal solution corresponds to sending no power in the reference signal but getting a perfect local signal ($\xi_2 \to \infty$). This is exactly the case for phase noise free PSK. This example also confirms our expectation that the conclusions reached from the Chernoff bound are likely to correspond to the actual system.

3. Double Filter DPSK: A final application of our bound is the case of double filter DPSK. Here we have the current and previous bits instead of the data signal and reference. Both signals have the same SNR and the filter processing is identical, i.e. $K = 1$. The reference vector $\vec{X}_2$ has to be modified so as to include the time delay as

$$X_2(k) = \frac{1}{T_1}\int_{(k-1)T_1 - T}^{kT_1 - T} e^{j\theta(t)}\, dt .$$

The conditional Chernoff bound with these parameters is

$$P_e(\vec{X}_1, \vec{X}_2) \leq (1-u^2)^{-M} \exp\left[\frac{1}{1-u^2}\frac{\xi}{M}\left(u^2(\|\vec{X}_1\|^2 + \|\vec{X}_2\|^2) - 2u\,\mathrm{Re}\vec{X}_2^H\vec{X}_1\right)\right]$$

for $0 \leq u < 1$. If we further specialize to the case with no phase noise we obtain

$$P_e \leq \min_{0\leq u<1}(1-u^2)^{-1}\exp\left(-\frac{2u\xi}{1+u}\right) \tag{5.20}$$

which is exactly 3 dB better than the Chernoff bound for FSK, thus retains all the desirable relations to the actual performance.

5.3.2 Chernoff–Jensen Approximation

The conditional Chernoff bound we obtained in Equation (5.17) depends on quadratic terms of phase noisy vectors $\vec{X}_1$ and $\vec{X}_2$. Unless $K = 1$, these quadratics have dependent components; therefore we must know the joint statistics of $\vec{X}_1$ and $\vec{X}_2$ to be able to remove the conditioning on the phase noise process. In the light of our experience with the statistics of $|X_1(k)|^2$ alone in Chapter 2, this may be a very difficult task. Even in the single filter case, one has the bound (with $v = \sqrt{K}u$)

$$P_e(X_1, X_2, M=1) \leq (1-v^2)^{-1}\exp\left[\frac{1}{1-v^2}\left(v^2\xi_1|X_1|^2 + v^2\xi_2|X_2|^2 - 2v\sqrt{\xi_1\xi_2}\,\mathrm{Re}\,X_2^*X_1\right)\right]$$

which requires the joint statistics of the random variable pair $|\sqrt{\xi_1}X_1 \pm \sqrt{\xi_2}X_2|^2$. Therefore the exact unconditioning of the bound seems infeasible. We have seen in Chapters 2 and 4 that, in the case of envelope detection of FSK and OOK signals, the interchange of the conditional error probability function for the double filter receiver and the phase noise expectation results in very close approximations to the actual error probability. Encouraged by the nature of this approximation we will apply this technique to get an estimate of the transmitted reference system performance. We will refer to the overall approximation for the error probability as a *Chernoff–Jensen approximation* to reflect both the method by which the conditional error probability is bounded and the method by which the conditioning is removed. Note that this approximation will not provide an upper bound on the performance since the conditional bound is not a concave function of $(\vec{X}_1, \vec{X}_2)$. However it is expected that due to the optimization of the Chernoff bound and the averaging of the double filter the excursion from the true performance will not be significant. This approximation overemphasizes the additive noise by upper bounding its effect, and underemphasizes the

phase noise by taking the phase noisy parameters at their means. Therefore, the values of M that will be predicted by our analysis will be smaller than the exact optimal, and conversely the predicted values of K will be larger than the exact optimal.

A check of Chernoff–Jensen approximation is the FSK case. The approximation yields

$$P_{e,CJ} = \min_{u,M}(1-u^2)^{-M} \exp\left[-\frac{u}{1+u}\xi\bar{X}(\gamma/M)\right]$$

where $\bar{X}$ is the mean of the squared envelope introduced in Chapter 2 and given by

$$\bar{X}(\gamma) = \frac{4}{\gamma}\left[1-\frac{2}{\gamma}(1-e^{-\gamma/2})\right] .$$

The comparison of this approximation with the actual performance obtained in Chapter 2 is shown in Figure 5-4. It is seen that the approximation satisfactorily estimates the performance in this case.

Now we apply the Chernoff–Jensen approximation to the double filter transmitted reference system. The conditional Chernoff bound in (5.17) requires three expectations to be found. These are

$$\begin{aligned} e_1 &= \mathrm{Re}\, E\, \vec{X}_2^H C \vec{X}_1 \\ e_2 &= \mathrm{Re}\, E\, \vec{X}_2^H C \vec{X}_2 \\ e_3 &= \mathrm{Re}\, E\, \vec{X}_1^H D \vec{X}_1 \end{aligned}$$

where the matrices C and D are defined as

$$\begin{aligned} C &= (I-u^2AA^T)^{-1} \\ D &= (I-u^2AA^T)^{-1}AA^T . \end{aligned}$$

Let's define the correlation matrices of the random vectors $\vec{X}_1$ and $\vec{X}_2$ as

$$\begin{aligned} H_{11} &= E\, \vec{X}_1\vec{X}_1^H \\ H_{22} &= E\, \vec{X}_2\vec{X}_2^H \\ H_{21} &= E\, \vec{X}_2\vec{X}_1^H . \end{aligned}$$

Then with the definition of the matrix operation $\odot$ as the sum of elementwise products, i.e.

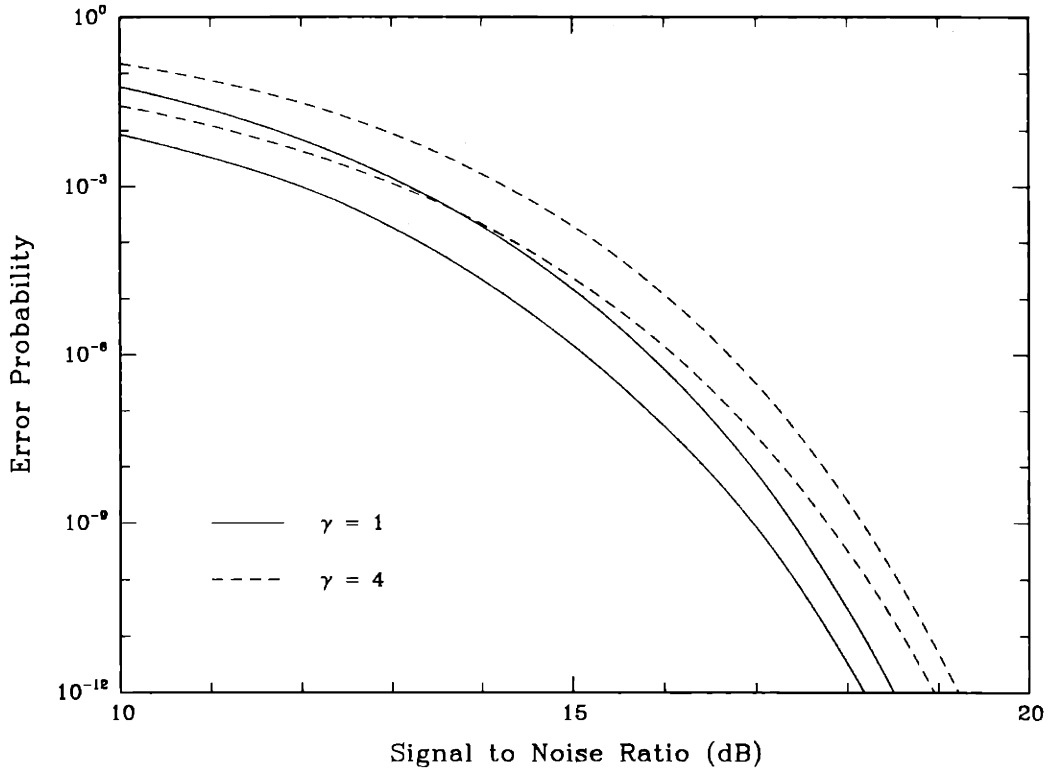

Figure 5-4: A comparison of the Chernoff–Jensen approximation with the actual performance for double filter FSK for $\gamma = 1$ and $\gamma = 4$.

$A \odot B = \sum_{i,k=1}^{M} A_{ik}B_{ik}$, we can compactly write the three expectations as

$$\begin{aligned} e_1 &= C \odot H_{21} \\ e_2 &= C \odot H_{22} \\ e_3 &= D \odot H_{11} \end{aligned}$$

where we have dropped the real parts since all the correlation matrices turn out to be real as will be seen. The correlation matrices are computed explicitly in Appendix 5.A, resulting in the following expressions:

$$H_{11}(i,k) = \begin{cases} \frac{2}{\alpha} - \frac{2}{\alpha^2}(1-e^{-\alpha}) & k = i \\ \left(\frac{1-e^{-\alpha}}{\alpha}\right)^2 e^{-\alpha(|k-i|-1)} & k \neq i \end{cases} \tag{5.21}$$

$$H_{22}(i,k) = \begin{cases} \frac{2}{\mu} - \frac{2}{\mu^2}(1-e^{-\mu}) & k = i \\ \frac{2}{\mu}\left(1 - \frac{|k-i|}{K}\right) + \frac{2}{\mu^2}\left[e^{-\alpha(K-|k-i|)} + (e^{-2\mu} - 2e^{-\mu})e^{\alpha(K-|k-i|)}\right] & 0 < |k-i| < K \\ \left(\frac{1-e^{-\mu}}{\mu}\right)^2 e^{-\alpha(|k-i|-K)} & |k-i| \geq K \end{cases} \tag{5.22}$$

$$H_{21}(i,k) = \begin{cases} \frac{1}{\mu\alpha}(1-e^{-\mu})(1-e^{-\alpha})e^{-\alpha(k-i-1)} & i < k \\ \frac{2}{\mu} - \frac{1}{\mu\alpha}(1-e^{-\alpha})\left[e^{-\alpha(i-k)} + e^{-\alpha(K-1-(i-k))}\right] & 0 \leq i-k < K \\ \frac{1}{\mu\alpha}(1-e^{-\mu})(1-e^{-\alpha})e^{-\alpha(i-k-K)} & i-k \geq K \end{cases} \tag{5.23}$$

where $\alpha \triangleq \pi\beta T_1 = \gamma/2M$, $\mu \triangleq \pi\beta T_2 = K\gamma/2M$.

To summarize, we have obtained the Chernoff–Jensen approximation as

$$P_e \simeq |C| \exp\left[-2u\sqrt{K\xi_1\xi_2}(C \odot H_{21}) + u^2 K\xi_2(C \odot H_{22}) + u^2\xi_1(D \odot H_{11})\right] \tag{5.24}$$

where the matrices C, D and H_{ij} are as defined previously. This approximation is to be minimized over u, ξ_1, ξ_2, K and M subject to the constraints

$$\begin{aligned} \xi_1 + \frac{\xi_2}{K} &= \frac{\xi}{M} \\ 0 \leq u &< \lambda_{\max}^{-1/2}(AA^T) \\ K, M &\in \{1, 2, \ldots\} . \end{aligned}$$

We will discuss the results of this optimization in Section 5.4. First we will consider a modification of the reference filter for possible performance improvement.

5.3.3 A Centered Reference Filter

In the previous analysis we have assumed that the information and reference filters integrate from $t-T_i$ to t to produce the output at time t for $i = 1, 2$ respectively. Since $T_2 = KT_1$ we may regard T_1 to be our unit of time. Then the first $K-1$ units of the integration window of the reference filter precedes the integration window of the information filter. For large K the distance in time between portions of the phase noise process $\theta(t)$ that affect the filter outputs will be large. Therefore the filter outputs may lose the phase coherence that they had at the input. The reason for using a K value that is greater than 1 is to gain robustness against additive noise by shrinking the filter bandwidth by a factor of K. However large K also means reduced phase coherence and hence reduced phase noise tolerance. To increase the phase coherence between the filter outputs, one has to minimize the maximum distance between the respective integration windows. For fixed size integration windows this means that the windows must be centered, i.e. if the information filter is integrating over $(t-T_1, t)$, then the reference filter must integrate over $(t - T_1/2 - T_2/2, t - T_1/2 + T_2/2)$. We insist on having the information filter noncentered because intersymbol interference would occur otherwise due to integration windows crossing the bit boundaries at sampling times. (We assume that sampling is done at times kT_1, $k = 1, \ldots, M$.) Clearly the reference filter we suggest here is noncausal. However this does not cause an implementation problem since the integrator input may be delayed by $T_2/2$ to create the same effect.

The analysis of Section 5.3.2 is valid for this case with minor modifications. The phase noisy reference vector $\vec{X}_2$ is now given by

$$X_2(k) = \frac{1}{T_2} \int_{(k-1/2)T_1 - T_2/2}^{(k-1/2)T_1 + T_2/2} e^{j\theta(t)}\, dt$$

It is convenient to assume that K is odd since this will ensure that the reference integration window consists of an integral number of chips of information integration window. Then with $K = 2N - 1$, one can write

$$X_2(k) = \frac{1}{K} \sum_{l=-(N-1)}^{N-1} X_1(k-l)\,.$$

The conditional Chernoff bound of (5.17) remains unchanged because the additive noise structure is the same. The only change will be in the Jensen approximation due to new correlation matrices. H_{11} is still given by (5.21) since $\vec{X}_1$ is not changed. H_{22} is also unchanged and given by (5.22) since a shift in the time origin does not affect the correlation

between $X_2(i)$ and $X_2(k)$. The cross correlation between $\vec{X}_1$ and $\vec{X}_2$ will change however. In fact, this is precisely the reason we introduced this new filter structure. In Appendix 5.A we obtain the new cross correlation matrix $\bar{H}_{21}$ as

$$\bar{H}_{21}(i,k) = \begin{cases} \frac{2}{\mu} - \frac{1}{\alpha\mu}(1-\epsilon^{-\alpha})\left[\epsilon^{-\alpha(N-1-|k-i|)} + \epsilon^{-\alpha(N-1+|k-i|)}\right] & |k-i| < N \\ \frac{1}{\alpha\mu}(1-\epsilon^{-\alpha})(1-\epsilon^{-\mu})\epsilon^{-\alpha(|k-i|-N)} & |k-i| \geq N\,. \end{cases} \tag{5.25}$$

Note that $\bar{H}_{21}$ is symmetric while H_{21} was not, this is due to the symmetry of the integration windows.

Equation (5.24) will give the performance for the system with this centered filter with the substitution of $\bar{H}_{21}$ for H_{21}. The performance will be discussed in Section 5.4.

5.4 Results and Discussions

We now present the results of the performance analysis of the double filter transmitted reference scheme under consideration. We first consider the system with the noncentered integrators. Optimization over the filter bandwidths, power distribution and Chernoff bound parameter has been performed numerically. The resulting error probability is shown in Figure 5-5 as a function of signal-to-noise ratio for various values of phase noise strength γ. The error probability obtained by Chernoff–Jensen approximation for double filter FSK is also shown on the same graphs. It is seen that for small values of γ, the reference transmission improves the performance considerably over FSK. However for $\gamma \geq 1$, the performance is identical to that of FSK. This is due to the fact that for large values of γ the difference in the bandwidth occupancies of the information and reference signals is small. Hence the filters become identical, which in turn imposes an even power distribution and thus FSK performance. The optimal power distribution does not seem to be correlated to the total power available, but only to the phase noise strength.

The numerical computations were also performed for the system in which the reference filter has a centered integration window as described in Section 5.3.3. The error probability curves are given in Figure 5-6 for various values of γ as well as the FSK performance. It is seen that this system has a considerably better phase noise tolerance than its noncentered equivalent. For example, for $\gamma = 4$ there is a distinct performance improvement with centered filters. A significantly less proportion of the total power is allocated to the reference signal. This is due to narrower reference filters that can be used without losing the phase coherence when the filter is centered. In Figure 5-7 we have tabulated the optimal values for

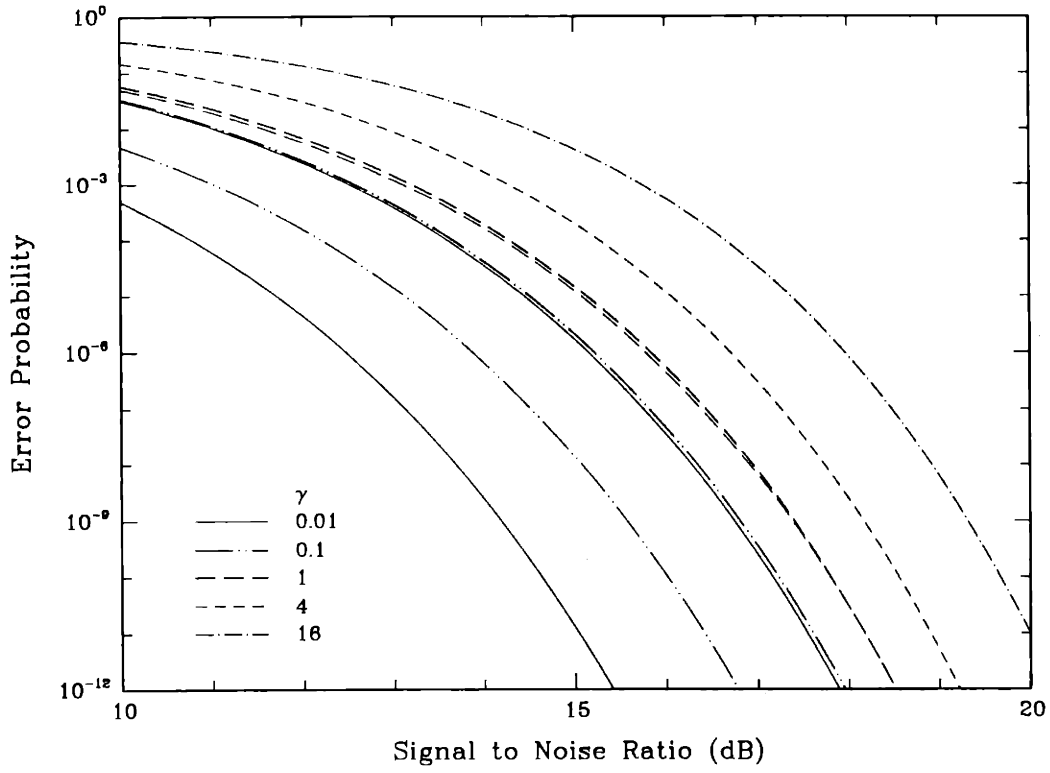

Figure 5-5: Error probability of transmitted reference system with noncentered reference filter as well as that of a double filter FSK system for various values of γ.

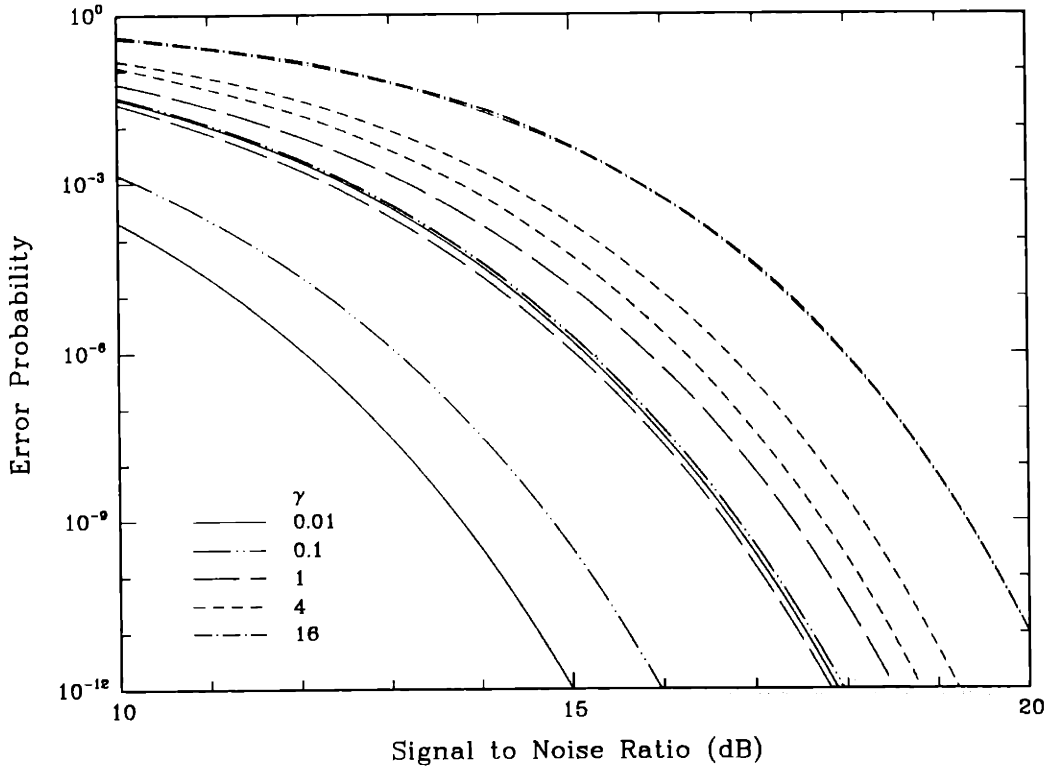

Figure 5-6: Error probability of transmitted reference system with centered reference filter as well as that of a double filter FSK system for various values of γ.

the bandwidth expansion factor M of the information filter and the bandwidth reduction factor K of the reference filter with respect to γ at an SNR level that achieves an error probability of 10^{-9}. It is seen that M increases with γ much faster with centered filters, and K decreases with γ much faster with noncentered filters. For both filter types K reaches a steady state value of 1 as expected.

In Figure 5-8 we compare the phase noise penalties of the two transmitted reference systems with respect to phase noise free DPSK at an error probability of 10^{-9}. The penalty for double filter FSK is also shown for comparison purposes. We conclude that for small values of γ, both transmitted reference systems have considerably better performance than FSK. While the system with noncentered filter saturates to FSK performance for $\gamma \geq 0.9$, the system with centered filter has an improved performance up to $\gamma = 8$. For the typical value of $\gamma = 1$, the centered filter has a gain of about 1 dB over FSK.

γ	Noncentered		Centered	
	K	M	K	M
0	∞	1	∞	1
0.006	21	1	71	1
0.01	18	1	41	1
0.05	7	1	15	1
0.1	4	1	9	1
0.5	2	1	7	3
1	2	2	5	4
2	1	2	3	4
4	1	4	3	7
16	1	10	1	10

Figure 5-7: Optimal values of K and M for various values of γ at a bit error probability of 10^{-9}.

Therefore, the transmission of a reference at an optimized power distribution and a double filter receiver with optimized filter bandwidths and proper filter structures achieve a performance that is the closest to ideal DPSK. This system is very promising for attaining robustness against phase noise for typical linewidth and bit rate values.

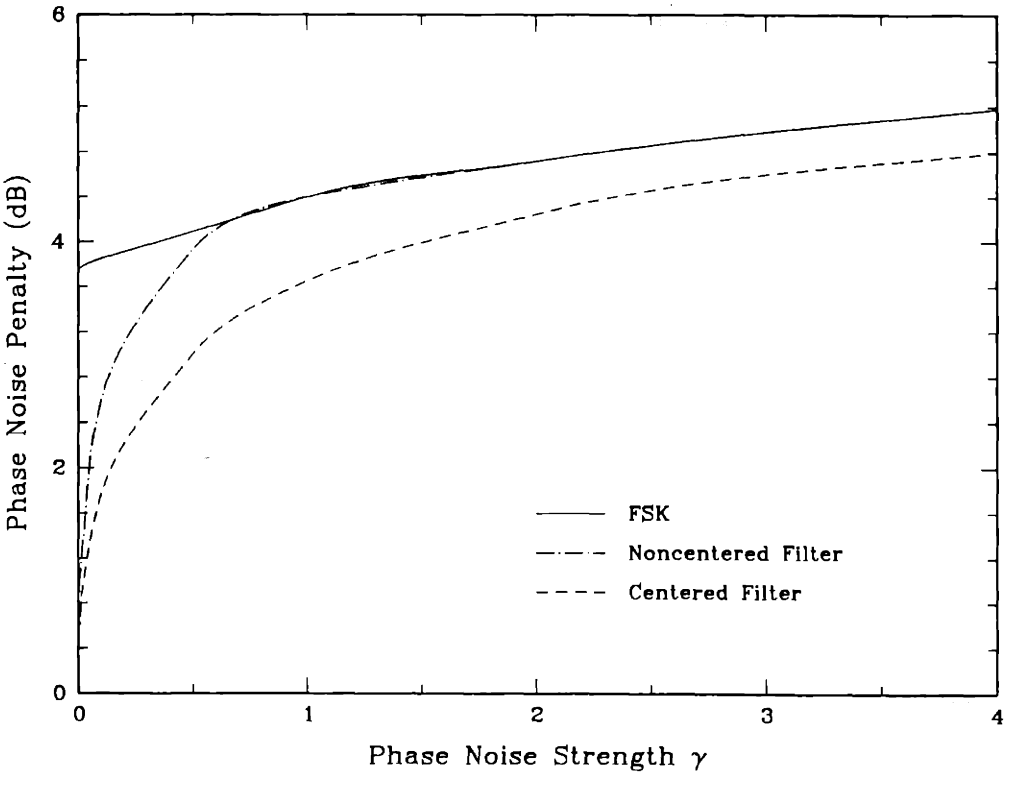

Figure 5-8: Phase noise penalty for noncentered and centered transmitted reference systems as well as double filter FSK at a bit error probability of 10^{-9}.

Appendix

5.A Calculation of Correlation Matrices

In this appendix, we obtain the auto- and cross-correlation matrices of the phase noisy vectors $\vec{X}_1$ and $\vec{X}_2$. We start with the autocorrelation matrix of $\vec{X}_1$, H_{11}. From the definition of $X_1(k)$ we have

$$\begin{aligned} H_{11}(i,k) &= EX_1(i)X_1^*(k) \\ &= \frac{1}{T_1^2}\int_{(i-1)T_1}^{iT_1}\int_{(k-1)T_1}^{kT_1} E\, e^{-j(\theta(t)-\theta(\tau))}\, d\tau\, dt\ . \end{aligned}$$

Now using the fact that $\theta(t) - \theta(\tau)$ is Gaussian with variance $2\pi\beta|t-\tau|$, we obtain

$$H_{11}(i,k) = \frac{1}{T_1^2}\int_{(i-1)T_1}^{iT_1}\int_{(k-1)T_1}^{kT_1} e^{-\pi\beta|t-\tau|}\, d\tau\, dt\ .$$

At this point there are two cases to consider: $i = k$ and $i \neq k$. For the first case we get by symmetry

$$\begin{aligned} H_{11}(i,i) &= \frac{2}{T_1^2}\int\int_{t>\tau} e^{-\pi\beta(t-\tau)}\, d\tau\, dt \\ &= \frac{2}{\alpha} - \frac{2}{\alpha^2}(1-e^{-\alpha}) \end{aligned} \tag{5.26}$$

where we have defined $\alpha = \pi\beta T_1$. For $i \neq k$, let's first assume $i > k$. Then

$$\begin{aligned} H_{11}(i,k) &= \frac{1}{T_1^2}\int_{(i-1)T_1}^{iT_1} e^{-\pi\beta t}\, dt \int_{(k-1)T_1}^{kT_1} e^{\pi\beta\tau}\, d\tau \\ &= \left(\frac{1-e^{-\alpha}}{\alpha}\right)^2 (1-e^{-\alpha(|i-k|-1)}) \end{aligned} \tag{5.27}$$

where we have introduced the absolute value in the second line artificially to make (5.27) valid for $i < k$ by symmetry. Equations (5.26) and (5.27) completely define the autocorrelation matrix H_{11} as given in Equation (5.21).

Now we consider the autocorrelation matrix H_{22} of $\vec{X}_2$. This can be written as the following integral

$$H_{22}(i,k) = \int_{iT_1-T_2}^{iT_1}\int_{kT_1-T_2}^{kT_1} e^{-\pi\beta|t-\tau|}\, dt\, d\tau\ .$$

For $i = k$, this is similar to H_{11}. Thus substituting T_2 for T_1 we get

$$H_{22}(i,i) = \frac{2}{\mu} - \frac{2}{\mu^2}(1 - e^{-\mu}) \tag{5.28}$$

where we have defined $\mu = K\alpha$. For the case $|i-k| \geq K$, the two integrals split with the result easily obtained as

$$H_{22}(i,k) = \left(\frac{1-e^{-\mu}}{\mu}\right)^2 e^{-\alpha(|i-k|-K)} . \tag{5.29}$$

Finally for the case $0 < |i-k| < K$, one has to consider the two regions in which the absolute value in the exponent of the integrand take different values. After a tedious, but straightforward calculation, one gets

$$H_{22}(i,k) = \frac{2}{\mu}\left(1 - \frac{|k-i|}{K}\right) + \frac{1}{\mu^2}\left[e^{-\alpha(K-|k-i|)} + (e^{-2\mu} - 2e^{-\mu})e^{\alpha(K-|k-i|)}\right] . \tag{5.30}$$

Equations (5.28), (5.29) and (5.30) define the autocorrelation matrix H_{22} as given in Equation (5.22).

Next we want to calculate the autocorrelation matrix H_{21}. Instead of performing a similar calculation to that of H_{11} which would be more involved due to the time overlaps between the defining integrals, we will recall the relation

$$X_2(i) = \frac{1}{K}\sum_{l=0}^{K-1} X_1(i-l)$$

and write the desired correlation as

$$H_{21}(i,k) = \frac{1}{K} E\, X_1(k) \sum_{l=0}^{K-1} X_1^*(i-l) = \frac{1}{K}\sum_{l=0}^{K-1} H_{11}(k, i-l) .$$

The result of the above will depend on whether the diagonal entries of H_{11} enter the summation or not. When $i-k \geq K$, or when $i < k$, the sum consists of nondiagonal entries only, while when $0 \leq i-k < K$ we have both types of terms in the series. For the case $i-k \geq K$, by using (5.27) we obtain

$$H_{21}(i,k) = \frac{1}{K}\left(\frac{1-e^{-\alpha}}{\alpha}\right)^2 \sum_{l=0}^{K-1} e^{-\alpha(i-k-l-1)}$$

$$= \frac{1}{\alpha\mu}(1-e^{-\alpha})(1-e^{-\mu})e^{-\alpha(i-k-K)} . \tag{5.31}$$

Similarly, for the case $i < k$ one gets

$$\begin{aligned} H_{21}(i,k) &= \frac{1}{K}\left(\frac{1-e^{-\alpha}}{\alpha}\right)^2 \sum_{l=0}^{K-1} e^{-\alpha(k-i+l-1)} \\ &= \frac{1}{\alpha\mu}(1-e^{-\alpha})(1-e^{-\mu})e^{-\alpha(k-i-1)} . \end{aligned} \tag{5.32}$$

For the case $0 \leq i-k < K$, one has the consider how the diagonal entries enter the series. Since H_{11} is symmetric and Toeplitz, we can use the convention $H_{11}(i,k) = h(|i-k|)$. With the convention, we can write for the case under consideration

$$H_{21}(i,k) = \frac{1}{K}\left[h(0) + 2\sum_{n=1}^{K-1-(i-k)} h(n) + \sum_{n=K-(i-k)}^{i-k} h(n)\right]$$

which yields

$$H_{21}(i,k) = \frac{2}{\mu} - \frac{1}{\alpha\mu}(1-e^{-\alpha})\left[e^{-\alpha(i-k)} + e^{-\alpha(K-1-(i-k))}\right] . \tag{5.33}$$

Equations (5.31),(5.32) and (5.33) define the cross-correlation matrix H_{21} as given in Equation (5.23).

Finally we want to calculate the cross-correlation matrix $\bar{H}_{21}$ for the case of the centered reference filter given in Section 5.3.3. Now the reference vector $\vec{X}_2$ is defined as

$$X_2(i) = \frac{1}{K}\sum_{l=-(N-1)}^{N-1} X_1(i-l)$$

so that the elements of $\bar{H}_{21}$ are

$$\bar{H}_{21}(i,k) = \frac{1}{K}\sum_{l=-(N-1)}^{N-1} H_{11}(k,i-l) .$$

Note that the only changes from the calculation of H_{21} are the upper and lower limits of the defining series. For $|i-k| \geq N$, the series contains only the off-diagonal elements of

H_{11} and the result is

$$\begin{aligned}\bar{H}_{21}(i,k) &= \frac{1}{K}\left(\frac{1-e^{-\alpha}}{\alpha}\right)^2 \sum_{l=-(N-1)}^{N-1} e^{-\alpha(|i-k|-l-1)} \\ &= \frac{1}{\alpha\mu}(1-e^{-\alpha})(1-e^{-\mu})e^{-\alpha(|k-i|-N)} \ . \end{aligned} \tag{5.34}$$

For the case with $|i-k| < N$, an accounting of the terms shows that with the same convention as before we get

$$\begin{aligned}\bar{H}_{21}(i,k) &= \frac{1}{K}\left[h(0) + 2\sum_{n=1}^{N-1-|i-k|} h(n) + \sum_{n=N-|i-k|}^{N-1+|i-k|} h(n)\right] \\ &= \frac{2}{\mu} - \frac{1}{\alpha\mu}(1-e^{-\alpha})\left[e^{-\alpha(N-1-|i-k|)} + e^{-\alpha(N-1+|i-k|)}\right] \ . \end{aligned} \tag{5.35}$$

Equations (5.34) and (5.35) define the new cross-correlation matrix as given in Equation (5.25).

Chapter 6

A Signal Space Analysis of Phase Noise

So far we have considered different modulation formats with various detection strategies, both optimal and suboptimal. We converted the optimal signal detection problem to an optimal vector detection problem via sampling in the time domain. In this chapter we take a different, perhaps more fundamental, approach to detecting phase noisy sinusoids in additive white Gaussian noise. This is the classical signal space approach used frequently in communication theory. In this approach, the signals are viewed as points in an infinite dimensional vector space where the directions are specified by a complete orthonormal basis of signals and the components of a signal in this representation are given by its projections on these basis signals. The problem is one of selecting a basis in which the resulting projections of the received signal are easily processed [55].

This approach is particularly fruitful in the problem of detecting one of finitely many known signals in additive white Gaussian noise. This is because a white Gaussian process $n(t)$ has independent projections on any set of orthogonal functions, i.e. the random variables

$$n_i = \int n(t)x_i(t)\,dt \quad i = 1, 2$$

are independent if (and only if)

$$\int x_1(t)x_2(t)\,dt = 0\,.$$

As a result, if the number of hypotheses is M, at most M signal directions are needed for detection; the rest of the directions will contain projections which are statistically independent of the true hypothesis and will therefore be irrelevant [37]. The required number of directions can be much less than M: for example for M-ary pulse amplitude modulation

(PAM) this number is 1, for M-ary quadrature amplitude modulation (QAM) it is 2.

6.1 Eigenfunctions of a Phase Noisy Sinusoid

When the signals to be detected are sinusoids with unknown but constant phases, then the relevant signal directions are the in-phase and quadrature sinusoids; the well-known envelope detector may be obtained using the signal space approach quite easily. When the unknown phase is time-varying, as is the phase noise process, the appropriate basis is not easily seen. Here by "appropriate" we again mean a basis for which there are only a finite number of relevant directions. Since the additive white Gaussian noise has independent projections for any basis, only the phase noisy sinusoid needs to be considered. It is more convenient to work with the complex signal

$$s(t) = A \exp\left[j\left(2\pi f_c t + \theta(t) + \phi\right)\right] . \tag{6.1}$$

The goal is to find a complete orthonormal basis $\{\phi_n(t)\}$ on the interval $(0, T)$ such that

$$s(t) = \sum_{n=0}^{\infty} s_n \phi_n(t)$$

where s_n are uncorrelated random variables. (The equality above is in the mean-square sense,i. e. $\lim_{N\to\infty} |s(t) - \sum_{n=0}^{\infty} s_n \phi_n(t)|^2$ integrates to 0.) The desired basis is the solution to the Karhunen-Loeve integral equation [15, 55]

$$\int_0^T R_s(t,\tau)\phi_n(\tau)\, d\tau = \lambda_n \phi_n(t) \quad n = 0, 1, \ldots \; 0 < t < T \tag{6.2}$$

where $R_s(t,\tau)$ is the autocorrelation function of $s(t)$ and λ_n are the eigenvalues associated with $\phi_n(t)$.

Before attempting to solve this integral equation we invoke a simple property to eliminate the amplitude and the carrier frequency.

Lemma 6.1 *If $\{\phi_{1n}(t), \lambda_{1n}\}$ are the eigenfunctions and eigenvalues for a wide-sense stationary random process $\{x_1(t)\}$, $\{x_2(t)\}$ is defined as*

$$x_2(t) = Ae^{j\omega_0 t} x_1(t)$$

where A and ω_0 are constants, then the associated eigenvalues and eigenfunctions satisfy

$$\begin{aligned} \phi_{2m}(t) &= e^{j\omega_0 t}\phi_{1m}(t) \\ \lambda_{2m} &= A^2\lambda_{1m} \end{aligned}$$

for all m.

Proof. Let R_1, R_2 be the autocorrelation function of x_1 and x_2 respectively. Then

$$R_2(t,\tau) = E\left(x_2(t)x_1^*(t)\right) = A^2 e^{j\omega_0(t-\tau)}R_1(t,\tau)\,.$$

Suppose ϕ_{1m} and λ_{1m} satisfy the Karhunen-Loeve equation for $s_1(t)$. Let ϕ_{2m} and λ_{2m} satisfy the statement of the lemma. Then

$$\begin{aligned} \int R_2(t,\tau)\phi_{2m}(\tau)\,d\tau &= A^2\int e^{j\omega_0(t-\tau)}R_1(t,\tau)e^{j\omega_0\tau}\phi_{1m}(\tau)\,d\tau \\ &= A^2 e^{j\omega_0 t}\lambda_{1m}\phi_{1m}(t) \\ &= \lambda_{2m}\phi_{2m}(t) \end{aligned}$$

The converse is also easily proven by assuming that some ϕ_{2m} and λ_{2m} satisfy the Karhunen-Loeve equation for $s_2(t)$ and then by showing that related quantities for $s_1(t)$ are also solutions in the same way as above. □

This lemma will be used to consider the unit-amplitude baseband phase noisy sinusoid $u(t)$ in the Karhunen-Loeve equation. In this case we have

$$R_u(t,\tau) = \epsilon^{-\pi\beta|t-\tau|}$$

and the left hand side of the integral equation, which we define as $f(t)$, becomes

$$f(t) = \int_0^t \exp\left[-a(t-s)\right]\phi_m(s)\,ds + \int_t^T \exp\left[a(t-s)\right]\phi_m(s)\,ds \tag{6.3}$$

where we have also defined $a \triangleq \pi\beta$. Differentiating both sides of the equation $f(t) = \lambda_m\phi_m(t)$ with respect to t, we obtain

$$-a\int_0^t \exp\left[-a(t-s)\right]\phi_m(s)\,ds + a\int_t^T \exp\left[a(t-s)\right]\phi_m(s)\,ds = \lambda_m\phi_m'(t) \tag{6.4}$$

and differentiating once more we get

$$\lambda_m \phi_m''(t) + (2a - a^2\lambda_m)\phi_m(t) = 0 \tag{6.5}$$

which is a linear homogeneous differential equation that can be easily solved in terms of λ_m. The solution is

$$\phi_m(t) = A_m e^{j\alpha_m t} + B_m e^{-j\alpha_m t} \tag{6.6}$$

where A_m and B_m are constants yet to be determined and α_m are related to the eigenvalues via

$$\alpha_m = \sqrt{\frac{2a}{\lambda_m} - a^2}\ . \tag{6.7}$$

In order to determine the eigenvalues, we need to resort to the integral equation (6.4). Inserting the solution in (6.6) into (6.4) we obtain, after some manipulations, that

$$e^{-at}\left(\frac{A_m}{a + j\alpha_m} + \frac{B_m}{a - j\alpha_m}\right) + e^{a(t-T)}\left(\frac{A_m e^{j\alpha_m T}}{a - j\alpha_m} + \frac{B_m e^{-j\alpha_m T}}{a + j\alpha_m}\right) = 0$$

must be satisfied for all $0 < t < T$. For any nonzero linewidth this is possible only when the coefficients of two linearly independent functions, e^{at} and e^{-at} are identically 0, i.e. α_m must be such that the linear system of equations

$$\begin{aligned} \frac{A_m}{a + j\alpha_m} + \frac{B_m}{a - j\alpha_m} &= 0 \\ \frac{A_m e^{j\alpha_m T}}{a - j\alpha_m} + \frac{B_m e^{-j\alpha_m T}}{a + j\alpha_m} &= 0 \end{aligned} \tag{6.8}$$

has a nontrivial solution for A_m, B_m. Thus we need

$$\frac{e^{-j\alpha_m T}}{(a + j\alpha_m)^2} = \frac{e^{j\alpha_m T}}{(a - j\alpha_m)^2} \tag{6.9}$$

to be satisfied. Note from Equation (6.7) that α_m is either real nonnegative or purely imaginary, since the eigenvalues are real and nonnegative. Since we are interested in small linewidths (small a) we will assume that α_m is real. In this case, the set of solutions becomes the solutions of the equation

$$2\arctan\frac{\alpha_m}{a} + \alpha_m T = m\pi \quad m = 0, 1, \ldots \tag{6.10}$$

We now have a mechanism to calculate the eigenvalues and the eigenfunctions. We can solve (6.10) for α_m and use them to calculate the eigenvalues via

$$\lambda_m = \frac{2a}{a^2 + \alpha_m^2} \tag{6.11}$$

and the eigenfunctions via Equation (6.6). (6.10) can not be solved analytically, so graphical methods will have to be used. It can be seen that for every m there exists a single solution for α_m. For $m = 0$, we have $\alpha_m = 0$, but this does not correspond to an eigenfunction since we have from (6.8) $A_0 + B_0 = 0$, while from (6.6) $\phi_0(t) = A_0 + B_0 = 0$.

Smaller values of α_m, which correspond to smaller m, are more significant since they result in larger eigenvalues. The following properties of the solutions α_m are easily observed and proved.

Lemma 6.2 *The solution α_m satisfy the following properties:*

i)

$$(m-1)\frac{\pi}{T} < \alpha_m < m\frac{\pi}{T}$$

ii)

$$\alpha_m - (m-1)\frac{\pi}{T} < \frac{2a}{\pi(m-1)}$$

iii)

$$\lim_{m\to\infty}\left[\alpha_m - (m-1)\frac{\pi}{T}\right] = 0$$

Proof. i) Since $\alpha_m > 0$, we have $0 < m\pi - T\alpha_m = 2\arctan(\alpha_m/a) < \pi$, from which the result follows.

ii) From (6.10) we get, $\alpha_m T - (m-1)\pi = \pi - 2\arctan(\alpha_m/a)$. Now we use $\arctan x \geq \pi/2 - 1/x$ to obtain

$$\alpha_m T - (m-1)\pi \leq \frac{2a}{\alpha_m}$$

which yields the desired result with the use of i).

iii) Follows immediately from the first two results. □

According to this lemma we can approximate α_m by $(m-1)\pi/T$ for sufficiently large m. The relative error in estimating the eigenvalues via this approximation can be easily bounded as

$$\frac{|\Delta\lambda_m|}{\lambda_m} \leq \frac{4aT}{\pi^2(m-1)^2}$$

showing that the approximation will be satisfactory when $m \gg \sqrt{aT}/\pi$. Thus we use for the eigenvalues of the original IF signal in (6.1)

$$\lambda_m \simeq \frac{2aA^2}{a^2 + ((m-1)\pi/T)^2}$$

for large m. Note that this is indeed a tight upper bound since α_m are underestimated.

We would like to have an estimate on the error in representing the phase noisy sinusoid by its projections on the first M eigenfunctions. It is a well-known fact that the mean square error in this representation is given as the sum of the remaining eigenvalues, i.e.

$$\epsilon_M \stackrel{\triangle}{=} \int_0^T E\left[\left|s(t) - \sum_{k=1}^{M} s_k \phi_k(t)\right|^2\right] dt = \sum_{k=M+1}^{\infty} \lambda_k$$

where the projections are defined in the standard way:

$$s_k = \int_0^T s(t)\phi_k^*(t)\, dt\,.$$

The following lemma shows that the representation error can be tightly bounded in terms of the signal energy $E_s = A^2T$ and the linewidth to bit rate ratio βT for large M.

Lemma 6.3

$$\frac{2}{\pi}E_s\left(\frac{\beta T}{M} - \frac{1}{3}\left(\frac{\beta T}{M}\right)^3\right) \leq \epsilon_M \leq \frac{2}{\pi}E_s\frac{\beta T}{M-1}$$

Proof. From the previous discussion, with $a = \pi\beta$ and $E_s = A^2T$, we have

$$\begin{aligned}\epsilon_M &= \sum_{k=M+1}^{\infty} \frac{2aA^2}{a^2 + ((k-1)\pi/T)^2} \\ &= \frac{2}{\pi}E_s\beta T \sum_{k=M}^{\infty} \frac{1}{k^2 + (\beta T)^2}\,.\end{aligned}$$

Using the fact that the function $(x^2 + \alpha^2)^{-1}$ is decreasing in x, we can bound the series above as

$$\int_{M-1}^{\infty} \frac{dx}{x^2 + \alpha^2} \geq \sum_{k=M}^{\infty} \frac{1}{k^2 + \alpha^2} \geq \int_{M}^{\infty} \frac{dx}{x^2 + \alpha^2}$$

which results in

$$\frac{1}{\alpha}\left(\frac{\pi}{2} - \arctan\frac{M-1}{\alpha}\right) \geq \sum_{k=M}^{\infty} \frac{1}{k^2+\alpha^2} \geq \frac{1}{\alpha}\left(\frac{\pi}{2} - \arctan\frac{M}{\alpha}\right) .$$

Finally to linearize the bounds in $1/M$ we use

$$\frac{1}{x} - \frac{1}{3x^3} \leq \frac{\pi}{2} - \arctan x \leq \frac{1}{x} \qquad \text{for } x \geq 0$$

and obtain the claimed result. □

The bounds in the lemma are asymptotically tight. They reveal that for a small representation error, more directions must be considered for larger signal energy and/or larger phase noise strength.

Having obtained the eigenvalues, we only need the coefficients (A_m, B_m) to complete the characterization of the signal eigenfunctions $\phi_m(t)$. To summarize, the IF eigenfunctions and eigenvalues are given by

$$\phi_m(t) = e^{j2\pi f_c t}\left(A_m e^{j\alpha_m t} + B_m e^{-j\alpha_m t}\right)$$

and

$$\lambda_m = A^2 \frac{2a}{a^2+\alpha_m^2}$$

where α_m are found graphically from Equation (6.10). (A_m, B_m) must satisfy Equation (6.8) which reduces to

$$A_m e^{-j\theta_m} + B_m e^{j\theta_m} = 0$$

where $\theta_m = \arctan(\alpha_m/a)$. Using (6.10) once again we obtain

$$B_m = (-1)^{m+1} e^{j\alpha_m T} A_m$$

resulting in

$$\phi_m(t) = A_m e^{j2\pi f_c t}\left(e^{j\alpha_m t} - (-1)^m e^{-j\alpha_m (t-T)}\right) .$$

A_m can now be obtained by normalizing $\phi_m(t)$ as

$$A_m = \left[2\left(T + \frac{\lambda_m}{A^2}\right)\right]^{-1/2} e^{-j\gamma^m}$$

where γ_m is an arbitrary phase. The choice of

$$\gamma_m = \begin{cases} \alpha_m T/2 & \text{for } m \text{ odd} \\ \alpha_m T/2 + \pi/2 & \text{for } m \text{ even} \end{cases}$$

simplifies the eigenfunctions to

$$\phi_m(t) = \left(\frac{2}{T + \lambda_m/A^2}\right)^{1/2} e^{j2\pi f_c t} \begin{cases} \cos \alpha_m(t - T/2) & m \text{ odd} \\ \sin \alpha_m(t - T/2) & m \text{ even} \end{cases}$$

which is a complete characterization of the eigenfunctions in conjunction with previous definitions of λ_m and α_m. The orthogonality of these eigenfunctions can be checked in a straightforward manner.

The structure of the eigenfunctions suggest a correlation of the received signal with sinusoids at frequencies $f_c \pm \alpha_m/2\pi$ for $m = 1, 2, \ldots$. It is not easy to see how these correlations will be processed for decision-making. However if we assume that they are squared and added, then the receiver is essentially sampling the power in the discrete spectral components spectral components within a bandwidth of the bit rate. The spectral sampling is nonuniform in the vicinity of the center frequency, but tends to get uniform as one moves away from f_c (large α_m). In fact as m gets large the spacing between the frequency samples becomes $1/2T$ which is the Nyquist rate.

The frequency sampling suggested by this analysis is the dual of time sampling approaches we pursued previously. This is an interesting observation in itself, but unfortunately not a useful one. Phase noise expands the basis of the signal from a single direction (the unique eigenfunction $\phi(t) = T^{-1/2} e^{j2\pi f_c t}$ on which the signal has nonzero projection) to infinitely many directions that we have obtained. This suggests that optimal detection strategies will be complicated– a fact we have repeatedly observed.

6.2 A Discrete Frequency Power Detector for FSK

We have observed that the signal space analysis suggests a sequence of correlations of the received signal with sinusoids of different frequencies. If the signal and noise components of these correlations are s_m and n_m respectively, the correlator outputs are

$$y_m = s_m + n_m \quad m = 1, 2, \ldots$$

where s_m are uncorrelated random variables with $E(s_m^2) = \lambda_m$, and s_m are independent Gaussian random variables with variance $N_0/2$. For frequency shift keying, the center frequency is either f_0 or f_1, hence two sets of correlations need to be performed resulting in $\{y_{0m}\}$ and $\{y_{1m}\}$. An intuitive way of processing these correlations is to add their powers and do a comparison:

$$\sum_{m=1}^{M} y_{0m}^2 \underset{1}{\overset{0}{\gtrless}} \sum_{m=1}^{M} y_{1m}^2$$

where M is the number of signal directions that the detector considers. We assume that $|f_1 - f_0|$ is large enough to ensure orthogonality as in Chapter 2. An accurate performance analysis of this receiver is possible in the style of Chapter 2. Here we will not be concerned with such an analysis; instead we demonstrate the issues that dictate the number of signal directions to be processed by the receiver.

Assuming that a "0" is transmitted we have

$$E\left(\sum_{m=1}^{M} y_{0m}^2\right) = \sum_{k=1}^{M} \lambda_k + \frac{MN_0}{2}$$

$$E\left(\sum_{m=1}^{M} y_{1m}^2\right) = \frac{MN_0}{2} .$$

Thus the signal to noise ratio at the decision variable is

$$\xi_M = \frac{\sum_{k=1}^{M} \lambda_k}{MN_0} .$$

An increment in the value of M from k to $k+1$ increases the signal power by λ_{k+1} while the noise power increases by N_0. Therefore the value of M should be chosen such that $\lambda_{M+1} < N_0 < \lambda_M$. Since for large m, λ_m can be written as

$$\lambda_m = \frac{2}{\pi} \frac{E_s \beta T}{(m-1)^2 + (\beta T)^2} ,$$

we obtain via $M \gg \beta T$

$$M_{\text{opt}} = \left\lceil \sqrt{\frac{2E_s \beta T}{\pi N_0}} \right\rceil \tag{6.12}$$

which, as expected, increases with phase noise strength and signal to noise ratio. An estimate of the error probability can be obtained via Gaussian approximation as $Q(\sqrt{\xi_M})$. For typical parameter values of $\beta T = 1$ and $E_s/N_0 = 20$ dB, the optimal number of signal

directions is 8, which results in 16 correlator branches in the receiver.

The important observation here is that the number of signal directions prescribed by the signal space analysis should be adjusted according to the additive noise level. An equivalent statement is that the frequency samples can not extend indefinitely since the signal component of a correlation away from the center frequency (frequency at which the spectral density has its peak) will be dominated by the additive white noise component.

Chapter 7

Phase Noise in Optical Networks

Optical communication networks have been the focus of intense research in the last decade. Because of the huge bandwidth and low loss offered by fiber-optic links, various multiple access methods, network architectures, routing and flow control algorithms, and communication protocols are currently under investigation. Perhaps the most fundamental of these issues is the mechanism in which the network resources will be allocated to the users in the network, that is the multiple access method to be employed. A variety of such methods have been suggested for optical networks, most notably Frequency Division Multiple Access (FDMA), Time Division Multiple Access (TDMA), and Code Division Multiple Access (CDMA).

Since the optical networks differ from traditional electronic networks mainly in the available frequency band for low loss transmission, frequency based multiplexing methods are more naturally incorporated into optical networking [56, 57]. While optical time division multiplexing is considered as an alternative to FDMA [58], the synchronization of a large number of users is still a formidable problem. Code based multiplexing methods are intuitively attractive since they don't require frequency or time scheduling, but simply require the a priori distribution of a code alphabet among the users. They also have the added benefit of network security since a receiver must know the right code to correctly decode a message. CDMA is a method of trading bandwidth with access coordination. Given the extra bandwidth available, it is conceivable that CDMA methods [59, 60] may be applied to certain optical networks in the future. However, some practical problems, most notably pulse dispersion in optical fibers, have to be solved for this to happen. The problem of small number of code words which limits the number of users must also be addressed [61].

We concentrate on frequency division multiplexed (FDM) optical networks here with a particular emphasis on the performance limitations imposed by phase noise. In a FDM

network, transmitters (or receivers) are assigned fixed nonoverlapping bands of the optical spectrum. There are two possible implementations of FDM.

Noncoherent FDM: Here on-off keying is used, and the receivers select the channel that they want to listen to by using optical filters and direct detection. There are two problems with this approach. One is that direct detection requires a large received power to maintain good error performance. The second is that tunable optical filters with narrow passbands are not expected to be available in the near future. Thus the channels have to be widely separated, which is usually called Wavelength Division Multiplexing (WDM) to reflect the fact that the channel separations are much higher than the electronic data rates. However the advance of optical filters [62] and optical amplifiers [63, 64] indicates a future where noncoherent FDM is a viable option.

Coherent FDM: Here the channel selection is accomplished via coherent detection. A tunable local oscillator laser followed by a photodetector brings the channel of interest to the IF range, and subsequent IF filtering provides further channel selection. Due to its superior sensitivity, possibility of dense channel spacing, and progress in tunable lasers, coherent FDM looks promising for optical networking.

Phase noise is an important factor in coherent FDM due to the spectral broadening that it causes. The required channel spacing between adjacent channels will be more than what it could be in the absence of phase noise. Therefore phase noise limits the efficiency with which the available optical bandwidth can be utilized. In this chapter we will attempt to quantify this efficiency degradation. First we need to evaluate the spectral occupancies of the modulation formats of interest in order to obtain an abstract model of spectral requirements of individual users.

7.1 Power Spectra with Phase Noise

The general model for the modulated output of an optical transmitter is

$$s(t) = \mathrm{Re}\left[A \exp\left(j(2\pi\nu_0 t + \theta(t))\right) \sum_k \bar{a}_k p(t - kT)\right] \tag{7.1}$$

where $\bar{a}_k$ is a modulation dependent data parameter, $p(t)$ is a pulse of duration T, and the rest of the parameters are as previously defined. For binary modulation formats with data

$a_k = 0, 1$, the parameter $\bar{a}_k$ is given in the following equation:

$$\bar{a}_k = \begin{cases} a_k & \text{OOK} \\ (1 - 2a_k) & \text{PSK} \\ (1 - 2a_{k-1} \oplus a_k) & \text{DPSK} \\ a_k e^{j2\pi f_d t} + (1 - a_k) e^{-j2\pi f_d t} & \text{FSK} \end{cases} \tag{7.2}$$

The modulation formats above except DPSK are memoryless. In general, memory causes complications in the spectral density computations [43]. However, the particular form of memory in DPSK is easily handled since its spectral density can be shown to be identical to that of PSK. Furthermore, all the modulation formats above have real and time-invariant $\bar{a}_k$ except FSK. We will first exclude FSK from our discussion and obtain a general form for the power spectral densities of the other formats. Later we show that the same form also applies to FSK.

The lemma below shows the reduction of DPSK to PSK as promised.

Lemma 7.1 *For independent and equiprobable binary data sequence $\{a_k\}$, DPSK modulated signal has the same power spectral density (PSD) as a PSK modulated signal.*

Proof. Clearly a modulation format affects the PSD of the modulated signal only through $\bar{a}_k$ in Equation 7.2. Thus we need to show that $\bar{a}_k$ has the same statistical description for DPSK and PSK. Let $b_k = a_k \oplus a_{k-1}$. Since $\bar{a}_k = 1 - 2a_k$ for PSK, and $\bar{a}_k = 1 - 2b_k$, we only need to show that when $\{a_k\}$ is an independent equiprobable sequence then so is $\{b_k\}$. This is easily seen to be true as follows.

$$\begin{aligned} \Pr(b_k = 0) &= \Pr(a_k = a_{k-1}) = \frac{1}{2} \\ \Pr(b_k = 0 \mid b_{k-1} = 0) &= \Pr(a_k = a_{k-1} \mid a_{k-1} = a_{k-2}) = \frac{1}{2} \end{aligned}$$

and similarly

$$\Pr(b_k = i_k \mid b_{k-1} = i_{k-1}, \ldots, b_1 = i_1) = \frac{1}{2} \quad \forall (i_1, \ldots, i_k) \in \{0, 1\}^k$$

Thus $\{b_k\}$ is an independent equiprobable sequence.

Note that this result would not hold if $\Pr(a_k = 0) = p \neq 1/2$, since $\Pr(b_k = 0) = p^2 + (1 - p)^2 \neq p$. □

For real, time-independent, and memoryless $\bar{a}_k$ the signal can be rewritten as

$$s(t) = A\cos(2\pi f_c t + \theta(t) + \phi)d(t) \tag{7.3}$$

where $d(t)$ is the baseband modulated waveform given by

$$d(t) = \sum_k \bar{a}_k p(t - kT)\ . \tag{7.4}$$

The main finding of this section is the following property (which will be later shown to be valid also for FSK) which states that the phase noise results in a power spectral density which is given by the convolution of a baseband spectral island of Lorentzian shape with the would-be PSD in the absence of phase noise.

Theorem 7.1 *The PSD of the phase noisy modulated signal $s(t)$ is given by the convolution of the PSD phase noise free modulated waveform $s_0(t)$ with the baseband Lorentzian spectrum :*

$$S_s(f) = S_{s_0}(f) * L(f)$$

where

$$L(f) = \frac{\beta/2\pi}{f^2 + (\beta/2)^2}$$

when $\bar{a}_k$ is real, time-independent, and discrete-time stationary.

Proof. We first note that the process $s(t)$ is not stationary in its given form since the modulation waveform $d(t)$ is not stationary. This problem can easily be overcome by the following standard observation. A constant timing mismatch between the carrier and the data waveform $d(t)$ will not change the frequency distribution of power. Such a timing mismatch can be artificially introduced as a random time origin in $d(t)$ to make the waveform stationary. Thus we modify $s(t)$ as

$$s(t) = A\cos(2\pi f_c t + \theta(t) + \phi)d(t + \alpha)$$

where α is uniformly distributed over $[0, T)$. The rest of the proof involves straightforward manipulation. We first find the autocorrelation function of $s(t)$.

$$\begin{aligned} R_s(u, v) &= A^2 E\left[\cos(2\pi f_c u + \theta(u) + \phi)\cos(2\pi f_c v + \theta(v) + \phi)\right] \\ &\quad \cdot E\left[d(u + \alpha)d(v + \alpha)\right] \end{aligned}$$

$$= A^2 E_1 E_2 \tag{7.5}$$

where we have labeled the first and second expectations as E_1 and E_2 respectively. E_1 was calculated in Chapter 1 as

$$E_1 = \frac{1}{2}\exp\left(-\pi\beta|u-v|\right)\cos\left(2\pi f_c(u-v)\right) . \tag{7.6}$$

For the second term we have

$$E_2 = \sum_n \sum_k E(\bar{a}_n \bar{a}_k) E_\alpha \left[p(u-nT+\alpha)p(v-kT+\alpha)\right] .$$

By the stationarity hypothesis $E(\bar{a}_n\bar{a}_k)$ is a function of only $n-k$, let $E(\bar{a}_n\bar{a}_k) = R_{\bar{a}}(k-n)$. The expectation over α, E_α, can be written as

$$\begin{aligned} E_\alpha &= \frac{1}{T}\int_0^T p(u-nT+\alpha)p(v-kT+\alpha)\, d\alpha \\ &= \frac{1}{T}\int_{u-nT}^{u-(n-1)T} p(x)p(x+v-u+(n-k)T)\, dx . \end{aligned}$$

Inserting the last line back into the expression for E_2, with a change of summation index, we obtain

$$\begin{aligned} E_2 &= \sum_i R_{\bar{a}}(i)\frac{1}{T}\sum_n \int_{u-nT}^{u-(n-1)T} p(x)p(x+v-u+iT)\, dx \\ &= \sum_i R_{\bar{a}}(i)\frac{1}{T}\int_{-\infty}^{\infty} p(x)p(x+v-u+iT)\, dx . \end{aligned} \tag{7.7}$$

Note from Equations 7.6 and 7.7 that both E_1 and E_2 depend on u, v only through $u-v$. Thus from Equation 7.5 $s(t)$ is stationary, and we have via $\tau = v-u$

$$R_s(\tau) = \frac{A^2}{2}\exp\left(-\pi\beta|\tau|\right)\cos\left(2\pi f_c\tau\right)\sum_i R_{\bar{a}}(i)\frac{1}{T}\int_{-\infty}^{\infty} p(x)p(x+\tau+iT)\, dx .$$

We now define $l(\tau)$ as

$$l(\tau) = \exp\left(-\pi\beta|\tau|\right)$$

and $m(\tau)$ as the rest of the factors in $R_s(\tau)$. If $L(f)$ and $M(f)$ denote the respective Fourier transforms, then

$$S_s(f) = L(f) * M(f) .$$

Since the phase noise free modulated signal $s_0(t)$, by definition, satisfies

$$s_0(t) = s(t)\,|_{\beta=0}\ ,$$

its PSD is $M(f)$. On the other hand, straightforward calculations show that $L(f)$ is given by

$$L(f) = \frac{\beta/2\pi}{f^2 + (\beta/2)^2}\ .$$

This completes the proof. □

One can show quite easily that the phase noise free PSD $S_{s_0}(f)$ can be written as

$$S_{s_0}(f) = \frac{A^2}{4}\left[Z(f - f_c) + Z(f + f_c)\right]$$

where

$$Z(f) = \frac{1}{T}\,|P(f)|^2\,S_{\bar{a}}(f)$$

and $S_{\bar{a}}(f)$ is the discrete Fourier transform of $R_{\bar{a}}(i)$:

$$S_{\bar{a}}(f) = \sum_i R_{\bar{a}}(i) e^{j2\pi f i T}\ .$$

It is easy to show that OOK and PSK (and thus DPSK) satisfies the stationarity condition of the theorem. For OOK, one obtains

$$R_{\bar{a}}(i) = \frac{1}{4} + \frac{1}{4}\delta_i$$

where δ_i is 1 if $i = 0$ and 0 if $i \neq 0$, and

$$S_{\bar{a}}(f) = \frac{1}{4}\delta(f) + \frac{1}{4}\ .$$

For PSK/DPSK, one has

$$\begin{aligned} R_{\bar{a}}(i) &= \delta_i \\ S_{\bar{a}}(f) &= 1\ . \end{aligned}$$

For FSK, the time-dependent formulation of (7.1)-(7.2) is not very helpful. Instead we write the FSK signal as a sum of two OOK signals modulated with complementary data

and with different carrier frequencies:

$$s(t) = A \sum_k [a_k \cos(2\pi f_1 t + \theta(t) + \phi_1) + (1 - a_k) \cos(2\pi f_2 t + \theta(t) + \phi_2)] p(t - kT + \alpha)$$

where ϕ_1 and ϕ_2 are two independent uniform phases. It is straightforward to mimic the proof of the theorem for this special case, and to show that the same convolution property holds. The phase noise free PSD in this case is

$$S_{s_0}(f) = \frac{A^2}{4} [Z(f - f_1) + Z(f + f_1) + Z(f - f_2) + Z(f + f_2)]$$

with $Z(f)$ being identical to that of OOK.

Our development so far applies to any pulse shape $p(t)$. In the case of a pulse shape which is unity over the bit duration, the spectrum will consist of spectral island of $\sin(x)/x$ form convolved with Lorentzian spectrum. The following general conclusions are immediate:

1. Phase noise results in broadening of the modulation spectrum, as in the case of the unmodulated carrier.

2. The bandwidth may be approximated by

$$B = \begin{cases} 2R + \beta & \text{OOK/PSK/DPSK} \\ f_d + 2R + \beta & \text{FSK} \end{cases}$$

   where R is the bit rate and $f_d = |f_1 - f_2|$ is the frequency separation between the FSK tones.

3. For negligible spectral broadening due to phase noise, the linewidth to bit rate ratio βT must be small.

The goal in going through these calculations was to obtain an estimate in the increase of band occupancy for various modulation formats so as to allow a unified treatment of FDM networks disregarding the details of modulation. The result that we will use in the following sections is that the width of the spectrum increases by an amount proportional to linewidth for all practical modulation formats. That is

$$B \simeq B_0 + \beta \tag{7.8}$$

where B_0 is the occupied bandwidth in the absence of phase noise.

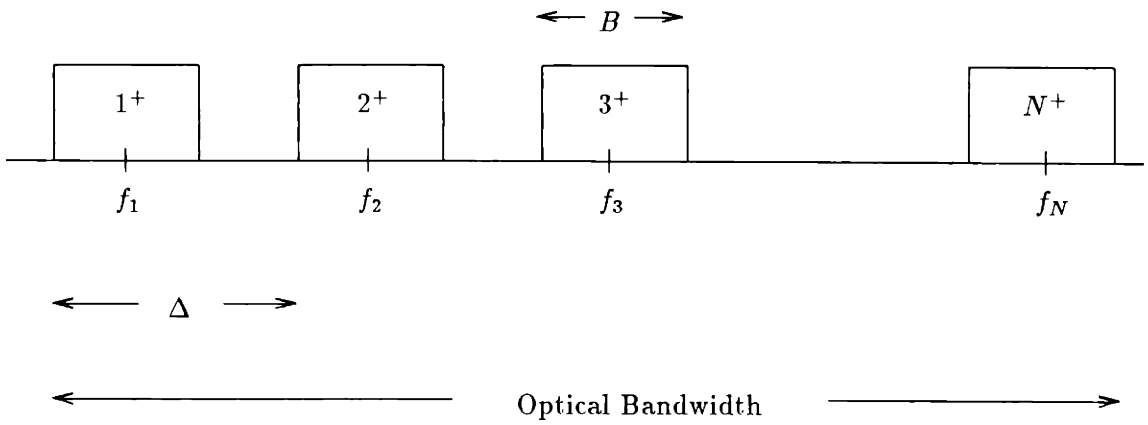

Figure 7-1: Typical channel allocation in a frequency division multiplexed network. The image bands are not shown.

7.2 Phase Noise and FDM

In a typical FDM network with N users the available bandwidth is divided into N channels of equal width as shown in Figure 7-1. In the figure, the center frequency of the ith channel, f_i, corresponds to the carrier frequency of ith user. The channels are placed Δ apart, and each channel has width equal to modulation bandwidth B (which includes phase noise effect). We assume users of identical rate.

We have mentioned that in noncoherent detection the channel spacing Δ must be much larger than the channel bandwidth B because of wide passband of optical filters. The requirement of large guard bands between adjacent channels results in poor spectral utilization. We define the spectral efficiency η as

$$\eta \stackrel{\Delta}{=} \frac{B_0}{\Delta} \tag{7.9}$$

where B_0 is the phase noise free modulation bandwidth. We would like η to be as close to unity as possible. For noncoherent FDM this is not likely to be the case.

At first glance, it seems that $\eta \simeq 1$ is possible with coherent FDM. This is certainly true in heterodyne radio, where a receiver, in order to listen to channel i, simply multiplies the received signal with $\cos(2\pi f_i t)$ and passes the resulting signal through a lowpass filter. However this is not true for optical heterodyning due to the square-law behavior of

photodetectors. The nonlinearity causes crosstalk between adjacent channels, resulting in interchannel interference (ICI) [65].

Let's suppose that a receiver wants to listen to channel i in coherent FDM. It will add a local oscillator field at frequency f_0 which is in the vicinity of f_i and photodetect the resulting lightwave. Let $s(t)$ be the received waveform and let

$$s_{LO}(t) = C\cos(2\pi f_0 t + \theta_{LO}(t))$$

be the local oscillator waveform. The resulting IF signal $r(t)$ will have the spectrum

$$R(f) = S(f) * S(f) + S_{LO}(f) * S_{LO}(f) + 2S(f) * S_{LO}(f)$$

where the first term is the signal cross signal (direct detection) term, the second term is the self-beat of the local oscillator (LO) signal, and the last term is is the desired signal cross LO term. A demonstration of these spectral components is given in Figure 7-2 for $f_{i-1} < f_{LO} < f_i$. Note that this is the only choice of f_0 which will not result in spectral overlapping of various signals. It is clear from the figure that the baseband is occupied by self-beat signal and LO components. The desired component of the signal cross LO signal is closest to baseband followed by other channels and ICI signals. The necessary conditions for no overlapping between the desired signal and undesired signals are

$$f_i - f_0 \geq \frac{1}{2}(3B + \beta) \tag{7.10}$$

$$f_0 - \frac{1}{2}(f_i + f_{i-1}) \geq \frac{1}{2}(B + \beta) \tag{7.11}$$

$$\Delta \geq (4B + 2\beta) \tag{7.12}$$

The first condition corresponds to nonoverlapping of the desired signal with baseband components, the other two conditions ensure that the two adjacent channels don't interfere.

There are several important conclusions that follow immediately.

1. Homodyne detection ($f_0 = f_i$) results in an overlap of the desired signal with the baseband self-beat terms, and therefore cannot be used here.

2. Large guard bands are necessary to avoid ICI. This is true even in the absence of phase noise, but is further worsened by the phase noise induced spectral broadening. Assuming $B_0 = 2R$, we obtain the maximum spectral efficiency as

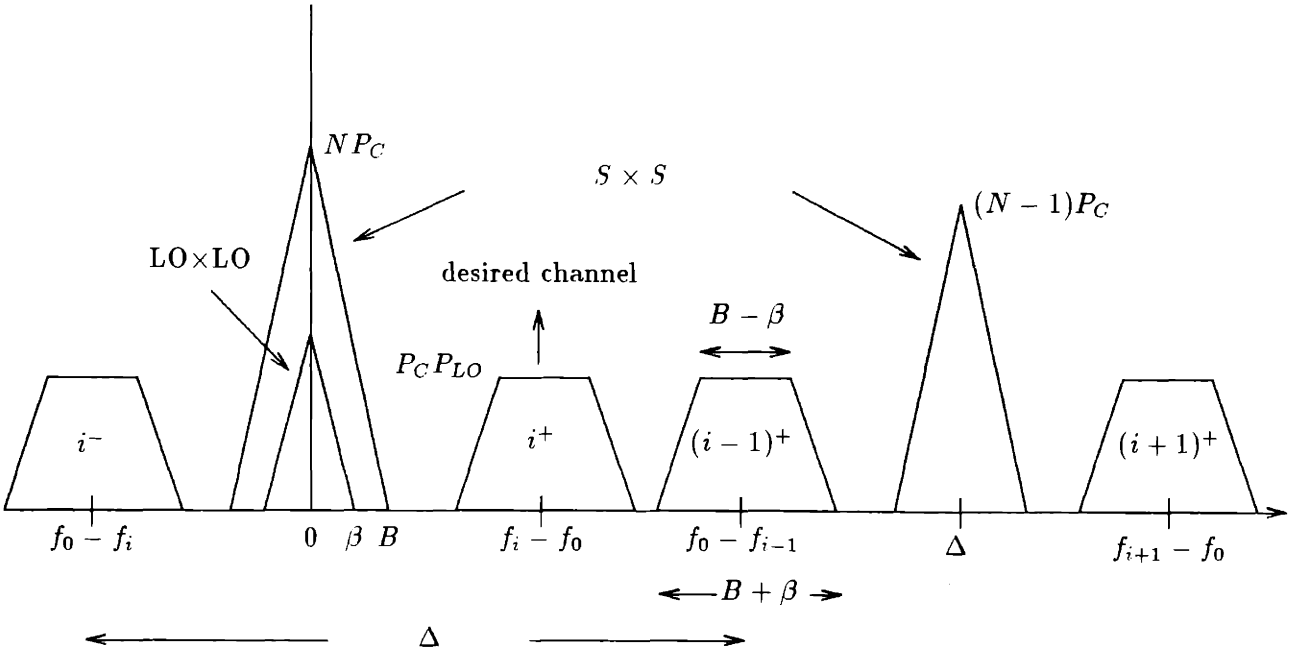

Figure 7-2: IF spectrum after heterodyne detection. The signal-cross-LO components are shown as trapezoids, while signal-cross-signal terms are shown as triangles. Amplitudes are accurate within multiplicative constants, P_C is the power per channel and P_{LO} is the LO power.

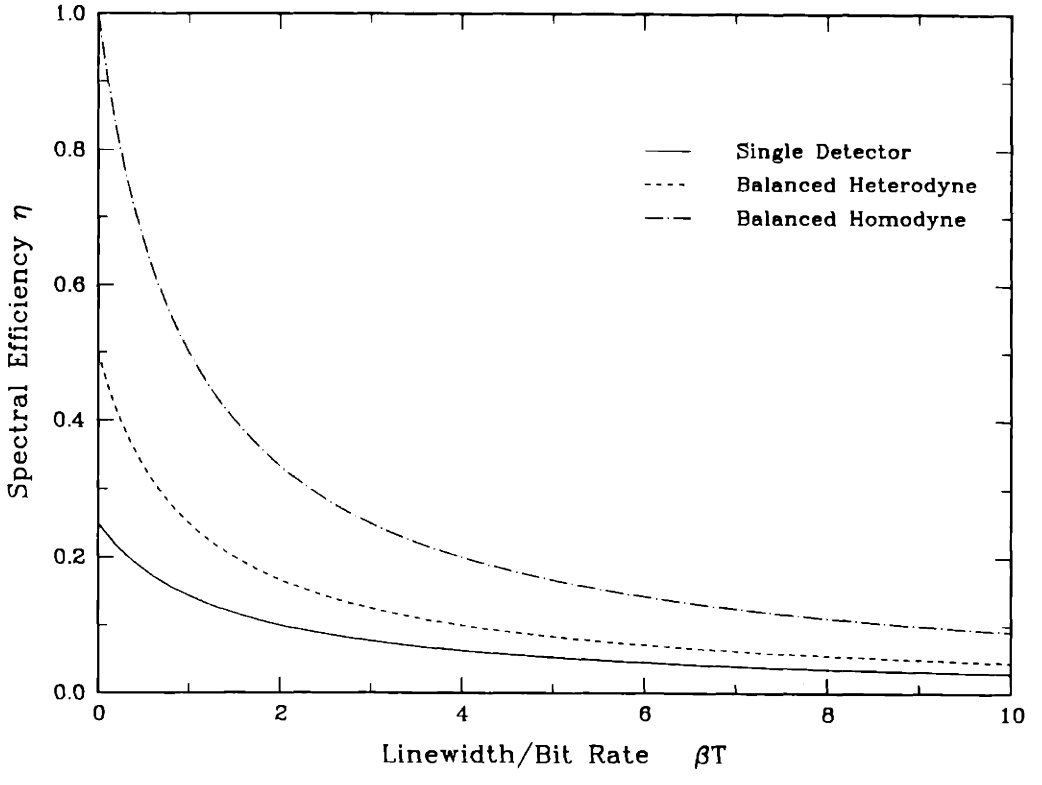

Figure 7-3: Spectral efficiencies of single receiver and balanced receiver FDM networks.

$$\eta = \frac{1}{4 + 3\beta T} \tag{7.13}$$

which is shown in Figure 7-3 (solid curve). It is seen that the spectral efficiency is 25% with no phase noise, 14% with $\beta T = 1$, and 10% with $\beta T = 2$. The channel spacing is seen to increase considerably with increasing phase noise strength.

3. The IF frequency $f_{IF} = f_i - f_0$ at which the IF processing will be done is not arbitrary. In fact, we get from (7.10) and (7.11) that f_{IF} must satisfy

$$3R + 2\beta \leq f_{IF} \leq \frac{\Delta}{2} - (R + \beta) .$$

At maximum spectral efficiency, this becomes $f_{IF} = 3R + 2\beta$. In this case the neighboring spectral islands are touching each other.

The need for precise control of the IF frequency for high spectral efficiency conflicts with the fact that controlling the frequency of a laser with precision in the IF range is a difficult task [66]. Thus, some additional inefficiency will have to be tolerated to accommodate the drift of the IF frequency from its desired value.

4. The height of signal cross signal spectra is independent of the LO power, while the height of signal cross LO terms is proportional to the LO power. Therefore if the LO power is very large and the number of channels N is not very large, then the components that result from signal self-beat are much weaker in power than the desired component. In this case the spectral overlapping around DC can be tolerated. The only requirement that has to be satisfied is that adjacent channels don't overlap which is achieved if $\Delta \geq 2B_0 + 4\beta$. The spectral efficiency η can be increased to close to 50% and homodyne detection can be used as well. One way to limit N can be implemented by a wideband optical filter, which passes only a limited number of channels, prior to photodetection.

5. The required IF filtering is bandpass, not lowpass. Lowpass-filtering will result in interference of DC terms with the desired channel. If the power in each channel is P_C and the LO power is P_{LO}, then the ratio of the desired power to the interference power will be

$$\frac{P_D}{P_I} = \frac{P_{LO} P_C}{N P_C} = \frac{P_{LO}}{N}$$

which decreases with increasing N.

6. Approximating the coherent photodetection process with ideal RF mixing (with a phase noisy oscillator) is only feasible when the LO power is very large in comparison to the total received power. In that case, one only needs to consider the adjacent channel interference. The necessary spacing conditions become

$$\Delta \geq \begin{cases} 2B_0 + 4\beta & \text{Heterodyne} \\ B_0 + 2\beta & \text{Homodyne} \end{cases}$$

Thus η can be made to approach 50% for heterodyne detection and 100% for homodyne detection. But there is still one drawback with homodyning. The mirror image of channel $i-k$ will overlap with channel $i+k$ for $k = 1, 2, \ldots$. Thus only channel i can be listened, while in heterodyne detection several channels can be listened in parallel by appropriate IF filtering.

7.3 FDM with Balanced Receivers

The photodetection model we have considered in the previous section consisted of a single photodetector. We have found that with a single photodetector configuration the spectral efficiency is at most 25% due to interchannel interference. In this section, we consider a receiver which employs two photodetectors, and we analyze its spectral efficiency.

The optical detector now consists of two photodetectors in *balanced* configuration [67]. This configuration is shown in Figure 7-4. The received optical field E_r and the LO field E_{LO} are the inputs to a 3 dB coupler. The coupler is a 2×2 linear device with the field transfer matrix

$$H = \frac{1}{\sqrt{2}} \begin{pmatrix} 1 & 1 \\ 1 & -1 \end{pmatrix}$$

so that the output branches have the fields

$$\begin{aligned} E_1 &= \frac{1}{\sqrt{2}}(E_r + E_{LO}) \\ E_2 &= \frac{1}{\sqrt{2}}(E_r - E_{LO}) \,. \end{aligned}$$

The power is conserved in the coupler since $H^T H = I$ where I is the identity matrix. The fields E_1 and E_2 are separately photodetected resulting in IF currents i_1 and i_2. We have,

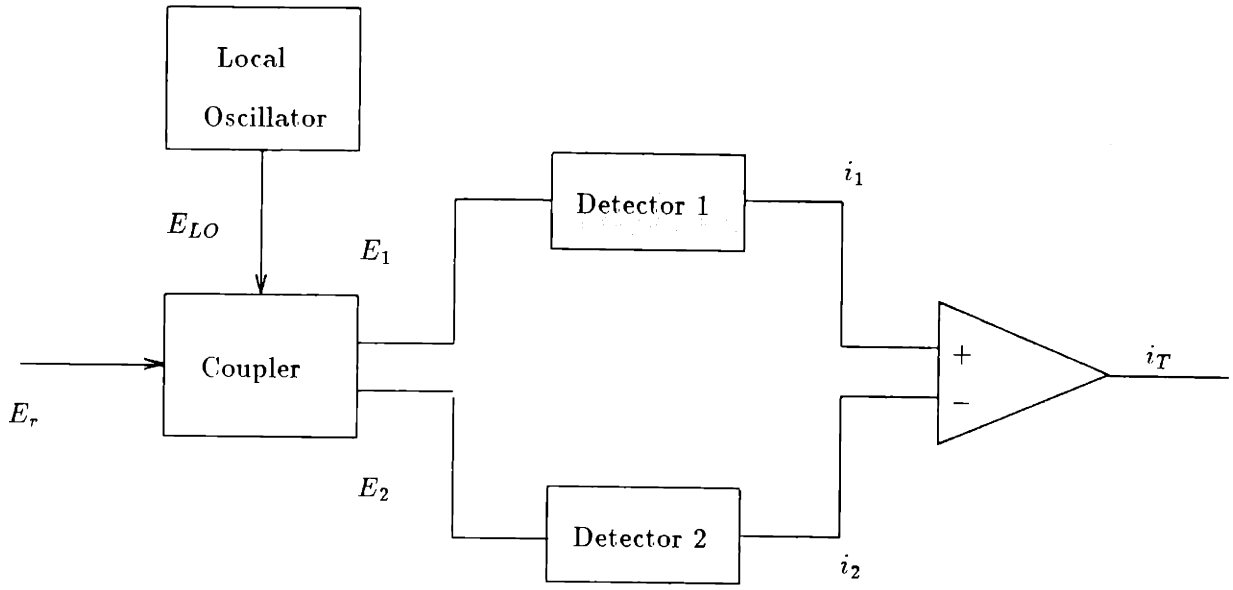

Figure 7-4: The balanced detector.

with the use of complex envelope notation,

$$\begin{aligned} i_1 &= K|E_1|^2 = \frac{K}{2}\left(|E_r|^2 + |E_{LO}|^2 + 2E_r^* E_{LO}\right) \\ i_2 &= K|E_2|^2 = \frac{K}{2}\left(|E_r|^2 + |E_{LO}|^2 - 2E_r^* E_{LO}\right) \end{aligned}$$

where it is assumed that the photodetectors are identical with responsivity K. The difference $i_1 - i_2$ does not contain the self-beat terms $|E_r|^2$ and $|E_{LO}|^2$. Thus balanced receivers eliminate an important source of interchannel interference, namely the signal cross signal interference [16, 17]. The only remaining source of interference is the image-band interference of adjacent channels. The situation is an exact analog of the single photodetector receiver with large LO power and small number of users. However this is realized by a simple insertion of an additional photodetector instead of a tunable optical filter, and without the limitation on the number of users.

The resulting spectral efficiency is easily found using the previous discussion to be

$$\eta = \frac{1}{2(1+\beta T)} \tag{7.14}$$

for heterodyne systems, and

$$\eta = \frac{1}{1 + \beta T} \tag{7.15}$$

for homodyne systems. Once again, homodyning improves the spectral efficiency by a factor of 2 at the expense of eliminating the possibility of parallel reception capability. The spectral efficiencies with balanced receivers are also shown in Figure 7-3. For balanced heterodyne systems, η is 50% with no phase noise, 25% with $\beta T = 1$, and 16.7% with $\beta T = 2$. This is a considerable improvement over single detector heterodyne FDM systems. Thus balanced receivers are most likely to be implemented in the coherent FDM networks of the future.

Chapter 8

Conclusions and Future Work

In this chapter, we present the conclusions from this thesis, and we point out open problems that may be considered for future work.

8.1 Conclusions

In this thesis, we have attempted to provide a study of the critical issues related to the phenomenon of phase noise. Our emphasis has been on the bit error performance of point-to-point links where the transmitter and receiver lasers are corrupted by significant phase noise. The degradation of the bit error performance is the most important effect of phase noise. Consequently, all but one chapter of this thesis has taken the bit error probability as the cost function that is to be minimized. Only in Chapter 7 we have used the spectral efficiency as the performance measure.

In the first three chapters, after the introduction, we considered three of the most fundamental and practical modulation formats: frequency, phase and amplitude modulations. While the analysis in Chapter 2 is applicable to any orthogonal modulation format, e.g. polarization modulation and pulse position modulation, it is likely that Frequency Shift Keying (FSK) with wide frequency deviation will be its major application in the foreseeable future. We have shown in Chapter 2 that envelope detection of binary FSK provides a system that is quite robust against phase noise: the performance degradation due to phase noise is within 3 dB even for conservative system parameters. The important point, however, is that this robustness is attained by appropriately modifying the receiver structure. The conventional envelope detector is very vulnerable to phase noise; it is only after widening the front-end filter bandwidth and adding a post-squaring filter that the system performance becomes satisfactory.

We have tried to emphasize the tradeoff between the phase noise and additive noise throughout the analyses in this thesis. It is the combination of these noise processes that degrade the performance to the extent we have seen; if one or the other of the two noises were absent the performance would be significantly better. Therefore, the system design must explicitly take this tradeoff into account and must attempt to optimally balance the effects of phase noise and additive noise. This approach was fruitful in the envelope detection of FSK and OOK signals as well as the joint signal/receiver design problem of transmitted reference systems.

We were not so successful in obtaining a good performance with phase modulated signals. We described form the outset that the problem was more challenging due to both the information and the noise being on the phase. Since previous performance analyses predicted poor performance, we tried to see what can be done optimally when the signal is phase modulated in the presence of phase noise. We were able to obtain the optimal decision rule after converting the continuous time problem into a discrete time problem by sampling. The resulting decision rule was unfortunately very complex. It didn't seem likely that it can be implemented in practice, neither did it seem likely that its performance can be analyzed in the general case. However, we feel it is important that the optimal receiver structure is known. It may be simplified to a point where it can be analyzed and/or implemented. Its performance can be simulated to estimate its contribution over simpler receivers. In fact, from the complicated structure we could obtain a decision rule, the angle difference rule, which can be both analyzed and implemented. As a by-product of the analysis, it became apparent that the error floors are not inherent in phase modulation, but rather they are a result of inflexible receivers. If a receiver is designed according to the relative strengths of additive noise and phase noise, then there is no error floor due to phase noise. While this result is conceptually nice, it still does not compensate for the fact that phase noise tolerance of the receiver structures we could analyze were extremely poor. How much of the poor performance is inherent in phase modulation, and how much of it is due to our inability to design and analyze better receivers is still an open question. We will elaborate on this further in the next section.

In Chapter 4, we considered another promising modulation scheme, the amplitude modulation. Using the techniques that were already developed for phase modulation, we started by obtaining the optimal receiver structure, which did retain its complexity. After analyzing a few special cases of the optimal receiver, we concentrated on the envelope detector structure. Since most of the necessary tools were available from the analysis of orthogonal signals, we could easily obtain the performance of binary On-Off-Keying (OOK) signals.

As a result, we observed that for peak-power constrained semiconductor lasers, OOK is inferior to FSK in performance. However the performance gap decreases from nearly 3 dB in the absence of phase noise to 1.5 dB when there is significant phase noise. These two modulation schemes are significant contenders for implementation in future coherent optical communication systems.

In the following chapter, we looked into the feasibility of transmitting a reference signal to help the receiver undo the lack of coherence imposed by phase noise. We started by reviewing the suggestions on how to perform reference transmission and the predictions of the performance. We showed that if the available transmitter power is equally divided between the information carrying signal and the reference signal then the performance of the system is limited to that of binary orthogonal systems, such as wide deviation FSK. Furthermore, we demonstrated that the wideband front-end filter is a poor choice, since it results in a nonsatisfactory performance. This is due to not properly balancing the tradeoff between phase noise and additive noise; a wideband filter overemphasizes phase noise at the expense of increasing the effect of additive noise. By jointly optimizing the signal and receiver parameters, one can achieve a significantly better performance. Namely, by allocating the available the available power optimally between the two signals, and also by optimizing the filters at the receiver, the performance of the transmitted reference schemes becomes much better than conventional single carrier transmission systems. As a result, these reference transmission systems are promising candidates for signaling mechanism in coherent optical systems.

We also briefly considered the problem of efficient bandwidth utilization in the presence of phase noise in a frequency division multiplexed optical network. After evaluating the bandwidth occupancies of various modulation schemes when the carrier is contaminated by the phase noise process, we showed that phase noise is a handicap in efficient packing of the optical spectrum. However with the use of balanced receivers, increased data rates and better semiconductor lasers, this effect does not seem as significant as the reliability degradation effect we have emphasized.

In conclusion, this thesis has been an attempt towards a comprehensive study of the effects of phase noise on coherent optical communication systems. We feel that the significance of the thesis not so much in the quantitative results that it provides, such as the bit error curves or bandwidth settings, but more in the increased conceptual understanding and modeling accuracy of phase noisy communications. For example, the method of obtaining the exact conditional error probability, which was successful in most cases, helps identify the fundamental parameters that affect the system performance. Similarly, the

idea of optimizing the receiver, and the signal when possible, to the extent it is analytically feasible and practically interesting, is an approach that improves the performance at little additional complexity or cost. Therefore it is hoped that some of the tools of this thesis will be used in the exciting and developing field of optical communications.

8.2 Future Work

As with any technical work, this thesis does not end the problems related to its topic. In fact, there are many open problems that remain and that need to be solved before we can claim that phase noise will not be a significant issue in coherent optical communications. We will briefly describe some of these problems in the following discussion.

8.2.1 Finite Frequency Separation in FSK

In our analysis, as well as in most analyses of FSK, it was assumed that the FSK signals are truly orthogonal. This means that the separation between the frequency tones is very large. It is not yet known whether this is critical to acceptable system performance. The quantitative effect of finite frequency separation must be analyzed to find a good balance between bandwidth occupancy of individual channels and the bit error performance. It is likely that the performance will not depend heavily on this separation, provided that it is above a certain threshold, and therefore that the effect of finite frequency separation is negligible.

8.2.2 Effect of Multiple Users on Bit Error Rates

This is an issue related to the previous point. We have always neglected the effect of neighboring channels in our error performance analyses. However, there will be an inevitable overlap between adjoining channels due to the tails of the modulated spectra. The extent of this interaction will put limits on the efficiency of spectral utilization that we considered in Chapter 7. This point has attracted the attention of researchers recently [68]. More work has to be done before we can get a clear understanding of how phase noise complicates the interuser interference from the viewpoint of reliability of end-to-end communication.

8.2.3 Double Filter Receivers for DPSK

As we have previously emphasized, the performance question of phase modulation is not completely answered yet. We are not sure whether DPSK is inherently intolerant to phase

noise or whether the receiver structures that we have proposed simply lack the required qualities. For example, the angle difference rule we have found in Chapter 3 eliminates the error floors and improves the performance by simply optimizing over the window of observation. However, this receiver is still one with a single filter. Single filter receivers were found to be inadequate against phase noise for other modulation schemes as well. The optimal receiver structure suggests a weighted nonlinear combination of the sample vectors which is far too complicated. However there may exist a simple mechanism, e.g. a linear combiner with optimized weights, that performs far better than known single filter receivers. Clearly some more work has to be done on DPSK before it is declared infeasible.

8.2.4 Statistics of Phase Noisy Random Variables

We have seen throughout this thesis that certain random variables, most notably the phase noisy squared envelope in envelope detection, are encountered frequently in the performance analysis of communication systems with phase noise. We employed certain approximations, e.g. exponential approximation and a mean value analysis, to overcome the difficulty that the statistics of these random variables are not available. It would be invaluable to have a compact statistical description of such random variables, for example through a closed-form probability density function or a moment generating function. Only then could we be absolutely certain about our performance predictions. The conditional error probability expressions we have found would be helpful in this context.

8.2.5 Capacity of a Phase Noisy Channel

The phenomenon of phase noise can be viewed as a distortion introduced by a channel. Then the channel could be modeled as having its input as a point on the two-dimensional Cartesian plane. The channel itself would have two blocks in cascade. The first block is a *rotation channel* the output of which is the rotation of the input around the origin. The angle of this rotation has the same memory structure as the Brownian motion. The second block is the well-known additive white Gaussian noise (AWGN) channel. The information-theoretic capacity of this cascaded channel is an interesting quantity to compute. The first channel has infinite capacity: one can convey infinitely many bits of information by just changing the energy by an infinitesimal increment. The second channel has a finite capacity which is explicitly known. The question here is whether the cascade of the two channels has the same capacity. While this may seem like an academic question its answer may be of practical importance in the light of advances in coded modulation for the AWGN channel

that approach the capacity.

8.2.6 Phase Noise in Direct Detection Systems

While this thesis has concentrated on coherent systems, phase noise is also a problem for direct detection systems. Since the current output of a photodetector is dependent only on the intensity of the incident field, phase noise would not affect the performance of a direct detection system if the input were a single sinusoidal. However systems in which the optical field is a sum of two or more fields suffer from phase noise in a mechanism that is similar to coherent systems. This is because the interfering signals play a similar role to that of the local oscillator in the sense that the cross terms will contain the effect of phase noise. Most direct detection systems will be hampered in this way, such as optical networks with multiple users sharing the same fiber, or systems with optical amplifiers where the optical noise introduced by the amplifier will serve as the interference. The robustness of these systems to phase noise must be analyzed to estimate the effect of phase noise and to devise possible remedies. The conditioning approach may be used in such an analysis with the necessary modifications for the Poisson statistics replacing the additive noise.

Bibliography

[1] C. H. Henry, "Theory of linewidth of semiconductor lasers," *IEEE Journal of Quantum Electronics*, vol. QE-18, pp. 259–264, February 1982.

[2] J. Rutman, "Characterization of phase and frequency instabilities in precision frequency sources: Fifteen years of progress," *Proceedings of the IEEE*, vol. 66, pp. 1048–1072, September 1978.

[3] M. W. Fleming and A. Mooradian, "Fundamental line broadening of single-mode GaAlAs diode lasers," *Applied Physics Letters*, vol. 38, pp. 511–513, April 1981.

[4] J. Salz, "Coherent lightwave communications," *AT&T Technical Journal*, vol. 64, pp. 2153–2209, December 1985.

[5] P. J. Lin, "Study of an all fiber polarization and phase diversity receiver," Master's thesis, Massachusetts Institute of Technology, 1991.

[6] L. G. Kazovsky and D. A. Atlas, "Miniature NdYAG lasers: Noise and modulation characteristics," *IEEE Journal of Lightwave Technology*, vol. 8, pp. 294–301, March 1990.

[7] P. S. Henry, "Lightwave primer," *IEEE Journal of Quantum Electronics*, vol. QE-21, pp. 1862–1879, December 1985.

[8] G. J. Foschini, L. J. Greenstein, and G. Vannucci, "Noncoherent detection of coherent lightwave signals corrupted by phase noise," *IEEE Transactions on Communications*, vol. COM-36, pp. 306–314, March 1988.

[9] S. Saito and Y. Yamamoto, "Direct observation of Lorentzian lineshape of semiconductor lasers and linewidth reduction with external grating feedback," *Electronics Letters*, vol. 17, pp. 325–327, April 1981.

[10] V. W. S. Chan, L. L. Jeromin, and J. E. Kaufmann, "Heterodyne lasercom systems using GaAs lasers for ISL applications," in *Proceedings of International Conference on Communications*, (Boston, MA), pp. 1201–1207, June 1983.

[11] J. E. Kaufmann, "Phase and frequency tracking considerations for heterodyne optical communications," in *Proc. Int. Telemetering Conf.*, (San Diego, California), September 1982.

[12] C. H. Henry, "Theory of the phase noise and power spectrum of a single mode injection laser," *IEEE Journal of Quantum Electronics*, vol. QE-19, pp. 1391–1397, September 1983.

[13] J. H. Shapiro, "Optical detection and communication." 6.453 Course Notes. MIT Cambridge, MA.

[14] J. R. Barry and E. A. Lee, "Performance of coherent optical receivers," *Proceedings of the IEEE*, vol. 78, pp. 1369–1394, August 1990.

[15] H. L. Van Trees, *Detection, Estimation, and Modulation Theory.* New York: John Wiley & Sons, 1968.

[16] L. G. Kazovsky, "Multichannel coherent optical communications systems," *Journal of Lightwave Technology*, vol. 5, pp. 1095–1102, August 1987.

[17] L. G. Kazovsky and J. L. Gimlett, "Sensitivity penalty in multichannel coherent optical communications," *Journal of Lightwave Technology*, vol. 6, pp. 1353–1365, September 1988.

[18] G. J. Foschini, G. Vannucci, and L. J. Greenstein, "Envelope statistics for filtered optical signals corrupted by phase noise," *IEEE Transactions on Communications*, vol. COM-37, pp. 1293–1302, December 1989.

[19] L. G. Kazovsky, "Impact of laser phase noise on optical heterodyne communications systems," *Journal of Optical Communications*, vol. 7, pp. 66–77, June 1986.

[20] I. Garrett and G. Jacobsen, "Phase noise in weakly coherent systems," *IEE Proceedings*, vol. 136, pp. 159–165, June 1989.

[21] I. Garrett, D. J. Bond, J. B. Waite, D. S. L. Lettis, and G. Jacobsen, "Impact of phase noise in weakly coherent systems: A new and accurate approach," *Journal of Lightwave Technology*, vol. 8, pp. 329–337, March 1990.

[22] L. G. Kazovsky and O. K. Tonguz, "ASK and FSK coherent lightwave systems: A simplified approximate analysis," *Journal of Lightwave Technology*, vol. 8, pp. 338–352, March 1990.

[23] L. G. Kazovsky, P. Meissner, and E. Patzak, "ASK multiport optical homodyne systems," *Journal of Lightwave Technology*, vol. 5, pp. 770–791, June 1987.

[24] W. C. Lindsey, "Error probabilities for rician fading multichannel reception of binary and N-ary signals," *IEEE Transactions on Information Theory*, vol. IT-10, pp. 339–350, October 1964.

[25] J. G. Proakis, *Digital Communications*. New York: McGraw-Hill, 1983.

[26] S. M. Ross, *Stochastic Processes*. New York: John Wiley & Sons, 1983.

[27] G. J. Foschini and G. Vannucci, "Characterizing filtered light waves corrupted by phase noise," *IEEE Transactions on Information Theory*, vol. IT-34, pp. 1437–1448, November 1988.

[28] P. A. Humblet. Private Communication, 1991.

[29] J. S. Young, "Performance of phase noisy optical systems with frequency stabilization," Master's thesis, Massachusetts Institute of Technology, 1991.

[30] M. Abramowitz and I. A. Stegun, *Handbook of Mathematical Functions*. New York: Dover, 1972.

[31] R. G. Gallager, *Information Theory and Reliable Communication*. New York: John Wiley & Sons, 1968.

[32] A. Papoulis, *Probability, Random Variables and Stochastic Processes*. New York: McGraw-Hill, second ed., 1984.

[33] R. V. Churchill and J. W. Brown, *Fourier Series and Boundary Value Problems*. New York: McGraw-Hill, third ed., 1978.

[34] L. J. Greenstein, G. Vannucci, and G. J. Foschini, "Optical power requirements for detecting OOK and FSK signals corrupted by phase noise," *IEEE Transactions on Communications*, vol. COM-37, pp. 405–407, April 1989.

[35] M. Azizoglu and P. A. Humblet, "Envelope detection of orthogonal signals with phase noise," Tech. Rep. LIDS–P–2010, Massachusetts Institute of Technology, Laboratory for Information and Decision Systems, December 1990.

[36] G. Arfken, *Mathematical Methods for Physicists.* Academic Press, 1985.

[37] J. M. Wozencraft and I. M. Jacobs, *Principles of Communication Engineering.* New York: John Wiley & Sons, 1965.

[38] N. M. Blachman, "The effect of phase error on DPSK error probability," *IEEE Transactions on Communications*, vol. 29, pp. 364–365, March 1981.

[39] J. E. Mazo, "On binary differential detection for coherent lightwave communication," *AT&T Technical Journal*, vol. 64, pp. 2467–2483, December 1985.

[40] M. R. Spiegel, *Mathematical Handbook of Formulas and Tables.* New York: McGraw-Hill, 1968.

[41] I. S. Gradshteyn and I. M. Ryzhik, *Tables of Series, Integrals and Products.* New York: Academic Press, 1980.

[42] G. Nicholson, "Probability of error for optical heterodyne DPSK system with quantum phase noise," *Electronics Letters*, vol. 20, pp. 1005–1007, November 1984.

[43] S. Benedetto, E. Biglieri, and V. Castellani, *Digital Transmission Theory.* Englewood Cliffs, NJ: Prentice-Hall, 1987.

[44] D. A. Shnidman, "The calculation of the probability of detection and the generalized Marcum Q-function," *IEEE Transactions on Information Theory*, vol. IT-35, pp. 389–400, March 1989.

[45] P. A. Humblet and M. Azizoglu, "On the bit error rate of lightwave systems with optical amplifiers," *Journal of Lightwave Technology*, 1991. To be published.

[46] K. Tamura, S. B. Alexander, and V. W. S. Chan, "Phase-noise canceled phase shift keying modulation for coherent optical communication systems," in *Optical Fiber Communications Conf,*, January 1988. Paper WG2.

[47] K. Tamura, S. B. Alexander, V. W. S. Chan, and D. M. Boroson, "Phase-noise canceled differential phase-shift-keying (PNC-DPSK) for coherent optical communication systems," *Journal of Lightwave Technology*, vol. 8, pp. 190–201, February 1990.

[48] S. Betti, F. Curti, G. D. Marchis, and E. Iannone, "Phase noise and polarization state insensitive optical coherent systems," *Journal of Lightwave Technology*, vol. 8, pp. 756–767, May 1990.

[49] I. Bar-David and J. Salz, "On dual optical detection: Homodyne and transmitted-reference heterodyne reception," *IEEE Transactions on Communications*, vol. 36, pp. 1309–1315, December 1988.

[50] R. Calvani, R. Caponi, and F. Cisternino, "Polarization phase-shift-keying: A coherent transmission technique with differential heterodyne detection," *Electronics Letters*, vol. 24, no. 10, pp. 642–643, 1988.

[51] Y. Imai, K. Iizuka, and R. T. B. James, "Phase-noise-free coherent optical communication system utilizing differential polarization shift keying (DPolSK)," *Journal of Lightwave Technology*, vol. 8, pp. 691–698, May 1990.

[52] W. C. Kwong and P. R. Prucnal, "Theory on multichannel CPFSK lightwave network with laser phase noise immunity," in *LEOS Summer Topical on Optical Multiple Access Networks*, (Monterey, California), pp. 66–67, July 25–27 1990.

[53] K. Tamura, "Phase-noise canceled differential phase-shift-keying (PNC-DPSK) for coherent optical communication systems," Master's thesis, Massachusetts Institute of Technology, 1989.

[54] M. Schwartz, W. R. Bennett, and S. Stein, *Communication Systems and Techniques.* New York: McGraw-Hill, 1966.

[55] C. L. Weber, *Elements of Detection and Signal Design.* New York: Springer-Verlag, second ed., 1987.

[56] K. Nosu and K. Iwashita, "A consideration of factors affecting future coherent lightwave communication systems," *Journal of Lightwave Technology*, vol. 6, pp. 686–694, May 1988.

[57] R. S. Kennedy and P. A. Humblet, "A white paper on fiber optic networks of the future." Unpublished, December 1986.

[58] R. S. Tucker, G. Eisenstein, and S. K. Korotky, "Optical time-division multiplexing for very high bit-rate transmission," *Journal of Lightwave Technology*, vol. 6, pp. 1737–1749, November 1988.

[59] J. A. Salehi, "Code division multiple-access in optical fiber networks–Part i: Fundamental principles," *IEEE Transactions on Communications*, vol. 37, pp. 824–833, August 1989.

[60] J. A. Salehi, A. M. Weiner, and J. P. Heritage, "Coherent ultrashort light pulse code division multiple access communication systems," *Journal of Lightwave Technology*, vol. 8, pp. 478–491, March 1990.

[61] M. Azizoglu, J. A. Salehi, and Y. Li, "Optical CDMA via temporal codes," *IEEE Transactions on Communications*, 1991. To be published.

[62] W. M. Hamdy, *Crosstalk in Direct Detection Optical FDMA Networks.* PhD thesis, Massachusetts Institute of Technology, 1991.

[63] M. J. O'Mahony, "Semiconductor laser optical amplifiers for use in future fiber systems," *Journal of Lightwave Technology*, vol. 6, pp. 531–544, April 1988.

[64] G. R. Walker, N. G. Walker, R. C. Steele, M. J. Creaner, and M. C. Brain, "Erbium-doped fiber amplifier cascade for multichannel coherent optical transmission," *Journal of Lightwave Technology*, vol. 9, pp. 182–193, February 1991.

[65] P. Healey, "Effect of intermodulation distortion in multichannel optical heterodyne systems," *Electronics Letters*, vol. 21, pp. 101–103, January 1985.

[66] P. A. Humblet and P. C. Li, "A new frequency distribution architecture for wavelength division systems," Tech. Rep. LIDS-P–2009, Massachusetts Institute of Technology, Laboratory for Information and Decision Systems, December 1990.

[67] G. L. Abbas, V. W. S. Chan, and T. K. Yee, "A dual detector optical heterodyne receiver for local oscillator noise suppression," *Journal of Lightwave Technology*, vol. 3, pp. 1110–1122, October 1985.

[68] G. J. Foschini and L. J. Greenstein, "Spectral efficiency of optical FDM systems impaired by phase noise," *IEEE Transactions on Communications*, 1991. To be published.